DISCLAIMER

This report was prepared as an account of work sponsored by an agency of the United States Government. Neither the United States Government nor any agency thereof, nor any of their employees, makes any warranty, express or implied, or assumes any legal liability or responsibility for the accuracy, completeness, or usefulness of any information, apparatus, product, or process disclosed, or represents that its use would not infringe privately owned rights. Reference herein to any specific commercial product, process, or service by trade name, trademark, manufacturer, or otherwise does not necessarily constitute or imply its endorsement, recommendation, or favoring by the United States Government or any agency thereof. The views and opinions of authors expressed herein do not necessarily state or reflect those of the United States Government or any agency thereof.

ORNL/TM--9146

DE84 016742

Environmental Sciences Division

NOTICE
PORTIONS OF THIS REPORT ARE ILLEGIBLE. It has been reproduced from the best available copy to permit the broadest possible availability.

Site Characterization Techniques Used at a Low-Level Waste Shallow Land Burial Field Demonstration Facility[1]

E. C. Davis, W. J. Boegly, Jr., E. R. Rothschild, B. P. Spalding, N. D. Vaughan,[2] C. S. Haase, D. D. Huff, S. Y. Lee, E. C. Walls,[3] J. D. Newbold,[4] and E. D. Smith

Date of Issue—July 1984

NUCLEAR WASTE PROGRAMS
(Activity No. AR 05 15 15 0; ONL-WL14)

ESD Publication No. 2306

1. Supported by the Office of Defense Waste and By-Product Management, U.S. Department of Energy.
2. Present address: Shell Landing, Route 2, Box 1738, Beaufort, North Carolina 28516.
3. Present address: Route 1, Box 322, Harriman, Tennessee 37748.
4. Present address: Stroud Water Research Center, Route 1, Box 512, Avondale, Pennsylvania 19311.

Prepared by the
OAK RIDGE NATIONAL LABORATORY
Oak Ridge, Tennessee 37831
operated by
MARTIN MARIETTA ENERGY SYSTEMS, INC.
for the
U.S. DEPARTMENT OF ENERGY
under Contract No. DE-AC05-84OR21400

MASTER

DISTRIBUTION OF THIS DOCUMENT IS UNLIMITED

LEGIBILITY NOTICE

A major purpose of the Technical Information Center is to provide the broadest dissemination possible of information contained in DOE's Research and Development Reports to business, industry, the academic community, and federal, state and local governments.

Although a small portion of this report is not reproducible, it is being made available to expedite the availability of information on the research discussed herein.

1

CONTENTS

LIST OF FIGURES

LIST OF TABLES

ABSTRACT

DAVIS, E. C., W. J. Boegly, Jr., E. R. Rothschild, B. P. Spalding, N. D. Vaughan, C. S. Haase, D. D. Huff, S. Y. Lee, E. C. Walls, J. D. Newbold, and E. D. Smith. 1984. Site characterization techniques used at a low-level waste shallow land burial field demonstration facility. ORNL/TM-9146. Oak Ridge National Laboratory, Oak Ridge, Tennessee. 170 pp.

The Environmental Sciences Division of the Oak Ridge National Laboratory has been investigating improved shallow land burial technology for application in the humid eastern United States. As part of this effort, a field demonstration facility (Engineered Test Facility, or ETF) has been established in Solid Waste Storage Area 6 for purposes of investigating the ability of two trench treatments (waste grouting prior to cover emplacement and waste isolation with trench liners) to prevent water-waste contact and thus minimize waste leaching. As part of the experimental plan, the ETF site has been characterized for purposes of constructing a hydrologic model. Site characterization is an extremely important component of the waste disposal site selection process; during these activities, potential problems, which might obviate the site from further consideration, may be found. This report describes the ETF site characterization program and identifies and, where appropriate, evaluates those tests that are of most value in model development. Specific areas covered include site geology (Sect. 4.1), soils (Sect. 4.2), and hydrology (Sect. 4.3). Each of these areas is further divided into numerous subsections, making it easy for the reader to examine a single area of interest. Site characterization is a multidisciplinary endeavor with voluminous data, only portions of which are presented and analyzed here. The information in this report is similar to that which will be required of a low-level waste site developer in preparing a license application for a potential site in the humid East, (a discussion of licensing requirements is beyond its scope). Only data relevant to hydrologic model development are included, anticipating that many of these same characterization methods will be used at future disposal sites with similar water-related problems.

1. EXECUTIVE SUMMARY

As part of Department of Energy (DOE) research and development (R&D) activities, the Oak Ridge National Laboratory (ORNL) has been investigating improved shallow land burial (SLB) technology for disposing of low-level waste (LLW) in humid environments. This technology includes improved disposal techniques such as grouting and lining of trenches, an evaluation of site characterization methodology, and the integration of site characterization data into site model development and application. A field-scale demonstration site, known as the Engineered Test Facility (ETF), has been established at ORNL to carry out these studies.

One of the major goals of the ETF is to evaluate various techniques that have been used to characterize the demonstration facility and that will likely be used to characterize large candidate sites in the eastern United States. Site characterization is an extremely important component of the site selection process; during these activities, potential problems, which might obviate the site from further consideration, may be identified. Further, information collected during site characterization will be used for licensing purposes to construct a hydrologic model of the site that can be used as a tool for making predictions about future site performance.

With the goal of obtaining enough information about the ETF site to construct a reliable hydrologic model, site characterization activities were initiated in 1981. This report summarizes the site characterization work completed to date and builds on previous work completed in 1982 (Vaughan et al. 1982). The three major categories of geology, soils, and hydrology were viewed as being the critical areas where information was needed, and each is treated in detail in Sects. 4.1, 4.2, and 4.3, respectively.

The ETF is located in Melton Valley, approximately 2 km south of ORNL. Geologically, it is within the Copper Creek thrust block and is underlain by strata of the Middle to Late Cambrian Conasauga Group. The specific formation is the Maryville Limestone, which consists of silty limestone interbedded with mudstones and shales. The structure of the formation is highly deformed with small-scale folding, several examples of which were exposed during trench excavation at the ETF. The formation is also heavily fractured, and flow through these fractures is believed to be quite significant during periods of heavy precipitation. Soil thickness, as measured from core samples and surface geophysical techniques, ranges from 2 to 7 m, being thinnest in the vicinity of experimental wells ETF-9, -1, and -2 (above a major limestone fold) and increasing in thickness to the northwest and southwest of the ETF experimental trenches.

Major emphasis in this report has been placed in shallow (<10 m) geological characterization, because this is the depth that will contain the LLW and in which groundwater movement and fluctuations are readily observed. Of perhaps equal importance is deeper geological site characterization, which is limited in this report to a description of geologic and geophysical logs of a deep well (ETF-16) located approximately 10 m northwest of the experimental trenches.

In addition to shallow geological characterization, radionuclide, chemical, and physical properties have been determined on core samples taken from a nearby site at depths of 5 to 35 m and

are included in the geological section (Sect. 4.1). These samples were taken from the Maryville Formation, identical to that portion of the Conasauga Group that underlies the ETF. A summary of important geologic characteristics of the ETF site is contained in Table 1.

The soil of the ETF site is described as being very shallow (A and B horizons), even taking into account the material removed during site clearing. The underlying C horizons were found to be highly leached (strongly acidic) and highly structured due to stratigraphic characteristics inherited from the bedrock. The soil's stratigraphic orientation was extremely variable in both dip and strike because of the folding and faulting. Root penetration was generally not noted below approximately 40 cm, presumably due to dense horizons and tight structure.

Measurement of distribution coefficients (Kd's) for seven radionuclides in soil samples collected from the ETF site indicates a range of 11.7 L/kg (^{125}I) to 64,100 L/kg (^{137}Cs). Extremely low

Table 1. Summary of Engineered Test Facility site characteristics

Oak Ridge, Tennessee[a]

Property	Unit	Value
Geology (see Sect. 4.1)[b]		
Radionuclide, chemical, and physical properties (mean of 23 samples, 5- to 35-m depth, Maryville Limestone)		
Kd, ^{85}Sr	L/kg	63.1
Kd, ^{134}Cs	L/kg	27,400
Kd, ^{58}Co	L/kg	2,720
Kd, ^{125}I	L/kg	9.4
Kd, ^{241}Am	L/kg	27,600
Kd, (Ca + Mg)	L/kg	56.0
Exchangeable Ca	meq/kg	113
Exchangeable Mg	meq/kg	19.1
Exchangeable Na	meq/kg	0.3
Exchangeable acidity	meq/kg	16.0
Cation exchange capacity	meq/kg	149
pH	$-\log[H^+]$	7.6
$CaCO_3$	%	17.1
Sand	%	76
Silt	%	13
Clay	%	11
Particle density	Mg/m^3	2.63
Soils (see Sect. 4.2)		
Radionuclide adsorption: mean Kd (0- to 2-m soil depth)		
^{241}Am	L/kg	5,670
^{85}Sr	L/kg	494
^{137}Cs	L/kg	64,100
^{60}Co	L/kg	782
^{125}I	L/kg	11.7
^{59}Fe	L/kg	46,800
^{51}Cr	L/kg	2,780

Table 1. (continued)

Property	Unit	Value
Chemical properties: mean (0- to 2-m soil depth)		
Exchangeable Ca	meq/kg	20
Exchangeable Mg	meq/kg	31
Exchangeable Na	meq/kg	1
Exchangeable K	meq/kg	3
Exchangeable acidity	meq/kg	154
Cation exchange capacity	meq/kg	210
Base saturation	%	26
Organic matter	%	0.37
$CaCO_3$	%	0
pH	$-\log[H^+]$	4.4
Water hardness	mM	0.12
Physical properties: (0- to 2-m depth)		
Bulk density	Mg/m^3	1.34
Total porosity	L/L	0.50
Sand	%	36
Silt	%	22
Clay	%	42
Clay mineralogy	Species	Illite > chlorite > vermiculite
Soil series		Montevallo
Soil classification	Family	Loamy-skeletal, mixed, thermic, shallow typic dystrochrept
Hydrology (see Sect. 4.3)		
Climatic factors		
Precipitation, mean annual at Oak Ridge	mm	1,388
Precipitation, mean annual at ORNL	mm	1,267
Precipitation, observed 1981	mm	1,022
Precipitation, observed 1982	mm	1,295
Surface water		
Peak discharge Flume I	L/s	57.8
Peak discharge Flume II	L/s	50.8
Low flow	L/s	0
Infiltration (saturated)		
Trench cover material	cm/s	13.3×10^{-5}
Undisturbed area	cm/s	1.56×10^{-5}
Groundwater		
Aquifer characteristics		
Transmissivity (T)	m^2/min	2.54×10^{-3}
Storage coefficient (S)		~0.01
Hydraulic conductivity	cm/s	6.31×10^{-5}
Effective aquifer thickness	m	67

Table 1. (continued)

Property	Unit	Value
Effective porosity		0.03
Water chemistry	Calcium/ bicarbonate	
Unsaturated zone		
Mean saturated hydraulic conductivity	cm/s	2.0×10^{-5}

[a]Location: Oak Ridge National Laboratory (ORNL) Solid Waste Storage Area 6; experimental trench area: 0.3 ha; Flume I drainage area: 0.65 ha; Flume II drainage area: 0.88 ha; monitoring wells: 44 (see Table 24).

[b]Formation: Maryville Limestone; lithology: silty limestone with interbedded mudstones and shales; strike: ~N50°E; dip: ~30°SE; structure: highly deformed by small-scale folding—heavily fractured.

Kd's ($\leq 10^{-1}$ L/kg) were not encountered for any soil samples, as might be the case with tritium. There was no observable pattern with depth for the Kd's of any of the radionuclides tested, nor were there any differences among the three profiles tested. Thus the best representation of these Kd values for unsaturated zone modeling purposes would be the averages and the standard deviations (Sect. 4.2). On a larger (30-m) depth scale extending into comparatively unweathered bedrock, there appeared to be some general decline in most radionuclide Kd's.

Cation exchange capacities averaged 210 meq/kg and were quite uniform in this characteristic. There appeared to be only a minor influence of vegetational nutrient cycling, as evidenced by the modest decline in exchangeable calcium with depth in each profile tested. A number of significant correlations were observed among the soil chemical properties. Of particular note are the correlations between exchangeable acidity and percent base saturation and pH ($r = 0.80$ and -0.72, respectively). This relationship is to be expected because the lower the soil pH, the more exchange sites that are occupied by acid cations (Al^{+3} and H^{+}) and, hence, the lower the percentage of these sites that are occupied by basic cations. Calcium dominated these exchangeable bases when the base saturation increased, which accounts for its high correlation ($r = 0.90$) with percent base saturation and its negative correlation with exchangeable acidity ($r = -0.73$). A summary of radionuclide, chemical, physical, and mineralogical properties for soils collected at the ETF site is contained in Table 1.

Hydrologic studies at the ETF site have focused on measurement of precipitation, surface runoff, and groundwater fluctuations (see Sect. 4.3). Precipitation for 1981 and 1982 at the ETF was 1022 and 1295 mm, respectively, 19% lower (1981) and 2% higher (1982) than the annual average for the ORNL site (1267 mm). Runoff in two drainage channels resulting from precipitation events is summarized in Appendix D, which shows that the maximum flow was observed on May 30, 1981 (57.8 L/s for Flume I and 50.8 L/s for Flume II). Mean peak discharge for the 30-month period of record was calculated as 10.5 L/s for Flume I ($n = 60$) and 10.0 L/s for Flume II ($n = 121$). These peak runoff values are being correlated with precipitation data so that expected maximum flows can be assigned for various amounts or classifications of precipitation. Because runoff during periods of no precipitation is insignificant when compared to that occur-

ring during storm activity, major effort has been on characterizing and measuring flow during storm events.

Water-table fluctuations have been measured for a period of 2 years and indicate that the yearly cycle is approximately 1 m, exhibiting a maximum in the winter and a minimum in the late summer. Response of water levels to rainfall events is rapid, usually on the order of 5–10 h, and water levels require several days to return to prestorm conditions. Deeper wells (30–70 m) located on site respond much less dramatically than the shallower wells (10 m deep) and appear to exhibit a <1-m annual fluctuation. Aquifer characteristics have been determined through a combination of tracer tests, pump tests, and in situ measurements of hydraulic conductivity (Table 1).

Tracer tests have been interpreted as showing rapid (60–65 d to peak concentration) movement of tracer along strike, between injection well ETF-1 and monitoring well ETF-3. The calculated value of a linear velocity is 0.17 m/d, based on the arrival time of the peak concentration of tracer. Values of hydraulic conductivity have been measured in each of the wells located at the ETF and appear to be spatially related to the fault structure found during trench construction. Mean hydraulic conductivity, based on these individual wells slug tests, is 6.31×10^{-5} cm/s. Pump test data have been evaluated using a curve-matching technique based on the Theis equation. From this analysis, an aquifer transmissivity of 2.54×10^{-3} m^2/min and a storage coefficient of 0.01 were calculated for the formation at the ETF site (Table 1).

In summary, the ETF site characterization activities have been under way for 2 years, with the goal of obtaining enough site-specific data to allow for hydrologic modeling. Constructing a reliable site model is one requirement for obtaining a license to construct and operate an SLB facility. However, no specific information is available to guide one in the modeling process. Work conducted at the ETF has focused on evaluating site characterization techniques relevant to hydroiogic modeling, anticipating that many of these same methods will be used for characterizing future disposal sites with similar water-related problems.

2. INTRODUCTION

Shallow land burial of industrial and municipal solid wastes has been the most common disposal practice in the United States (Wilson 1977). The principal reasons for this have been that land for disposal has been easy to obtain and the methods used are relatively inexpensive. Even though SLB is a common practice, it has not proved to be the ideal solution for solid waste disposal. Love Canal, and other instances where ground and surface water pollution have resulted from industrial waste disposal operations, has increased public awareness of the hazards inherent in improper land disposal. Passage of the Resource Conservation and Recovery Act (RCRA) of 1976 has dramatically changed the procedures required to obtain permission to operate a land disposal facility (U.S. Congress 1976). Careful consideration of site selection, characterization, and design is now incorporated in the RCRA disposal regulations [U.S. Environmental Protection Agency (EPA 1982)].

Like other industrial wastes, essentially all LLW produced in the United States has been disposed using SLB practices. Some of these LLW sites have provided less than ideal geological/hydrological site conditions and, as a result, have led to localized groundwater contamination outside of the burial trench boundaries. In addition, most sites in humid regions have experienced problems with trench cover subsidence. Although these occurrences have not resulted in significant off-site movement of radioactivity or exposure of the general public, their presence raises concern with the long-term performance of SLB facilities. As a result, DOE and the U.S. Nuclear Regulatory Commission (NRC) have initiated R&D activities for improved methods of waste disposal, including waste classification, site selection, site characterization, design, operation, and closure-postclosure maintenance operations for such facilities. In addition, both DOE and NRC have prepared regulations for commercial (NRC) and defense (DOE) facilities that include guidance concerning site selection, design, operation, and closure-postclosure of such facilities (DOE 1983, NRC 1982).

As part of DOE R&D activities, ORNL has designed and constructed an experimental facility (ETF) to investigate and demonstrate the application of improved engineering practices to the design of land disposal facilities in geographic areas where precipitation equals or exceeds the evapotranspiration (Boegly and Davis 1983). Although many of the precipitation-related problems encountered could be avoided by locating SLB facilities in arid areas, the presence of a large portion of the nuclear-waste-generating facilities in humid areas (eastern United States) and the high costs and legal constraints associated with shipping wastes across country indicate that disposal facilities are required in these climates. Thus the experimental work associated with the ETF focuses on anticipated waste leaching and contaminant transport problems associated with disposal in humid climates. Though the work is specific to the ORNL site, results are applicable to other humid sites experiencing similar water-related problems.

Four major objectives were considered in designing the ETF (Table 2). The first was to experimentally verify improvements in SLB procedures that minimize, through the application of a grout or a liner, the potential for contact between the buried waste and water. Other objectives included

Table 2. Objectives of the Engineered Test Facility

1.	Evaluation of cement-based grouting and liners as trench treatments to reduce infiltration
2.	Evaluation of certain site characterization techniques needed to model the site
3.	Integrating site characterization data with model development
4.	Construction and validation of a model describing site performance

assessment of site characterization techniques as they relate to understanding the ETF site, construction of a site model using measured site characteristics determined in Objective 2, and verification of the model by comparison to site performance data. Although not considered a major objective, an evaluation is being made of the effects of grouting and lining on subsidence of trench covers. As proposed, the ETF does not address the verification of DOE or NRC site selection criteria or the prevention of plant or animal intrusion.

The purpose of this report is to present, discuss, and where appropriate evaluate the site characterization information collected as a part of Objective 2. The nature of this information collection activity was directed at the need to understand and model the site in order to evaluate the performance of two trench treatments (Objective 1) and was not an effort to determine if the site were suitable for long-term storage of radioactive wastes using conventional disposal techniques. Much of the information reported can be used in site selection characterization; however, considerably more information would be required to meet present licensing requirements.

This report is one in a series of reports (Vaughan et al. 1982; Davis, Spalding, and Vaughan 1982; and Boegly and Davis 1983) and focuses on the data needs for characterizing the ETF site, how these needs were met, and the methods deemed best for obtaining this information. Although experimental determination of necessary modeling parameters (e.g., rainfall, hydraulic conductivity, and aquifer characteristics) is somewhat investigator dependent, this report attempts to evaluate the procedures available for determining the parameters of interest and suggests methods that are most desirable on the basis of time, cost, and accuracy.

3. SITE DESCRIPTION

The Oak Ridge Reservation (about 23,900 ha) is located in a broad valley between the Cumberland Mountains, which lie to the northwest, and the Great Smoky Mountains, which lie to the southeast. The reservation is located about 40 km west of Knoxville, Tennessee, and about 241 km east of Nashville, Tennessee. (See Fig. 1 for its location relative to surrounding communities.)

Prevailing winds in the area are usually either up-valley, from west to southwest, or down-valley, from east to northeast. Daytime winds are usually southwesterly; nighttime winds, usually northeasterly. Wind velocities are somewhat decreased by the mountains, and tornadoes rarely occur in the valley. The coldest month is normally January, but differences between the mean temperatures of the three winter months of December, January, and February are comparatively small. July is usually the hottest month, but again differences in mean temperatures for June, July, and August are small. The average daily temperature range is about 12°C, with the greatest average range in spring and fall and the smallest in winter.

Precipitation is more than adequate for agriculture and is normally well distributed through the year. Winter and early spring are the seasons of heaviest precipitation, with the monthly maximum normally occurring January to March. A secondary maximum occurs in the month of July, because of afternoon and evening thundershowers. September and October are usually the driest months. Periods of five consecutive days without measurable precipitation occur about four or five times per year, but rarely are there ten consecutive days without measurable precipitation. Light snow usually occurs in all of the months from November through March, but the total monthly snowfall is often only a trace [U.S. Department of Commerce (DOC) 1981].

ORNL is located in the southwest portion of the reservation (Fig. 1) and has been in operation since 1942. Low-level radioactive solid wastes have been disposed of at ORNL since its inception; to date six burial grounds (presently termed Solid Waste Storage Areas, or SWSAs) have been used for this purpose (Sease et al. 1982). The first three locations were chosen mainly due to proximity to the waste sources, whereas the last three were located following recommendations of geologic and hydrologic studies (Boyle et al. 1982). To date about 170,000 m^3 of LLW has been buried in ORNL solid waste storage areas (Gilbert/Commonwealth 1980).

During the early planning stages of the ETF, a listing of five criteria for selection of the proposed demonstration site was formulated. These were: (1) the site should be close to or a part of an existing burial ground, (2) the site should be near ORNL, (3) the site should be capable of handling LLW, (4) the site must not be strongly influenced by nearby operations, and (5) the site should be representative of conditions anticipated in burial operations in humid climates. As a result of these criteria, a 0.3-ha site was selected and reserved in 1980.

The ETF site is located within a portion of ORNL's SWSA 6, an area of the reservation that has been, and is currently being, used for LLW disposal operations (Figs. 2 and 3). Although geologic and hydrologic investigations were not undertaken prior to selecting the site, it does meet all

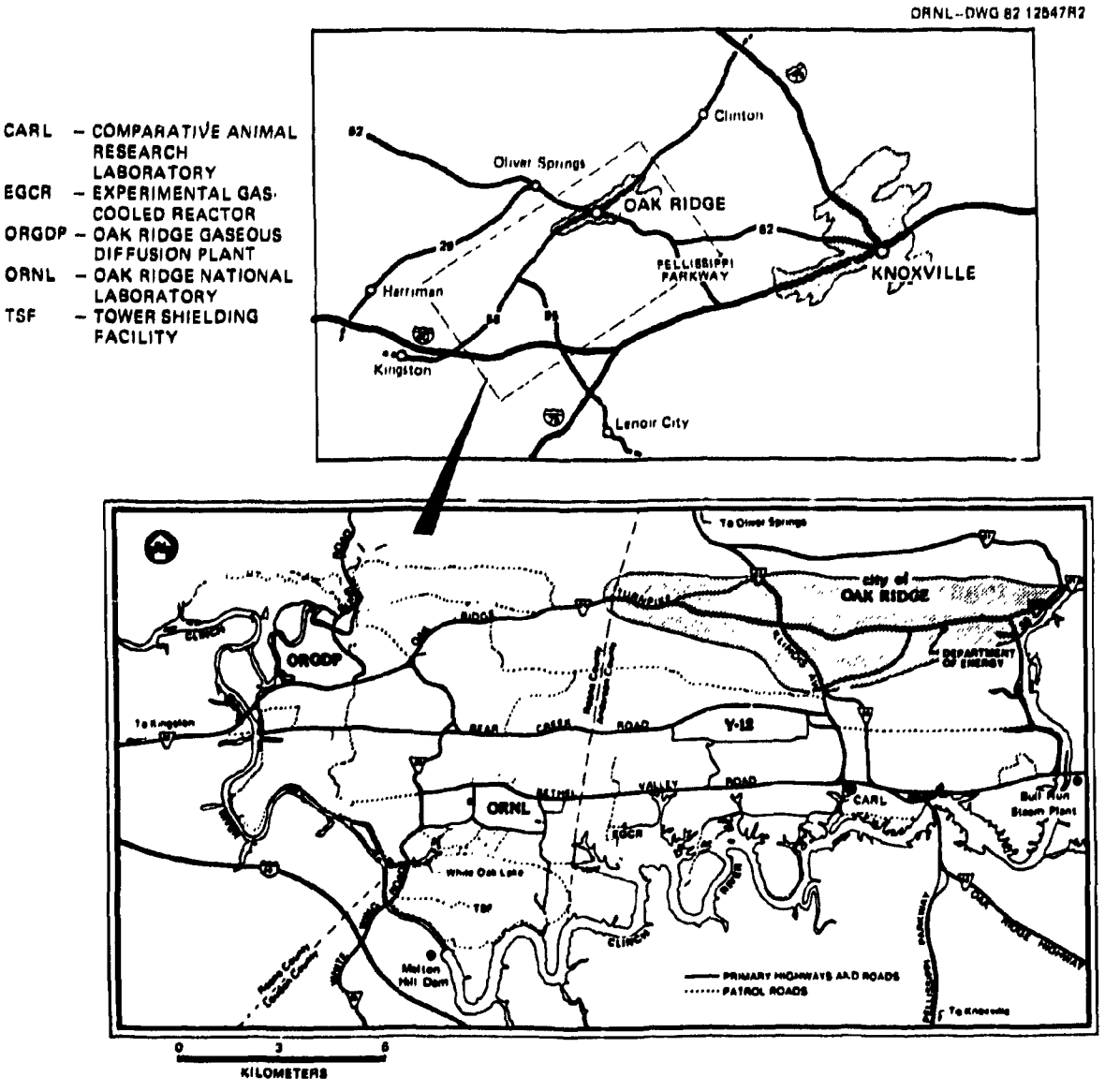

Fig. 1. Map showing location of Oak Ridge National Laboratory on the Oak Ridge Reservation and the relationship to surrounding communities.

five of the criteria specified above. Previous studies of ORNL burial operations (Appendix A) in this area have provided considerable background information on the meteorologic, geologic, and hydrologic properties of SWSA 6; however, detailed information on the specific area in which the ETF is located did not exist. Thus site characterization of the ETF has received a great deal of attention.

The ETF is located on a small hillock characteristic of SWSA 6. Surface topography is such that one portion of the rainfall drains southeasterly and another southwesterly, into two small drainage channels that eventually form small creeks and drain southward into White Oak Lake (Fig. 3). Much of SWSA 6 has been cleared of trees and, after trench construction, planted in grass to minimize surface erosion. A group of LLW trenches are located on the hillock immediately

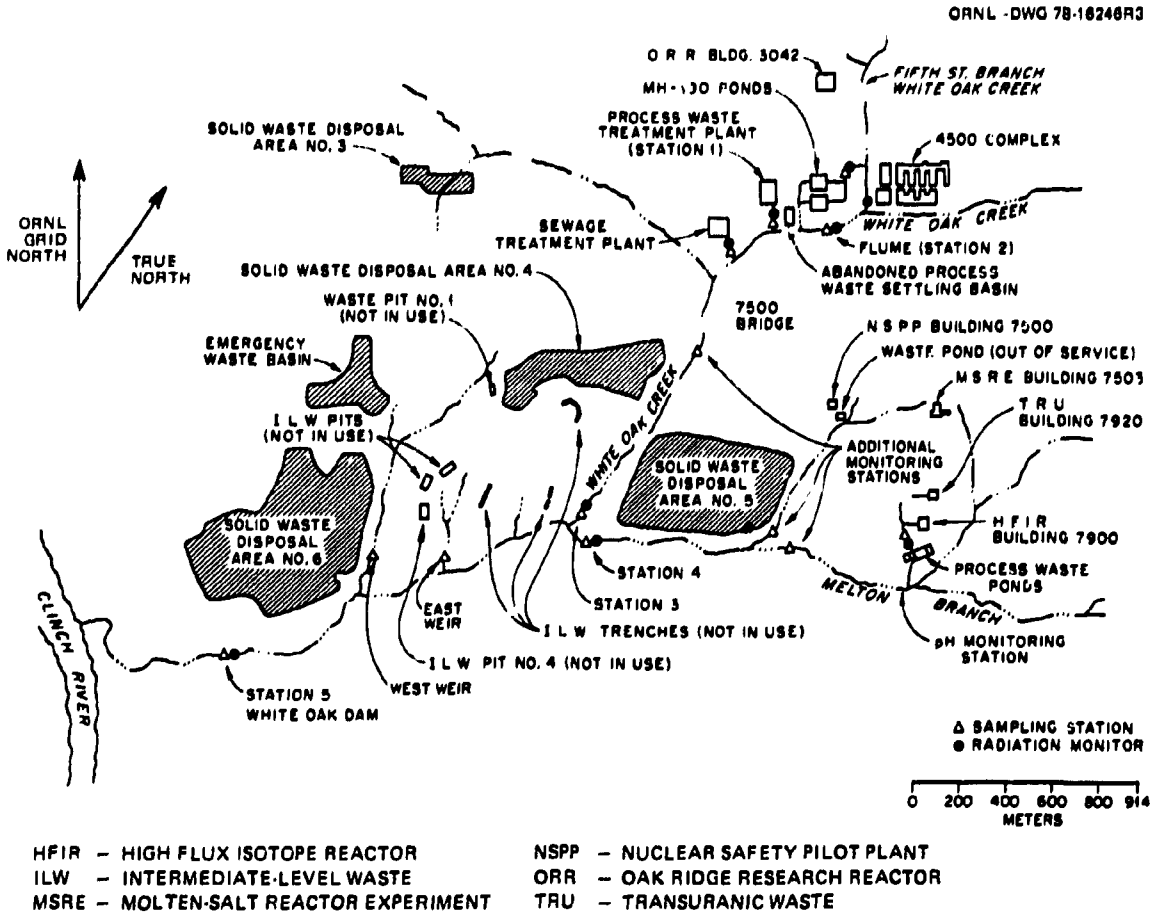

Fig. 2. Location of Solid Waste Storage Areas at Oak Ridge National Laboratory.

to the east of the ETF and share the eastern drainage channel. No burial activity is presently taking place to the north, west, or south of the site. At current production rates, SWSA 6 is estimated to have enough capacity to receive LLW for the next 6–8 years (until 1990–1992) (Sease et al. 1982).

At present, nine experimental trenches located at the ETF have been designed, constructed, treated according to the experimental plan, and closed by application and compaction of a soil cover (Davis, Spalding, and Vaughan 1982). Several previously existing wells and a total of 52 monitoring wells have been located on site as part of the groundwater monitoring program. In addition, two surface-water monitoring stations, a shed housing a data logging device for the groundwater fluctuation monitoring program, and a continuous-recording rain gauge have been located on site. Figure 4 presents a plan view of the site illustrating the surface topography and location of experimental trenches, wells, and other monitoring stations established at the ETF.

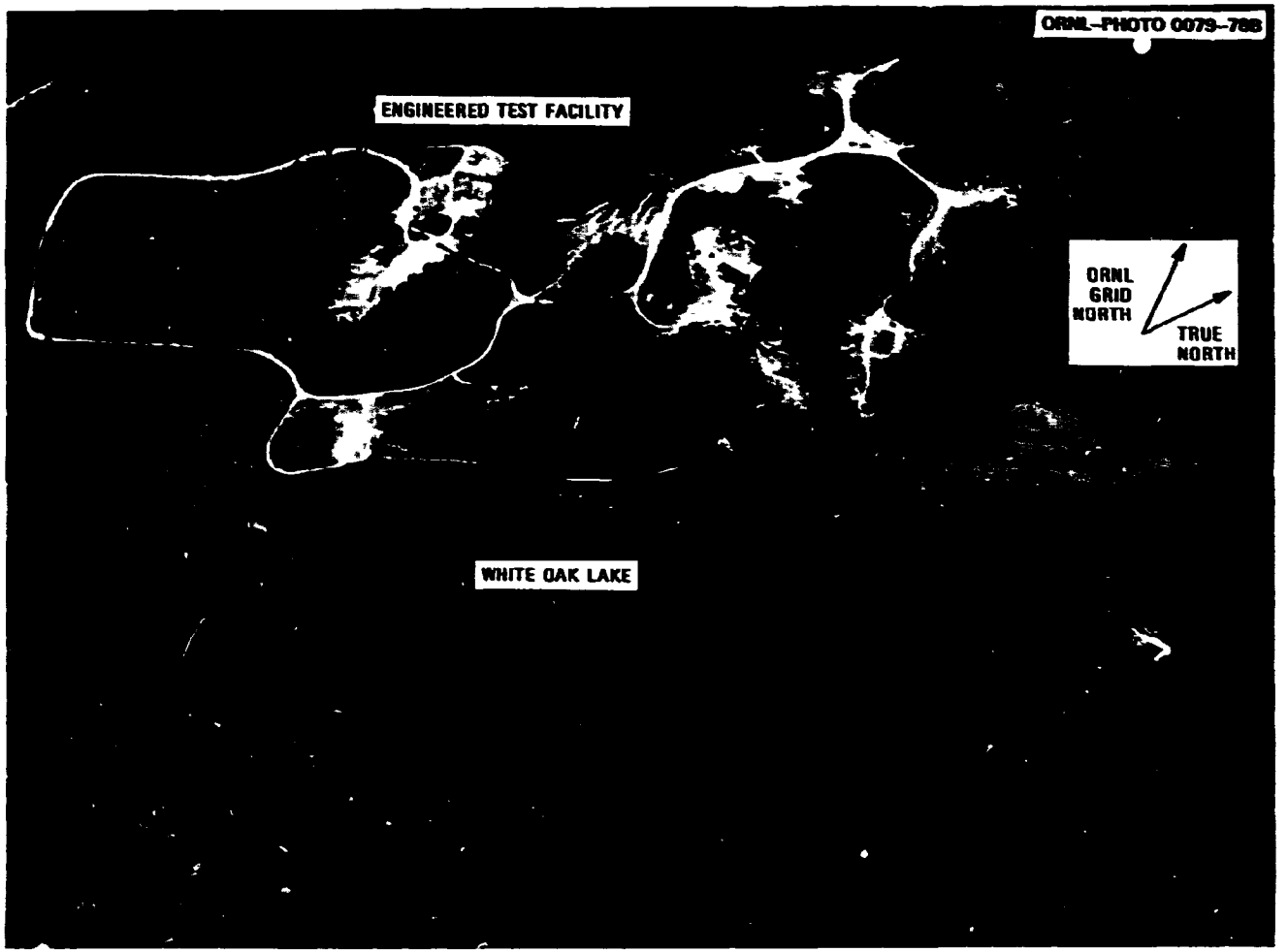

Fig. 3. Aerial view of Solid Waste Storage Area 6 showing approximate location of the Engineered Test Facility.

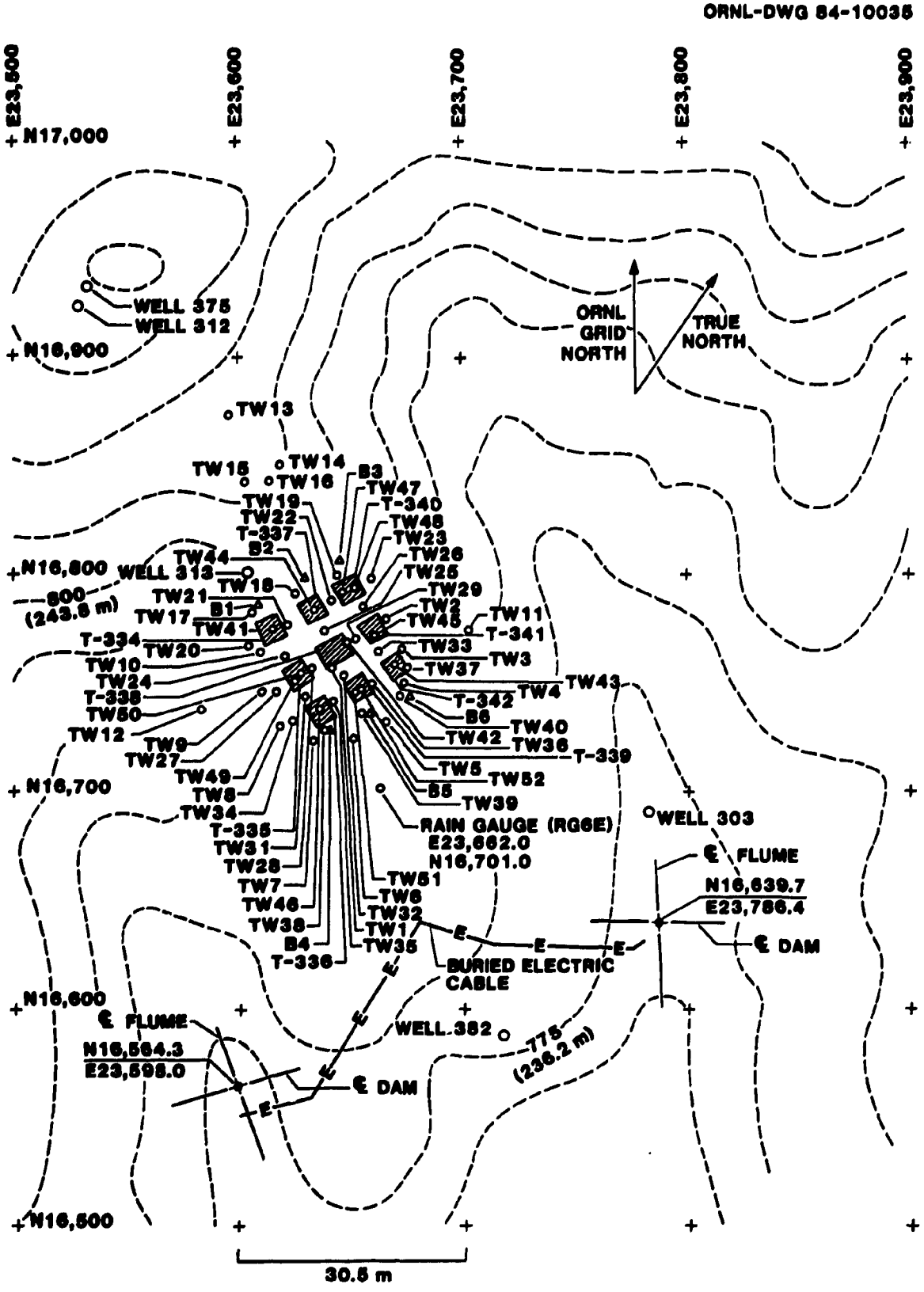

Fig. 4. Plan view of the Engineered Test Facility showing experimental trenches, monitoring wells, and surface water monitoring stations.

4. SITE CHARACTERIZATION

One of the primary objectives of the ETF is to evaluate the effectiveness of improved SLB practices (trench lining and grouting) for application at disposal sites located in humid climates. To do this requires a site characterization program that establishes background conditions and supplies the necessary data for construction and validation of a site hydrologic model. Site characterization activities at the ETF have concentrated on a study of those areas important to model development. These include an investigation of both near-surface and bedrock geology, soils, climatic factors, and surface and groundwater hydrology. The information included in this characterization study is no different from what might be required to license an LLW site; however, certain (e.g., ecological and socioeconomic) areas not of interest to site hydrologic modeling have been omitted. Thus the reader should be aware that this report is not representative of site characterization activities for purposes of licensing but, rather, for purposes of model development and application.

4.1 GEOLOGY

4.1.1 Regional Geology

The DOE Oak Ridge Reservation lies in the Valley and Ridge Province of East Tennessee (Fenneman 1938) (Fig. 5). At this locality, the Valley and Ridge Province is 30 to 40 km wide and is characterized by alternating, elongate, northeast-trending, parallel ridges and valleys. Maximum topographic relief in the area is about 187 m (McMaster 1963). Differential erosion of the northeast-striking Paleozoic strata has influenced the topography and is largely responsible for the development of parallel ridges and valleys. Structural strike of the strata varies from N45° E to N60° E; and the structural dip, which is toward the southeast, varies between 20° and 40° (Stockdale 1951). The overall character and alignment of the Valley and Ridge Province topography are controlled by the geometry of major thrust faults that developed during the Appalachian orogeny, about 250 million years ago. Although minor earthquakes do occur in the area, unrelated to the Paleozoic mountain building, the region is generally seismically inactive (Bolinger 1975).

The area of interest to this report is geographically located in Melton Valley, approximately 2 km south of ORNL, within the DOE Oak Ridge Reservation. Geologically, the study area is within the Copper Creek thrust block (Fig. 6, area C) and is underlain by strata of the Middle to Late Cambrian Conasauga Group. The regional stratigraphic and lithologic variations within the Conasauga Group are discussed in Hasson and Haase [submitted to American Association of Petroleum Geologists (AAPG) 1983].

The Conasauga Group was deposited as part of a major marine transgression over a subsiding carbonate-rimmed tidal flat that extended from the craton eastward to the shelf margin (Hasson and Haase submitted to AAPG 1983). The Conasauga Group in the study area is approximately 550 m thick. Structural features of the Conasauga are related to fault motion along the Copper Creek Fault, a regionally significant, low-angle thrust fault, striking N50–60° E and dipping to

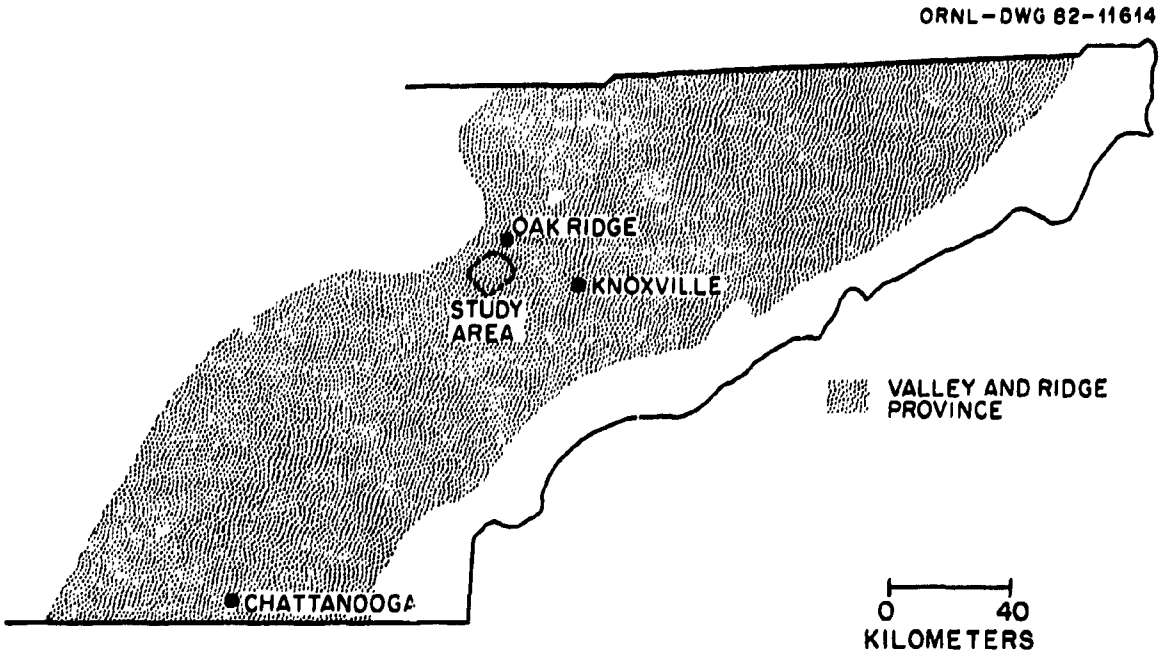

Fig. 5. Study area within the Valley and Ridge Province.

the southeast, which is a result of a regional deformation event that took place about 250 million years ago and created the valley and ridge topography typical of East Tennessee. Thrust fault motion developed much internal deformation throughout the Conasauga Group. Typical features observed are numerous secondary low-amplitude isoclinal folds, secondary bedding plane thrust faults, reverse high-angle faults, and joint sets (Sledz and Huff 1981). The Conasauga Group is lithologically very heterogeneous, consisting basically of alternating siltstones, silty limestones, limey shales, and mudstones. It consists of six formations in the Oak Ridge vicinity (Haase and Vaughan 1981), which are, in ascending order, Pumpkin Valley Shale, Rutledge Limestone, Rogersville Shale, Maryville Limestone, Nolichucky Shale, and Maynardville Limestone (Fig. 7). The relatively erosion-resistant limestone-rich formations tend to form hillocks along their outcrop extent. The ETF site is underlain by such a limestone-rich formation, the Maryville, and is located on one of the characteristic hillocks. At the Oak Ridge locality, the Maryville is typically composed of ribbon-bedded and interclastic limestones and dark gray shales and mudstones (Haase and Vaughan 1981). Isopach and lithofacies maps for the Maryville Formation are shown in Fig. 8.

4.1.2 Site-Specific Geology

4.1.2.1 Lithology

Examination of rock cores taken during drilling of wells ETF-1, -3, -4, -5, -6, -11, -12, and -16 (for a location of cores see Fig. 4) indicates that the Maryville is a gray to gray-black massive- to medium-bedded silty interclastic limestone and ribbon-bedded silty limestone interbedded with a thin-bedded mudstone/shale. The limestone ranges from a silty lime mud (or micrite) to a fine-grained crystalline material (or microspar). The interclastic lithology has micritic clasts with microspar matrices and is locally oolitic. The shale and mudstone are calcareous and locally very

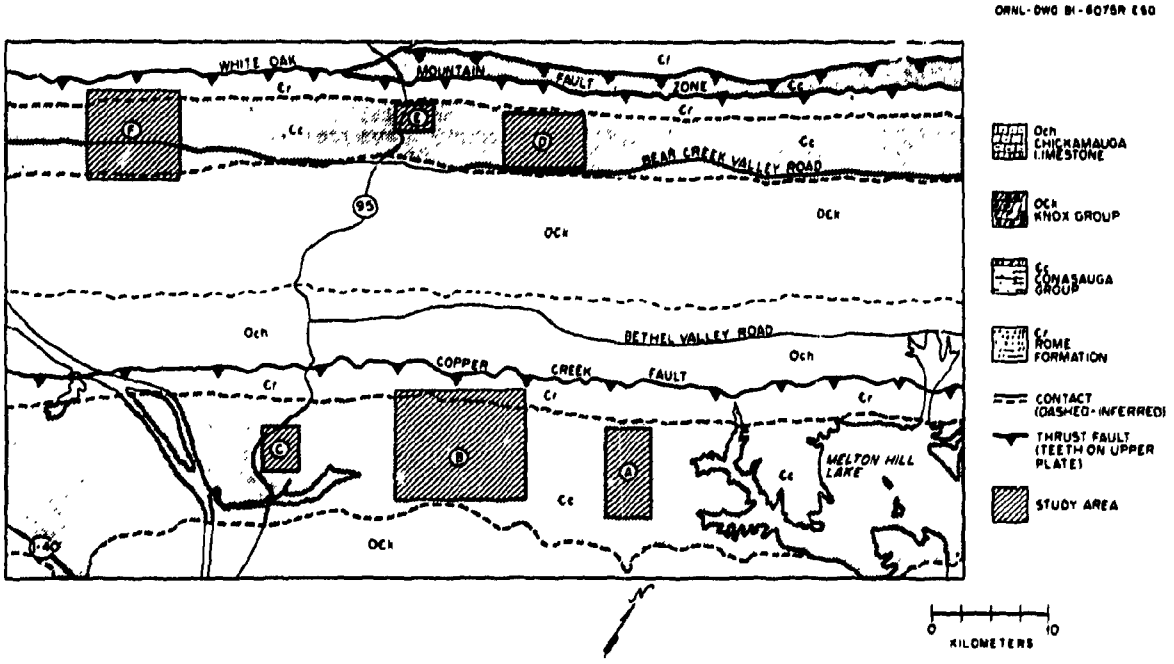

Fig. 6. Geologic map of a portion of the Oak Ridge Reservation. The Engineered Test Facility site is in area C. The symbols adjacent to formation names are indicative of lithology: the Chickamauga is generally a silty limestone; the Knox, a sandy dolomite; the Conasauga, a calcareous shale; and the Rome, a silty sandstone. *Source*: W. M. McMaster, *Geologic Map of the Oak Ridge Reservation* (geologic), ORNL/TM-713, Union Carbide Corp. Nuclear Div., Oak Ridge Natl. Lab. (1963).

rich in detrital muscovite, which is oriented parallel to bedding planes. Bedding geometry in the shale ranges from a parallel- to a wavy-bedded pattern. Locally, discontinuous lenticular-bedded stratification is also present.

The longest core (76 m) taken at the ETF site was from well ETF-16. The geologic log is shown in Fig. 9. Figures 10 and 11 show two geophysical logs for well ETF-16. The natural gamma log indicates the lithologic variation within the Maryville Formation. A high gamma response indicates zones that have more natural radioactivity than surrounding rock. These zones are usually associated with shales as compared to limestones (due to ^{40}K content). The neutron attenuation log responds to the attenuation of emitted neutrons by the surrounding rock. Low backscatter usually indicates the presence of water (thus porosity) within a given zone. The log taken at well ETF-16 indicates a general decrease in porosity with depth. Geologic logs for other cores taken at the ETF site can be found in Appendix B.

All of the cores exhibit numerous joints and fractures, some of which are filled. Fracture-filling material varies from white to pink, fine to coarse, crystalline calcite. The calcite may be accompanied by dolomite, pyrite, marcasite, bladed gypsum, or other minerals. Small-scale (<0.25-m) solution cavities are also observed in cores. The solution cavities have local coatings of iron oxides, gypsum, and carbonates. Further information on fracture width, distribution, and wall chemistry in the near-surface Conasauga close to ORNL can be found in Sledz and Huff (1981) and Krumhansl (1979).

Selected core samples were studied by X-ray diffraction techniques to determine their clay mineralogy. A total of eight samples was collected at depths of 6.6 m, 7.3 m, 7.6 m, 8.1 m,

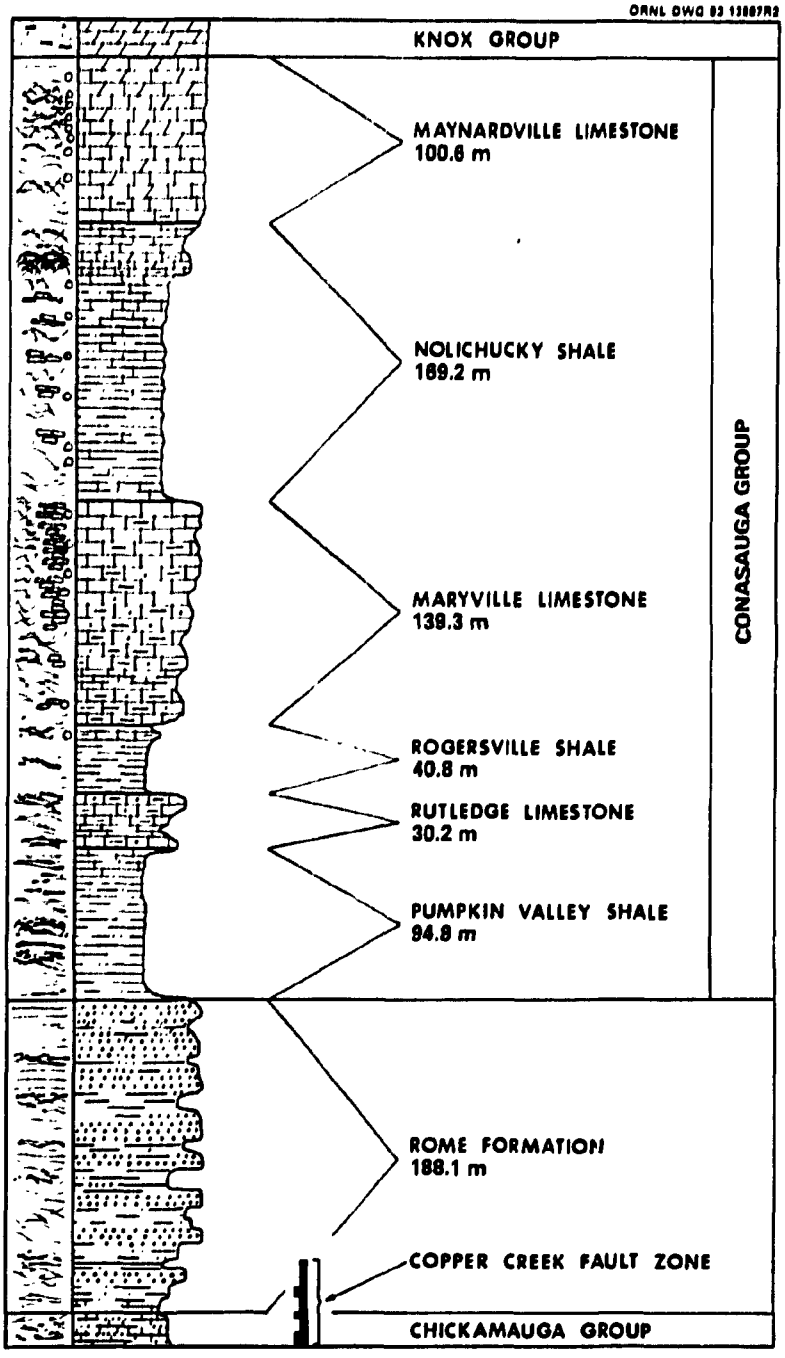

Fig. 7. Stratigraphic column for the Conasauga Group in the Oak Ridge, Tennessee, vicinity. See Appendix B for a description of lithologic symbols. *Source*: C. S. Haase, *Subsurface Geologic Data for the Conasauga Group on the USDOE Reservation*, ORNL/TM-9158, to be published at Oak Ridge National Laboratory.

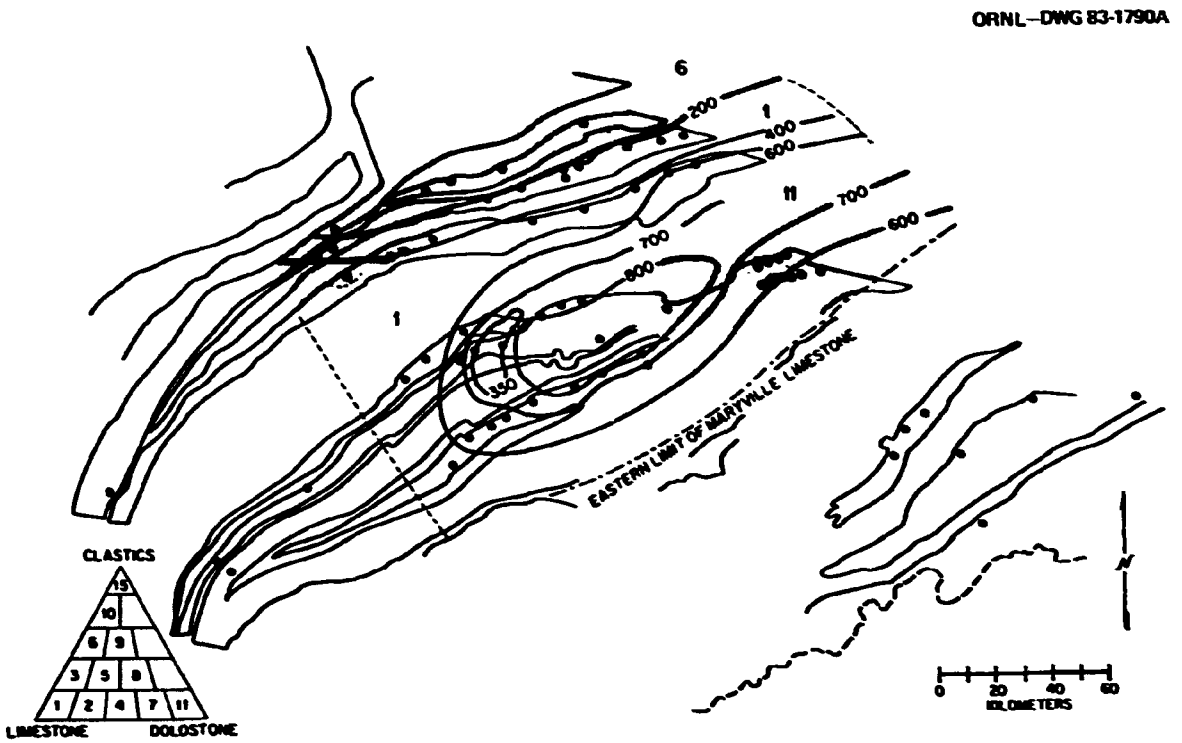

Fig. 8. Isopach and lithofacies map for the Maryville Formation. Dots indicate data points, and dashed lines the limit of interpretation. Heavy solid lines are isopach contours in feet; light solid lines indicate thrust fault traces. The heavy dashed line is the Tennessee–North Carolina border. The lithofacies triangle is broken into 20% intervals.

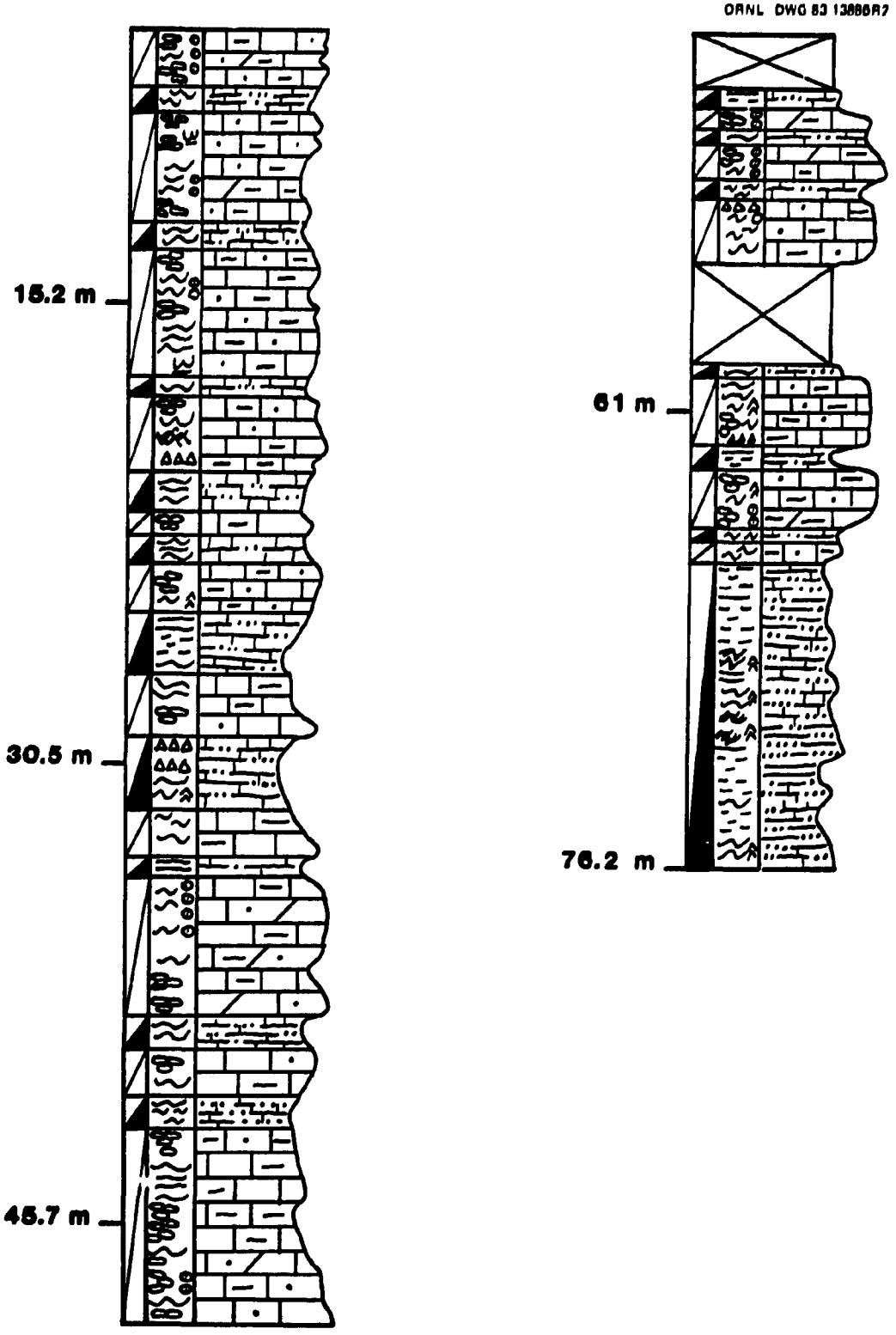

Fig. 9. Geologic log for well ETF-16. See Appendix B for a description of lithologic symbols.

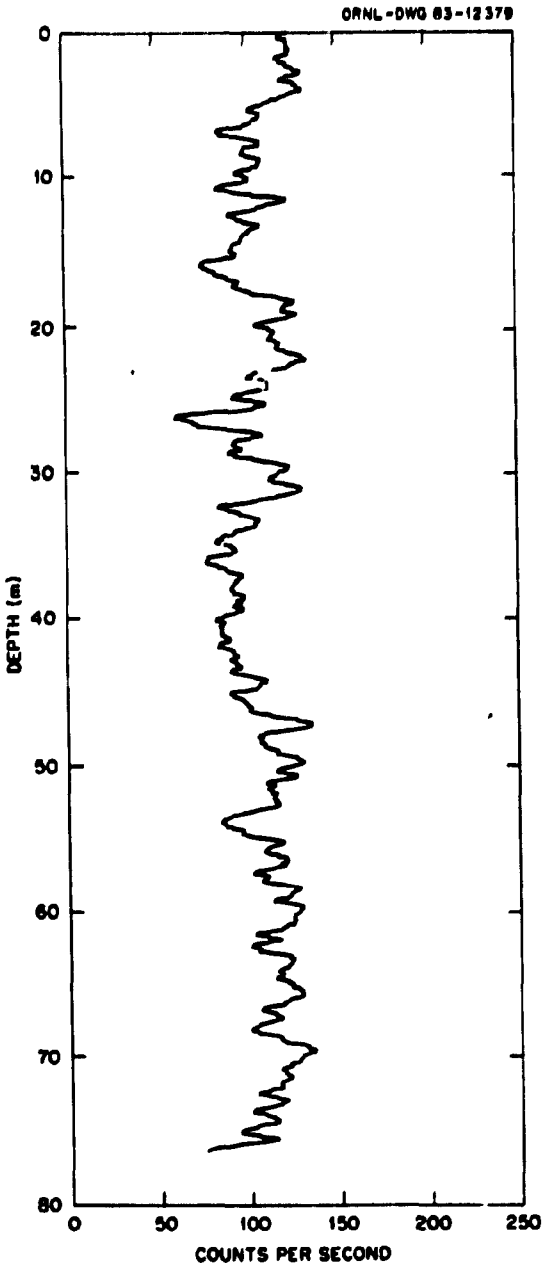

Fig. 10. Natural gamma-ray log for well ETF-16.

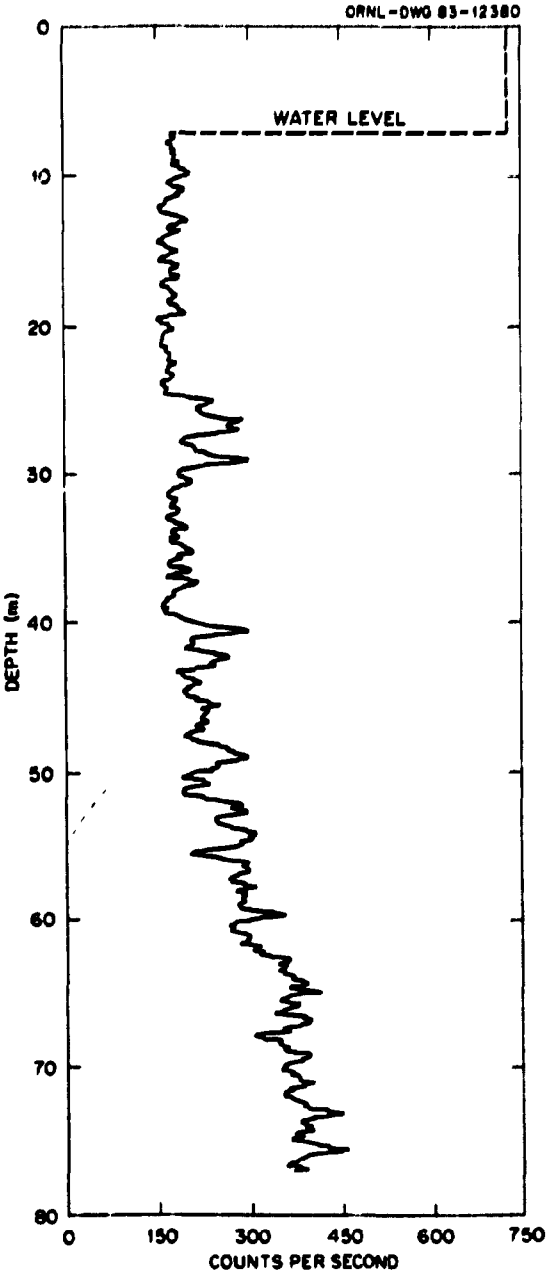

Fig. 11. Neutron attenuation log for well ETF-16.

8.4 m, and 8.8 m from wells ETF-1, -3, -11, and -12. The samples were disaggregated by crushing using a mortar and pestle, grinding for a short time in a ball mill, and subsequently dissolving the carbonate constituent with a (pH 5) sodium acetate–acetic acid solution (approximately 1 *N*). Both whole-rock- and size-fractionated X-ray diffraction analyses were carried out following the standard procedures of Jackson (1974). Size fractions studied were 45 to 2 μm (silts), 2 to 0.2 μm (coarse clay), and <0.2 μm (fine clay). Air-dried, glycolated, and potassium- and magnesium-saturated preferred orientation (to the 001 crystallographic direction of the minerals) specimens

were prepared and X-ray diffractograms obtained for the 2- to 0.2- and <0.2-μm fractions for each sample. X-ray diffraction data indicated that chlorite, illite, and mixed layer illite/vermiculite were the major clay mineral constituents (Table 3). Locally, smectite and mixed-layer illite/smectite are minor trace constituents; however, kaolinite is absent. Much of the illite is probably detrital and, along with plagioclase feldspar and quartz, makes up the major constitutent of the 45- to 2-μm-size fraction. Whole-rock, random powder orientation X-ray analyses indicate the presence of either calcite or dolomite or both, in addition to the above-mentioned clays, plagioclase and (locally) potassium feldspars, and quartz. Mineralogically, the patterns were similar, suggesting a reasonable level of homogeneity in the sequence for the site.

Table 3. Clay mineralogy for rock samples from wells ETF-1, -3, -11, and -12

In order of abundance

Depth (m)	Size fraction (μm)	Clay mineralogy
ETF-1, 6.6	<0.2	Illite, chlorite, illite/smectite[a]
	2–0.2	Illite, chlorite
	45–2	Chlorite, illite
ETF-1, 8.8	<0.2	No sample
	2–0.2	Chlorite, illite
	45–2	Illite, chlorite, illite/smectite
ETF-3, 7.3	<0.2	Illite, chlorite
	2–0.2	Illite, chlorite
	45–2	Chlorite, illite, illite/smectite (vermiculite)
ETF-3, 8.1	<0.2	Illite, chlorite
	2–0.2	Illite, chlorite
	45–2	Chlorite, illite
ETF-3, 8.4	<0.2	Illite, chlorite
	2–0.2	Illite, chlorite, smectite
	45–2	Chlorite, illite/vermiculite or smectite
ETF-3, 8.8	<0.2	Illite, chlorite
	2–0.2	Illite, chlorite, vermiculite
	42–2	Chlorite, illite, vermiculite (?)[b]
ETF-11, 8.8	<0.2	Illite, chlorite
	2–0.2	Illite, chlorite, smectite (?)
	45–2	Chlorite, illite
ETF-12, 7.6	<0.2	Illite, chlorite
	2–0.2	Illite, chlorite
	45–2	Illite, chlorite

[a] / = Interstratified association.
[b] (?) = Trace amount, tentative identification.

4.1.2.2 Structure

The structure of the Maryville Limestone at the ETF site has been strongly influenced by deformation along the Copper Creek Fault (Fig. 6). Deformational structures such as folds, faults, and joints are superimposed on depositional features such as the interclastic breccias and various styles of bedding that vary from lenticular to cross-bedded and wavy to evenly bedded planar (see geologic logs in Appendix B). Two major joint/fracture orientations can be found in the Conasauga and are near the ETF site (Siedz and Huff 1981). The first is a high-angle joint set that is generally found to strike perpendicular to geologic strike. The second type of movement is along bedding planes where slickensides, polishing, and offset can be found, indicating displacement. Locally, fracture distribution and orientation are controlled by structural deformities such as folds and small-scale thrusting. The size of fractures, some of which have been chemically widened to form solution cavities, ranges up to 15 cm; however, most fractures are from 1 to 15 mm in width, and the majority are from 1 to 3 mm.

The dip of bedding planes, as measured with respect to the side of the core, is highly variable over small lateral or vertical distances. It ranges from 30° to vertical, depending on the nature of the structures that have been intercepted by the bore hole.

The Conasauga Group weathers to a saprolite in which structural features and lithologic variations are still distinct but the rock is chemically altered. Most carbonate cement is leached out, but purer limestone beds are still intact. Because of chemical alteration and leaching, fractures tend to be widened, and the rock is structurally less competent. The extent of weathering is usually recognizable by color (saprolite is usually brown or tan as opposed to gray), by poor core recovery, or by auger refusal.

Surface geophysical techniques suggested the presence of two discontinuities that were interpreted to be fold structures. When the experimental trenches were excavated in June 1981, the presence of two anticlinal folds was revealed. Bedrock structures are well preserved in the weathered zone of the Conasauga, so it was possible to locate the folds and to measure bed orientation on the saprolite exposures in the trenches. Portions of the two fold areas that were revealed in the trenches are shown in Fig. 12.

One fold is a tight anticlinal fold in both saprolite and bedrock, plunging to the northeast (southern fold axis in Figs. 12 and 13). The northern limb of the anticline dips to the northwest at between 44° and 52°, while the other limb dips between 47° and 70° to the southeast. The core of the fold is highly deformed, presumably as a result of the shale layers yielding plastically and the limestone layers yielding in a brittle manner (Fig. 13). Fractures are concentrated in the anticlinal core but are also evident on the limbs.

A second anticlinal fold occurs as shown in Fig. 12. Its northern limb dips to the northeast at between 32° and 57°, while the southern limb dips southeast at between 28° and 56°. This fold, however, is entirely within the weathered portion of the bedrock.

4.1.2.3 Chemical properties

The chemical and radionuclide adsorption properties of the saprolite-bedrock continuum were characterized using samples of cuttings collected during the drilling of a 35-m-deep borehole in a nearby area of Melton Valley. This borehole was located approximately 3 km northeast of the ETF site but at approximately the same stratigraphic position within the Maryville Limestone (Fig. 7) of the Conasauga Group. Samples were collected every 1.5 m, sieved to <2 mm, and

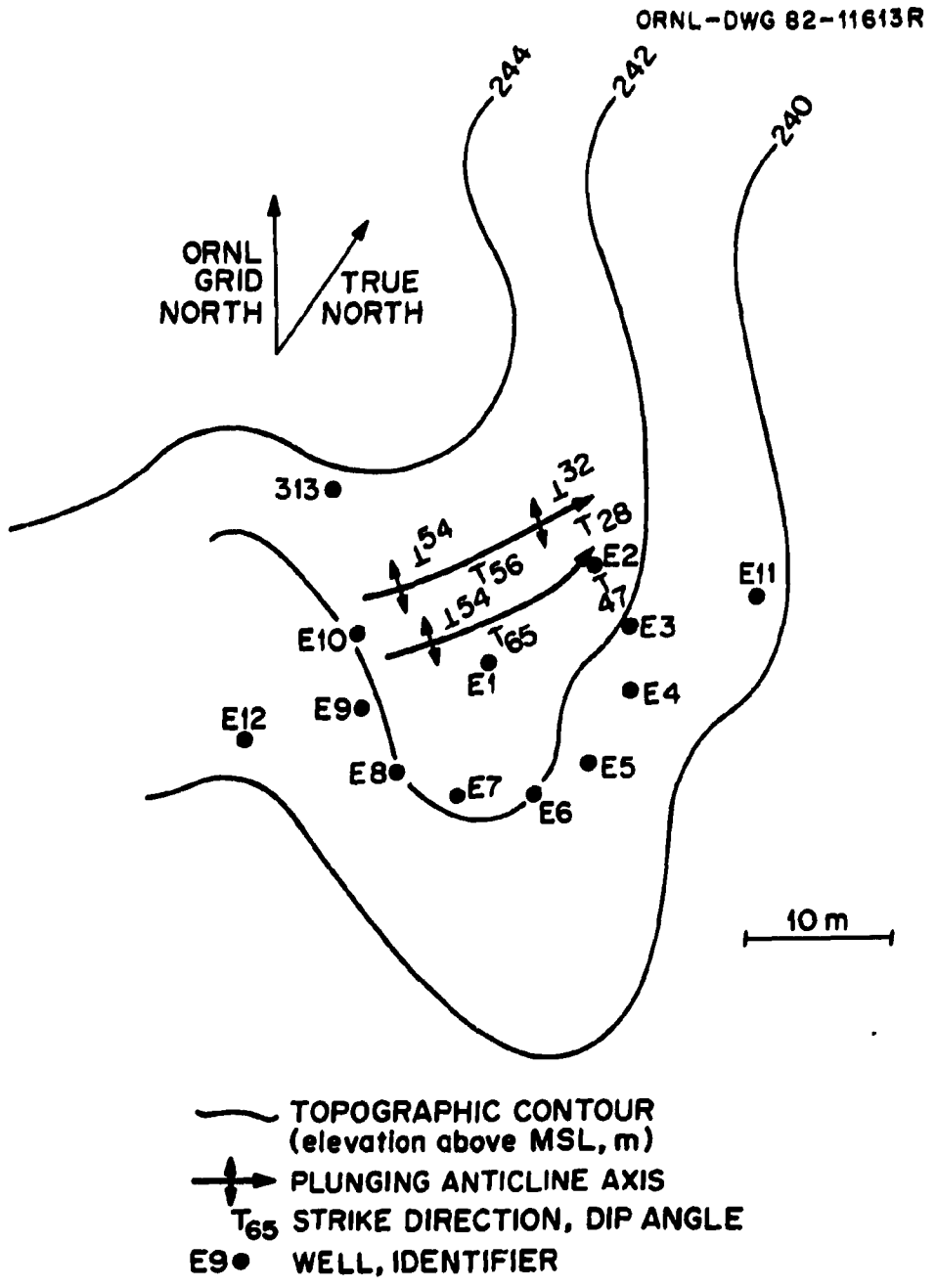

Fig. 12. Geologic structures found in the Engineered Test Facility site.

air-dried (70°C). Radionuclide Kd's, chemical analyses, and physical property determinations were performed as described in Sect. 4.2. Figure 14 depicts the Kd's of five radionuclides as well as the hardness determining cations (calcium plus magnesium). One of the more salient characteristics is the decline in ^{85}Sr Kd with depth, which parallels the distribution of hardness cations. Two radionuclides, ^{125}I and ^{241}Am, showed little variation with depth, while both ^{134}Cs and ^{58}Co exhibited a gradual decline with depth as less weathered rock was encountered. Only the shallowest sample

Fig. 13. Anticlinal fold (Trench 335, east wall) exposed during trench excavation. Fractures are concentrated in the hinge zone of the fold. (Note 0.75-m section of backhoe arm in upper lefthand corner of photograph for scale.)

ORNL–DWG 83-11498R

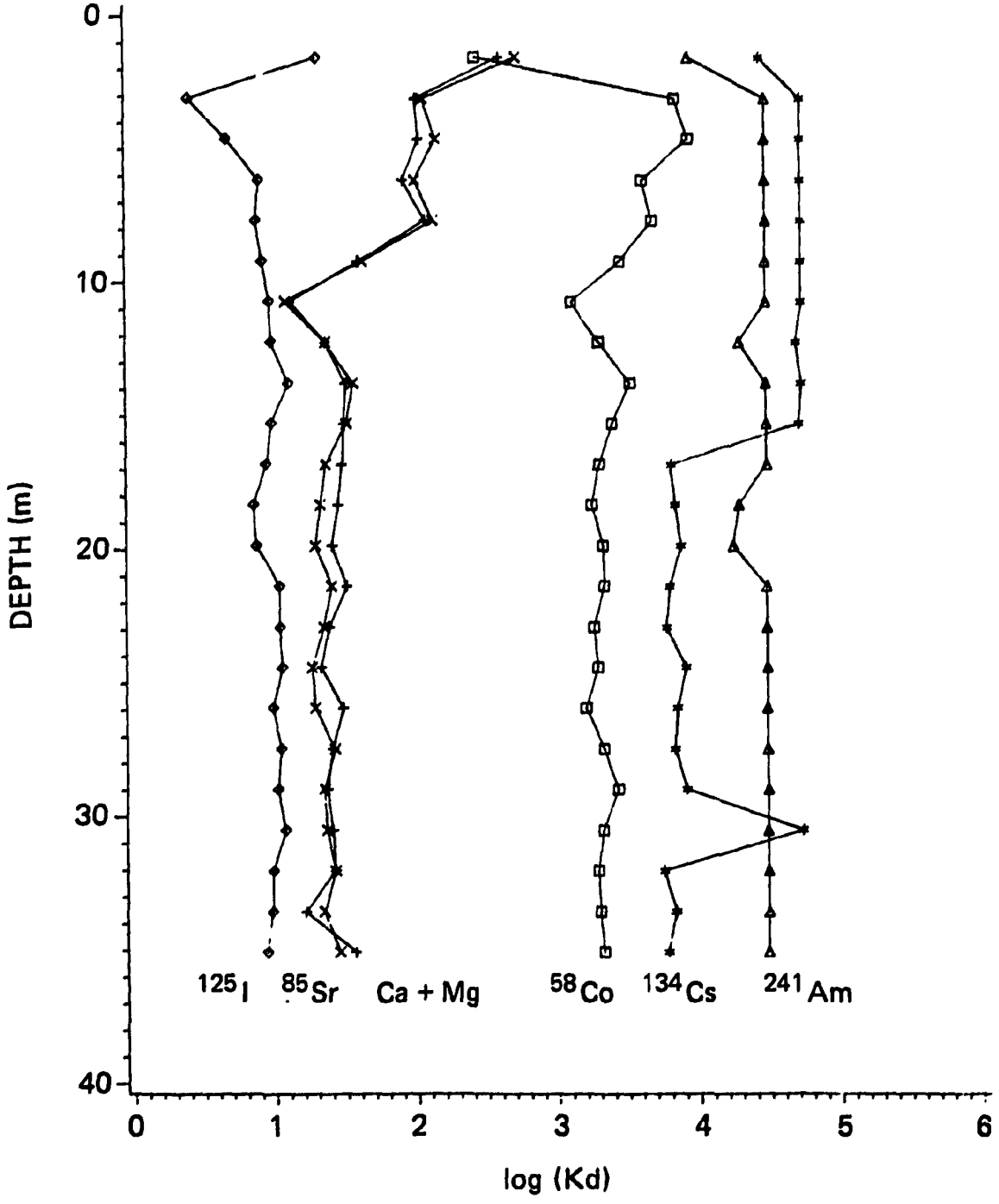

Fig. 14. Distribution coefficients of ^{125}I, ^{85}Sr, ^{58}Co, ^{134}Cs, and ^{241}Am and hardness cations (calcium and magnesium) with depth within the Maryville Limestone of the Conasauga Group.

within this borehole was similar to the soil profile samples discussed in the soils section; this top sample tended to be much higher in ^{85}Sr and ^{125}I Kd's and significantly lower in ^{58}Co, ^{241}Am, and ^{134}Cs Kd's.

The chemical properties of these borehole samples exhibited a more consistent depth relation (Fig. 15). The upper profile samples showed greater total exchangeable cations than deeper samples. As expected for the weathering of a limestone, most of these exchangeable cations were calcium. The decline with depth of exchangeable calcium and total cations is indicative of the degree of weathering of the Maryville Limestone. As the limestone and its clay mineral components weather, more cation exchange sites become functional (i.e., measurable by cation exchange analyses) as their surfaces become exposed. The additional chemical and physical properties presented in Table 4 also support this general conclusion. Although limestone was present throughout the depth of the borehole, only in the top sample had the calcium carbonate ($CaCO_3$) weathered to the degree that the saprolite was acidic; all other samples were above pH 7, reflecting the presence of residual carbonate. The apparent clay contents within the Maryville Limestone declined with depth and indicated the stronger aggregation of the rock at depth. Thus the general conclusion that the Maryville Limestone becomes more inert to cation and radionuclide adsorption with depth is supported by both the chemical and physical characteristics.

4.1.3 Surface Geophysical Characterization

4.1.3.1 Background

Three surface geophysical methods were used at the ETF site to aid in the characterization process: shallow electrical resistivity, shallow seismic refraction, and ground penetrating radar (GPR). The objective was to examine, in some detail, the surface geophysical characteristics of the ETF site in an attempt to gather as much information as possible about the zone in which the experimental trenches were to be located. In addition, because core examination and trench excavation activities had been completed or were planned as a part of the experimental design, this was an excellent opportunity to verify surface geophysical techniques with more expensive, time-consuming field observations. An evaluation of the three techniques could therefore be made regarding their applicability to LLW disposal site characterization.

4.1.3.2 Seismic refraction method

The seismic refraction method is based on the fact that elastic waves travel through different earth materials at different velocities (Dobrin 1960). The denser the material, the higher the wave velocity. In groundwater investigations · · technique has been used to determine such features as the depth to bedrock, the presence of . ..ed bedrock channels, the thickness of surficial fracture zones in crystalline rock, and the areal extent of potential aquifers (Freeze and Cherry 1979). The depth of penetration depends on the strength of the energy source, which can range from an explosion at the ground surface to a simple hammer blow on a steel plate resting on the ground. Receivers, or geophones, set up in a line radiating outward from the energy source are used to detect the arrival of the elastic wave and to construct a seismograph. A set of seismograph records can be used to derive a graph of the arrival time of the signal versus distance from shot point to geophone, which can be used to calculate layer depths and their seismic velocities.

ORNL–DWG 83-11499R

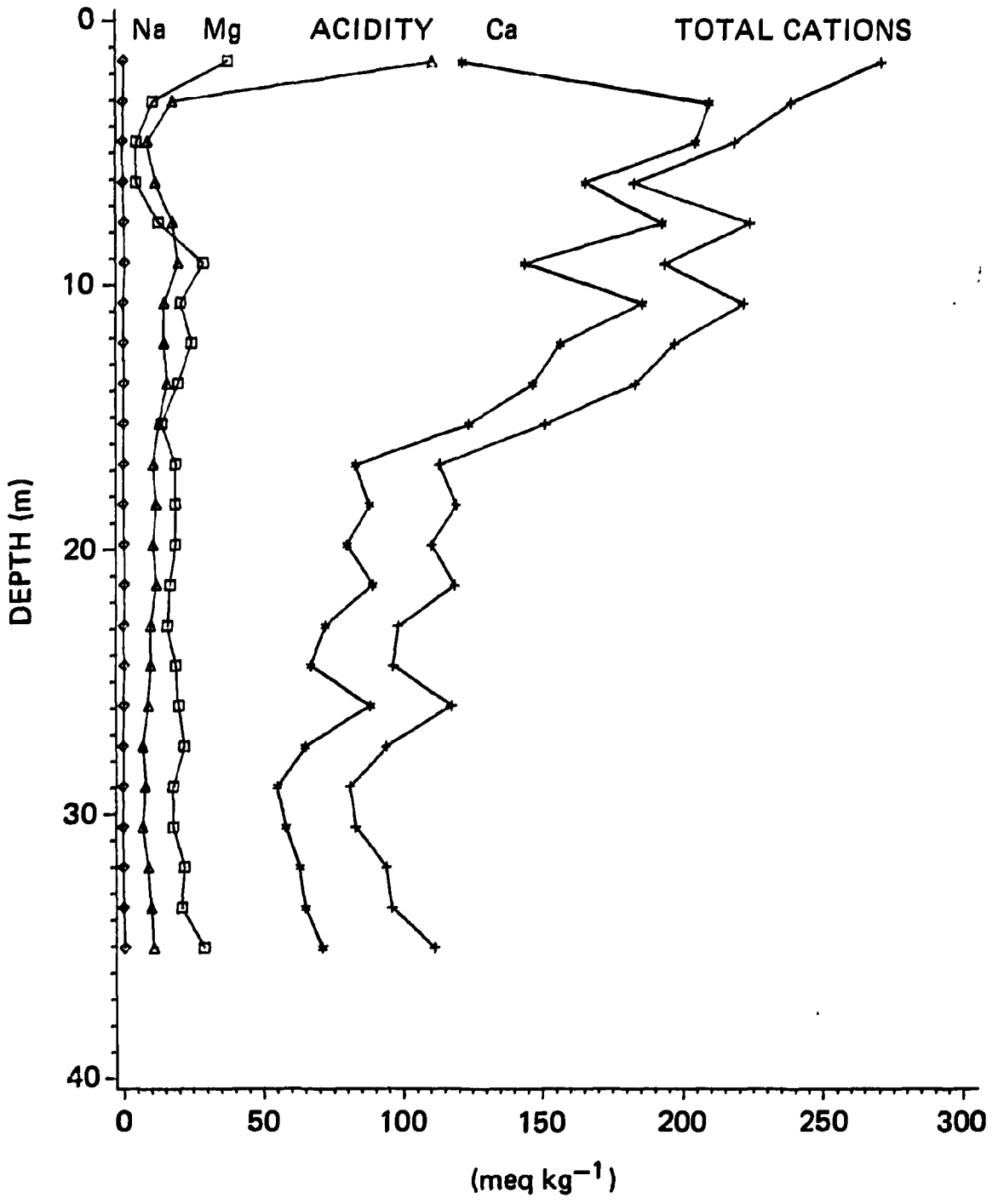

Fig. 15. Exchangeable sodium, magnesium, calcium, acidity, and total cations with depth within the Maryville Limestone of the Conasauga Group.

Table 4. Physical and chemical properties of depth increments of a borehole within the Maryville Limestone of the Conasauga Group

Depth (m)	pH	$CaCO_3$ (%)	Sand (%)	Silt (%)	Clay (%)	Particle density (Mg/m^3)
1.5	5.4	0.2	63	18	19	2.61
3.0	7.7	6.4	68	21	12	2.61
4.6	7.7	18.2	74	13	12	2.61
6.1	7.7	27.9	72	16	12	2.61
7.6	7.6	21.9	66	16	18	2.63
9.1	7.7	5.4	59	21	19	2.64
10.7	7.6	27.2	67	19	14	2.63
12.2	7.3	25.8	66	19	15	2.63
13.7	7.4	18.9	67	15	18	2.64
15.2	7.4	16.7	73	14	12	2.64
16.8	7.6	10.6	77	12	10	2.63
18.3	7.6	7.3	75	14	11	2.63
19.8	7.8	6.7	79	13	8	2.63
21.3	7.8	9.1	80	10	10	2.63
22.9	7.8	18.9	81	11	8	2.62
24.4	7.9	26.8	82	11	7	2.63
25.9	7.8	26.2	82	10	8	2.63
27.4	7.8	26.2	86	7	7	2.63
29.0	8.0	22.3	90	5	5	2.57
30.5	7.7	26.0	82	11	7	2.62
32.0	7.9	11.7	82	11	7	2.63
33.5	7.7	21.0	87	6	7	2.64
35.0	7.9	10.9	80	12	7	2.64

Three transects were established at the ETF site to run both a refraction and reflection seismic survey (Fig. 16). Unlike the refraction method, which gives a more detailed structural picture, reflection provides only enough data to approximate the depths to particular rock layers (Dobrin 1960). For the refraction surveys, the geophone (receiver) was set at 3-m intervals from the transmitter (strike plate), up to a distance of 33 m. Then a reversed seismic profile was performed, which requires reversing the starting points of the geophone and transmitter. For the reflection survey, the common depth point (CDP) method was used. This requires that both the transmitter and the geophone be moved from a common point to enhance the reflected signal. A more detailed discussion of these two techniques can be found in several review papers that deal specifically with geophysical applications in groundwater exploration (McDonald and Wantland 1961, Hobson 1967, and Lennox and Carlson 1967).

Analysis of the refraction data began by considering a site model consisting of horizontal layers. While this model did not adequately account for all the data, the distance-arrival time curves did show a distinct break in slope (velocity change) at about 15 m from the source in all transects. Analysis for a nonhorizontal site model was attempted, using refraction data from both the original and the reversed seismic profiles. The two travel-time graphs, when superimposed, showed two dipping discontinuities, which were interpreted to be a folded structure. When excavation of the site was initiated, existence of the folded structure (Fig. 13) was confirmed. The CDP results, how-

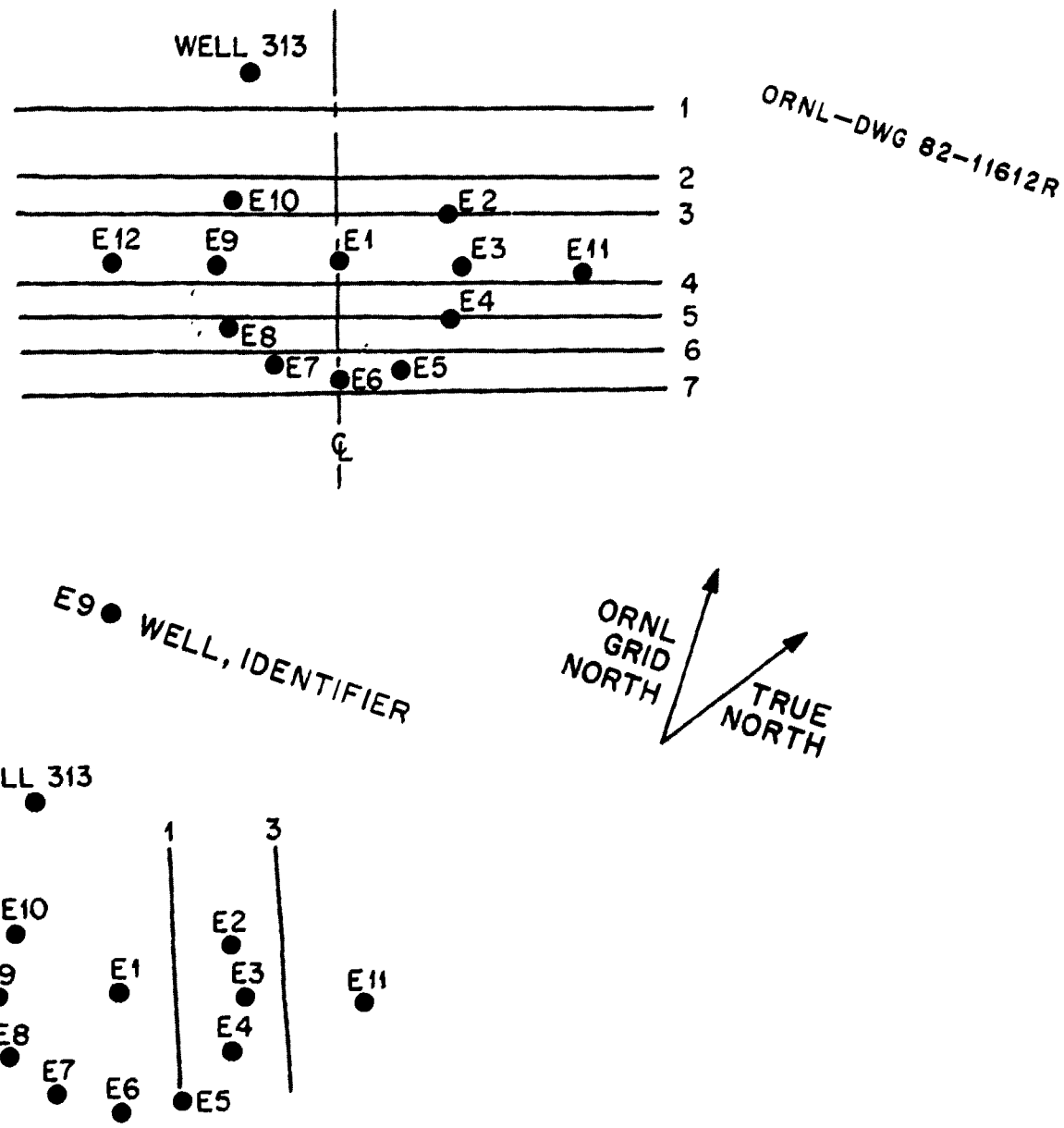

Fig. 16. Survey transects for the resistivity (top) and seismic (bottom) surveys.

ever, provided only an average depth to the fold. Thus the seismic results were found to be useful for providing a semiqualitative indication of site structure and complexity, but seismic studies appear to be best considered as a supplement to more direct observation methods at SLB sites.

4.1.3.3 Electrical resistivity

The electrical resistivity of a formation is defined as:

$$\rho = RA/L\,, \tag{1}$$

where

R = resistance to electric current for a unit soil block,
A = block cross-sectional area,
L = block length.

In an electrical resistivity survey, an electric current is passed into the ground through a pair of current electrodes, and the potential drop is measured across them. The spacing of the electrodes controls the depth of penetration. At each setup, an apparent resistivity is calculated on the basis of the measured potential drop, the applied current, and the electrode spacing.

Electrical resistivity surveys are of two general types: profiling and sounding. Profiling employs fixed electrode-spacing and thus samples a fixed depth. It is normally used for mapping the areal extent of such things as zones of groundwater with high salt concentrations. Sounding, which was used in this study, examines variations of resistivity with depth at a fixed location and is thus useful for determining stratigraphic and water-table elevation information. Details of the principles and application of electrical resistivity are well known and may be found in reference texts (e.g., Dobrin 1960).

Application of electrical resistivity to the ETF site employed the Wenner electrode configuration (Dobrin 1960). Seven transects were established normal to those used in the seismic survey as shown in Fig. 16. The electrodes were spaced at 1, 2, 3, 4, 5, 6, 8, and 20 m around the established center on each transect; and the apparent resistivities were calculated from the potentials measured at each spacing. The apparent resistivity values were then summed for each line, and the cumulative resistivity values were plotted against the electrode spacing (Dobrin 1960). Breaks in slopes were interpreted as media changes, and the first major one was interpreted as the soil-bedrock interface.

The estimated depths to bedrock based on the resistivity survey were compared to those determined by well-drilling activities (Fig. 17). Agreement between the two appears to be good, showing that soil depth at the site ranges from 2 to 7 m and becomes shallower as one moves along the centerline approaching well ETF-1. Again this relatively shallow soil depth was confirmed during trench construction when a folded structure was encountered at this location.

4.1.3.4 Ground penetrating radar (GPR)

The principle of GPR operation involves the generation of a pulse train of electromagnetic radiation in the frequency range of 10–1000 MHz. In accordance with the laws of classical electromagnetism, the wave propagates, with material dependent attenuation, through a given medium (the earth). When the wavetrain encounters a material or boundary of different dielectric properties, the wave is partially reflected. This reflected wave is then detected, and the time interval

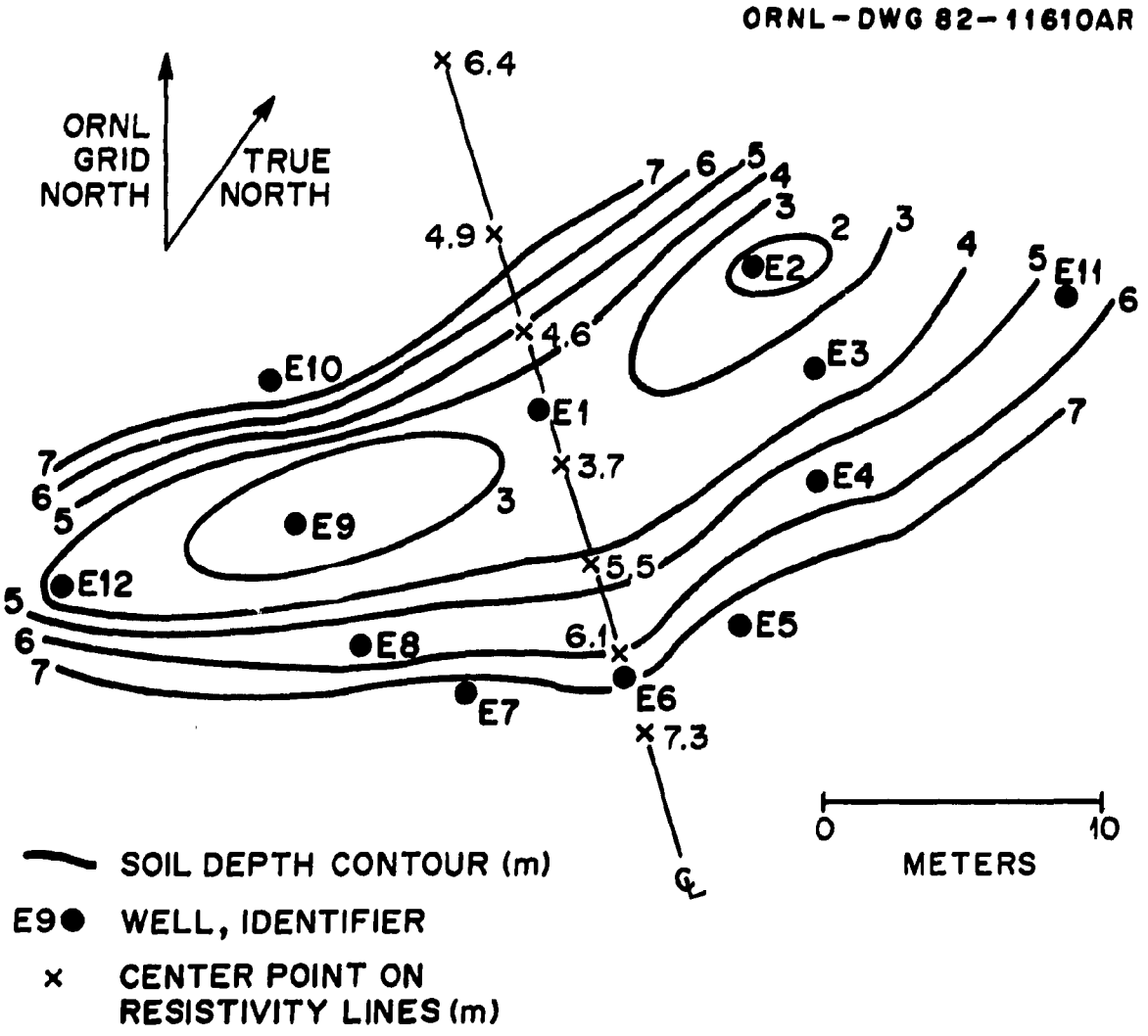

Fig. 17. Soil depths calculated from resistivity survey compared with measured soil depth contours from cores.

between transmission and detection is recorded. With knowledge of the velocity of propagation, the time interval can be converted to a range or depth (Geo-Centers Inc. 1982).

The probing depth is determined by the frequency selected and the electromagnetic properties of the soil, principally the conductivity and the dielectric constant. A summary of the physical properties that affect the propagation and attenuation of electromagnetic signals in several common media is shown in Table 5. Careful analysis of the reflected pulse, combined with a knowledge of the electromagnetic properties of the soil, can reveal information such as water content, subsurface density variation, and the location and depth of buried objects.

From August 25 through August 30, 1982, Geo-Centers Inc. (Newton Upper Falls, Massachusetts) was contracted to conduct a GPR survey of the ETF. The survey was scheduled for late summer in order to take advantage of the expected low soil moisture conditions, which, if too high, can limit the depth of GPR penetration (Table 5). A 7.6-m grid system was established at the site

Table 5. Approximate VHF (very high frequency) electromagnetic parameters of typical earth materials

Material	Approximate conductivity σ (mho/m)	Approximate dielectric constant	Depth of penetration
Air	0	1	Max (km)
Limestone (dry)	10^{-9}	7	
Granite (dry)	10^{-8}	5	
Sand (dry)	10^{-7} to 10^{-3}	4 to 6	
Bedded salt	10^{-5} to 10^{-4}	3 to 6	
Freshwater ice	10^{-5} to 10^{-4}	3 to 6	
Permafrost	10^{-4} to 10^{-2}	4 to 8	
Sand, saturated	10^{-4} to 10^{-2}	30	
Freshwater	10^{-4} to 3×10^{-2}	31	
Silt, saturated	10^{-3} to 10^{-2}	10	
Rich agricultural land	10^{-2}	15	
Clay, saturated	10^{-2} to 1	8 to 12	
Seawater	4	81	Min (cm)

for reference purposes, and two radar scan lines were selected: one over the experimental trench area and one along the perimeter access road (Fig. 18).

An example of a radar profile conducted at 300 MHz along line 78E is shown in Fig. 19. Interpretation of the scan by Geo-Centers indicates two complex folds at a depth of approximately 1 m at location 27N and 40N. In addition, a series of anticlines and synclines were identified in the region 60N and 70N, the most pronounced being that on the east wall of Trench 335 shown in Fig. 13. Results of the GPR survey proved to be difficult to interpret, and one must rely on the judgment of a trained operator. Further confounding of the interpretation resulted from high soil-moisture conditions, which did not allow identification of the groundwater surface. At best, GPR is a developing surface geophysical technique and, based on the results of the survey conducted at ORNL, would have limited applicability to disposal site characterization in humid areas.

4.1.4 Evaluation

The Conasauga Group is extremely complex, and work at the ETF has provided a better understanding of its makeup. Interpretation of soil thickness based on the electrical resistivity survey compared well with data from well drilling operations, and both will provide a soil depth contour map that is extremely important to waste disposal operations. The seismic refraction survey identified two dipping discontinuities at the ETF site, interpreted as folded structures, and is a valuable tool for a semiqualitative evaluation of site structure and complexity. Ground penetrating radar had several limitations, including the complexity of data interpretation, the inability to maneuver the truck-mounted equipment over the site, and the shallow penetration due to soil moisture.

To date, the focus of the ETF geologic characterization has been on the area in the immediate vicinity of the experimental trenches. However, the description of the geologic properties of the site, and therefore the hydrologic characteristics, is being expanded both laterally and vertically to give a better three-dimensional picture of water movement. This additional effort in geologic characterization is required both for general hydrologic modeling of the site and for trench treatment evaluation.

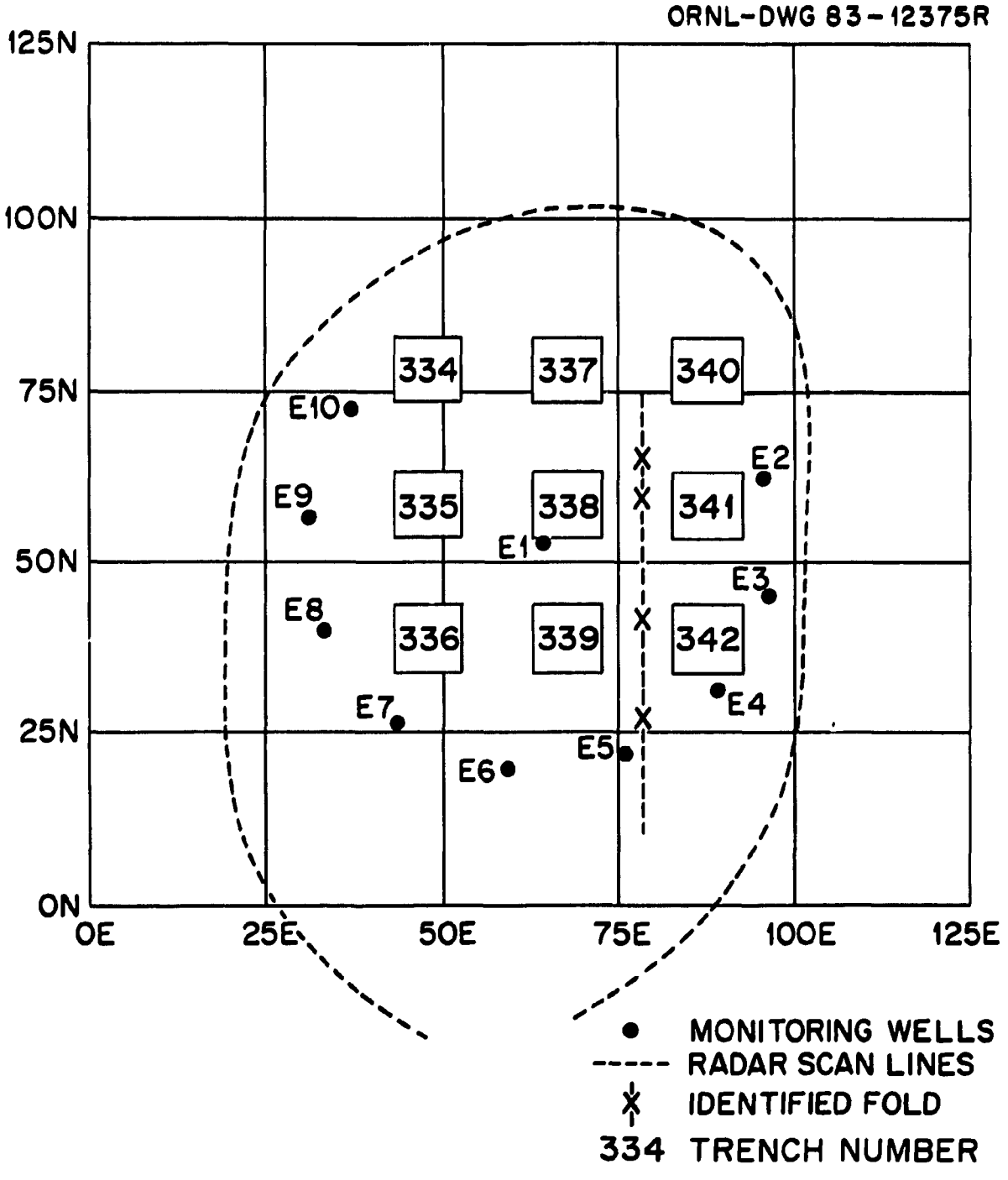

Fig. 18. Map showing Engineered Test Facility trench layout and 7.6-m grid system for ground penetrating radar survey.

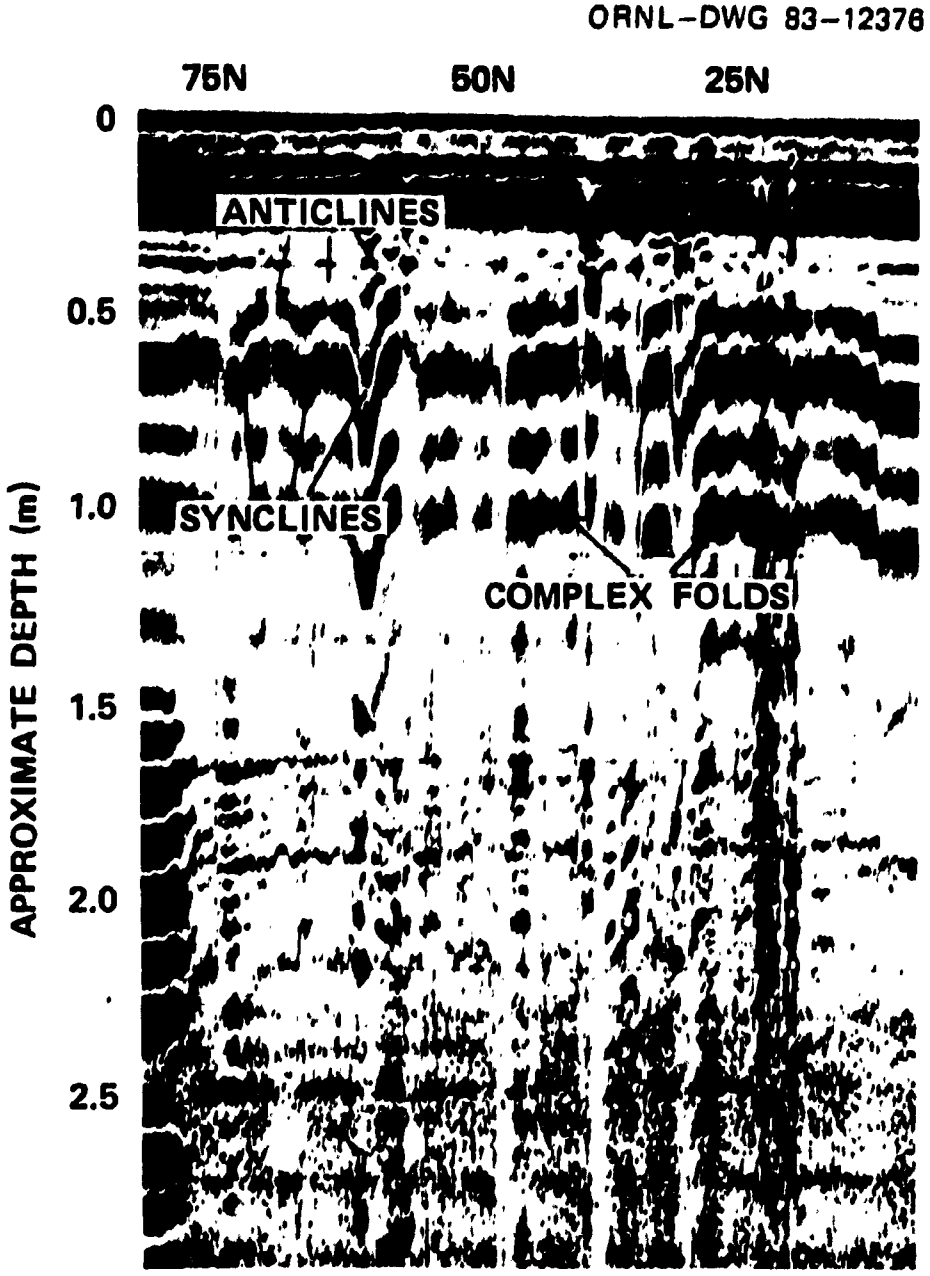

Fig. 19. Radar profile along Line E78 at 300 MHz. Small anticline exposed in Trench 338 during excavation indicated by arrow along with other associated folded structures. Strong "ringing" reflections at approximately 22N are caused by shallow instrumentation cables.

4.2 SOILS

4.2.1 Radionuclide Adsorption Properties

4.2.1.1 Background

A basic question that must be addressed by any site characterization is how fast various radionuclides will move after initial contact with the soil under prevailing hydrologic conditions. One of the major factors in the attenuation of radionuclide migration is their degree of adsorption to the soil or rock of the disposal site formation. The prevailing experimental approach to this question is to determine in the laboratory the degree to which a radionuclide is partitioned between an actual or simulated groundwater and the earthen material from the site. Because radionuclide adsorption is frequently dependent on the time of interaction between the water and earthen material, such determinations are often performed for long enough intervals to reach an equilibrium, the condition thought to be the most useful or stable. But if equilibrium requires months to attain and groundwater velocities at a particular site are in the order of meters per day, then the measurement of adsorption at equilibrium conditions should, be considered, at best, an academic exercise. Likewise, quite a few other laboratory experimental conditions, if not carefully considered, would lead to unrealistic results (i.e., results that would lead to an inaccurate description of the migration of radionuclides at the site).

The two general laboratory methods for the measurement of soil adsorption, batch and column elution, both have restrictions in their utility for site characterization. Column elution techniques appear to simulate field conditions more than batch or static "test tube" methods. They seem to have the advantage that the derived Kd's are determined from the breakthrough of the radionuclide under dynamic flow conditions. In fact, however, they are often determined under arbitrary flow rates selected for convenience of the experimenter rather than for their simulation of field conditions. Most always they are performed on reconstituted materials rather than undisturbed cores, which further compromises their justification on the basis of simulating field conditions. Perhaps the most serious drawback to column elution studies is that they are time-consuming (i.e., expensive) to perform. If the adsorption characteristics of a number of samples, representing the various earthen materials encountered at a site, need to be determined for a number of radionuclides, then the use of column elution techniques becomes cost-prohibitive. In addition, because of the large elution volumes required and column dispersion, the determination of Kd's greater than 100 L/kg by column elution is virtually impossible. Thus column elution was not selected, nor is it recommended for estimating Kd's in the laboratory.

Consideration of the problem of radionuclide migration necessitates focusing on particular radionuclides so that those that might potentially compromise site performance can be singled out from the many that pose significantly less hazard. To achieve this, a typical low-level solid waste must be defined, and an estimate must be made of the amount of each radionuclide it contains. The variability of LLW makes such a definition difficult, but, for purposes of illustration, one defined waste stream was selected. Boiling water reactor filter sludge (BWRFS) is one of the highest activity LLWs identified by NRC (NRC 1981) and contains one of the broadest ranges of potentially hazardous radionuclides. These estimates of concentrations in the waste, coupled with an estimate of their environmental mobility like the geologic retardation factors also estimated by NRC (NRC 1981), allow these radionuclides to be compared for potential migration from an SLB trench. A hazard rating for each radionuclide can be calculated by factoring in its inherent radio-

logical toxicity as measured by its maximum permissible concentration (MPC) for the unrestricted use of water (NRC 1979):

$$\text{hazard rating} = \text{concentration in BWRFS}/(\text{Rd} \times \text{MPC}), \quad (2)$$

where

Rd = geologic retardation factor,
MPC = maximum permissible concentration.

Such hazard ratings (Table 6) provide a quantitative method to compare radionuclides that occur at differing concentrations in the waste, that are adsorbed to differing degrees by the soil in which

Table 6. A generic hazard evaluation of radionuclides encountered in the disposal of low-level radioactive waste

Radionuclide	Concentration in BWRFS[a] (Ci/m^3)	Soil Rd[b]	MPC[c] (mCi/L)	Hazard rating[d]	Rank
^{3}H	1.26×10^{-2}	1	3×10^{-3}	4.2	5
^{14}C	7.78×10^{-4}	10	8×10^{-4}	9.7×10^{-2}	8
^{55}Fe	1.44×10^{0}	2640	8×10^{-4}	6.8×10^{-1}	6
^{59}Ni	1.49×10^{-3}	1750	2×10^{-4}	4.3×10^{-3}	10
^{60}Co	2.41×10^{0}	1750	5×10^{-5}	$2.8 \times 10^{+1}$	4
^{63}Ni	3.25×10^{-2}	1750	3×10^{-5}	6.2×10^{-1}	7
^{94}Nb	4.70×10^{-5}	4640	3×10^{-6}	3.4×10^{-3}	11
^{90}Sr	2.37×10^{-3}	36	3×10^{-7}	$2.2 \times 10^{+2}$	2
^{99}Tc	5.00×10^{-5}	4	3×10^{-4}	4.2×10^{-2}	9
^{129}I	1.33×10^{-4}	4	6×10^{-8}	$5.5 \times 10^{+2}$	1
^{135}Cs	5.00×10^{-5}	350	1×10^{-4}	1.4×10^{-3}	
^{137}Cs	1.33×10^{0}	350	2×10^{-5}	$1.9 \times 10^{+2}$	3
^{235}U	3.32×10^{-7}	3520	3×10^{-5}	3.1×10^{-6}	
^{238}U	2.61×10^{-6}	3520	4×10^{-5}	1.9×10^{-5}	
^{237}Np	6.38×10^{-11}	1200	3×10^{-6}	1.8×10^{-8}	
^{238}Pu	4.66×10^{-4}	3520	5×10^{-6}	2.6×10^{-2}	
^{239}Pu	2.36×10^{-4}	3520	5×10^{-6}	1.3×10^{-2}	
^{241}Pu	1.15×10^{-2}	3520	2×10^{-4}	1.6×10^{-2}	
^{242}Pu	5.18×10^{-7}	3520	5×10^{-6}	2.9×10^{-5}	
^{241}Am	1.56×10^{-4}	1200	4×10^{-6}	3.2×10^{-2}	12
^{243}Am	1.05×10^{-5}	1200	4×10^{-6}	2.2×10^{-3}	
^{243}Cm	2.97×10^{-7}	1200	5×10^{-6}	5.0×10^{-5}	
^{244}Cm	2.24×10^{-4}	1200	7×10^{-6}	2.7×10^{-2}	

[a]BWRFS = Boiling Water Reactor Filter Sludge per U.S. Nuclear Regulatory Commission (NRC). *Source:* NRC, *Licensing Requirements for Land Disposal of Radioactive Waste,* Draft Environmental Impact Statement on 10CFR Pt. 61, Main Report, NUREG-0782, vol. 2, 1981, Table 3.3.

[b]Based on Case 1, soils with moderate permeability (NRC 1981, Table 5.2).

[c]MPC = Maximum permissible concentration for unrestricted use of water per NRC (1979). *Source:* NRC, *USNRC Rules and Regulations, Pt. 20, Standards for Protection Against Radiation, Revised January 1, 1979,* 1979, Table 5.2.

[d]Hazard rating = BWRFS concentration/(Rd × MPC).

they must migrate, and which have inherently different radiological toxicities. Such hazard ratings can be used to formulate a ranking system for determining which radionuclides ought to be investigated for site characterization. One can also see what makes a radionuclide like ^{129}I exhibit the highest hazard rating; many other radionuclides occur at higher concentrations in BWRFS, but most have much higher soil Rd's and much greater MPCs. The rankings follow the order: $^{129}I > {}^{90}Sr > {}^{137}Cs > {}^{60}Co > {}^{3}H > {}^{55}Fe$, etc., with all of the actinide radioisotopes being of lower hazard than the fission and activation products. This hazard rating system merely serves to justify site characterization efforts on the six most hazardous radionuclides. In addition to the fission and activation products, the most hazardous of the actinides, ^{241}Am, was also investigated. In several cases, a less hazardous and more analytically facile radioisotope was selected for Kd determination, that is, ^{85}Sr, ^{125}I, or ^{59}Fe.

4.2.1.2 Methods

For the Kd determination of each radionuclide, a weight of soil equivalent to 5.00 g of oven-dried material was placed in a 30-mL polypropylene "Oak Ridge" centrifuge tube. To this was added 20.0 mL of a bulk sample of stream water collected from the eastern drainage of the ETF site. This stream water sample, filtered twice through Whatman No. 1 paper to remove suspended material, exhibited a pH of 7.2, an electrical conductivity of 460 dS/m, and a hardness of 263 mg/L as $CaCO_3$, which properties remained unchanged during the several weeks required to complete the Kd determinations. This sample was also analyzed for elemental composition (EPA 1979), including calcium, magnesium, sodium, potassium, strontium, cobalt, and cesium; these were found to be 57, 10.9, 5.0, 3.2, 0.24, 0.01, and 0.005 mg/L, respectively.

To the resulting soil water suspension was added a 1-mL aliquot of a stock carrier-free radioisotopic solution. These stock solutions were prepared by diluting the radioisotope into 100 or 50 mL of tap water. The following total activities of each isotope were employed: ^{125}I (1.9 MBq), ^{137}Cs (9.3 MBq), ^{85}Sr (1.7 MBq), $^{60}Co(II)$ (7.6 MBq), $^{59}Fe(III)$ (1.9 MBq), $^{51}Cr(III)$ (0.2 MBq), and ^{241}Am (1.1 MBq). After shaking lengthwise for one week at 100 oscillations per minute, the soil water suspension was centrifuged at 3600 RCF (relative centrifugal force, 3530 m/s^2) for 10 min and an aliquot removed from the supernatant for activity determination. In the case of ^{137}Cs, ^{85}Sr, ^{60}Co, ^{59}Fe, or ^{51}Cr, a 5-mL aliquot was placed in a 25-mL-capacity plastic scintillation vial and counted directly in a well-type sodium iodide gamma detector. In the case of either ^{125}I or ^{241}Am, a 0.5-mL aliquot was placed in a 7-mL-capacity plastic scintillation vial with 5 mL of liquid scintillation cocktail (Aquasol, New England Nuclear), and the activity was determined with a Prias liquid scintillation counter. With the five gamma-emitting radioisotopes, only the channels within the photopeak were counted, using a multichannel analyzer to divide the gamma spectrum into 200 channels between 0.1 and 2.0 MeV. Blanks were run concurrently to correct for background counting rates in the photopeak of interest. With ^{125}I, the predetermined program of instrument settings was employed, and with ^{241}Am, a counting window between 20 and 100% of full scale was selected. The external standard ratio method was used to correct color and chemical quenching of samples during liquid scintillation counting, but only a few samples manifested such interferences. Triplicate standards for each radioisotope, composed of 1 mL of stock solution in 20 mL of creek water but without soil, were counted concurrently with each batch of samples. By taking the ratio of sample counts to their standards, the fraction adsorbed by each soil (i.e., the relative amount disappearing from solution) was computed from the background-corrected

counting rates. Absolute counting efficiencies therefore did not need to be determined; and because of the generally high activities employed, spectrum stripping did not need to be performed to correct for contributions of other isotopes.

From the observed counting rates (cpm) of sample and standards, the fraction of radioisotope can be calculated:

$$\text{fraction adsorbed} = \frac{(\text{standard} - \text{background}) - (\text{sample} - \text{background})}{(\text{standard} - \text{background})} \qquad (3)$$

From this fraction adsorbed, the Kd of the radioisotope can be calculated:

$$\text{Kd} = \frac{(\text{fraction adsorbed})(\text{volume of solution})}{(1 - \text{fraction adsorbed})(\text{weight of soil})} \quad , \qquad (4)$$

where the volume of solution is the total of 20.0 mL of creek water plus 1 mL of radicisotopic stock solution plus the moisture added with the soil and where the weight of soil is the equivalent oven-dried weight of soil.

4.2.1.3 Results and discussion

The measured Kd's are listed in Table 7 for the three soil profiles from Trenches 334, 338, and 342. Radioisotopes, including ^{241}Am, ^{137}Cs, and ^{59}Fe, exhibited extremely high Kd's. There was an upper limit to the Kd that could be measured in these cases, which was imposed by a combination of the background counting rates and the activity of isotope employed; these maximum measurable Kd's were calculated to be 30,000, 190,000, and 59,000 L/kg for ^{241}Am, ^{137}Cs, and ^{59}Fe, respectively. Any calculated Kd that exceeded these upper limits was set equal to them for presentation in Table 7. The detection limits for the other radioisotopes were not approached for any of the samples; these values were 36,000 (^{85}Sr), 160,000 (^{60}CO), 54,000 (^{125}I), and 8300 L/kg (^{51}Cr). These detection limits were determined by using a minimum detectable sample counting rate of three standard errors of the background counting rate above the background counting rate; the Kd corresponding to this sample counting rate was then calculated using Eqs. (3) and (4). Above this calculated Kd, it is difficult to distinguish the sample counting rate from background counting rate.

The relative uncertainty in the reported Kd's in Table 7 is neither of constant magnitude nor of constant percentage. An excellent discussion of these uncertainties can be found in Baes and Sharp (1983) and will not be repeated here. Nonetheless, the Kd's are reported to three significant figures. In general, extremely high Kd's (i.e., $>10^5$ L/kg) will have unsymmetrical confidence limits; a typical 95% confidence interval would range from 10^6 to 10^4 L/kg. Extremely low Kd's (i.e., $<10^{-1}$ L/kg) were not encountered for any samples, as might be expected for ^3H as water, and would be subject to the same large range of uncertainty. Actually, such large confidence intervals are not particularly cumbersome to interpret. If a Kd is above 10^4 L/kg, a precise confidence interval would be superfluous because Kd's of such magnitude indicate that the radionuclide will not move in the formation. Likewise, extremely low Kd's are not worth learning with great precision because the radionuclide will behave like water and a determination of any difference in the rate of migration of the radionuclide to that of water in the formation could not be measured experimentally. Thus Kd's in the range 10^0 to 10^3 L/kg are most useful to determine with precision because these radionuclides will move in the formation at velocities slower than those of groundwater yet fast enough that they might migrate to uncontrolled areas.

Table 7. Distribution coefficients of selected radionuclides for soils from three depth profiles of the Engineered Test Facility site

Trench	Depth (cm)	Kd (L/kg)						
		^{241}Am	^{85}Sr	^{137}Cs	^{60}Co	^{125}I	^{59}Fe	^{51}Cr
334	20	17,100	342	18,400	435	21.4	44,600	895
334	40	4,620	79	29,100	102	18.5	59,000	5,460
334	60	1,950	117	28,500	117	22.8	59,000	3,190
334	100	2,770	544	58,900	570	2.2	59,000	615
334	130	1,720	724	104,000	730	1.1	7,840	482
334	150	2,160	831	67,100	725	4.2	59,000	238
334	180	5,810	757	190,000	845	10.5	59,000	445
334	200	2,000	548	52,900	825	11.3	59,000	126
338	20	7,820	236	32,000	223	4.1	10,900	4,240
338	40	5,610	298	64,800	293	11.1	59,000	7,290
338	60	1,750	408	49,700	385	1.0	59,000	3,610
338	100	3,220	759	57,400	1,740	18.6	59,000	112
338	130	2,020	782	34,700	675	0.3	9,570	1,460
338	150	5,240	248	64,800	1,020	3.8	59,000	48
338	180	4,040	458	69,600	762	2.6	33,000	334
338	200	17,100	126	48,000	4,810	0.1	4,120	17
342	20	3,220	224	49,900	219	10.1	12,500	8,300
342	40	2,720	383	52,500	311	14.8	59,000	5,300
342	60	30,000	729	75,200	560	13.8	59,000	8,300
342	100	1,77υ	327	48,500	388	23.0	56,200	327
342	130	2,160	415	91,200	447	14.0	59,000	1,350
342	150	4,370	678	96,500	889	31.7	59,000	572
342	180	3,840	821	75,100	839	24.0	59,000	424
342	200	3,220	1,010	78,900	854	16.0	59,000	120
Mean		5,670	494	64,100	782	11.7	46,800	2,220
Standard deviation		6,630	266	34,600	929	9.0	20,700	2,780

In absolute terms, the significance of a potential hazard posed by a radionuclide cannot be assessed from the magnitude of the Kd. Even if the total inventory of radionuclide in the waste and its inherent radiological hazard are taken into account as discussed above, the adequacy of a given Kd to retard radionuclide migration depends on the hydraulic conductivities and gradients within the formation. If hydraulic conductivities are low, then even low Kd's will be adequate to allow radioactive decay before a significant radiological dose is delivered to some predetermined boundary. Such assessments are the major goal of the site model; therefore, the Kd's are critical parameters for the modeling effort.

Table 7 also shows that there is no observable pattern with depth for the Kd's of any of the radionuclides and no differences among the three profiles. Thus the best representation of these Kd values for modeling purposes would be the averages and their standard deviations as presented at the bottom of the table. On a larger depth scale extending into comparatively unweathered bedrock (i.e., to depths of 30 m), there appeared to be some general decline in most radionuclide Kd's (Geology, Sect. 4.1).

Many of the Kd's were difficult to relate to other soil chemical properties. This was attempted by a correlation matrix (Table 8). Although most correlations were not large, several have mechanistic explanations worthy of note. The correlation of the behaviors of soil calcium and magnesium with radiostrontium (r = 0.83) was particularly interesting. The hardness Kd in Table 8

Table 8. Correlation coefficients between radionuclide distribution coefficients and the chemical and physical characteristics of soils from the Engineered Test Facility site

Property	Kd (L/kg)						
	^{85}Sr	^{137}Cs	^{60}Co	^{125}I	^{51}Cr	^{59}Fe	^{241}Am
% Organic matter	−0.55	−0.46	ns[a]	ns	0.42	ns	ns
% Sand	ns	−0.42	ns	−0.40	ns	−0.46	ns
% Silt	ns	ns	ns	ns	ns	ns	ns
% Clay	ns	0.49	ns	ns	ns	ns	ns
Exchangeable							
Ca^{+2}	−0.43	ns	0.81	ns	ns	−0.54	ns
Mg^{+2}	0.49	0.43	ns	−0.54	−0.45	ns	ns
Na^{+}	0.46	0.43	0.54	ns	−0.59	ns	ns
K^{+}	−0.56	−0.42	ns	ns	0.46	ns	ns
H^{+}/Al^{+3}	0.42	0.51	−0.53	0.59	ns	0.64	ns
Cation exchange capacity	ns	0.51	0.46	ns	ns	ns	ns
pH	ns	ns	0.88	−0.44	ns	−0.51	0.47
Bulk density	ns	ns	ns	−0.52	ns	−0.44	ns
Hardness Kd	0.83	0.45	ns	ns	−0.44	ns	ns

[a]ns = not significant at the 5% level.

was calculated by determining the hardness of the equilibrium water in the ^{85}Sr Kd determination and dividing it into the amount of exchangeable calcium and magnesium in the soil plus that which was adsorbed from the starting creek water hardness. The similarity of radiostrontium behavior in soil to that of calcium has been established previously (Spalding 1980) with similar soils, so their similar behavior in the ETF soils is not surprising.

For other radionuclides, only correlation coefficients greater than 0.80 are worth trying to define a mechanistic explanation. The correlation between the Kd for ^{60}Co and either soil pH or exchangeable calcium may be related to the similarity of Ca(II) and Co(II); the correlation with soil pH may be fortuitous because exchangeable calcium was strongly correlated (r = 0.89) with the soil pH. Other correlations seem too low to merit mechanistic arguments. One major reason for the generally poor correlation with soil chemical properties is the comparatively narrow range of these properties encountered at the ETF site. All soil samples except one can be described as strongly acid soils with very low levels of exchangeable basic cations: that is, calcium, magnesium, potassium, and sodium. Although organic matter, texture, and bulk densities varied more widely than these chemical characteristics, they would not necessarily be expected to be strongly related to the presumably more Kd-influencing chemical characteristics.

What is equally important is that the radionuclide Kd's exhibited little relationship with each other (Table 9). Such lack of correlation would make it impossible to use the behavior of one

Table 9. Correlation coefficients among radionuclide distribution coefficients of soils of the Engineered Test Facility site

Radionuclide	^{85}Sr	^{137}Cs	^{60}Co	^{125}I	^{51}Cr	^{59}Fe	^{241}Am
^{85}Sr		0.51	ns[a]	ns	ns	ns	ns
^{137}Cs			ns	ns	ns	ns	ns
$^{60}Co(II)$				ns	ns	ns	ns
^{125}I					ns	0.52	ns
$^{51}Cr(III)$						ns	ns
$^{59}Fe(III)$							ns

[a]ns = not significant at the 5% level.

radionuclide as a surrogate for another. In terms of site characterization, such lack of correlation would mandate that each Kd be determined individually.

4.2.1.4 Evaluation

As discussed previously with reference to Table 6, only the more hazardous radionuclides were evaluated for their Kd's in this site characterization. To put these numbers in perspective, most of these Kd's correspond to retardation coefficients, Rd's, at least an order of magnitude greater than the typical Rd's listed by NRC in its generic environmental impact statement (NRC 1981) and repeated in Table 10. The relationship between Rd and Kd is defined:

$$Rd = 1 + (Kd\ \rho/\theta), \tag{5}$$

where ρ = bulk density of the soil, usually between 1.0 and 1.8 kg/L, and θ = porosity in L/L, usually between 0.60 and 0.30. A typical value for ρ/θ for most subsoils would be 3.5 kg/L; for the ETF site, ρ/θ = 2.7 kg/L. Perhaps one of the most attractive characteristics of the ETF site is the very large retardation it poses for the migration of these radionuclides. Theoretically even ^{129}I would be retarded quite significantly in the formation at the ETF. To illustrate how these Rd's would be used in the site model, consider a hypothetically large inventory of ^{129}I buried within the central trench at the ETF. Using a mean value of 2.0×10^{-7} m/s for the hydraulic conductivity of the site formation, a hydraulic gradient of -0.1 m/m, and a total porosity of 0.50, a nonadsorbing tracer would require 24 years to migrate the 30 m to the surface water drainage point on the east side of the ETF:

$$V_l = -(K_l/\theta)(d\phi/dl) = 4 \times 10^{-8}\ m/s\ , \tag{6}$$

where V_l = average linear velocity of groundwater, K_l = hydraulic conductivity, and $d\phi/dl$ = hydraulic gradient. This calculation neglects dispersion and assumes both uniform flow through the formation and a seasonally stable hydraulic gradient. Actually, all these variables are spatially and/or time dependent, and the finite element modeling of the site will represent a quantitative method of describing their dynamics. If a radionuclide like ^{129}I exhibited a migration velocity 31 times slower than that of the groundwater, then its arrival time at the same surface seep would be 744 years. Any peak of radioactivity arriving at this surface seep would also be greatly diluted because of both dispersion and the kinetics of leaching from the waste. This sample calculation

serves only to describe how well radionuclides should be retained, in theory, at the ETF site. In the 0.2-m soil zone, the total porosity approaches the effective porosity, or that porosity which actually functions in groundwater conduction. For deeper soils, and especially for bedrock, the effective porosity, n, probably approaches 0:05 or below; hence, the retardation times calculated above and listed in Table 10 could well be reduced by an order of magnitude.

Table 10. Comparison of Engineered Test Facility (ETF) retardation factors, Rd's, and U.S. Nuclear Regulatory Commission (NRC) generic Rd's

Radionuclide	Mean ETF soil Kd (L/kg)	Calculated ETF soil Rd[a]	NRC generic Rd[b]
^{85}Sr	494	1,320	36
^{137}Cs	64,100	172,000	350
^{60}Co	782	2,100	1,750
^{125}I	11.7	31.4	4
^{59}Fe	46,800	125,000	2,640
^{241}Am	5,670	15,200	1,200

[a]Rd = 1 + Kd (ρ/θ), where ρ = 1.34 kg/L and θ = 0.50.

[b]Based on Case 1, soils of moderate permeability. *Source:* NRC, *Licensing Requirements for Land Disposal of Radioactive Waste,* Draft Environmental Impact Statement on 10CFR Pt. 61, Main Report, NUREG-0782, vol. 2, 1981, Table 5.2.

Considering the magnitude of many of these Kd's, it would be virtually impossible to determine these in the field. As illustrated above, velocities of only a few meters per year would make such determinations impractical. Likewise, laboratory soil columns also become impractical because of the large breakthrough volumes and the number of isotopes and soils to be studied. Thus laboratory batch mode Kd determinations are the only feasible alternative for site characterization.

4.2.2 Soil Chemical Properties

4.2.2.1 Background

The soil total elemental composition can be misleading because many elements can be present in largely insoluble mineral phases; other phases, representing only a small fraction of the total elemental composition, can be the active phases in determining the equilibrium solubility of an element in groundwater. Many of the radionuclides in LLW, such as ^{90}Sr or ^{137}Cs, will present a virtually insignificant perturbation to the stable isotopic elemental composition of the soils through which they migrate. The radioisotopes added through leaching of the waste will behave as tracers for the much larger pool of elemental mass of the active or labile phase of their corresponding stable isotopes. Hence, the chemistry of the radioisotope and of the element is determined by these active phases.

In humid regions, the generally most active soil phase, which determines groundwater quality, is the soil cation exchange complex. The nature and quantities of cations on the soil's exchange sites should be the primary concern of soil chemical characterization. In arid regions because of limited profile leaching, soil development is much less advanced; residual, more soluble minerals, for ex-

ample, halite, gypsum, trona, and soda ash, can be present and exert the dominant influence on groundwater quality. In humid regions, however, the source of most of a soil's exchangeable basic cations is often the weathering of sparingly soluble $CaCO_3$. Thus the depth of weathering and the residual content of this phase are important determinants for a site characterization.

In the classification of groundwaters by geochemical type (Stumm and Morgan 1981), the amounts of dissolved cations are often determined to be in equilibrium with $CaCO_3$. In the absence of carbonate, much less soluble minerals, such as quartz, feldspars, and phyllosilicates, determine groundwater quality and generally result in groundwaters of much lower ionic strength than those influenced by carbonate. The fluxes of carbon dioxide (CO_2), required to dissolve carbonate, are generally supplied by plant root respiration and decomposition of soil organic matter, particularly in its zone of concentration near the soil surface. Plants are also responsible for much of the elemental cycling that occurs in a soil profile. Cations are brought aboveground by the growing vegetation. During plant senescence, these cations are released to the surface soil horizons, where weathering and repeated plant uptake continue. Such elemental cycling can be extremely important in radionuclide movement for elements such as ^{90}Sr, which behave like calcium in soil; they can be mined out of buried waste by vegetation and brought to the soil surface. Similarly, ^{137}Cs often behaves like soil potassium and can be cycled in the soil profile in a manner analogous to ^{90}Sr. The characterization of this elemental cycling requires a determination of the kinds and quantities of exchangeable cations (e.g., calcium, magnesium, potassium, sodium, aluminum, and hydrogen) within soil profiles. The summation of all these cations equates with the soil's cation exchange capacity. This capacity represents the primary determinant by which any cation, whether a radioactive or stable isotope, added in buried waste will be retarded by soil. It is therefore the single most important property for the chemical characterization of soil.

Related to the nature of the soil's indigenous exchangeable cations is the soil pH. This property is generally related to the fraction of a soil's exchange sites that are occupied by acidic cations, that is, Al^{+3}, H^{+}, and, sometimes, Mn^{+2}. It is therefore a good index of soil weathering, particularly if the soil parent material contains carbonate, as does the Conasauga Group at the ETF. In general, a pH of less than 6.5 indicates that a soil will not contain any carbonate and that, as the pH of the soil delines below this, the amounts of exchangeable calcium and magnesium will also decline. The amount of $CaCO_3$ present in a soil is also a useful weathering index; none of the ETF soil profiles contained any $CaCO_3$ as evidenced by their extremely low pHs. However, $CaCO_3$ is a major component of the Conasauga Group; significant amounts of $CaCO_3$ can be found at greater depth beneath the soil zone (see Sect. 4.2).

The degree of profile interaction with vegetation can be determined by the soil's organic matter content. All soil profiles exhibit an organic matter content that declines with depth and results from the distribution of plant roots. However, the depths and absolute amounts of organic matter can vary enormously among soil types. The degree of influence of organic matter on soil properties is considered so important that it forms the basis for classifying many soils at the highest level (i.e., the soil order). Organic matter is also a source of cation exchange in soil and is the source of many specific adsorptions, for example, organic pesticides or other organic species that might be present in waste. Thus the soil profile's organic matter content is extremely valuable for site characterization.

Many standard techniques exist for soil characterization. Those described by the Soil Conservation Service [U.S. Department of Agriculture (USDA) 1972] are oriented toward soil classification; they tend to be the most useful for site characterization because their purpose makes them the

most generic. Another source of generic soil characterization methods is the American Society of Agronomy (1982); its methods tend to be somewhat biased toward agricultural characterization, but most have evolved into quite generic ones because of the diversity of agricultural goals they must address. Other procedures for soil testing [e.g., American Society for Testing Materials (ASTM) 1958] tend to be oriented toward engineering properties and therefore have less application for chemical characterization.

4.2.2.2 Methods

Soils were collected and processed as described in the section on physical properties (Sect. 4.2.3.2). Soil exchangeable cations were determined by elemental analyses of calcium, magnesium, potassium, and sodium (EPA 1979) in 1 *M* ammonium acetate, pH 7, extracts (Chapman 1965). Exchangeable acidity was determined by the $BaCl_2$-triethanolamine method (Peech 1965). Cation exchange capacity was calculated as the sum of exchangeable cations and exchangeable acidity. Soil pH was measured with a glass electrode using a 4:1 (v:w) water:soil ratio. Organic matter content was determined by the Walkley-Black method (Allison 1965). Percent base saturation was computed as the ratio of exchangeable bases (calcium, magnesium, potassium, and sodium) to the cation exchange capacity.

The carbonate carbon content of the soil was determined in a manner similar to the procedure of the Soil Conservation Service (method 6E3, USDA 1972) except that a sealed, rather than a flow-through, system was employed for collecting evolved CO_2. Because this modification represents a significant deviation from the standard procedure, it needs to be described in detail and its accuracy tested by applying it to standards containing variable amounts of $CaCO_3$. Into a 500-mL, large-mouth, screw-cap, polystyrene jar, was weighed 1.00 g of soil or rock. Within this large jar was also placed a 50-mL large-mouth screw-cap glass jar containing 5.00 or 10.00 mL of 1 *M* sodium hydroxide (NaOH) solution. While tilting the large jar to segregate the contained soil on the elevated portion of its bottom, 20 mL of a 1 *M* sulfuric acid (H_2SO_4)–5% ferrous sulfate ($FeSO_4$) solution was added; the screw cap was then secured and the jar returned to an upright position, allowing the H_2SO_4-$FeSO_4$ solution to contact and wet the soil. If the $CaCO_3$ content of the soil was greater than 1%, then a pronounced effervescence was noted. After allowing the jar to remain unperturbed for 72 h, the smaller jar of NaOH was removed and sealed with its screw cap until titration. After adding 10 mL of 1 *M* barium chloride ($BaCl_2$) to the NaOH, the residual alkalinity was titrated with 1 *M* hydrochloric acid (HCl) to the phenolphthalein endpoint. The difference between the amounts of titrant required for blanks and sample was converted into an amount of evolved CO_2. The carbonate content of the soil or rock was expressed as a weight percent of $CaCO_3$, equivalent to the evolved CO_2. Standards of chemically pure $CaCO_3$ were run to test the accuracy and validity of the method. The regression between milligrams of $CaCO_3$ found *(Y)* and $CaCO_3$ added *(X)* was:

$$Y = 0.95X + 4.2 \quad (r = 0.994, n = 9) \tag{7}$$

over the range of 50 to 450 mg $CaCO_3$, that is, 5 to 45% $CaCO_3$ by weight. The minimum detectable amount of $CaCO_3$ was 0.1%.

An additional measurement of the soil solution concentration of calcium and magensium was made by measuring hardness (American Public Health Association 1980). This was performed using a 20 mL aliquot of a batch of creek water collected from the eastern drainage of the ETF

site (see Sect. 4.2.1). This water was equilibrated with 5.00 g of soil for 6 d by shaking in a centrifuge tube.

4.2.2.3 Results and discussion

The chemical properties of the three soil profiles are summarized in Table 11. The general picture of these soils can be described as highly leached, strongly acidic soils. In only one case (Trench 338, 200-cm depth) was any significant influence of residual carbonate observed; this sample had the largest exchangeable calcium content and was the only sample with a pH > 5. This generalized chemical property description for the ETF soils correlates well with the visual description in the physical properties section (Sect. 4.2.3). Nonetheless, these soils have considerable

Table 11. Chemical properties of three soil profiles from the Engineered Test Facility site

Trench	Depth (cm)	Exchangeable (meq/kg)						BS[b] (%)	OM[c] (%)	pH	Hardness (mM)
		Ca	Mg	Na	K	Acidity	CEC[a]				
334	20	28	29	1	5	148	221	30	1.40	4.3	0.16
334	40	26	16	1	5	177	224	21	1.40	4.0	0.42
334	60	17	18	1	5	153	195	21	0.26	4.2	0.22
334	100	5	52	1	4	143	205	30	0.15	4.4	0.06
334	130	5	57	1	4	140	206	32	0.14	4.4	0.04
334	150	4	50	1	2	155	212	27	0.11	4.3	0.06
334	180	3	51	2	2	212	270	22	0.11	4.3	0.06
334	200	6	44	1	2	152	206	26	0.11	4.3	0.06
338	20	32	35	1	6	136	210	35	1.24	4.4	0.20
338	40	21	32	1	5	154	213	28	0.83	4.4	0.14
338	60	9	28	1	3	151	193	22	0.30	4.3	0.06
338	100	8	30	1	3	156	198	21	0.16	4.4	0.04
338	130	21	44	1	3	138	207	33	0.11	4.4	0.08
338	150	20	26	1	3	140	190	26	0.27	4.6	0.14
338	180	64	34	1	4	114	218	47	0.09	4.7	0.10
338	200	168	30	1	2	59	260	77	0.11	5.8	0.56
342	20	15	16	1	2	127	161	21	0.41	4.4	0.12
342	40	10	17	1	4	144	176	18	0.45	4.3	0.16
342	60	5	23	1	4	168	201	16	0.21	4.6	0.04
342	100	5	15	1	2	146	169	13	0.29	4.3	0.04
342	130	3	27	1	4	201	236	15	0.28	4.2	0.10
342	150	4	30	1	3	208	246	15	0.12	4.3	0.06
342	180	4	26	1	1	200	232	14	0.20	4.3	0.04
342	200	4	25	1	1	163	194	16	0.07	4.2	0.04
Mean		20	31	1	3	154	210	26	0.37	4.4	0.12
Standard deviation		34	12	0	1	32	26	14	0.41	0.3	0.13

[a]CEC = cation exchange capacity.
[b]BS = base saturation.
[c]OM = organic matter.

cation exchange capacities averaging 210 meq/kg and were quite uniform in this characteristic. There appeared to be only a minor influence of vegetational nutrient cycling, as evidenced by the modest decline in exchangeable calcium with depth in each profile. Deeper strata, when encountering carbonate rock, would be expected to be quite high in exchangeable calcium. It should be noted that during the clearing of the original forest vegetation from the site, the original A and most of the B soil horizons were removed; these horizons tend to be quite shallow on these soils anyway. An unperturbed A horizon of this profile would have an organic matter content ranging from 3 to 6% (Spalding 1980); notably, the highest found in the surface horizons of these profiles was only 1.4%, a condition indicative of the A horizon removal.

The exchangeable magnesium and potassium contents seem to be largely independent of depth. In both cases, the ambient levels of these exchangeable cations probably represents a steady-state weathering of illite. Micaceous minerals (vermiculite and illite) dominate the mineralogy of these soils (see Sect. 4.2.3). The prevailing view of clay formation is that vermiculite weathers from mica, that is, illite (Douglas 1977). This process becomes very plausible for the Conasauga Group, where weathering occurs in a magnesium-rich environment. As the illite weathers, it will release potassium to the exchange complex of the soil. The presence of illite in these soils is the source of the strong ^{137}Cs fixation properties of these soils (Jacobs and Tamura 1960).

A number of significant correlations were observed among the soil chemical properties (Table 12). Of particular note are the correlations between exchangeable acidity and percent base saturation and pH ($r = -0.80$ and -0.72, respectively). This relationship is to be expected because the lower the soil pH, the more exchange sites that are occupied by acidic cations (Al^{+3} and H^+) and, hence, the lower the percentage of these sites that are occupied by basic cations. Calcium dominated these exchangeable bases when the base saturation increased, which accounts for its high correlation ($r = 0.90$) with percent base saturation and its negative correlation with exchangeable acidity ($r = -0.73$). Other correlations in Table 12 do not appear large enough to merit significant mechanistic discussion.

Table 12. Correlation coefficients among chemical properties of soil samples from three depth profiles at the Engineered Test Facility site

Property	Exchangeable					CEC[a]	BS[b] (%)	OM[c] (%)	pH
	Ca	Mg	Na	K	Acidity				
Exchangeable									
Ca		ns[d]	ns	ns	−0.73	ns	0.91	ns	0.89
Mg			0.52	ns	ns	ns	ns	ns	ns
Na				−0.53	ns	0.64	ns	ns	ns
K					ns	ns	ns	0.68	ns
Acidity						ns	−0.80	ns	−0.72
CEC							ns	ns	ns
BS								ns	ns
OM									ns

[a]CEC = cation exchange capacity.
[b]BS = base saturation.
[c]OM = organic matter.
[d]ns = not significant at the 5% level.

4.2.2.4 Evaluation

Soil chemical properties reflect the nature of the mineral phases present. In site characterization, these properties should be compared for consistency with the results of the mineralogical analyses. The presence of carbonates, for example, is inconsistent with a strongly acidic soil or a low percent base saturation. In addition, soil chemical properties usually correlate with certain physical properties. For example, a soil with a very coarse texture (e.g., 90% sand) would not be expected to have a cation exchange capacity in excess of 50 meq/kg; nor would a soil, whose clay mineralogy was dominated by kaolinite, be expected to exhibit a cation exchange capacity much above 100 meq/kg.

A number of soil chemical properties were not examined on the ETF samples because other characteristics obviated their measurement. Included among these properties would be salinity and oxidation-reduction potential. The low exchangeable sodium content of these soils indicates that no excess sodium chloride (NaCl), sodium carbonate (Na_2CO_3), or sodium sulfate (Na_2SO_4) was present. Likewise, the low pH indicated that no alkaline salts were present, as might be expected in extremely arid environments. The relatively high values and chromas of these soil horizon colors (see Sect. 4.2.3) indicated that all these horizons were in oxidizing environments; oxidation-reduction potential measurement would therefore be superfluous. Soil colors, particularly in the C horizon material where the influence of organic matter is minimal, tend to be determined by iron oxides which acquire very low values and chromas when reduced. In addition, $CaCO_3$ was not observed in any soil sample from the ETF; this is not surprising because these acidic soils would not be stable environments for carbonates.

A number of other common chemical soil tests were not examined (e.g., available P and the many availability tests for essential plant micronutrients) because these tests were developed as an aid for agricultural production rather than as descriptions of fundamental chemical interactions. The behavior of many radioisotopes (e.g., ^{60}Co and ^{55}Fe) will be determined by their interaction with the available pools of the more abundant stable isotopes already in the soil. The soil adsorption reactions of many of these elements have been studied for some time and tend to follow reasonably well-established mechanisms (Ellis and Knezek 1972). Each element or radioisotope will follow some empirical adsorption isotherm; the investigations of these isotherms was not judged to be particularly important for site characterization in a generic sense. As can be seen from the rather large Kd's for such radioisotopes (Sect. 4.2.1), these isotopes will not migrate very far within the formation, so a more detailed knowledge of their adsorption behavior would only be of academic interest.

In terms of site modeling, these soil chemical properties can be quite influential. The nature and quantities of exchangeable cations determine the starting conditions of the soil formation before waste burial. Among the many changes caused by the introduction of waste, biodegradable constituents will function as a source of cations (usually H^+ and the Al^{+3}, which this H^+ will dissolve from the soil) that will migrate through the soil formation. The flux of these cations, with their associated anions, will have to be described as a cation exchange process and addressed by the site model. Microbiological production of soluble organic acids can also result in enhanced carbonate weathering, which a site model will also have to address. Likewise, the metabolism of such biodegradable materials will generate a considerable oxygen demand, which, in turn, will perturb the oxidation-reduction status of some portion of the formation. Such conditions could alter the adsorption characteristics of some radioisotopes, for example, ^{60}Co and ^{55}Fe.

The interaction of the site formation with the buried waste necessitates that almost as much effort be spent on waste characterization as on the site. Although this waste characterization is not

the subject of this report, a number of important waste properties can be identified. First, the biodegradability of the waste needs to be determined. Second, the nature and leachability of its constituents must be determined, with particular emphasis on how these vary during the course of microbiological degradation. The influence of biodegradation on the corrosion of nonbiodegradables, for example, metals, also needs to be determined. If significant amounts of dissolved cations result from metallic corrosion, then these will have dramatic influences on the cation exchange properties of the soils. Finally, as pointed out above, the influence of reducing conditions on the solubility of various soil mineral phases should also be measured because such conditions will result from even minor amounts of microbiological activity in a region of the soil where oxygen (O_2) availability is limited by diffusion through the upper soil layers. Such waste biodegradation will also likely affect some physical soil properties, particularly hydraulic conductivities. Soil pores can become clogged with microbiological exudates and debris, with resulting decreases in hydraulic conductivity (Klute 1965). The duration of such effects on the long-term scale is unknown, but such processes could have a dramatic effect on site performance.

4.2.3. Soil Physical Properties and Morphology

4.2.3.1 Background

Mineralogical composition and the size and arrangement of mineral particles in a soil formation determine most of its bulk physical properties. These properties include hydraulic conductivity, porosity, strength, water-holding characteristics, compressibility, and erodibility. Many of these same properties are either the resultants or the causative agents of soil development. Thus they influence the classification of soils in the current USDA system (USDA 1975), which is based on the degree of development of the soil solum, with certain caveats for widely differing parent materials. Because this soil classification is useful in describing and understanding the processes that have given rise to the present soil and because these processes will enable predictions for the future development of the soil, this soil classification is most pertinent for site characterization. This information should be of particular use in assessing the long-term landform stability of a formation, with due consideration for any operational perturbations.

Among the physical properties considered most useful for site characterization are texture, bulk density, and structure. These parameters describe the size distribution of the primary soil particles, the degree to which these particles are packed, and the nature of the secondary arrangement of the primary particles, respectively. These properties can sometimes be correlated with hydraulic properties, such as conductivity, but hydraulic properties are somewhat independent and should be measured in the field with little soil structure perturbation. Texture and bulk density are, of necessity, measured in the laboratory using retrieved samples. Texture is often considered predictive of hydraulic conductivity; soils of fine texture, that is, composed mainly of clay particles, will have smaller pores between particles than coarser soils and, hence, exhibit lower hydraulic conductivities. However, the arrangement of the primary particles, that is, structure, often can result in larger pore sizes and therefore, greater hydraulic conductivities. Thus, two soils of the same texture can have vastly different hydraulic conductivities.

Bulk density, ρ, is another property that is easily measured but difficult to interpret. It is inversely related to the soil porosity, θ:

$$\theta = [1 - (\rho/\text{particle density})] . \quad (8)$$

Particle density is the density of the primary soil particles. It can be measured or, more commonly, assumed to equal 2.65 kg/L, which is the density of most silicate minerals in soils (e.g., quartz, feldspars, and phyllosilicates). The inference is often made that the greater the soil porosity (i.e., the lower the bulk density), the greater the soil hydraulic conductivity. Such a generalization can, of course, be grossly misleading. The pore size distribution and interconnectedness and not the porosity control the soil permeability to water. Often, a fraction of the total porosity is composed of such small pore sizes in comparison to larger pores that, effectively, it does not participate in water movement through the soil. This has led to the definition of an effective porosity as that fraction of the porosity which functions in fluid transport. Experimentally, this effective porosity can only be addressed in the field because the retrieval of unperturbed samples of the soil formation is, at best, quite difficult. Even if the technical difficulties of retrieving an unperturbed sample for laboratory hydraulic characterization could be overcome, such measurements would apply only to that small sample. Because of the widely inherent spatial variability within the formation, the laboratory measurements may only be representative of a small fraction of the formation. In situ field testing over much larger volumes of the formation would yield more useful site characterization data and could likely be obtained with less effort and expense.

None of the common geotechnical properties of the site were measured. These properties would include such indices as compressibility, shear strength, bearing capacity, modulus of rupture, and Atterberg limits. Such parameters are more useful for describing the properties of the soil or rock for construction purposes. Their utility for predicting site performance would be purely incidental; hence, they were not considered important for this level of site characterization. These characteristics would affect the site selection process in a minor way by their effect on construction strategies to be used at the site. The hydrologic suitability of a site for LLW disposal can be judged independently of any knowledge of these parameters.

4.2.3.2 Methods

Bulk densities were determined using cores retrieved from depth increments of the eastern wall of Trench 334, the western wall of Trench 338, and the eastern wall of Trench 342 (Fig. 20). A soil corer (Clements Associates, Inc.) with a cellulose acetate liner (2.06 cm inside diameter × 31.5 cm long) was hammered into the selected depth; using the removable handle, the core was retrieved by hand twisting. The liner was removed and both ends sealed with plastic caps. A 5.0-cm-long section of the core was removed by cutting with a carbide-tipped rotary saw. Some obvious compression was noted at both ends of the core, which obviated the use of either 5-cm end section for this determination. The soil was expressed from the cut liner section and oven-dried at 80°C for 16 h. The bulk density was calculated from the oven-dried weight and the known volume of the liner section. Total porosity was then calculated using Eq. (8) and assuming a particle density of 2.65 kg/L.

An additional sample of about 500 g was collected with a shovel from a 10-cm-diam area around each core hole. These samples were stored in polyethylene bags and dried as above. The soil was then sieved to <2 mm by rubbing batches over wire cloth for about 30 s. These soil samples were used for determination of texture by the hydrometer method (Day 1965) and also for determination of chemical properties (Sect. 4.2.2) and radionuclide adsorption properties (Sect. 4.2.1). In the hydrometer texture determination, the 50-g sample was dispersed by shaking with 600 mL of water and 100 mL of 5% sodium hexametaphosphate. Hydrometer readings were taken only after

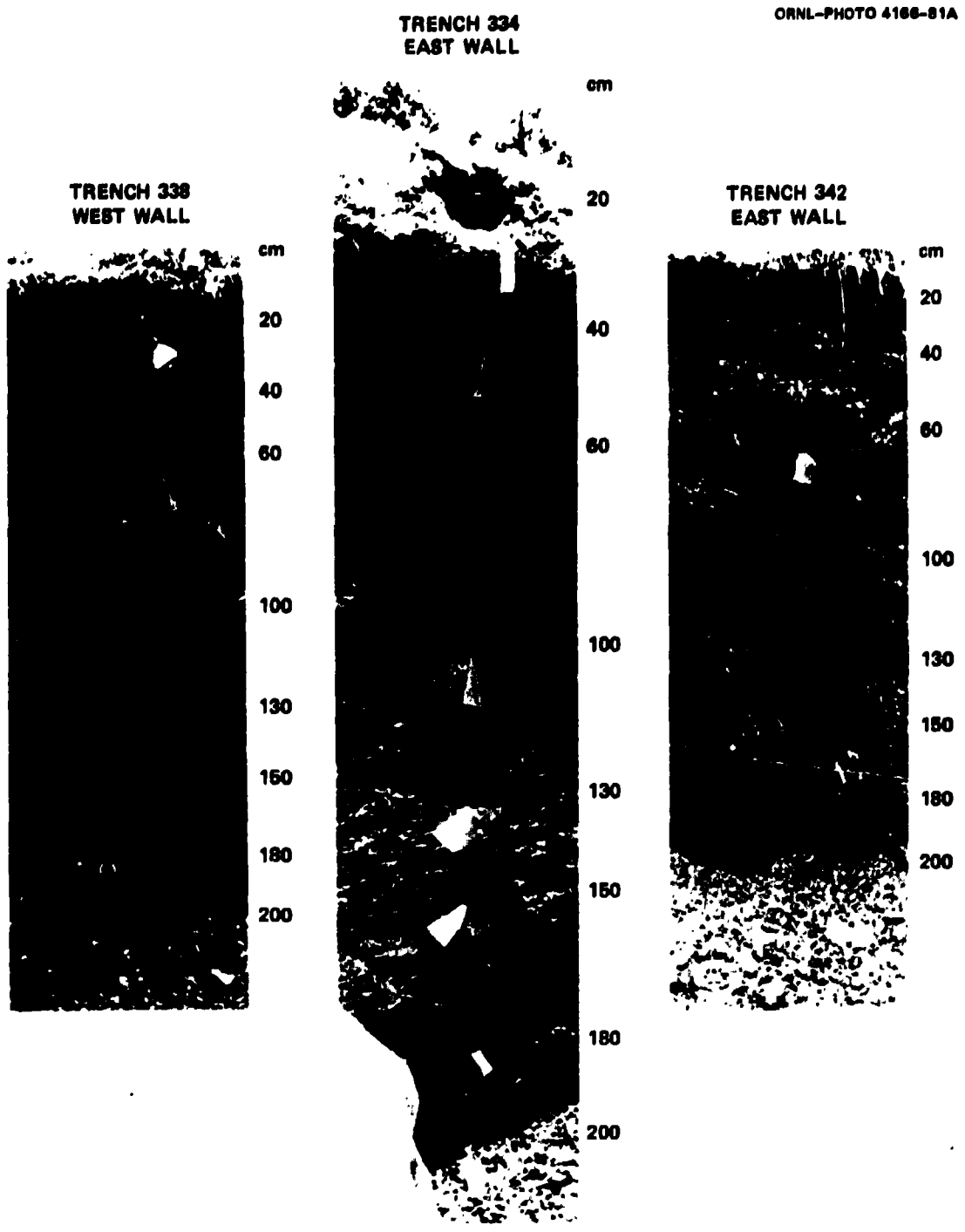

Fig. 20. Profiles of three trench walls sampled for bulk densities and chemical properties. Flags indicate where cores were taken.

40 s and 2 h of sedimentation, which correspond to the sedimentation times of particles >50 μm (sand) and >2 μm (sand and silt), respectively. The percentage of sand, silt, and clay was then calculated from these readings.

Two soil profiles (Trench 335, north wall, and Trench 338, south wall) were employed for a field morphological description (Fig. 21). Two horizons of unique visual character from Trench 340 walls were also described (Fig. 22). The descriptive techniques are summarized in the Soil Survey Manual (USDA 1951). Soil color was determined in the moist condition by spraying dry horizons of the profile when necessary. Texture was determined by feel. Because of the quite variable strength of the rock aggregates, such field textures can be misleading; stable aggregates rather than primary particles would be felt. Aggregate structure and plant root density and penetration were also noted. Acidities were determined with retrieved samples using a pH meter and a 1:1 (w:v) soil paste.

Composite samples were collected from each described horizon and separated into four fractions: >45 μm, 45 to 2 μm, 2 to 0.2 μm, and <0.2 μm (Day 1965). Split samples of the clay fractions (<2 μm) were cation saturated with either K^+ or Mg^{+2} and mounted on glass slides for preferred orientation X-ray diffraction analysis (Whittig 1965). After initial X-ray diffraction of the magnesium-saturated sample, ethylene glycol was added to the clay (Jackson 1974) and the sample reexamined to identify any swelling clay (i.e., smectites). The silt fraction, 45 to 2 μm, was analyzed as a random powder. Qualitative identification of clay minerals was made by the location of diffraction peaks and their behavior with differing cation saturation and solvation. Semiquantitative analysis, that is, the relative ranking of the amounts of the clay minerals present, was determined from diffraction peak intensity. Similar mineral identifications were performed for the random powder diffraction patterns of the silt fractions, but no relative ranking was performed because of the inherent differences in peak intensities of the minerals.

Identifications of soil series at the ETF site were made by fitting series field and laboratory characteristics with the nearby Anderson County, Tennessee, Soil Survey (USDA 1981). Taxonomical classifications were made by comparing these descriptions with the generic descriptions (USDA 1975). The Conasauga Group in Bethel Valley extends eastward into Anderson County; and many terrains, which are similar to the ETF hillock, exist within this mapped area. The ETF is located in Roane County, Tennessee, but the county soil survey (Swann et al. 1942) is of marginal value for site characterization because its resolution was too large to identify the ETF site. In addition, both the mapping units and the soil classification system have changed since that time.

4.2.3.3 Results and discussion

The bulk densities and textures of the three depth profiles at the ETF site are listed in Table 13. The variation in bulk density and porosity showed no pattern with depth. The obvious differences in stratification at the various depths can be seen in Fig. 20, and the widely varying bulk densities reflect this heterogeneity. It should be noted that the cores for the bulk density determinations were taken perpendicular to the east or west walls of the three trenches; thus the entire core would be within a single stratum. During the comparatively dry conditions when these cores were taken (June 1982), quite noticeable differences were observed in the moisture status among the strata. These observations obviously reflect differences in the hydraulic properties among the layers. but because of the qualitative nature of these observations, no attempt was made to correlate them with the quantitative measurements of bulk density and texture. The patterning of such variability of

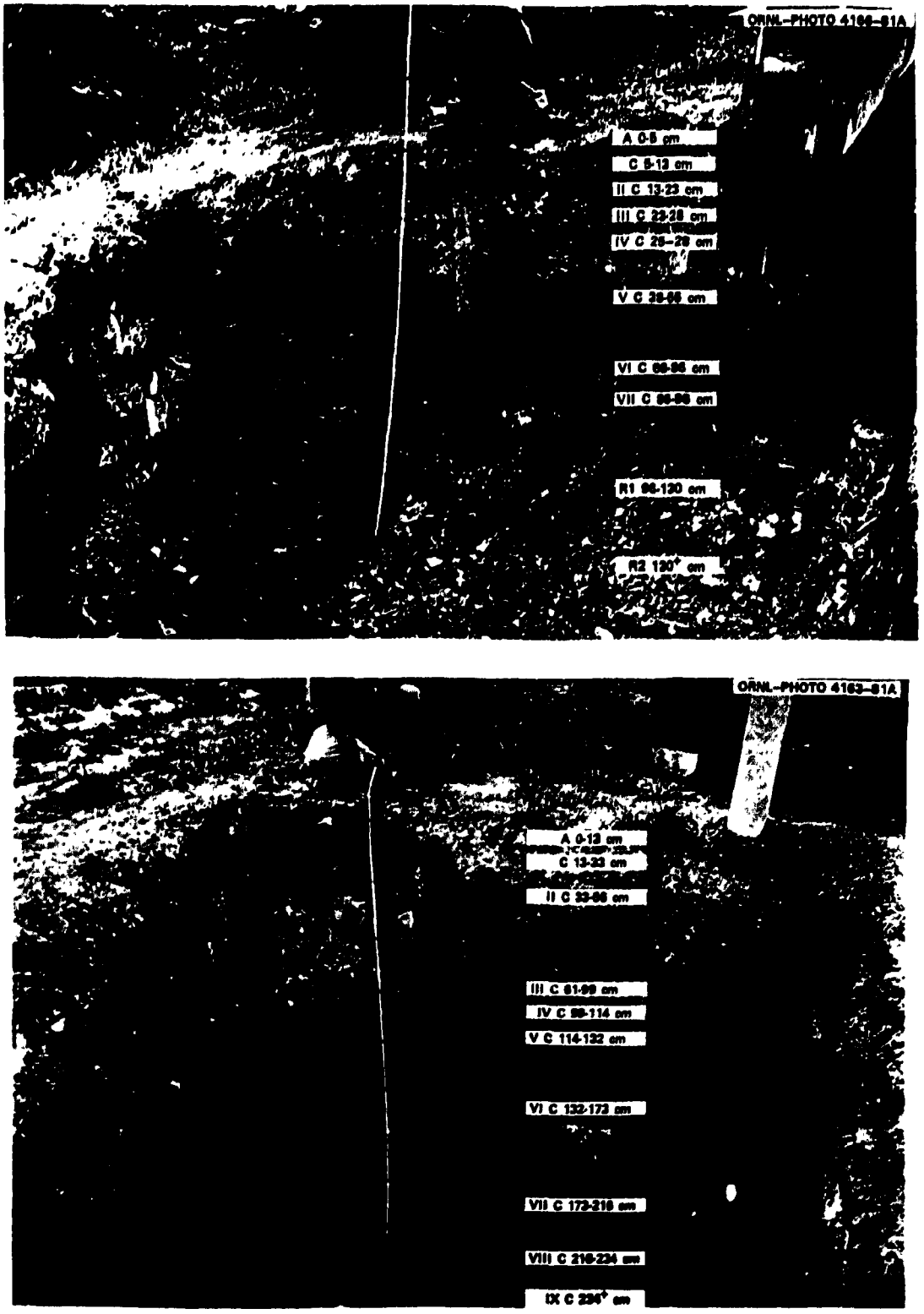

Fig. 21. Soil horizons and depths (cm) for the north wall of Trench 335 (top) and the south wall of Trench 338 (bottom).

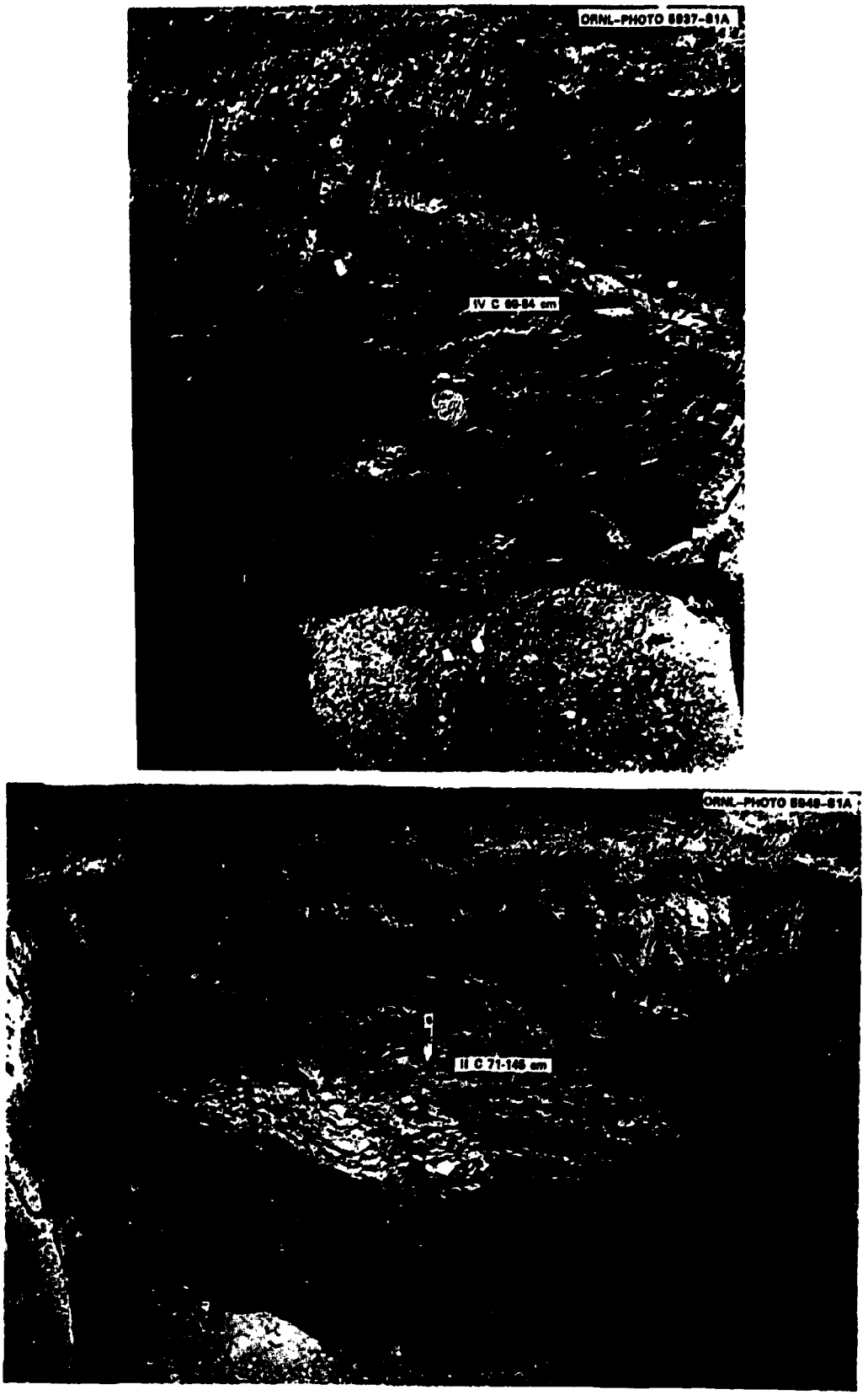

Fig. 22. Soil horizons and depths (cm) for the north (top) and south (bottom) walls of Trench 340.

Table 13. Physical properties of three soil profiles from the Engineered Test Facility site

Trench	Depth (cm)	Bulk density (Mg/m^3)	Total porosity (L/L)	Sand (%)	Silt (%)	Clay (%)
334	20	1.26	0.52	30	22	48
334	40	1.09	0.59	27	20	52
334	60	1.27	0.52	45	24	31
334	100	1.47	0.45	53	12	35
334	130	1.59	0.40	41	17	42
334	150	1.64	0.38	24	25	51
334	180	1.33	0.50	8	20	72
334	200	1.23	0.54	39	26	36
338	20	1.24	0.53	23	23	53
338	40	1.19	0.55	28	24	48
338	60	1.45	0.45	41	32	28
338	100	1.12	0.58	34	29	38
338	130	1.77	0.33	57	23	21
338	150	0.97	0.63	36	29	35
338	180	1.38	0.48	54	23	24
338	200	1.62	0.39	59	17	24
342	20	1.26	0.52	46	19	35
342	40	1.46	0.45	29	22	49
342	60	1.51	0.43	24	17	59
342	100	1.33	0.50	45	23	32
342	130	1.22	0.54	45	22	32
342	150	1.28	0.52	27	13	60
342	180	1.02	0.62	21	27	51
342	200	1.32	0.50	34	28	39
Mean		1.34	0.50	36	22	42
Standard deviation		0.20	0.0	13	4	13

bulk soil properties is manifested on such a small scale that it would be of only very limited use in the macro scale modeling of the site.

The textures presented in Table 13 represent only the particle sizes of the sample that could be attained by shaking the soil overnight in the sodium hexametaphosphate dispersing agent. Although such dispersion is generally adequate for most soils, the procedure will probably not disperse many aggregates of weathered shale and siltstone into their primary particles. Thus the sand fractions will be overestimated in these textures. These aggregates seem to be cemented with iron oxides, a condition that would make reducing agents, such as sodium dithionite, seem attractive for attaining the primary particles. Nonetheless, the reported textures are probably more useful because they represent water-dispersible aggregates; these would be the particle sizes subject to movement by soil erosion rather than the primary particles.

The field descriptions for the other three trench wall profiles are given in Tables 14 to 16. The generalized description of all profiles is that of a very shallow soil solum (A and B hori-

Table 14. Soil profile description of Trench 335 (north wall)

Horizon	Depth (cm)	Description
A	0–5	Brown (7.5 YR 4/6) silt loam; medium to coarse granular structure; moderately friable; pH = 4.8; many fine roots; smooth boundary
C	5–13	Finely laminated dull yellow-orange (10 YR 7/2) and dark brown (10 YR 3/2) weatherd siltstone; very coarse platey rock structure; pH = 5.0; few roots; smooth boundary
IIC	13–23	Dull orange (10 YR 7/4); weathered sandstone; very coarse platey rock structure; pH = 4.7; clay and iron oxide coating; few roots
IIIC	23–28	Finely laminated dull yellow-orange (10 YR 7/2) and dark brown (10 YR 3/3) weathered siltstone; very coarse platey rock structure; pH = 4.7; brown and brownish black iron and manganese coating; few roots
IVC	25–38	Brown (7.5 YR 4/4); silt loam; moderate, medium coarse granular structure; weathered platey siltstone fragments; firm; pH = 4.9; iron and manganese coating
VC	38–66	About same as IIIC; pH = 4.7
VIC	66–86	Dark reddish-brown (5 YR 3/4); other features of silt loam are same as IVC; pH = 4.9
VIIC	86–96	Finely laminated dull yellow-orange (10 YR 6/3) and brownish-black (10 YR 2/2) slightly weathered siltstone; very coarse platey rock structure; pH = 5.2; heavy manganese coatings
R1	96–130	Slightly weathered rock, undulating
R2	130^{+}	Rock

zons), even taking into account the material removed during site clearing. The underlying C horizons were highly leached (strongly acidic) and highly structured because of stratigraphic characteristics inherited from the bedrock. The soil's stratigraphic orientation was extremely variable in both dip and strike because of the folding and faulting present. The C horizon aggregates have iron and manganese hydrous oxide coatings appearing at shallow depth. Root penetration was generally not noted below 40 cm from the surface; the dense horizons and tight structure of the weathered rock must offer too much resistance to the displacement required for root growth.

The clay mineralogy of the selected soil samples is summarized in Table 17. In the silt fraction, considerable quartz and plagioclase were noted. Their abundance, however, cannot be quantitatively ranked, like the clay minerals in Table 17, because there are inherent differences in X-ray diffraction peak intensities influenced by particle size and orientation. As discussed in the Chemical Properties section (Sect. 4.2.2), the abundant vermiculite in these samples appears to be a weathering product of illite and chlorite. During and after sedimentation in the marine environment, both illite and chlorite minerals will form from swelling clays by uptake of potassium and magnesium, respectively. It should be noted that this is, at least, the second time these minerals have gone

Table 15. Soil profile description of Trench 338 (south wall)

Horizon	Depth (cm)	Description
A	0–13	Light brown (7.5 Y 5/6) silt loam; moderate medium to coarse granular; friable; pH = 4.7; many fine roots; smooth boundary
C	13–33	Light reddish-brown (5 YR 5/8) loam; moderate coarse granular to platey structure; firm; pH = 4.6; few roots; iron oxide coating
IIC	33–66	Light reddish-brown (5 YR 5/8) loam; highly weathered, finely laminated shale structure; firm; pH = 4.4; black manganese coatings; smooth boundary dipping 60°SE
IIIC	66–99	Dull yellow (2.5 YR 6/4) interbedded with light brown (2.5 YR 5/6) silt loam; highly weathered finely laminated shale structure; friable; pH = 4.4; very extensive manganese coating
IVC	99–114	Dark brown (7.5 YR 3/4) smeared color, loam; weak fine platey structure; friable; pH = 4.4; very extensive manganese coating and nodules
VC	114–132	Same as IVC but sand is finer; pH = 4.5
VIC	132–173	Light yellowish-brown (2.5 YR 6/6) sandy loam; highly weathered, finely laminated siltstone (rock structure was well preserved); friable; pH = 4.6
VIIC	173–216	Light yellowish-brown (2.5 Y 6/6) sandy loam; moderately weathered coarse siltstone; hard; pH = 5.3
VIIIC	216–234	Same as VC; pH = 5.0
IXC	234+	Olive brown (2.5 Y 4/4) fine sand; moderately weathered, fine sandstone; hard; pH = 5.5

Table 16. Soil profile description of Trench 340

Horizon	Depth (cm)	Description
IVC[a]	69–84	Brownish-black (7.5 YR 3/2) and orange (7.5 YR 7/6) silt loam; laminated, platey structure; moderately friable; pH = 5.3; heavy manganese coating; silt grains; no roots; clay filling fractures
IIC[b]	71–145	Dull yellow brown (10 YR 5/3) sand; medium to coarse structureless; friable; pH = 5.3; weathered sandstone; very little original structure preserved

[a]North wall.
[b]South wall.

Table 17. Mineralogy of silt and clay fractions of Engineered Test Facility soils

Sample	Size (μm)	Clay mineralogy
IV R2	<0.2	Illite > chlorite
IV R2	2–0.2	Chlorite > illite > vermiculite/smectite[a]
IV R2	45–2	Undifferentiated intergrades
IV R1	<0.2	Illite = chlorite
IV R1	2–0.2	Chlorite > illite > vermiculite/smectite
IV R1	45–2	Illite > chlorite > vermiculite/smectite
V IXC	<0.2	Illite > chlorite > smectite
V IXC	2–0.2	Illite > chlorite > nonswelling vermiculite
V IXC	45–2	Chlorite = vermiculite = illite
V IIC	<0.2	Illite > chlorite
V IIC	2–0.2	Chlorite > illite > nonswelling vermiculite
V IIC	45–2	Chlorite > vermiculite/smectite > illite

[a] / = interstratified association.

through soil genesis, because the Conasauga Group resulted from collection of eroded material from other soils.

Soils at the ETF site would be generally mapped in the Montevallo series (USDA 1981). These are shallow, well-drained upland soils formed from material weathered from acid shale. The solum (A and B horizons) of these soils is quite shallow (<50 cm), and the C horizon contains >35% coarse fragments. If the percentage of coarse fragments in the C horizon were <35%, then the soil would be in the Armuchee series. If the solum were >50 cm thick, then the soil would fall in the Sequoia series. All of Melton Valley would contain soils of the Armuchee-Montevallo-Hamblin association (USDA 1981). Soils in Melton Valley as it traverses the Clinch River to the southeast into Loudon County are mapped as the Litz-Sequoia-Lindside association (USDA 1961). Supposedly, this difference can be ascribed to a change in soil series nomenclature since the time Loudon County was surveyed. Whatever the nomenclature, the genetic description of the soils at the ETF is quite consistent. The soil family is a typic dystrochrept (USDA 1975). In everyday translation, this refers to a very strongly leached solum weathering from a rather highly leached parent material. It is classified as an inceptisol because the depth of the solum (i.e., the genetic horizons) is very limited. The frequent dissection of the slopes, on which these soils develop, leads to a comparatively unstable surface material, which erodes at a rate approximately equivalent to the rate of solum formation; hence, the solum remains shallow. If the C horizon were more weathered, that is, contained fewer coarse fragments, then the family classification would become an Ochreptic Hapludult (Armuchee series); this would be an ultisol because of the greater profile development, which, in turn, is facilitated by its location on more stable landforms. The modifier, Ochreptic, means that the soil tends to resemble an inceptisol but has adequate horizonization to be classified as an ultisol. The Sequoia series would be the extreme of this genetic sequence and classified as a typic Hapludult; here, the profile development is much advanced over the Armuchee series, and the

soil becomes more typical of the central concept of an ultisol. It should be pointed out that any soil mapping unit will contain areas that are more correctly described by other soil series; the mapping unit will contain mostly the indicated series, but genetic deviations are inherent.

4.2.3.4 Evaluation

The shallow depth of the soils at the ETF is indicative of their naturally high erosion rates even under natural vegetation. During the operational phases of SLB, careful soil management is required to avoid significant surficial erosion. The depth of paralithic contact is often within 1 m of the surface; lithic contact is usually within the saturated zone, that is, from 3 to 7 m below the surface. The depths of these transitions are often arbitrarily measured and depend on the judgment of the stratigrapher. One characteristic often used for differentiation is the first persistent appearance of shaly limestone within the core; this transition often occurs somewhat beneath the average water-table depth where weathering is, presumably, less severe. The groundwater and surface water quality showed a great influence of limestone interaction as evidenced by its hardness and alkalinity (see Hydrology, Sect. 4.3). Although the waste will be buried in the highly leached (i.e., limestone-free), unsaturated zone, all groundwater leaving the site will show a strong influence of limestone interaction. Conceivably, the hydraulic conductivities of the less weathered (limestone) saturated zone could be expected to be less than those of the highly leached unsaturated zone. This was apparently not the case (see Sect. 4.3). Thus although the chemical properties of these two zones can differ dramatically, the hydraulic properties do not exhibit the same differences.

Such properties as bulk density and porosity will be needed for site modeling. Mean values appear to be the most useful for this modeling because there were no apparent depth correlations for these parameters. Bulk densities greater than about 1.8 kg/L generally indicate an impermeable zone. No such horizons were noted at the ETF, indicating that a hydraulic continuity exists among the pedologic and paralithic zones. As discussed previously, the soil textures were also of very little value for ETF site characterization. Textures become very ambiguous as the strength of aggregates becomes great enough to obviate dispersion into primary particles. At other sites, texture would have considerable utility if applied to a formation with a deeper soil solum. At the ETF, practically all of the solum was removed during vegetation clearing, leaving only the nonplastic C and paralithic horizons. In general, textural discontinuities can be very informative about soil development at a site. Textures, determined by feel using an experienced hand, can be almost as accurate as laboratory determinations. They are, of course, much cheaper to measure and can be performed in the field.

Soil surveys can be extremely useful in site evaluation. Although soil series nomenclature is not particularly important per se, it does provide a genetic description of how the soils were formed. Recent soil surveys also contain considerable information on drainage, erodability, and suitability for various uses, such as sanitary landfills. Even if the sites under consideration have not been mapped recently, surveys can often be found for nearby and related areas with similar lithologies. Soil classification is particularly useful because it reflects the processes thought to be responsible for the soil formation. Such processes can indicate landform stability (an important component in planning for site closure) as well as rates of genetic development, that is, the chemical and physical processes active in the zone where the waste is to be buried. Much of this qualitative information will not enter directly into site modeling, but its consideration becomes more important in the long-term planning of the site.

4.3 HYDROLOGY

4.3.1 Climatic Factors

4.3.1.1 Background

The hydrologic characteristics of a region are determined largely by its geology and geography, with climate playing a dominant part. Among climatic factors that establish the hydrologic features of a region are the amount and distribution of precipitation; the occurrence of snow and ice; and the effects of wind, temperature, and humidity on evapotranspiration and snowmelt (Linsley et al. 1975). Perhaps the most critical of these climatic factors is precipitation. In its many forms, precipitation drives the hydrologic cycle and is thus of extreme importance to any level of site characterization. Like information on temperature, humidity, and wind speed and direction, statistics concerning precipitation at or near a potential disposal site are often available from the Environmental Data and Information Service of the National Oceanic and Atmospheric Administration (NOAA). Depending upon the location of the site of interest, this readily available data source is often all that is needed to adequately determine important climatic factors needed for site characterization and preliminary modeling.

The U.S. Nuclear Regulatory Commission has stated that meteorological data are needed primarily for three analyses: the determination of a site water budget; an analysis of airborne pathways; and the determination of the frequency, probability, and potential consequences of severe meteorological phenomena (Siefken et al. 1982). For analysis of the site water-budget and the airborne pathway, NRC recommends that the site characterization program include measurements of the amount, type, and temporal distribution of precipitation, dates and depth of frost penetration, and dates and thickness of snow cover. It also recommends that the program include continuous recordings of air and soil temperature, wind speed, wind direction, surface humidity, dew point, and atmospheric pressure. Air and soil temperatures are typically needed at several levels up to 1 m above or below the ground surface, respectively. Further, NRC states that atmospheric stability is typically estimated from wind speed and wind direction fluctuations at about 2 and 10 m; these parameters should be measured continuously at both levels.

For purposes of the ETF site characterization and hydrologic model construction, monitoring efforts have focused on amount and intensity of precipitation. Local climatological data summaries, such as the one published for the NOAA monitoring station in Oak Ridge, Tennessee (DOC 1981), were judged adequate in providing much of the additional meteorological data recommended by NRC. Because of the close proximity of the Oak Ridge and ETF monitoring stations, it would not be cost-effective to establish a second meteorological station at the ETF site to collect similar data.

4.3.1.2 Methods

Precipitation measurements at the ETF site are made using a Belfort Instrument Company 30-cm dual-traverse rain gauge (Model 9432) (Fig. 23). The location of the instrument relative to the experimental trenches and monitoring wells is shown in Fig. 4. The rain gauge is serviced once each week according to manufacturer's operating instructions. Maintenance consists of changing the 8-d chart paper, winding the clock, and emptying the collection/weighing bucket. The instrument is designed to record both the amount and the intensity of precipitation on a continuous basis by weighing the collected rainfall, and it has experienced only minimal downtime, usually due to extremely low temperatures.

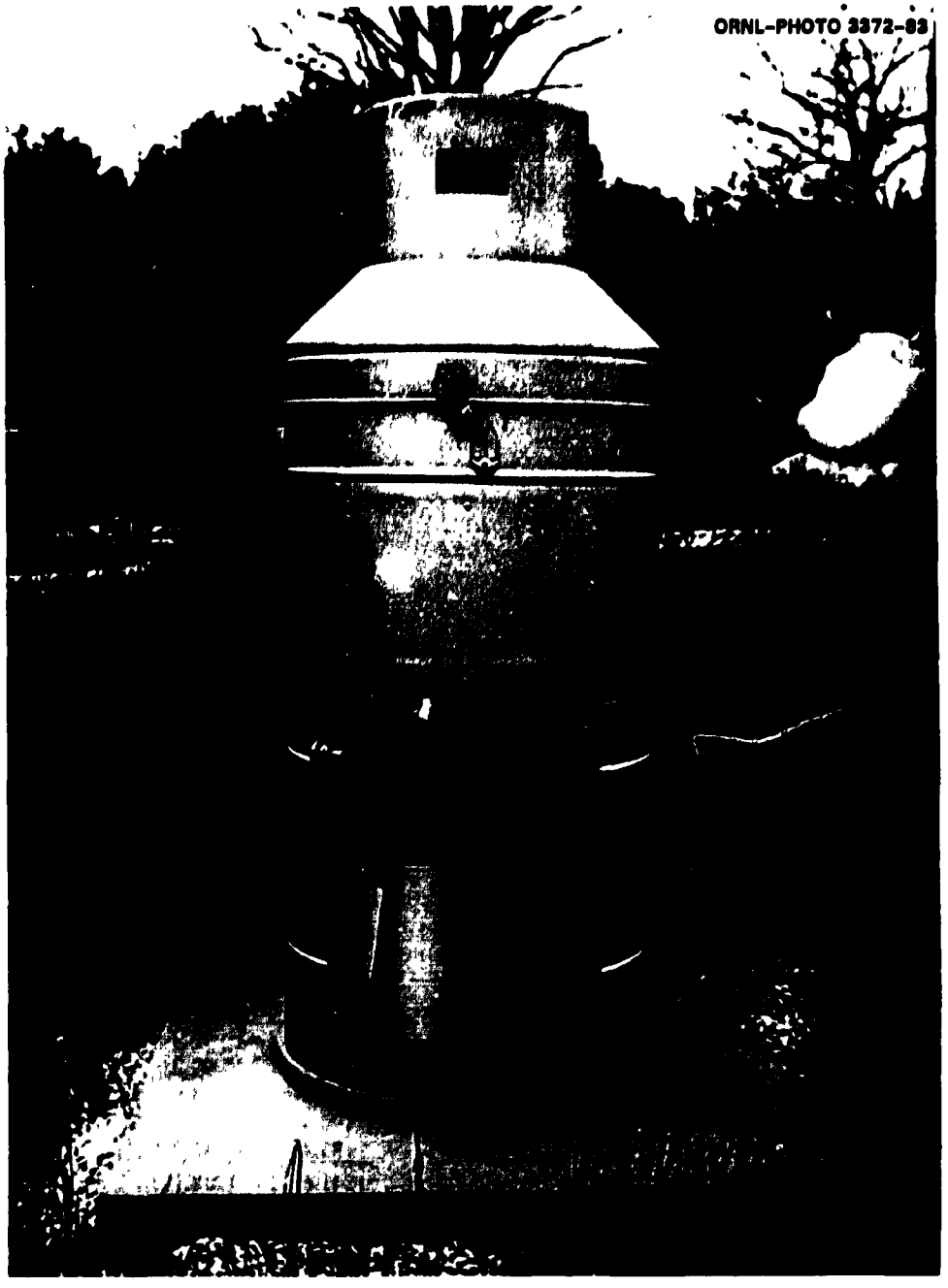

Fig. 23. Rain gauge located at the Engineered Test Facility site.

4.3.1.3 Results and discussion

Precipitation data have been collected at the ETF site since August 11, 1980. Tables in Appendix C present daily summaries for the 32-month period spanning August 1980 to March 1983. Monthly precipitation summaries for this same period of record are shown in Table 18. Also included in the table are data from the nearby precipitation monitoring station located in Oak

Table 18. A comparison of precipitation data collected at the Engineered Test Facility (ETF) and the Oak Ridge sites

Month	ETF site (mm)	Record mean[a] (mm)	Oak Ridge site (mm)	Record mean[b] (mm)
		1980		
Aug	35.6[c]	81.3	52.6	96.3
Sep	68.6	88.1	84.1	92.2
Oct	45.1	64.5	27.4	74.9
Nov	102.9	93.0	115.6	116.1
Dec	45.7	138.7	51.3	141.0
Total	297.9[c]	465.6	331.0	520.5
		1981		
Jan	23.5	117.1	23.6	137.4
Feb	123.2	128.0	119.1	120.6
Mar	69.9	140.7	91.2	153.9
Apr	95.2	108.2	116.3	109.0
May	101.6	82.8	67.3	106.4
Jun	117.5	97.0	114.3	105.2
Jul	73.0	127.8	61.5	135.1
Aug	73.6	81.3	79.0	96.3
Sep	71.1	88.1	99.1	92.2
Oct	92.1	64.5	124.2	74.9
Nov	76.2	93.0	81.3	116.1
Dec	104.8	138.7	104.6	141.0
Total	1021.7	1267.2	1081.5	1388.1
		1982		
Jan	158.8	117.1	170.2	137.4
Feb	126.4	128.0	137.7	120.6
Mar	159.4	140.7	157.5	153.9
Apr	59.7	108.2	70.9	109.0
May	48.9	82.8	89.4	106.4
Jun	67.9	97.0	54.6	105.2
Jul	134.0	127.8	178.0	135.1
Aug	89.5	81.3	117.1	96.3
Sep	62.2	88.1	134.9	92.2
Oct	60.3	64.5	49.5	74.9
Nov	153.0	93.0	198.4	116.1
Dec	175.3	138.7	183.4	141.0
Total	1295.4	1267.2	1541.6	1388.1
		1983		
Jan	38.1	117.1	44.4	137.4
Feb	105.4	128.0	111.0	120.6
Mar	54.6	140.7	65.3	153.9
Total	198.1	385.8	220.7	411.9

[a]Mean [illegible] based on data taken from the Oak Ridge National [illegible]atory (ETF) site for the period 1951 thr[illegible]

[illegible] based on data taken from the Oak Ridge site [illegible] through 1981.

[illegible] began operation on August 10, 1980. Nu[illegible]e low due to missing data covering the perio[illegible] through 10.

Ridge, Tennessee (DOC 1981). These data have been included so that one can see the variability in precipitation totals that occurs between relatively close (approximately 14 km) monitoring stations. For example, in July 1982 total precipitation recorded at the ETF gauge was 134 mm, whereas the total at the Oak Ridge station was 178 mm, 33% higher. Many of these monthly discrepancies can be attributed to localized thundershower activity.

In general, the precipitation data collected at the ETF site show lower than average rainfall for the last 5 months of 1980 and also for calendar year 1981. Total rainfall for 1981 was 1021.7 mm, 19% lower than the annual average of 1267.2 mm reported by NOAA (DOC 1972) for the ORNL site. Total rainfall at the ETF for calendar year 1982 was higher than for 1981 (1295.4 mm), only 2% higher than the annual average. Figure 24 illustrates monthly precipitation totals measured at the ETF site for calendar years 1981 and 1982. For comparison purposes monthly averages based on 33 years of record (1948–1981) at the Oak Ridge site have been included. A simple comparison of bar heights in Fig. 24 reveals that 1981 was a drier-than-average year, with only February, June, and October exceeding expected monthly averages. In contrast, 1982 exhibited 5 months in which expected monthly averages were exceeded.

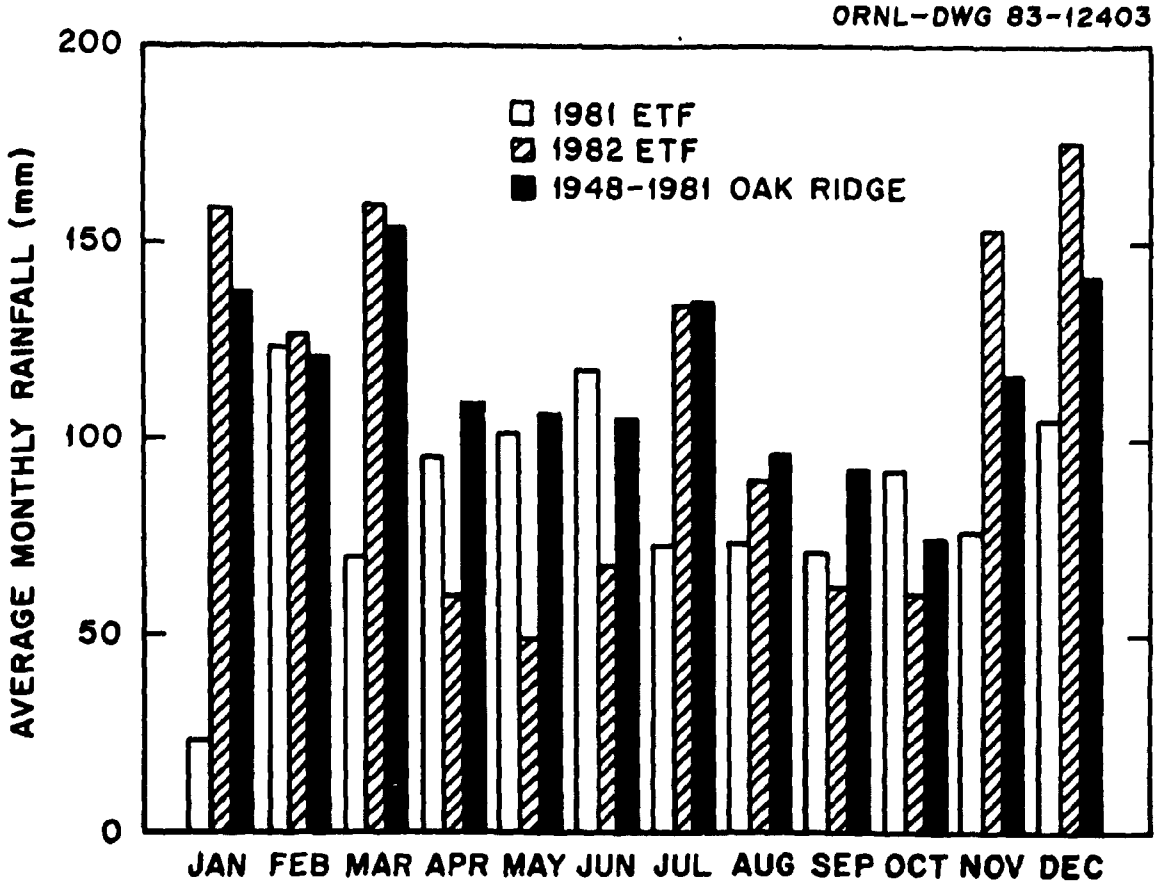

Fig. 24. Monthly rainfall for the Engineered Test Facility (ETF) site, 1981 and 1982.

4.3.1.4 Evaluation

The purpose of monitoring precipitation at a potential LLW disposal site is to gather background site characterization information that can be used in developing a hydrologic model of the site. Depending on the resolution of the model (i.e., is the model concerned with a 1-ha site or a 10,000-ha site), more than one rainfall monitoring station may be required. In the case of the ETF, the relatively small area (approximately 1 ha) warranted the use of a single monitoring station, the results from which could easily be compared to existing monitoring stations at ORNL and Oak Ridge. Trends in data obtained from the ETF monitoring station correlate well with those from other precipitation monitoring stations in the vicinity and have been a useful site characterization resource.

4.3.2 Surface Water Hydrology

4.3.2.1 Background

In characterizing a potential LLW disposal site, both the quality and the quantity of surface water are important. The quality of surface drainage is determined through a water sampling and chemical analysis program, while the quantity of drainage is determined through hydrologic studies. Depending on the size of the site in question, this surface water hydrology study can be quite complex. Aerial photography and topographic mapping of the site may be necessary to locate features such as drainage divides, size of drainage areas, surface gradients, and streams draining the site. Estimates of runoff coefficients; infiltration rates; and channel slope, cross section, and roughness may need to be made in order to model the response to various rainfall events as well as to calculate expected water heights during flood conditions. Many of these site-specific characteristics are endorsed by NRC (Siefken et al. 1982) in addition to more regional considerations, such as examination of users of surface water, adjacent municipal water supplies, and water rights.

In characterizing the surface water hydrology at the ETF, several of the above-mentioned study areas do not apply. For example, because the site is located on a hillock within a region of East Tennessee characterized by ridges and valleys (elevation of 236–244 m above MSL) and the lengths of each of the two streams draining the site are less than 100 m, the issue of flooding becomes trivial (Fenneman 1938). Also, because the ETF is located on federal land, within a portion of an existing DOE LLW disposal site, the issue of uses of surface water by industries or adjacent municipalities becomes less important. With this in mind, characterization of the surface water hydrology at the ETF site has focused on the relevant issues of measurement of surface infiltration, measurements of storm-induced flow in drainage channels, and chemical analysis of samples taken from drainage channels.

4.3.2.2 Methods

Surface drainage flow measurements. Two Parshall flumes (I and II), equipped with automated flow meters (Manning Inc. Model F-3000A) and flow-proportional water samplers (Manning Inc. Model S-4040), were placed in the two channels that drain the ETF to measure the amount of water that runs off the site and to establish points for collecting samples for chemical analyses. The locations of the two flumes are shown in Fig. 4, while Figs. 25 and 26 are photographs of each station, showing flume positioning and associated water-level monitoring and sampling equipment.

To ensure that shallow subsurface flow moving in the stream channels is included in the water-budget accounting (i.e., is forced to flow through the flume where it can be measured), a polyvinyl

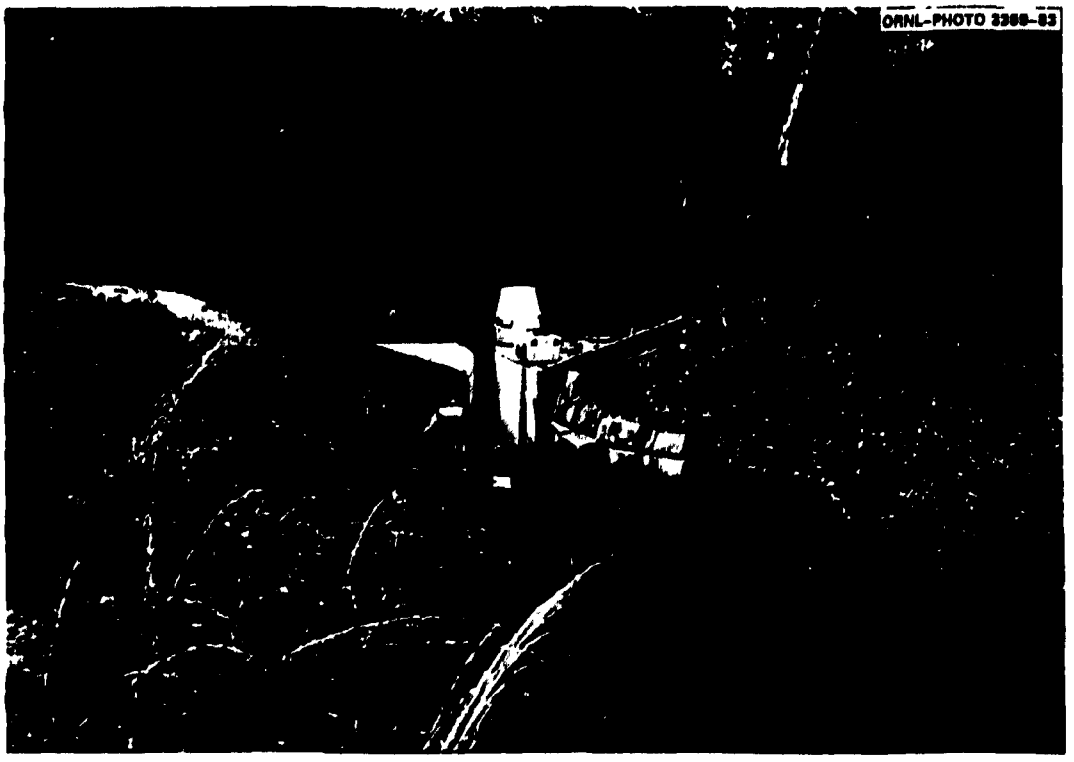

Fig. 25. Surface water monitoring Station I.

Fig. 26. Surface water monitoring Station II.

chloride (PVC) liner was used in construction to form a cutoff wall or barrier to subsurface flow. During excavation it was placed approximately 2 m below the channel bottom at a location about 4 m upstream of each flume. Subsurface flow is thereby preferentially directed through the flumes rather than under or around them. A summary of design statistics related to Flumes I and II is presented in Table 19.

Table 19. Summary of statistics for Engineered Test Facility Flumes I and II

Parameter	Flume I	Flume II	Parameter	Flume I	Flume II
ORNL coordinates			Flow range[a]		
North	16,564.3	16,639.7	Maximum, L/s	252	252
East	23,598.0	23,786.4	Minimum, L/s	2.5	2.5
Drainage area, ha	0.65	0.88	Observed flow		
			Maximum, L/s	57.8	50.8
Upstream channel			Minimum, L/s	0	0
length, m	60	100			
Throat width, cm	22.9	22.9			

[a]Range of measurable flows in a Parshall flume with a 22.9-cm throat.

Table 19 shows that the operating range for Parshall flumes with a 22.9-cm throat width is from 2.5 to 252 L/s (a differential of a factor of 100) which corresponds to a depth of water in the approach ranging from 3 to 61 cm. This wide measuring range and high maximum flow measurement capability make these flumes excellent for measuring flow resulting from extreme precipitation events occurring at the ETF site. For example, the highest recorded flow through each flume occurred on May 30, 1981, and was measured at 57.8 L/s for Flume I and 50.8 L/s for Flume II. These peak flows are approximately 22% of the 252 L/s maximum design flow for these particular flumes. Thus it is quite unlikely that the maximum flow in the drainage channels will ever exceed the flow measurement capacity of the flumes.

Surface water sampling. A surface-water sampling and chemical characterization program was initiated that includes periodic sampling at each of the two flume sites. A mixture of flow-proportional and grab samples from the two streams has been taken since construction of the flumes was completed in 1980. Samples of surface water are included with groundwater sample sets and are analyzed for the same chemical parameters of interest listed in Appendix F.

Surface infiltration. Not all the precipitation that falls on a watershed will result in direct runoff. A portion of the precipitation will be intercepted and/or transpired by vegetation, evaporate from the ground surface, or infiltrate the soil and either be held by capillary forces or enter the underlying aquifer. The percentage of rainfall that infiltrates the surface is by no means constant; it changes with such seasonal variables as soil moisture and vegetative cover. To adequately define surface infiltration, one might take the approach of measuring infiltration rates under a variety of soil moisture conditions that may relate to different seasonal conditions. In this manner a relationship between infiltration and soil moisture conditions for a particular site could be established. In addition, infiltration could be estimated indirectly from runoff coefficients. A series of runoff coefficients for a watershed could be determined over some period of time; and from these data an average runoff coefficient for various seasons, or other appropriate intervals of time, could be deter-

mined. Surface infiltration could then be calculated as the amount of rainfall to fall on the watershed less the measured volume of runoff. Regardless of how surface infiltration rates are derived, they are important components of the site water-budget.

To determine rainfall infiltration rates at the ETF site, a group of six infiltrometers were installed around the site at locations shown in Fig. 45. Two of the infiltrometers were located outside the matrix of experimental trenches, on relatively undisturbed soil with established grass cover, and four were placed between trenches on the site cover material. The method of determining rate of water intake under saturated conditions using two concentric cylinders was followed (Bertrand 1965).

During March 1983, surface infiltration testing was initiated. Each of the six infiltrometers was periodically filled with water for several days before testing to ensure saturated conditions in the vicinity of the infiltrometers. Three infiltration tests were conducted during the 4-d period from March 4 to March 8. Each test consisted of filling the center of the two concentric steel rings (diameter = 40.6 cm) with water to a depth of approximately 15 cm. The fall in head was then monitored for a 1-d period or until the water level in the center ring dropped to below 5 cm. By using this technique, several infiltration rates could be calculated at a single station at the ETF, and the geometric mean infiltration rate for the six stations could be used as an estimate of overall site infiltration.

4.3.2.3 Results and discussion

Surface drainage flow measurements. The two Parshall flumes located at the ETF site were put into service in October 1980. For the 30-month period of record, including October 1980 to March 1983, 60 runoff events were recorded at Flume I, and 121 events at Flume II. The discrepancy in the number of recorded runoff events is attributed to the difference in size of the drainage areas and the difference in length of time the two flow recording devices were out of service. Because the drainage area (0.65 ha) contributing to flow at Flume I is smaller than the area (0.88 ha) contributing to flow at Flume II and because the flow recording device monitoring flow through Flume I has been less reliable, half the number of runoff events have been recorded at Flume I. Appendix D tables summarize each of the runoff events recorded at the ETF site.

The data presented in these tables indicate that the maximum discharge measured at Flumes I and II during storm activity was 57.8 and 50.8 L/s, respectively. Mean peak discharge for the 30-month period of record was 10.5 L/s for Flume I and 10.0 L/s for Flume II, with standard deviations of 11.8 and 10.9 L/s, respectively. These peak runoff values are being correlated with precipitation data so that expected maximum flows can be assigned for various amounts or classifications of precipitation. This type of information is essential to the site water modeling effort.

In addition to peak discharge, tables in Appendix D also list the flow recovery time, which is defined as the time required for flow in the channel to return to base flow conditions following occurrence of peak runoff. This recovery time is obviously dependent upon soil moisture conditions, which are generally a function of the time since the previous rainfall event and range from less than 10 min for short, intense rainfall events to 36 h for longer, less intense events. These rather short recovery times are characteristic of small headwater streams draining relatively small watersheds.

Correlation between flow at either flume and the rain total at the gauge for individual events is evident. For purposes of illustration, two separate storm events were selected as representative of runoff conditions during winter periods, when vegetation is dormant, and during summer, when

vegetation is growing. The two events occurred in November 1980 and in June 1981. The hydrographs shown in Figs. 27 and 28 are representative of winter and summer rainfall and runoff at areas 1 and 2 (Fig. 29) A simple hydrograph separation of quick flow and delayed flow indicates that over 60% of the precipitation that fell on subcatchment area 1 and about 46% of the rainfall in area 2 were discharged as quick flow (Fig. 27). During the early summer event (Fig. 28) in June 1981, the quick flow at area 1 was about 43% of rainfall. At area 2, quick flow was only 29% of rainfall.

Examination of the hydrograph in relation to observed rainfall shows that area 1 is quite responsive, as would be expected on shallow soils with sparse grass cover. A very short lag time (~15 min) exists between peaks in rainfall and corresponding runoff. The amount of rainfall that runs off as quick flow corresponds well with simulated values (about 50% during November) for a grassed area on Montevallo soils. There is an obvious delay and reduction in peak flow for area 2. This could result from the impoundment of water (from over 90% of the sub-basin) in the swale

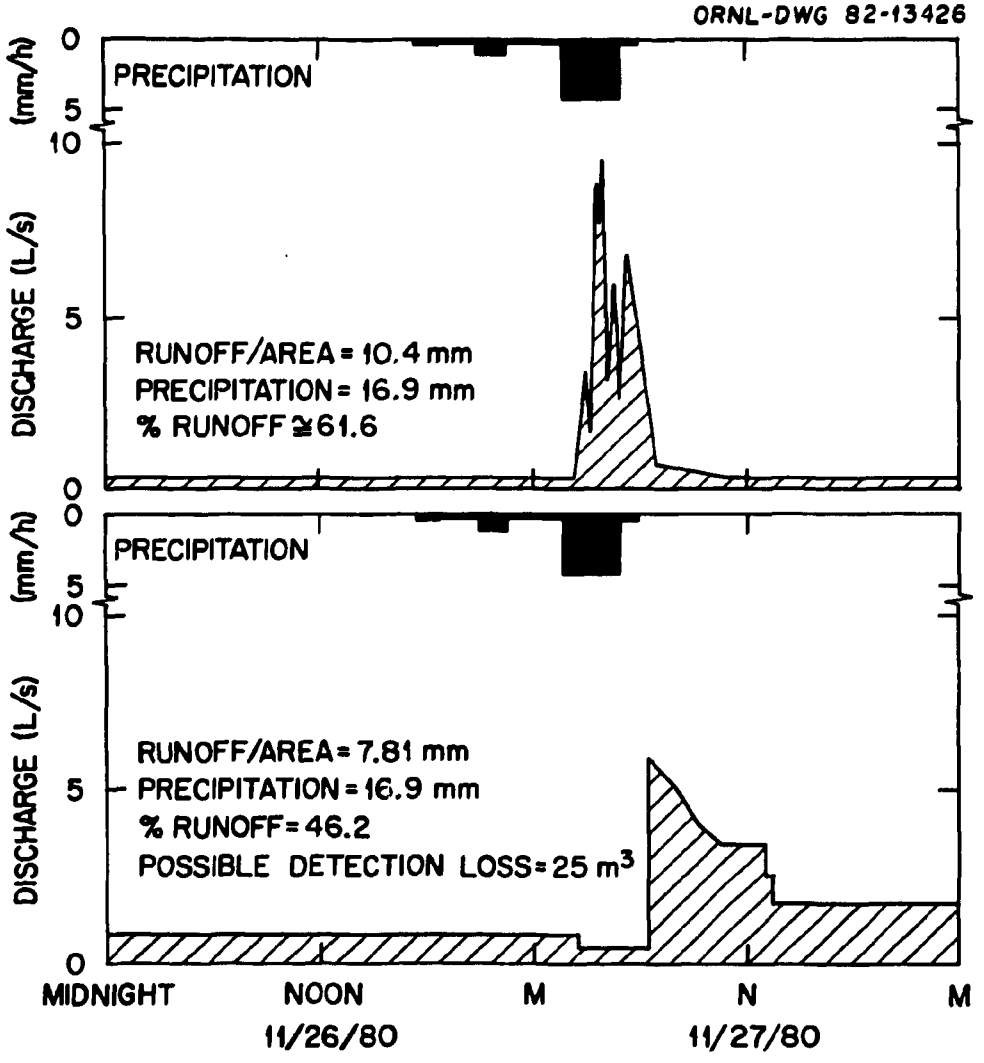

Fig. 27. Flume hydrographs for a winter storm event (top, area 1; bottom, area 2).

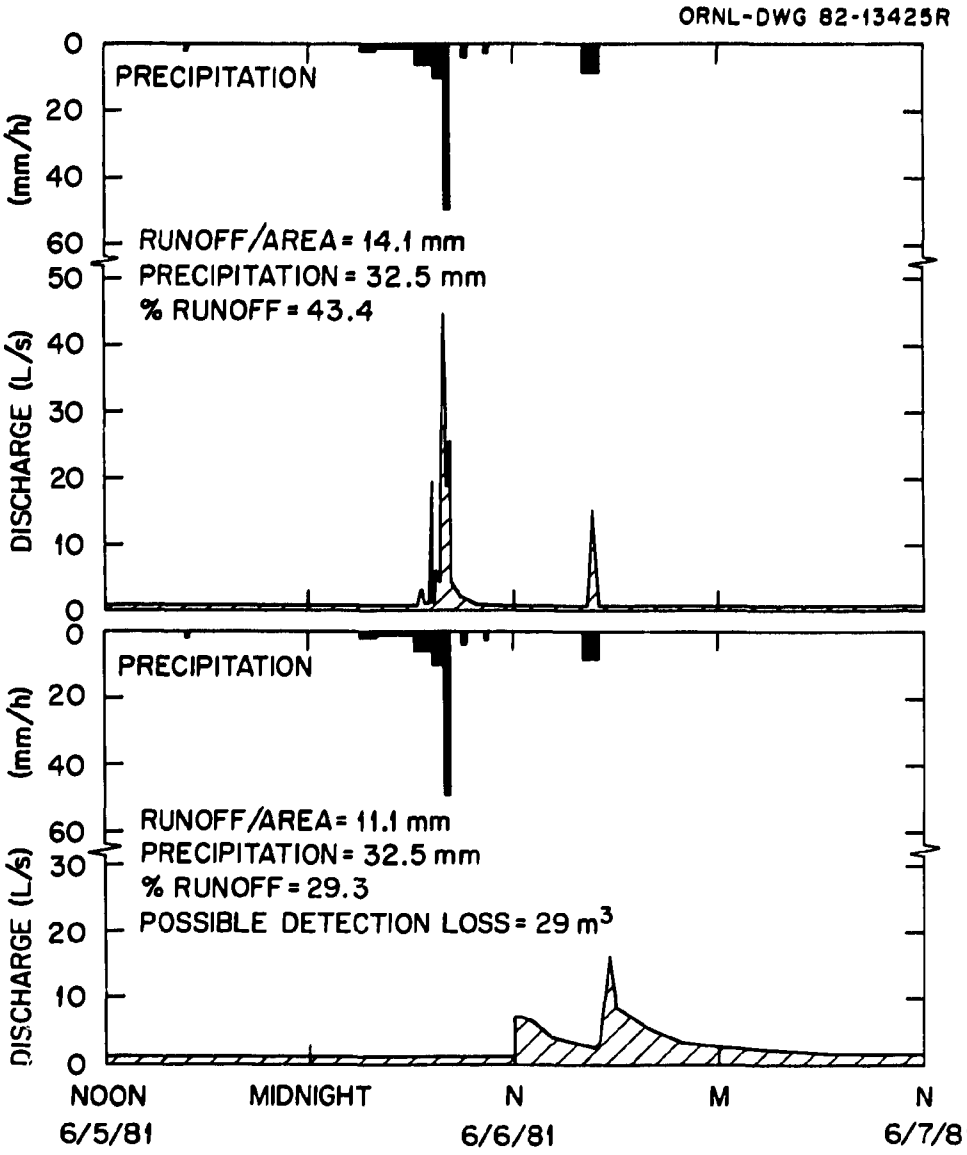

Fig. 28. Flume hydrographs for a summer storm event (top, area 1; bottom, area 2).

above the point where the access road crosses the stream channel (Fig. 29). Water is released from the swale via a culvert pipe, but not until a sufficient pool has accumulated to raise the water above the base of the pipe (elevation = 236.78 m). For the two storms examined, this amounts to about 25 to 30 m^3 of water, assuming uniform runoff per unit area for both catchments. Apparently the initial runoff is impounded and lost via later seepage and evaporation. In addition, the pool causes an attenuation of peak flows, even after runoff through the culvert has been established.

Between rainfall events, especially during the dry months of the year, flow in the two channels approaches zero. Under these conditions flow is less than the minimum detectable flow rate (2.5 L/s) for the Parshall flume, and data collected from the automated flow meters become meaningless. To quantify the flow during these dry months, periodic bucket gauging of flow

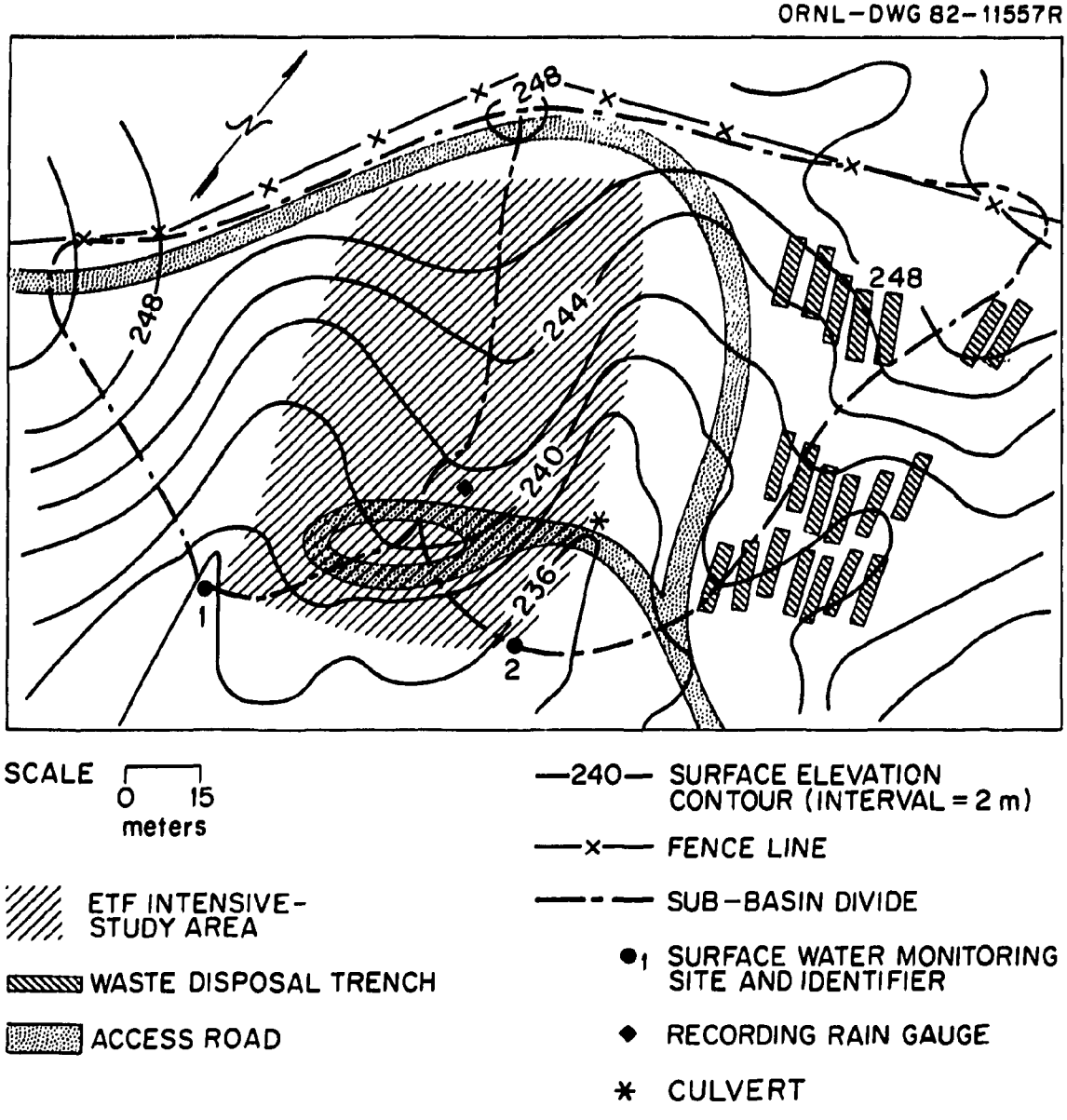

Fig. 29. Map showing location of the flumes and rain gauge and the delineation of drainage basins.

through the two flumes is carried out. Table 20 summarizes flow measurements taken using this method for April and May of 1983.

Although the streams were not dry during this period of time, flow was quite low, on the order of 0.04 L/s. This is approximately 60 times lower than the flume minimum design flow and would result in a total of only 3500 L of water passing through the flume in a day. This same volume could pass through the flume in 6 min during an average storm event with peak runoff of 10 L/s. Thus only a trivial amount of water drains from the ETF site under dry weather conditions.

Surface water sampling. Water quality and radionuclide analyses (see Appendix F) were performd once a quarter to determine baseline conditions at the site. In addition to these quarterly

Table 20. Summary of low flow measurements taken at the Engineered Test Facility site[a]

Date	Flume I (L/s)	Flume II (L/s)
04-18-83	0.08	0.14
04-22-83	0.04	0.05
04-25-83	0.06	0.09
04-26-83	0.04	0.05
04-29-83	0.04	0.04
05-02-83	0.04	0.03
05-03-83	0.07	0.06
05-06-83	0.04	0.03

[a]Flow was measured using the bucket gauge method.

samples, weekly grab samples have been collected and routinely monitored for pH and electrical conductivity, two simple measurements that can be used to detect changes in water quality (Table 21). Missed samplings were due in part to equipment problems and/or the lack of water to sample. The analyses generally indicate surface runoff from a mixed carbonate and siliceous terrane (Hem 1959). As expected, however, the water quality varied somewhat due to natural and anthro-

Table 21. Electrical conductivity (EC) and pH of runoff samples collected at the Engineered Test Facility site

Date	Flume I		Flume II		Date	Flume I		Flume II	
	pH	EC (μS/cm)	pH	EC (μS/cm)		pH	EC (μS/cm)	pH	EC (μS/cm)
04-24-81	6.6	320	6.9	260	01-04-83	7.1	169	7.6	367
08-11-81	7.0	240	6.7	*a*	01-11-83	7.0	150	7.4	365
06-28-82	7.4	*a*	7.2	*a*	01-18-83	6.8	160	7.1	382
07-06-82	7.8	*a*	7.7	*a*	01-25-83	7.4	128	7.5	310
07-12-82	7.2	406	7.4	392	02-01-83	7.2	145	7.5	370
07-26-82	7.9	246	8.1	380	02-08-83	6.9	110	7.2	262
08-02-82	7.8	399	8.2	422	02-15-83	7.2	133	7.4	313
08-16-82	7.4	316	7.2	558	02-22-83	7.3	160	7.4	390
08-23-82	7.3	288	7.5	524	03-01-83	7.3	159	7.3	380
09-08-82	8.3	263	8.0	536	03-08-83	7.3	170	7.3	381
09-22-82	7.6	273	7.5	526	03-15-83	7.3	170	7.5	405
11-16-82	7.3	219	7.6	509	03-22-83	7.0	152	7.0	373
11-30-82	7.5	276	7.5	513	03-29-83	7.1	167	7.3	391
12-07-82	7.4	293	7.6	499	04-06-83	6.7	102	7.2	265
12-14-82	7.1	150	7.4	350	04-12-83	7.2	165	6.9	370
12-21-82	6.8	150	7.3	333	04-19-83	7.1	170	7.2	380
12-28-82	7.2	100	7.4	250	04-26-83	7.2	172	7.3	385

[a]Measurement not made.

pogenic input. For example, vegetation surrounding the flumes was different: Flume I is located in a stand of trees and thus receives leaf litter; Flume II is in a grassed area, receiving no leaf litter. Algae were also present at times in the vicinity of the flumes. Additionally, construction being carried on at the site, such as trench excavation and well drilling, had an impact on the water quality as sediment and cuttings were transported to the flumes. Another possible source of variation in water quality between streams is the application of fertilizer which likely causes elevated nitrogen (nitrate) levels, particularly in the spring.

The radionuclide analyses for the two flumes showed very different results. For both surveys Flume I water samples did not have any of the radionuclides (^{3}H, ^{137}Cs, ^{60}Co, ^{90}Sr, and gross-alpha) in quantities above background. Except for ^{3}H, water from Flume II yielded the same results. The ^{3}H levels were on the order of 10^{3} to 10^{4} Bq/L, and the tritium probably originates in the eastern portion of the drainage area, which has been used for waste burial (Fig. 29). To check the validity of the quarterly results and obtain more detailed information, a series of water samples was taken from Flume II at shorter intervals. Analytical results are shown in Table 22. A comparison of ^{3}H concentration and the precipitation record at the same times and dates indicates a dilution of ^{3}H-containing groundwater with surface runoff. The May 30-1705 sample registered $<1 \times 10^{2}$ Bq/L ^{3}H and was taken in a 15-min interval in which 15.2 mm (0.6 in.) of rain fell. Apparently the volume of runoff diluted the concentration of ^{3}H, because within 75 min the count returned to the 10^{3} Bq/L level, at which time the rainfall rate had slackened considerably. The actual mechanism may be related to the mixing of runoff with shallow subsurface flow; however, more work is required to better understand this phenomenon. In any case, results clearly demonstrate the importance of detailed monitoring of surface runoff in the study of contaminant migration.

Surface infiltration. Results of three surface infiltration tests conducted at six locations on the ETF site are summarized in Table 23. Data are in units of centimeters per second and were calculated using the following equation:

$$I = \frac{S}{A}, \tag{9}$$

where

I = saturated surface infiltration rate (centimeters per second),
S = slope of the line with abscissa equal to time and ordinate equal to a summation of the change in water volume in the inner ring as a function of time (cubic centimeters per second),
A = area of the inner ring (square centimeters).

Generally, the line from which the slope S is derived tends to exhibit curvature near the origin (Philip 1957), especially if the test is not initiated near saturated conditions. As time progresses, the line straightens and infiltration slows to a constant rate. An example of infiltration data taken from ring 6 is shown in Fig. 30.

The data in Table 23 are perhaps bests summarized by differentiating between the two infiltrometers located on the undisturbed soil (1 and 2) and the four infiltrometers located on the cover material between the experimental trenches (3, 4, 5, and 6). The geometric mean infiltration rate for the undisturbed soil was 1.56×10^{-5} cm/s, while that of the cover material was 13.3×10^{-5} cm/s. The mean for the undisturbed soil compares well with similar data from

Table 22. Radionuclide analysis for Flume II water samples (Bq/L)

Time and date	^{3}H	^{137}Cs	^{60}Co	Gross-alpha	^{90}Sr
1100					
03-16-81	25,000 ± 1,000	<0.5	<0.7	3.8 ± 4.9	0.21 ± 0.34
1300					
03-23-81	24,000 ± 1,000	<0.4	<0.5	2.5 ± 2.8	0.18 ± 0.36
0900					
03-30-81	11,000 ± 1,000	<0.3	<0.5	3.1 ± 4.6	0.20 ± 0.36
0050					
04-05-81	4,700 ± 200	<0.8	11 ± 2	3.8 ± 4.7	0.18 ± 0.36
0350					
04-05-81	8,900 ± 300	<0.5	<0.4	1.1 ± 2.8	0.24 ± 0.43
1200					
04-07-81	1,700 ± 100	<0.4	0.52 ± 0.45	2.2 ± 4.3	0.11 ± 0.40
1250					
04-14-81	21,000 ± 1,000	<0.5	0.71 ± 0.67	4.4 ± 5.1	0.45 ± 0.44
0010					
04-20-81	4,500 ± 200	<0.6	<0.8	5.9 ± 4.5	0.27 ± 0.42
1050					
04-20-81	5,400 ± 300	<0.3	<0.5	3.8 ± 4.8	0.77 ± 0.73
1430					
04-20-81	9,400 ± 300	<0.3	<0.4	1.1 ± 2.8	0.08 ± 0.33
1520					
04-20-81	11,000 ± 1,000	<0.5	<0.6	4.0 ± 4.3	0.51 ± 0.43
1340					
04-27-81	20,000 ± 1,000	<0.5	0.9	2.4 ± 3.8	0.29 ± 0.44
0930					
05-04-81	21,000 ± 1,000	<0.6	<0.8	5.4 ± 5.7	0.35 ± 0.41
1325					
05-11-81	20,000 ± 1,000	<0.6	<0.7	3.9 ± 3.6	0.28 ± 0.41
1310					
05-18-81	3,100 ± 200	0.39 ± 0.33	0.63 ± 0.42	4.3 ± 5.2	0.38 ± 0.47
1300					
05-25-81	15,000 ± 1,000	0.54 ± 0.35	<0.4	2.4 ± 4.3	0.01 ± 0.02
1033					
05-26-81	15,000 ± 1,000	<0.5	<0.7	5.2 ± 5.5	0.37 ± 0.43
2015					
05-27-81	2,900 ± 200	<0.5	<0.6	2.7 ± 3.0	0.25 ± 0.44
1705					
05-30-81	<100	<0.4	<0.4	4.0 ± 4.9	0.13 ± 0.39
1830					
05-30-81	2,100 ± 200	<0.3	<0.4	2.2 ± 3.5	0.90 ± 1.2
0240					
05-31-81	4,000 ± 200	<0.5	<0.6	2.9 ± 3.6	0.12 ± 0.36
0545					
06-02-81	10,000 ± 1,000	<0.6	<0.7	4.4 ± 6.0	0.20 ± 0.39

Table 23. Surface infiltration measurements under saturated conditions, (cm/s) × 10^{-5}

Method of flooding using concentric steel rings[a]

Test	Infiltrometer					
	1	2	3	4	5	6
1	*b*	3.78	14.7	27.9	11.2	8.4
2	2.78	0.85	9.93	28.1	11.5	8.76
3	1.72	0.61	6.36	40.6	13.0	8.54

[a]*Source:* A. R. Bertrand, "Rate of Water Intake in the Field," in *Methods of Soil Analysis*, Pt. 1, *Agronomy* 9, 197–209, American Society Agron., Madison, Wis.

[b]Measurement not made.

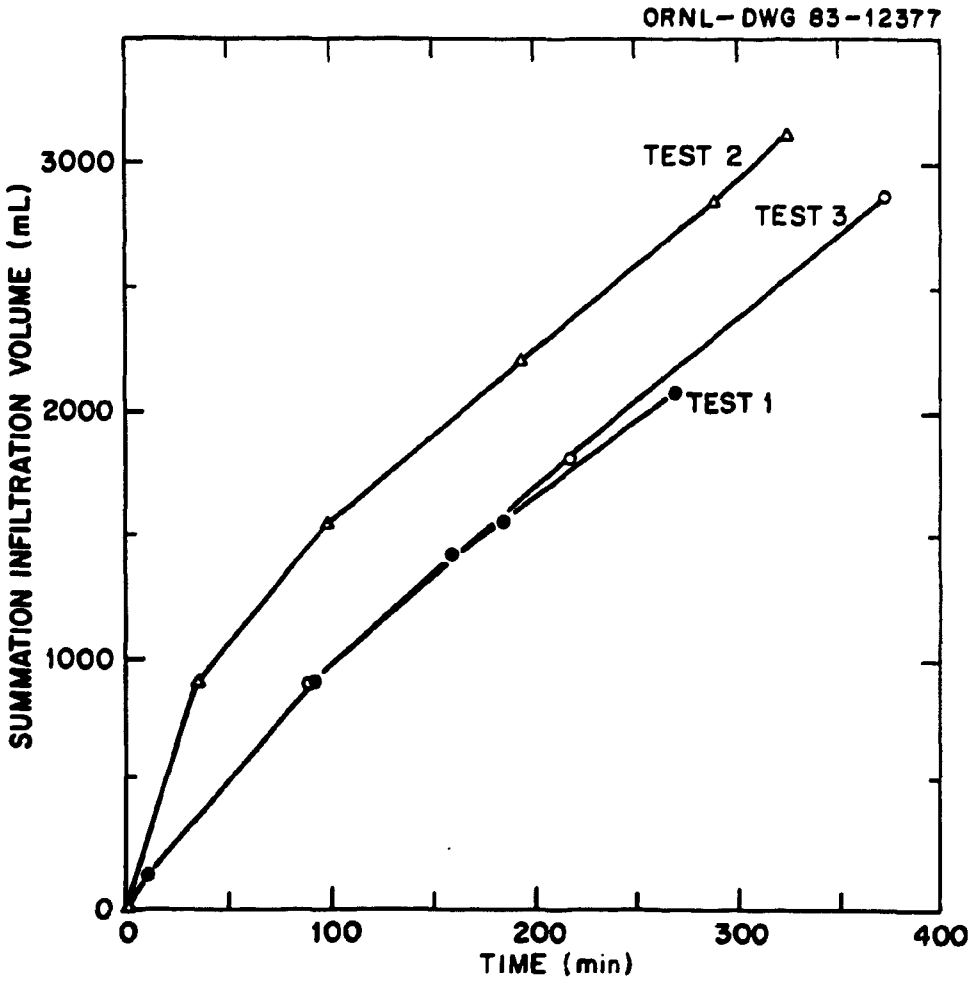

Fig. 30. Infiltration data collected from three tests using ring 6.

weathered shale (Luxmoore et al. 1981) reported to have an infiltration rate with a geometric mean value of 2.3×10^{-5} cm/s. In comparison, the mean value for the disturbed cover material is approximately ten times greater than the undisturbed value and can be attributed to the lack of adequate "settling time." This hypothesis will be tested by taking additional infiltration rate measurements as the trench cover material settles with age.

4.3.2.4 Evaluation

Evaluation of the surface water monitoring program at the ETF indicates that the two water sampling and flow monitoring stations are adequate in characterizing surface runoff. The Parshall flumes are particularly useful in monitoring discharge during extreme precipitation events, but lack the sensitivity to measure flows <2.5 L/s. In addition, equipment malfunctions such as battery failure, clock failure, and automatic-flow-meter component failure have resulted in a significant amount of downtime and subsequent loss of flow data.

Radioactivity resulting from ^{3}H has been identified and monitored at Flume II and is presumed to originate from an existing group of trenches immediately east of the ETF. Water samples taken from Flume I have not been found to contain any radioactivity above background levels. This establishment of background chemical and radiochemical characteristics is an integral part of the overall site characterization process.

4.3.3 Groundwater Hydrology

4.3.3.1 Background

Groundwater may be the most significant pathway for migration of radionuclides at humid waste disposal sites (Siefken et al. 1982). For this reason, characterization of groundwater at the ETF has received major attention, both from the standpoint of field experimental and monitoring work, as well as from site modeling efforts. Work has concentrated in a variety of areas, including development of a water-table elevation monitoring system, design and interpretation of a series of tracer studies, sampling and analysis to establish background water quality, and employment of various experimental techniques commonly used to quantify aquifer characteristics.

To study the groundwater characteristics of the ETF, an array of 40 wells was installed at the site. Table 24 summarizes well design and construction characteristics. Well ETF-1 is at the center of the site, surrounded by wells ETF-2 through -10 in a radial pattern (approximately 10 m from well ETF-1 at 30° intervals). Wells ETF-1 through -10 are about 10 m deep. Wells ETF-11 and -12 are to the east and west, respectively, of the trenches and are about 15 m deep. Wells ETF-13 through -16 constitute a well nest upflow from the test area and vary from 14 to 75 m in depth. The remaining wells are all very shallow (7 m) and are densely clustered around or in the experimental trenches. Also, on the edge of the ETF site (see Fig. 4) are several wells that are used as part of the ongoing monitoring program for SWSA 6 (wells 312, 313, 362, 375). All wells were gravel-packed around the screen, and then the annular space was sealed to the ground surface with a mixture of cuttings and bentonite. After completion, the wells were developed by flushing and pumping.

4.3.3.2 Aquifer characteristics

In order to predict patterns and rate of solute movement at the ETF, a description is needed of the physical properties of the media in which groundwater flows. The major properties that need to

Table 24. Summary of design and construction characteristics of wells located at the Engineered Test Facility

ETF well	ORNL[a] coordinates		Top of casing elevation (m)	Well depth[b] (m)	Casing I.D. (cm)	Casing height[c] (cm)	Borehole diameter (cm)	Screen length (m)	Screen type[d]
	North	East							
1	16,755.97	23,641.19	243.72	8.75	15.2	81	20.3	1.2	S-PRF
2	16,778.27	23,665.16	242.88	9.69	15.2	61	20.3	1.2	S-PRF
3	16,764.91	23,672.79	243.10	9.40	15.2	74	20.3	1.2	S-PRF
4	16,749.15	23,673.34	242.52	9.38	15.2	76	20.3	1.2	S-PRF
5	16,732.49	23,665.30	242.47	9.22	15.2	84	20.3	1.2	S-PRF
6	16,724.10	23,650.96	242.48	9.17	15.2	79	20.3	1.2	S-PRF
7	16,723.19	23,633.64	242.25	9.27	15.2	71	20.3	1.2	S-PRF
8	16,729.23	23,618.57	241.96	9.07	15.2	74	20.3	1.2	S-PRF
9	16,745.32	23,610.28	242.25	9.42	15.2	71	20.3	1.2	S-PRF
10	16,763.48	23,609.83	243.32	9.47	15.2	51	20.3	1.2	S-PRF
11	16,773.04	23,702.57	241.73	15.11	15.2	76	20.3	2.4	S-PRF
12	16,737.94	23,584.36	241.62	15.27	15.2	76	20.3	2.4	S-PRF
13	16,871.96	23,596.33	247.57	76.42	15.2	94	25.4	3.0	S-PRF
14	16,849.23	23,618.51	245.99	28.83	10.2	63	15.2	3.0	S-PRF
15	16,841.45	23,603.47	246.05	14.25	10.2	51	15.2	3.0	S-PRF
16	16,841.45	23,614.14	245.92	74.52	10.2	58	15.2	3.0	S-PRF
17	16,782.86	23,606.38	243.68	5.71	7.6	8	15.2	1.8	PVC-SLT
18	16,791.16	23,624.78	244.17	5.94	7.6	23	15.2	1.8	PVC-SLT
19	16,799.41	23,643.83	244.34	6.12	7.6	23	15.2	1.8	PVC-SLT
20	16,769.52	23,606.72	242.89	6.65	7.6	5	15.2	1.8	PVC-SLT
21	16,776.48	23,621.54	243.64	6.22	7.6	8	15.2	1.8	PVC-SLT
22	16,788.03	23,641.20	243.95	6.86	7.6	8	15.2	1.8	PVC-SLT
23	16,797.92	23,659.16	243.62	6.20	7.6	5	15.2	1.8	PVC-SLT
24	16,762.61	23,620.24	242.91	6.60	7.6	8	15.2	1.8	PVC-SLT
25	16,773.88	23,637.95	243.43	6.58	7.6	0	15.2	1.8	PVC-SLT
26	16,784.95	23,655.52	243.50	6.45	7.6	0	15.2	1.8	PVC-SLT
27	16,745.55	23,616.44	242.40	6.22	7.6	10	15.2	1.8	PVC-SLT
28	16,756.48	23,632.12	243.04	6.20	7.6	8	15.2	1.8	PVC-SLT
29	16,769.40	23,651.35	243.33	6.32	7.6	8	15.2	1.8	PVC-SLT
31	16,743.16	23,628.76	242.35	5.26	7.6	0	15.2	1.8	PVC-SLT
32	16,753.22	23,646.40	242.93	6.04	7.6	0	15.2	1.8	PVC-SLT
33	16,764.51	23,662.09	242.89	6.10	7.6	0	15.2	1.8	PVC-SLT
34	16,732.38	23,623.74	241.94	6.68	7.6	0	15.2	1.8	PVC-SLT
35	16,740.99	23,641.55	242.68	6.27	7.6	8	15.2	1.8	PVC-SLT
36	16,749.06	23,658.60	242.81	6.45	7.6	5	15.2	1.8	PVC-SLT
37	16,757.00	23,674.92	242.55	6.53	7.6	5	15.2	1.8	PVC-SLT
38	16,727.75	23,637.84	242.18	6.71	7.6	0	15.2	1.8	PVC-SLT
39	16,735.81	23,654.86	242.56	6.76	7.6	5	15.2	1.8	PVC-SLT
40	16,743.62	23,671.35	242.41	6.30	7.6	8	15.2	1.8	PVC-SLT
312	16,922	23,529	247.98	5.79	16.8	9	*e*	5.99	S-PRF
362	16,588	23,718	237.15	2.44	16.8	83	*e*	2.39	S-PRF
375	16,935	23,531	248.86	7.92	7.6	78	*e*	3.05	PVC-SLT

[a]Oak Ridge National Laboratory.
[b]Depth of well from ground to bottom of casing.
[c]Height from ground to top of casing.
[d]S = steel casing; PVC = polyvinyl chloride plastic casing; PRF = perforated casing; SLT = slotted.
[e]Missing information.

be evaluated are hydraulic conductivity, effective porosity, and storage coefficient. The Conasauga Group is extremely lithologically and structurally heterogeneous and is therefore expected to be hydraulically heterogeneous. Thus in order to characterize the aquifer, estimates of properties as well as their spatial distributions are required. The distribution and magnitude of aquifer properties will result in a geological aquifer description, which includes information on areal extent of the aquifer, aquifer thickness, heterogeneity, anisotropy, and the nature of primary and secondary porosities.

The first aquifer characterization tests to be performed at the site were tracer tests conducted by researchers from Indiana University. The tracers were a homologous series of chlorofluorocarbons: 1,2-$C_2Cl_2F_4$ (F-114), 1,1,2-$C_2Cl_3F_3$ (F-113), and 1,1,2,2-$C_2Cl_4F_2$ (F-112). They were introduced into well ETF-1 at a depth of 8.4 m and agitated with a slug of water. The water level in the well was adjusted so that the addition of excess fluid would not create any lasting perturbations to the groundwater flow system. Samples were taken immediately after injection to determine the initial fluorocarbon concentration. All water samples during this test were collected using a bailer because the fluorocarbons would be preferentially vaporized and lost if a vacuum pump were used (Cooper 1981). Results of the test are shown in Figs. 31 and 32, which show all elution data and those for well ETF-3, respectively. Figure 33 shows the head gradient through time from the injection well to observation wells.

The highest concentrations of tracers were observed at well ETF-3 (Figs. 31 and 32), which lies on a line that generally parallels the regional strike of the Conasauga Group. The simultaneous appearance of elution maxima for each tracer is a strong indication of minimal interaction between the tracers and formation, because each tracer was expected to be retarded to a differing degree. The calculated value of linear velocity is 0.17 m/d, based on the arrival time of the peak concentration of tracer. Using this linear velocity, a hydraulic gradient of 0.094 (m/m), and an effective porosity of 0.10, the computed hydraulic conductivity is 0.18 m/d. There is some uncertainty associated with the effective porosity estimate. Reasonable values for the effective porosity of a fractured shale range between 0.01 and 0.10 (based on Freeze and Cherry 1979), but measurements for the appropriate-depth zone are not available at the ETF.

Cooper (1981) presented data that suggest very rapid movement of tracer F-112, as evidenced by the presence of tracer in some of the wells within 5 to 8 d of injection, when the first samples were taken (Fig. 31). Examination of detailed results presented by Cooper (1981) shows tracer was present in all wells, although it was most pronounced in wells ETF-2, -3, -7, and -8. (Concentrations of tracer are low, less than 10% of subsequent peaks.) Wells ETF-2, -3, -7, and -8 are all oriented along the strike-joint set. Although it is not possible to define the first arrival of tracer precisely, apparent velocities, based on first arrivals, were of the order of 1 to 2 m/d. This range of apparent velocity suggests an intrinsic permeability of 1.4×10^{-12} to 2.8×10^{-12} m^2 (1.4 to 2.8 Darcy) for the bulk material (assuming porosity is 0.10) or 1×10^{-14} to 2×10^{-14} m^2 (0.01 to 0.02 Darcy) for a fracture system having a porosity of 0.0007. Sledz and Huff (1981) estimated an intrinsic permeability of 0.10 Darcy for the fracture system only. Cooper (1981) deduced that the flow direction suggests secondary permeability that formed preferentially along the strike-joint set. Calculations of travel time for flow in fractures using results presented by Sledz and Huff (1981) indicated that the first peak arrival would occur in about 4 to 10 d, depending on fracture porosity. Examination of data for tracer F-112 by Cooper (1981) suggests that a primary pulse of tracer had already passed through wells ETF-2, -4, -5, -6, -9, and -10 when the first samples were taken at 5 d after injection. These wells line up along the strike of the

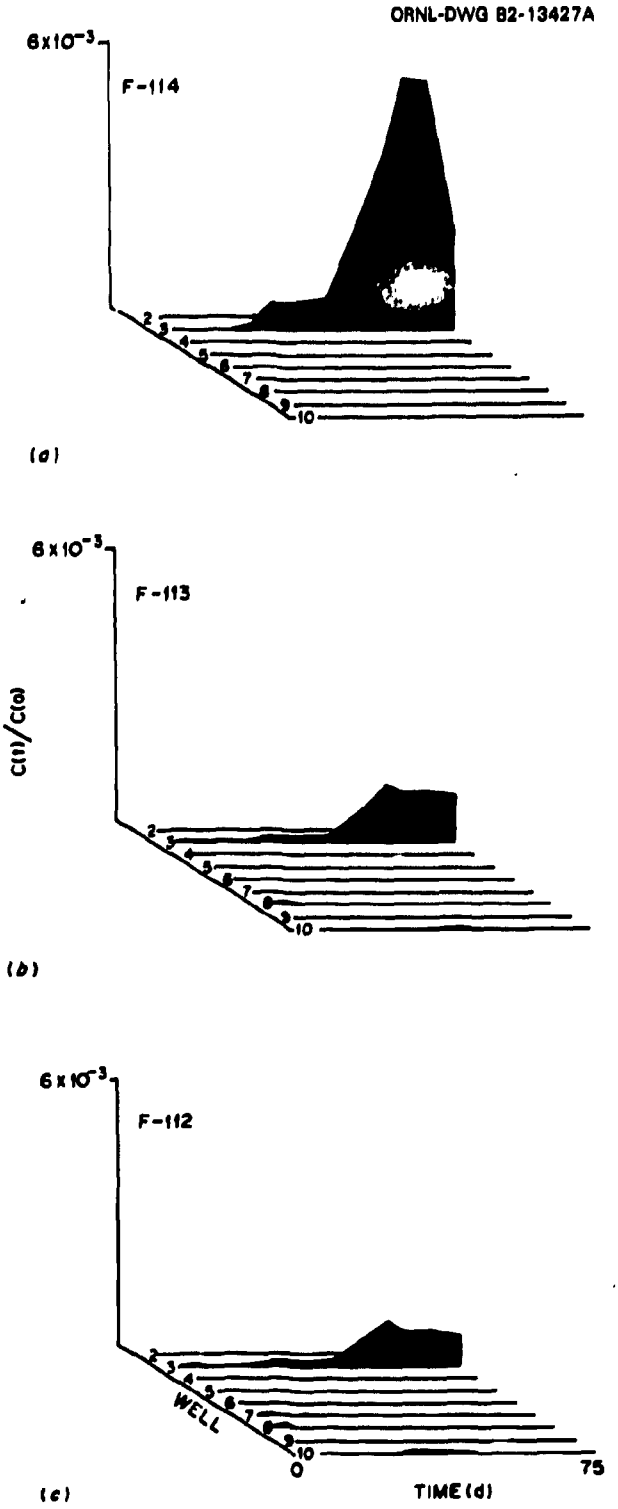

Fig. 31. Elution peaks for tracers F-114 (*a*), F-113 (*b*), and F-112 (*c*) for wells ETF-2 through -10. *Source*: W. T. Cooper, "Interactions Between Organic Solutes and Mineral Surfaces and the Significance in Hydrogeology," Ph.D. thesis, Indiana University, Bloomington, Ind., 1981.

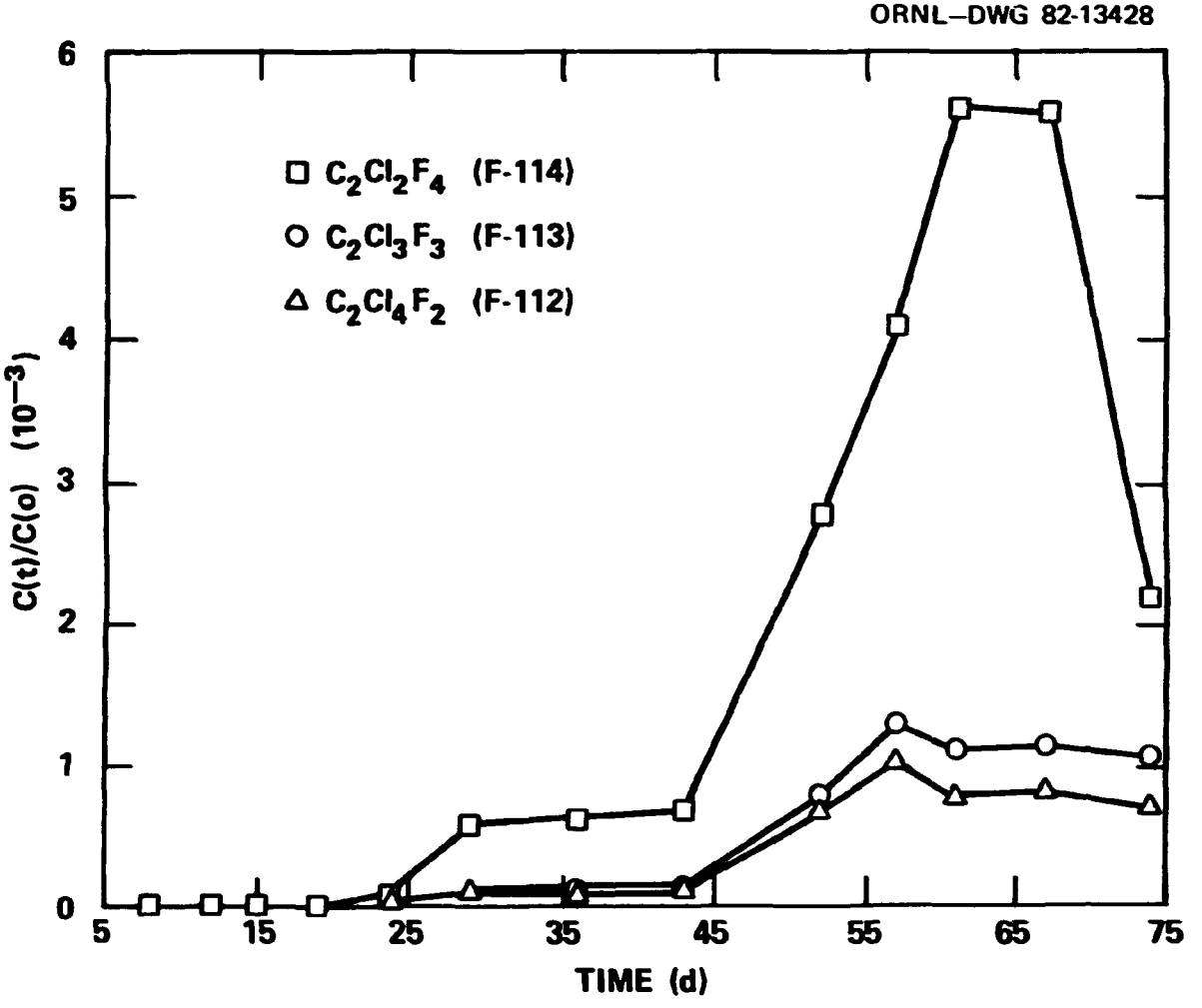

Fig. 32. Tracer peak arrival in relative concentrations. *Source:* W. T. Cooper, "Interactions Between Organic Solutes and Mineral Surfaces and the Significance in Hydrogeology," Ph.D. thesis, Indiana University, Bloomington, Ind., 1981.

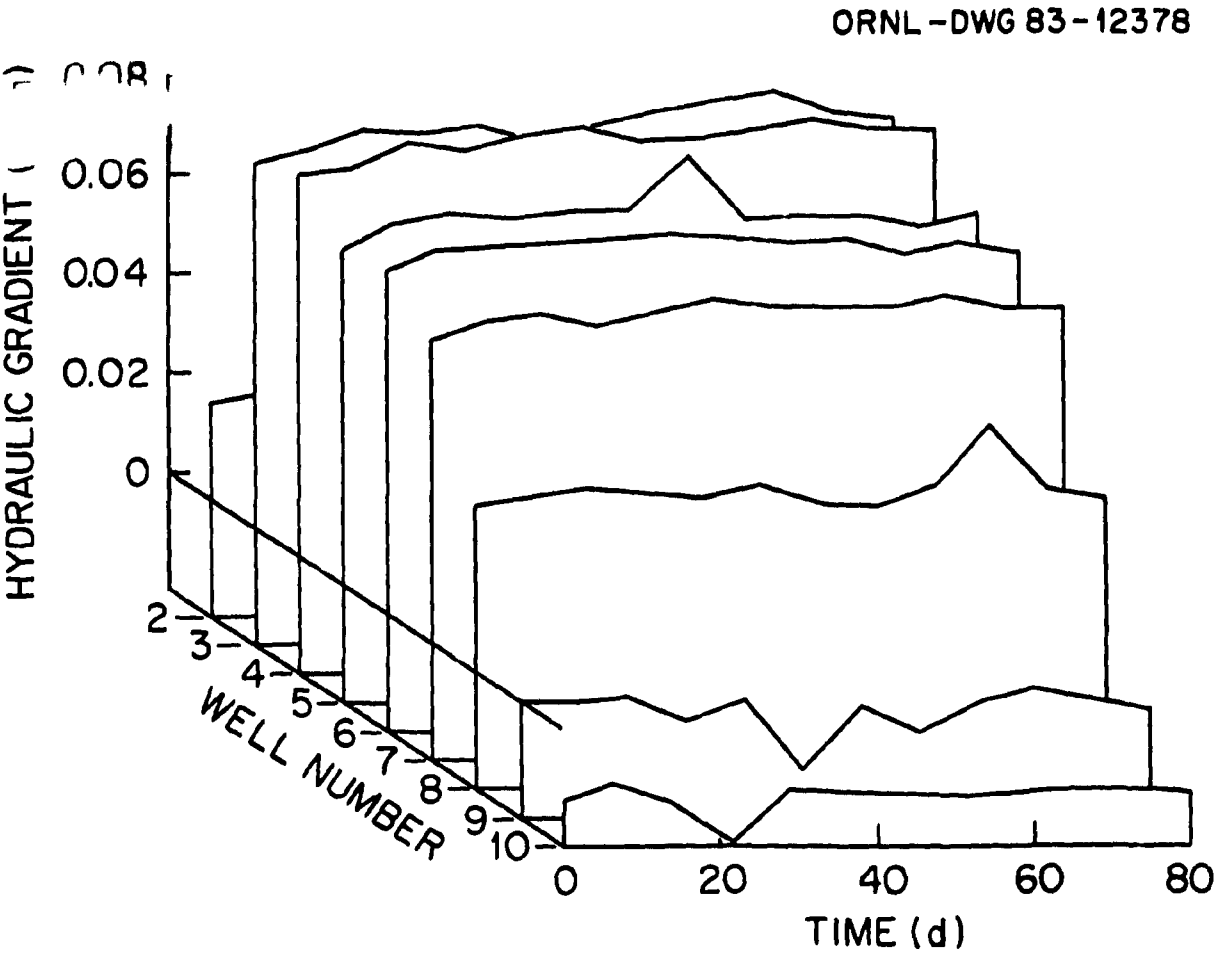

Fig. 33. Hydraulic gradient through time between well ETF-1 and observation wells.

formation and along an angle away from the strike that corresponds directly to a secondary fracture joint set identified by Sledz and Huff (1981). The pattern of tracer arrival at well ETF-3 is attenuated compared with expected migration rates in fractures but is, by far, the largest peak with regard to the mass of tracer. This peak is expected if flow is along the steepest hydraulic gradient (see Fig. 33), suggesting that bulk transport via intergranular flow is probably the significant part of groundwater migration at the ETF. Individual fractures are important and dominate quick movement but are volumetrically less significant than the surrounding media. The intergranular portion of the aquifer at the ETF is most likely a combination of primary porosity and a secondary porosity of very densely spaced and weathered joint system. This joint system is well developed along geologic strike (bedding planes) as well as perpendicular to strike. These tracer tests thus indicate the importance of both rapid migration pathways associated with fractures as well as slower intergranular flow paths that are controlled by the bulk hydraulic properties of the deep residuum and bedrock.

In order to determine aquifer transmissivity and storage coefficient, several pumping tests were performed. During well development, it was found that well ETF-12 was found to be the most productive well at the ETF; therefore, it was used as the pumping well for the aquifer testing. The first

pumping test performed lasted 7 h. The results were not satisfactory, because of equipment failures, varying pumping rates, and insufficient pump time. A second pumping test was run in June 1982, which lasted for 24 h. The pumping rate was 3.29 L/min throughout the test. Water level responses were measured in the pumping well (ETF-12) and in wells ETF-1 through -11. Drawdown data for all wells were obtained successfully using continuous level recorders with strip charts, but recovery data were lost due to equipment malfunction. Figure 34 shows lines of equal draw-

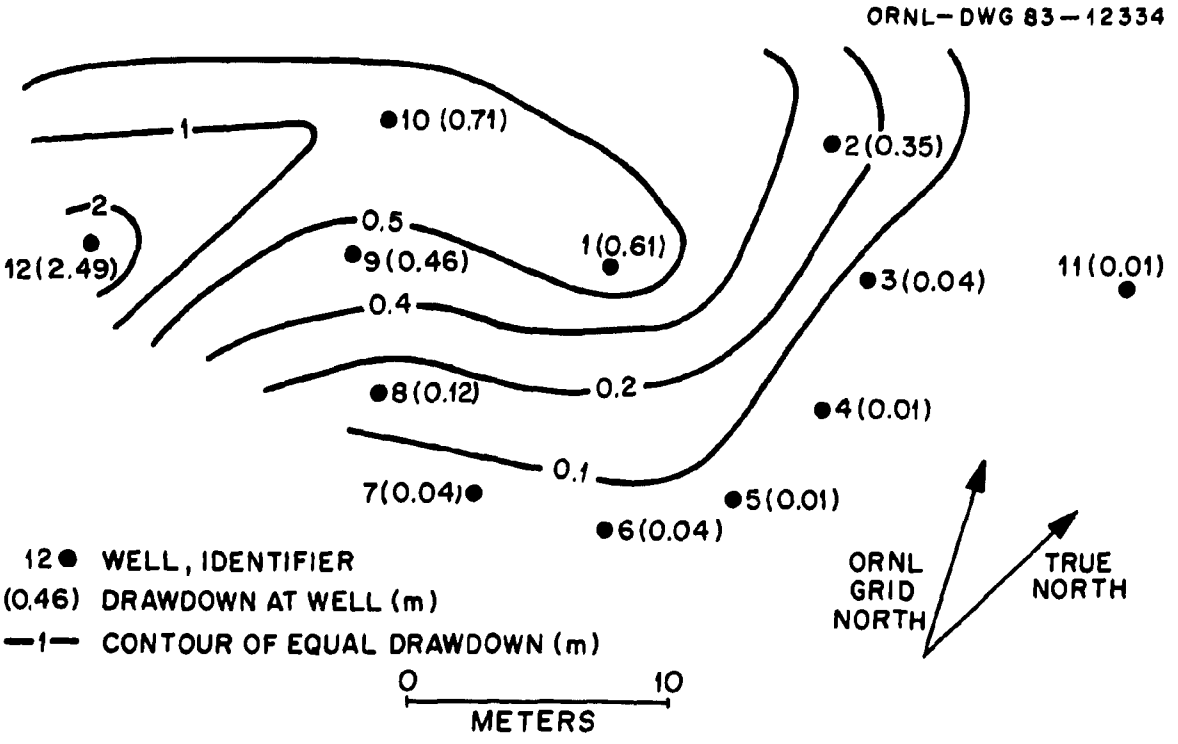

Fig. 34. Drawdown pattern at the end of the 24-h pumping test.

down after 24 h, that is, the final cone of depression. The elongated drawdown pattern indicates the heterogeneity of the aquifer. This pattern can result from the variable hydraulic conductivity of the media, a strong anisotropic effect (high permeability along strike), or structural control of water movement. In reality, it is most likely a combination of effects. There are two anticlines observable at the ETF in the very near surface. The orientation of the axes and limbs were discussed in Sect. 4.1.2. The extent of these features (the wells are completed about 7 m below the observation of the anticlines) and the orientation of the axial planes of the folds are uncertain. The presence of these folds does affect weathering, and soils appear to be thinnest above these features and thicker on the flanks (see Fig. 17). Weathered material is most likely of higher hydraulic conductivity (see following discussion on slug tests); therefore, a linear expression of hydraulic conductivity and drawdown is expected to develop due to the geologic structures observed at the ETF. The structures will also have a local effect on the distribution of fractures which may also impact the flow regime.

An interesting phenomenon that occurred during both pump tests was water-level recoveries in pumping well ETF-12 and, to some extent, in observation wells (notably ETF-10). It is not unusual

for water-level declines to cease or to slow down during a pump test; this may be caused by the intersection of the cone of depression with a surface water body or a highly transmissive portion of the aquifer. Three explanations for the actual recoveries in water levels exist. The first is the Noordbergum effect (Bouwer 1978), which is due to a response lag in the drainage of excess pore pressure from a loading event. This is common in fine-grained materials. The second explanation is similar except it says that water may be derived from fractures or solution zones that respond to loading due to dewatering. Finally, undetected changes in the pumping rate may have occurred.

Plots of drawdown versus time for wells ETF-1, -3, -8, -9, -10 are shown in Fig. 35. These wells line up approximately along the minor and major axes of the cone of depression. Many techniques

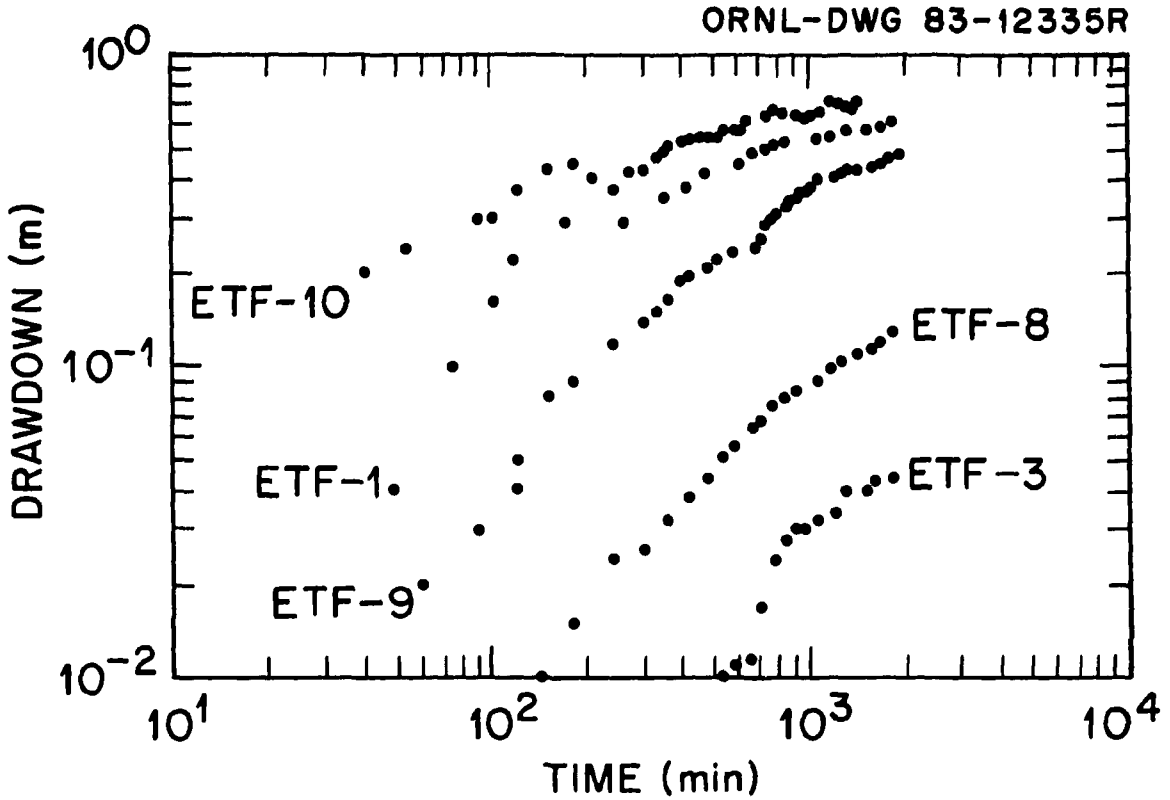

Fig. 35. Drawdown versus time for wells ETF-1, -3, -8, -9, and -10.

are available for analyzing pumping test data (Lohman 1972). The standard approach is to use a curve-matching technique based on the Theis equation. Many assumptions are inherent in the technique, including: (1) the flow is horizontal and radial in nature, (2) the aquifer is infinite in areal extent, (3) the pumping well is fully penetrating, and (4) the aquifer is homogeneous and isotropic. If any of these conditions are not met, deviations from a perfect Theis response will occur. Corrections, however, can be made, so the curve-matching technique is not as limiting as it might appear. Results show that the data for all the wells fit on a Theis curve, and the results are quite consistent (see Table 25). The transmissivity (hydraulic conductivity × aquifer thickness) calculated is actually a bulk average for the portion of the aquifer between the pumping well and the observa-

Table 25. Values of transmissivity and storage coefficient for wells ETF-1, -3, -8, -9, and -10

Well	Transmissivity (m^2/min)	Storage coefficient
ETF-1	1.59×10^{-3}	5.12×10^{-4}
ETF-3	4.36×10^{-3}	.01
ETF-8	3.74×10^{-3}	.03
ETF-9	1.25×10^{-3}	.01
ETF-10	1.74×10^{-3}	3.34×10^{-4}
Average	2.54×10^{-3}	~.01

tion well. Plotted in Fig. 36 are the vectors for transmissivity (T) and the storage coefficient (S) (the volume of water an aquifer releases from or takes into storage per unit surface area per unit change in head). Except for well ETF-9, T appears greatest along geologic strike, as was expected. The average T was found to be 2.54×10^{-3} m^2/min. Storage coefficient values were more variable; all were low for an unconfined aquifer (S values for unconfined aquifers generally range from about 0.3 down to 0.003). The average value for S was determined to be about 0.01.

A second analysis was performed based on nonradial flow techniques. In this analysis, flow is assumed to be predominately through a single vertical fracture in or near the vicinity of the anticlines at the ETF. In this case, graphs of drawdown versus the square root of time were used. Using the graphical approach presented by Gringarten and Witherspoon (1972), estimates of 3.2×10^{-4} to 1.4×10^{-3} m^2/min were obtained for the transmissivity of the aquifer matrix surrounding the hypothetical vertical fracture.

To obtain direct, in situ measurements of hydraulic conductivity, a series of slug tests were conducted in wells ETF-1 through -40. Slug tests are small-scale pump-in/pump-out tests observing water-level recovery after instantaneous injection or removal of water. In this case, a solid aluminum rod (0.006 m^3) was used to instantaneously displace a volume of water equal to its own volume. The method of analysis used is based on Hvorslev (1951) [also described in Freeze and Cherry (1979)] and results in a measurement of hydraulic conductivity (K) for a zone immediately surrounding the screen of the well being tested. A total of 36 wells at the ETF site was tested, and the average value of K for each well is shown in Table 26 (each well was tested at least two times, and the analysis took into consideration the varying well geometrics). Figure 37 shows the distribution of K values at the ETF. The log of K values was used because K is generally log-normally distributed (Freeze 1975) and the distribution of values at the ETF supports this premise.

Based on the distribution of K, a mean ($\bar{x}$) and standard deviation (σ) were calculated. Noted in Table 26 are all wells above and below 1 σ of the mean, that is, which wells statistically stand out among the background values of K. More of the deeper monitoring wells (ETF-1 through -16) had higher than average hydraulic conductivities when compared to the shallow wells (ETF-17 through -40). This is most likely due to slightly different construction techniques between the two sets of wells; therefore, only comparisons within "groups" of wells are made. Wells with higher K values appear between anticlines in a trough through the center of the site. This also coincides well with soil depths. Again, this is at the depth of the shallow well screens, which may or may not lie directly beneath mapped features; that is, the vertical extent of shallow features is uncertain.

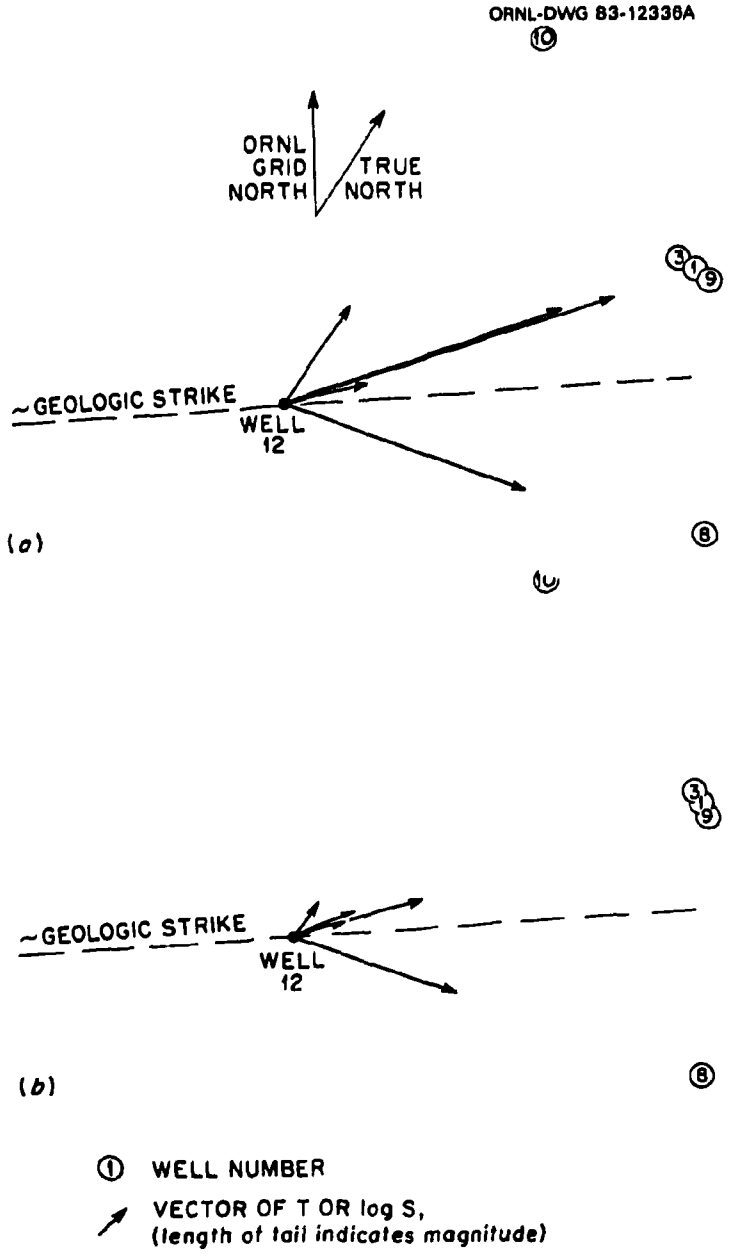

Fig. 36. Vectors for (*a*) transmissivity (T) and (*b*) log of storage coefficient (S).

Using the log-normalized mean value for hydraulic conductivity (6.31×10^{-5} cm/s) and the values of T from the pumping test, an approximate value for aquifer thickness can be obtained. The value calculated will actually be an effective thickness (based on the pumping test) because no true aquifer "bottom" exists at the ETF. Using the transmissivity from the Theis analysis ($T = 2.54 \times 10^{-3}$ m^2/min), a thickness of 67.09 m was calculated. Based on the geology, this value seems reasonable. Using the average T value from the Gringarten and Witherspoon analysis, a thickness of about 22 m was calculated.

Table 26. Results of hydraulic conductivity measurements in wells ETF-1 through -40

ETF well[a]	Mean value of K (cm/s) × 10^{-5}	Log of K × 10^5	Statistical significance	ETF well[a]	Mean value of K (cm/s) × 10^{-5}	Log of K × 10^5	Statistical Significance
1	31.0	1.49	H[b]	22	4.5	.65	
2	2.3	.36		23	6.0	.78	
3	5.0	.70		24	60.0	1.78	H
4	13.0	1.11		25	7.6	.88	
5	30.0	1.48	H	26	4.7	.67	
6	39.0	1.59	H	27	2.2	.34	
7	20.0	1.30		28	0.92	−.04	L
8	31.0	1.49	H	29	2.2	.34	
9	5.1	0.71		31	2.4	.38	
11	24.0	1.38		32	2.9	.46	
12	41.0	1.61	H	33	238.0	2.38	H
13	1.7	.23		34	2.1	.32	
14	2.3	.36		35	1.5	.18	L
15	0.66	−.18	L[c]	36	3.0	.48	
16	2.9	.46		37	7.9	.90	
17	0.96	−.02	L	38	9.7	.99	
20	23.0	1.36		39	4.3	.63	
21	1.1	.04	L	40	5.6	.75	

[a]Data for wells ETF-10, -18, -19, and -30 are not included.
[b]H = high K values (≥1 σ).
[c]L = low K values (≤1 σ).

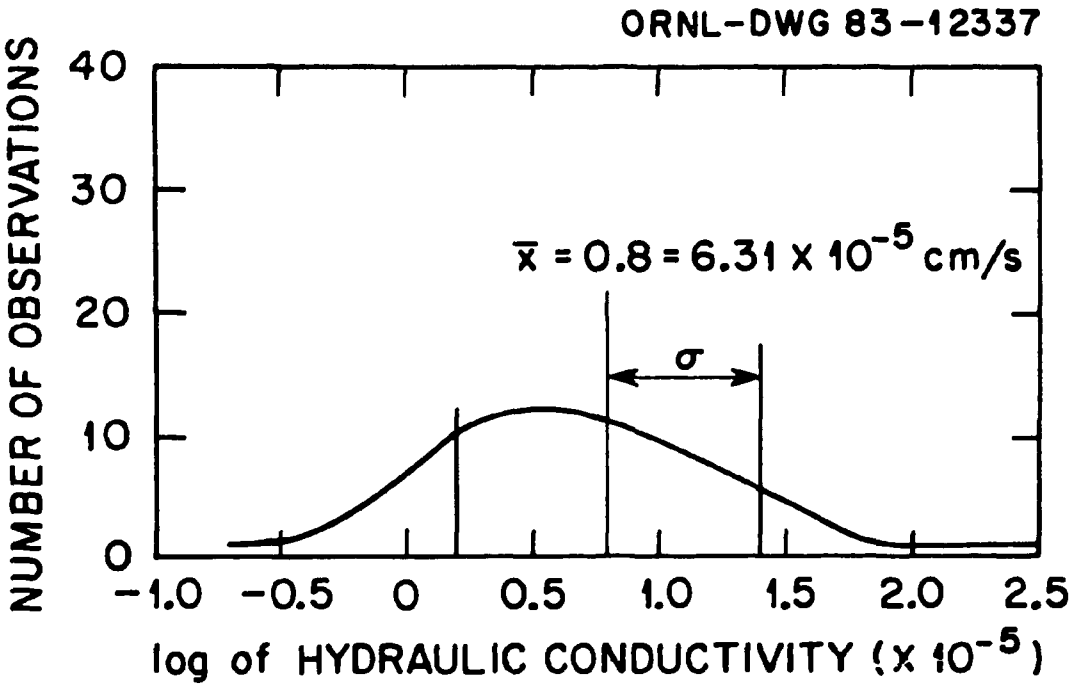

Fig. 37. Distribution of measured hydraulic conductivity values.

The groundwater velocities from earlier tracer tests and the hydraulic conductivities from slug tests can be combined to calculate an effective porosity for the intergranular media at the ETF. Using Darcy's Law, a value of 0.03 for effective porosity is calculated. This is within the range calculated for fractured shales.

$$V_l = -(K_l/\theta)(d\phi/dl), \tag{10}$$

where

V_l = linear velocity = 0.17 m/d,
K_l = hydraulic conductivity = 6.31×10^{-5} cm/s,
ϕ = effective porosity,
$d\theta/dl$ = gradient = −0.094.

By using a variety of testing methods (tracers, pumping tests, and slug tests), all major aquifer characteristics have been estimated. The determined variability and magnitude of transmissivity, storage coefficient, hydraulic conductivity, effective porosity and aquifer thickness, as well as qualitative estimates of anisotropy and heterogeneity can all be used to model water and solute movement at the ETF site. Table 27 summarizes the ETF aquifer characteristics that have been discussed in this section.

Table 27. Summary of Engineered Test Facility aquifer characteristics

Method	Parameter	Value
Tracer test	Average linear velocity	0.17 m/d
Pump test	Transmissivity (T)	1.25×10^{-3} to 4.36×10^{-3} m²/min
	Storage coefficient (S)	5×10^{-4} to 0.01
Well slug test	Hydraulic conductivity (K)	6.31×10^{-5} cm/s
Darcey equation	Effective porosity (θ)	0.03
	Effective aquifer thickness	67 m

4.3.3.3 Water-table fluctuation monitoring and groundwater flow system

Water levels are monitored continuously in 15 wells, numbered ETF-1 to -15, located on the ETF site (see Fig. 4). The ORNL coordinates of these wells, as well as other important characteristics, have been summarized in Table 24. Of the 15 wells, 12 were constructed at the ETF site as a part of an initial site-characterization tracer study and are arranged in an arc-shaped array around ETF-1. Wells ETF-13, -14, and -15 lie to the north of the site and were constructed for purposes of monitoring deeper site groundwater. For a detailed description of ETF well design and construction, refer to Boegly and Davis (1983).

Each of the 15 wells is equipped with a Belfort Instrument Co. portable liquid level recorder (Cat. 5-FW series), which records on a paper chart the vertical movement of a float resting on the water surface. In addition, each recorder has a 5-V potentiometer, which converts float level to a voltage. The voltages from the 15 recorders are fed to a single data logger, which records the voltages at preset intervals (normally 13.88 min) on a casette tape.

The paper chart turns on a drum at one rotation per week, actuated by a mechanical spring. Charts are replaced each week, at which time the depth to the water in each well is manually measured for calibration purposes. The tape cassette is normally replaced every 2 weeks, also in conjunction with manual calibration measurements. A marked measuring point at the top of each well casing provides a reference elevation for converting depths to water-level elevations. Figure 38 illus-

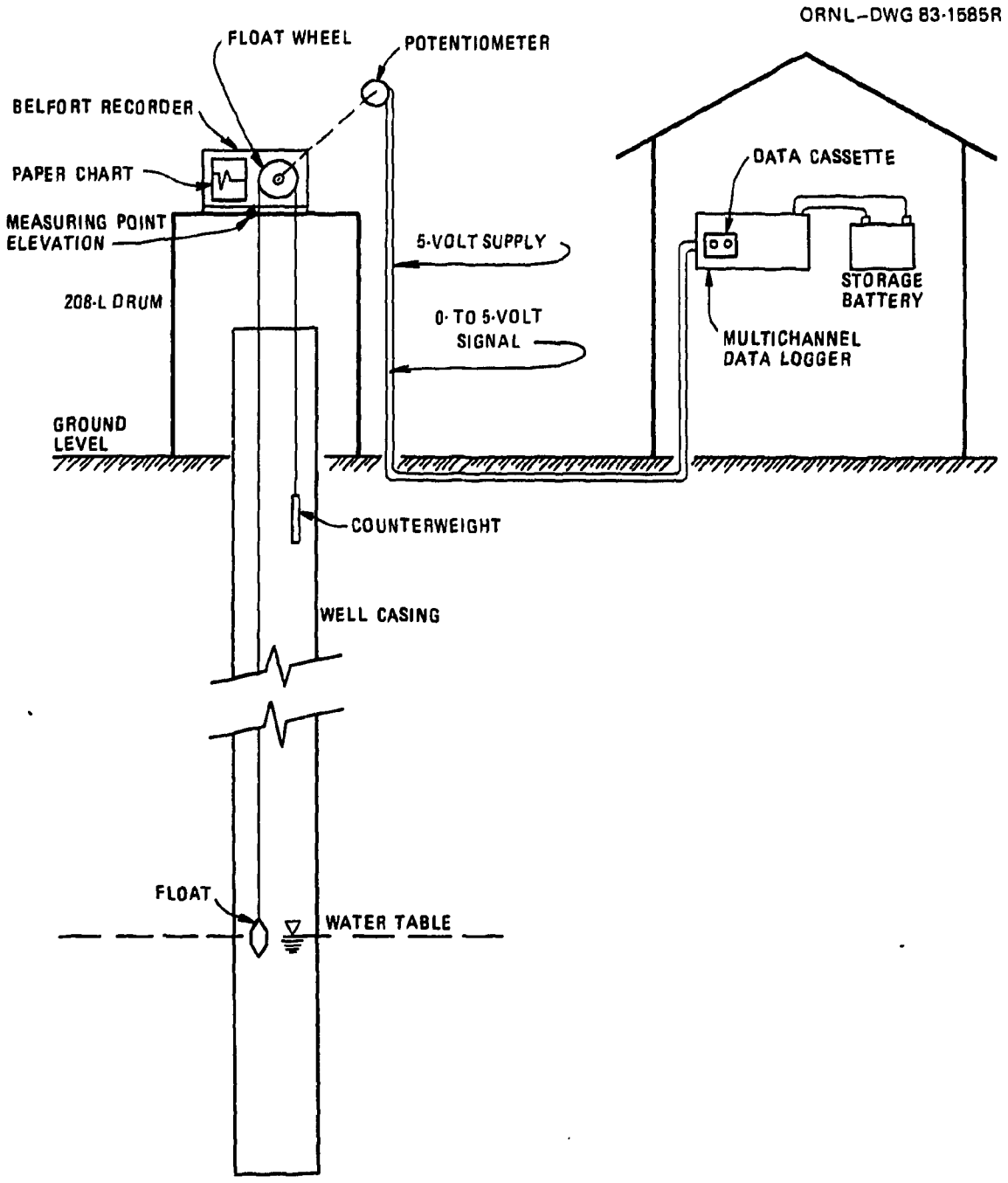

Fig. 38. Schematic of Engineered Test Facility water-table monitoring system.

trates the ETF water-table monitoring system showing one of the wells, a Belfort recorder, and connections to the multichannel data logger.

Water-table monitoring began in mid-June 1980, with weekly elevation readings taken manually as the automated system was being set up. The system was first applied to wells ETF-1 through -12 and later expanded to include wells ETF-13 through -15. At present, more than 2 years of water-table data are available for wells ETF-1 through -12, including more than 6 months of data from all 15 wells. The data thus reflect both long-term trends as well as a large number of short-term responses to storm events.

Mean monthly water-table elevations (summarized in Appendix E) illustrate the longer term cyclic trend that occurs within a given year. For example, both 1981 and 1982 exhibit minimum water-level elevations during the late summer months (August to September) and maximum elevations during the winter months (January to April). This corresponds with the monthly rainfall totals summarized in Fig. 24, which also exhibit a yearly cycle with highs in the winter months and lows in the late summer. In addition, evapotranspiration is highest in the late summer and lowest in the winter months.

In general, monthly averaging of water elevations suggests that the wells at the ETF site exhibit a yearly fluctuation of approximately 1 m. Even considering a smaller time increment when the data are not averaged, this 1-m elevation differential is often observed during storm activity. During storms, the response in the wells is rapid, usually on the order of several hours, but the water level requires several days to return to prestorm levels (Fig. 39). Table 28 summarizes the response in the ETF wells to a single storm event which occurred on February 1 and 2, 1983. The table presents two lag times. The first is the time from the beginning of the rainfall (5 p.m. February 1) to the beginning of the rise in water level in the well. The second lag time is from the beginning of the rainfall to the peak water level in the well. In general, the wells took approximately 5 h to respond to the rainfall, and all wells but ETF-5, -6, and -7 took approximately 9 h to reach a peak water elevation. These three wells took considerably longer (22 h) to reach a peak water elevation. The wells remained at peak conditions for from 0.2 to 1.2 h (excluding well ETF-5) and then slowly, over a period of several days, returned to prestorm conditions (Fig. 39). The maximum rise in water elevation was noted in well ETF-2 (87 cm), and the minimum response was in well ETF-6 (27 cm). Recorders on wells ETF-13 through -15, which are also a part of the water-level fluctuation monitoring system, were not operating during this particular storm event; however, similar examination of other storm events indicates that these deeper wells take longer to respond to a rainfall event, and the magnitude of the response is less than for the shallower wells ETF-1 through -12.

Depth to water varies across the ETF site, although, in the center of the array of experimental wells, the water averages approximately 4.2 m below ground surface. To illustrate this, equipotential lines have been drawn for the site and compared to surface (topographic) contours (Fig. 40). These lines, constructed from data collected on five dates during 1980 and 1981, indicate that the flow of groundwater is primarily in a southeasterly direction. In all examples, the equipotential lines generally parallel the strike of the bedrock, and the piezometric surface does mimic topography. The bend in the contours near well ETF-3 appears to be a permanent feature, whose exact shape varies with hydrologic conditions.

On a monthly basis, water levels are taken manually from all wells at the ETF site. Levels on December 31, 1982, represent approximately the maximum level reached throughout the year (see water-table trend discussion above), and equipotential contours for these data are shown in Fig. 41.

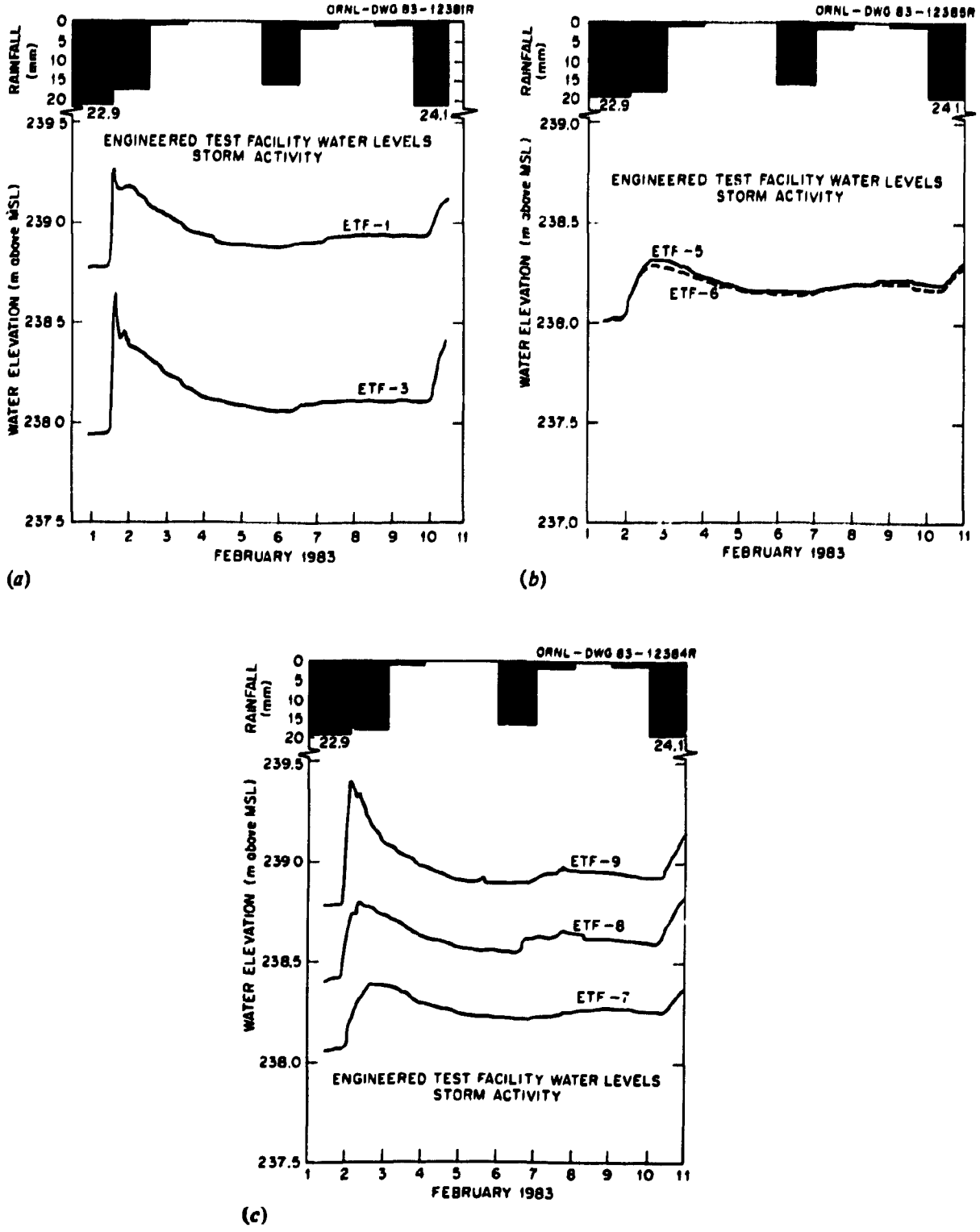

Fig. 39. Groundwater response to rainfall events, February 1–11, 1983. Data were collected from wells: (*a*) ETF-1 and -3, (*b*) ETF-5 and -6, (*c*) ETF-7 through -9, (*d*) ETF-10 through -12, and (*e*) ETF-13 and -15.

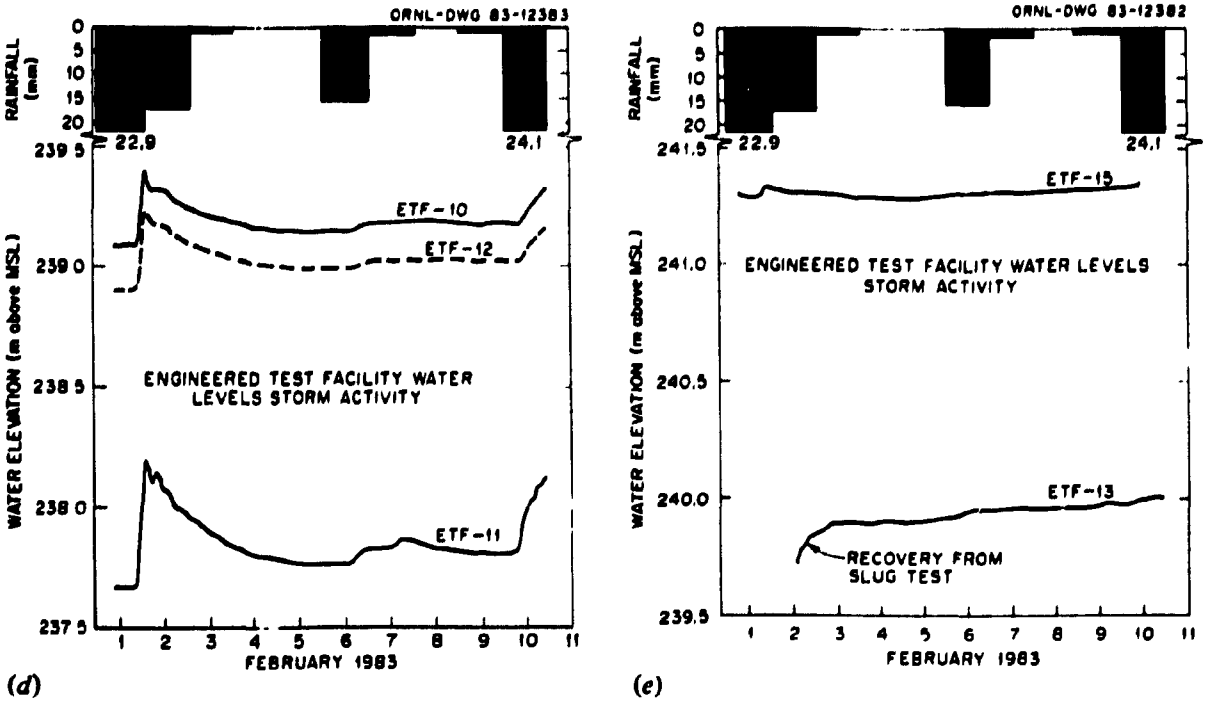

Fig. 39. (continued).

Table 28. Well response to a single precipitation event

Rainfall started 5 p.m., Feb. 1, 1983,
and ended 4 a.m., on Feb. 2, 1983
(precipitation total = 40 mm)

ETF well	Lag time[a] (h)	Lag time[b] (h)	Time at peak[c] (h)	Change in water elevation[d] (cm)
1	5.2	9.3	0.2	48
2	5.2	8.4	0.2	87
3	5.2	9.1	1.2	69
5	4.2	22.5	8.8	28
6	4.2	22.5	1.2	27
7	4.5	22.3	0.9	32
8	4.2	10.9	0.7	32
9	4.9	9.8	0.7	58
10	4.9	9.1	0.2	31
11	4.7	9.3	0.5	51
12	4.7	9	0.9	32

[a]Time from beginning of rainfall to beginning of water-level rise.
[b]Time from beginning of rainfall to peak water level in well.
[c]Time that water level stayed at peak.
[d]Total rise in water level due to the storm event.

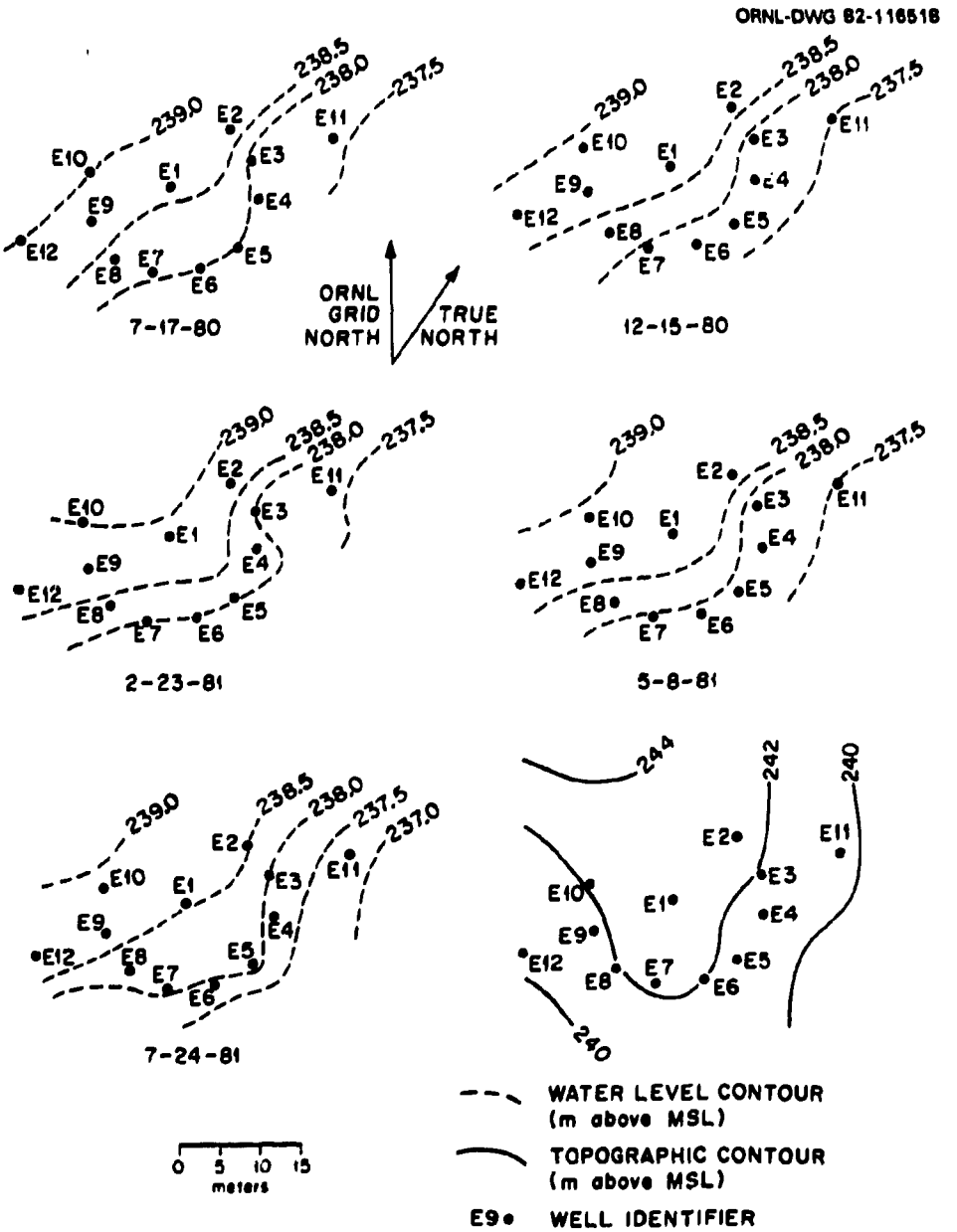

Fig. 40. Water-table elevations for five dates in 1980 and 1981 compared to surface topography.

Included in this figure are equipotential lines for the very near surface water-table system (wells ETF-17 through -40) and a zone slightly deeper (about 3 m deeper than these shallow wells) constructed from data from wells ETF-1 through -12. Because two well sets of different depths were used, vertical gradients are apparent in Fig. 41 and are seen as a slight shift or offset in a given equipotential line. For the deeper system depicted as solid lines in Fig. 41, the contours are similar

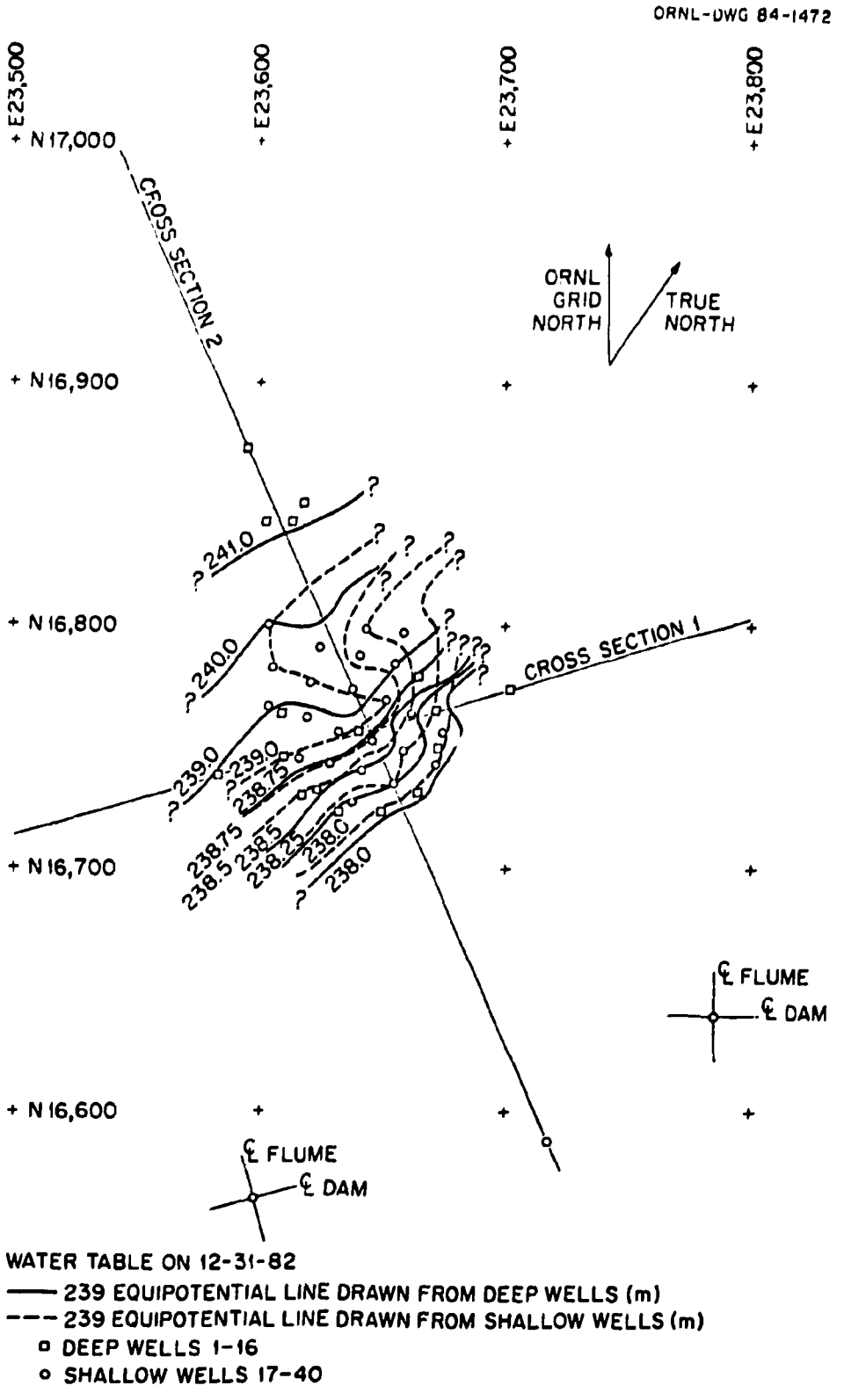

Fig. 41. Equipotential water contours for the Engineered Test Facility site.

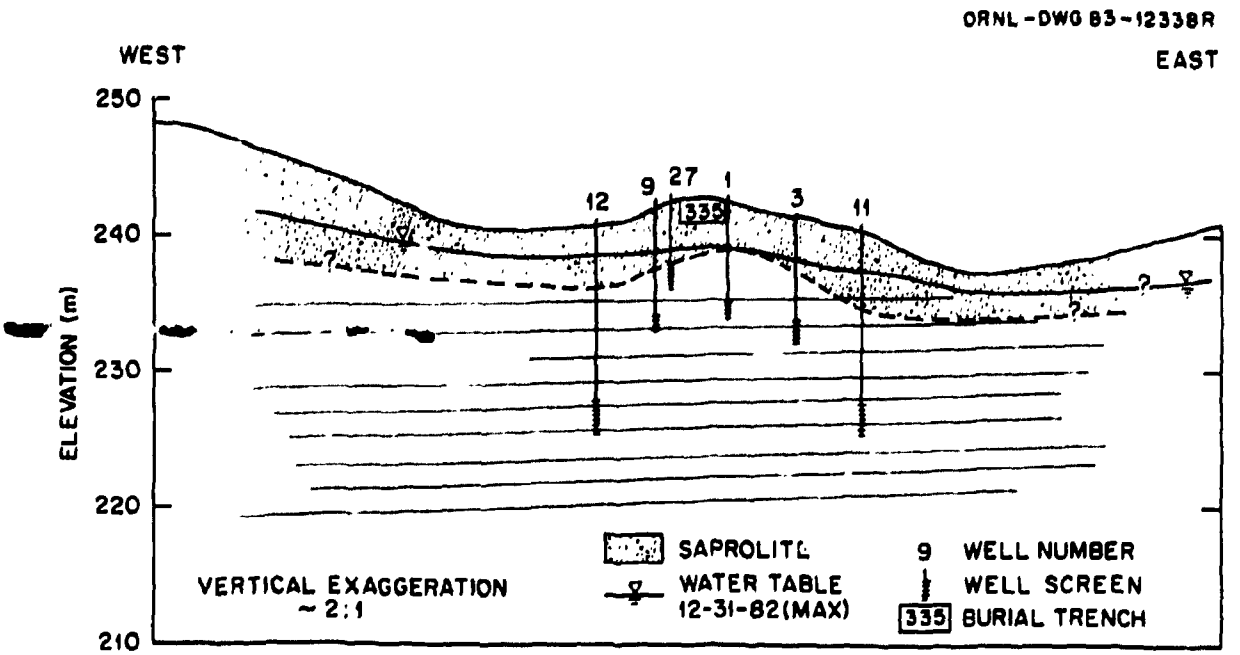

Fig. 42. Cross section 1 of the Engineered Test Facility site. See Fig. 41 for exact location.

to those recorded on previous dates (Fig. 40). Based on these data, the direction of flow would be southeasterly, roughly between wells ETF-1 and ETF-3 (this was also indicated by the tracer test).

In the southeast portion of the ETF, contours based on the shallow wells (depicted as broken lines on Fig. 41) are similar to those from the deeper wells; however, as one moves northward, differences between the shallow and deep systems become apparent An elongated mound of water is shown in this region; it is situated above the axis of the southernmost of the two anticlines located during geologic investigations (Fig. 12). This groundwater mound shows up in contours constructed from all sampling dates and appears to be directly related to soil thickness (Fig. 17).

The near-surface groundwater flow regime at the ETF site is quite complex and results from the complex geology and topography of the site. Figure 41 illustrates this point and emphasizes the importance of knowing both the vertical gradients and the exact location and depth of a contaminant source to predict accurately contaminant transport at the site.

Figures 42 and 43 are cross-sectional views of the ETF site (see Fig. 41 for location of cross sections). Both figures include the general geometry of the bedrock, the thickness of the weathered zone as estimated from well logs, and maximum water-level elevations from the shallow wells. In Fig. 42 the cross section runs approximately along geologic strike (about east-west). The mimicking of both weathering depth and groundwater levels to surface topography is apparent. Figure 43 shows a cross section that runs approximately perpendicular to geologic strike. The groundwater mound and the complex geology can both be seen. The nature of the deeper groundwater flow system is influenced by geologic structure. Shown in this figure is a breccia zone observed in the logging of well ETF-16. Well ETF-14 is completed in or very near this zone. Water levels taken from this well nest (ETF-13 through -16) show much higher elevations in wells ETF-14 and -15 than any of the other wells (Fig. 43). It appears that this zone is acting as a semi-independent confined aquifer. For December 31, 1982, vertical gradients of 0.004 were measured between wells

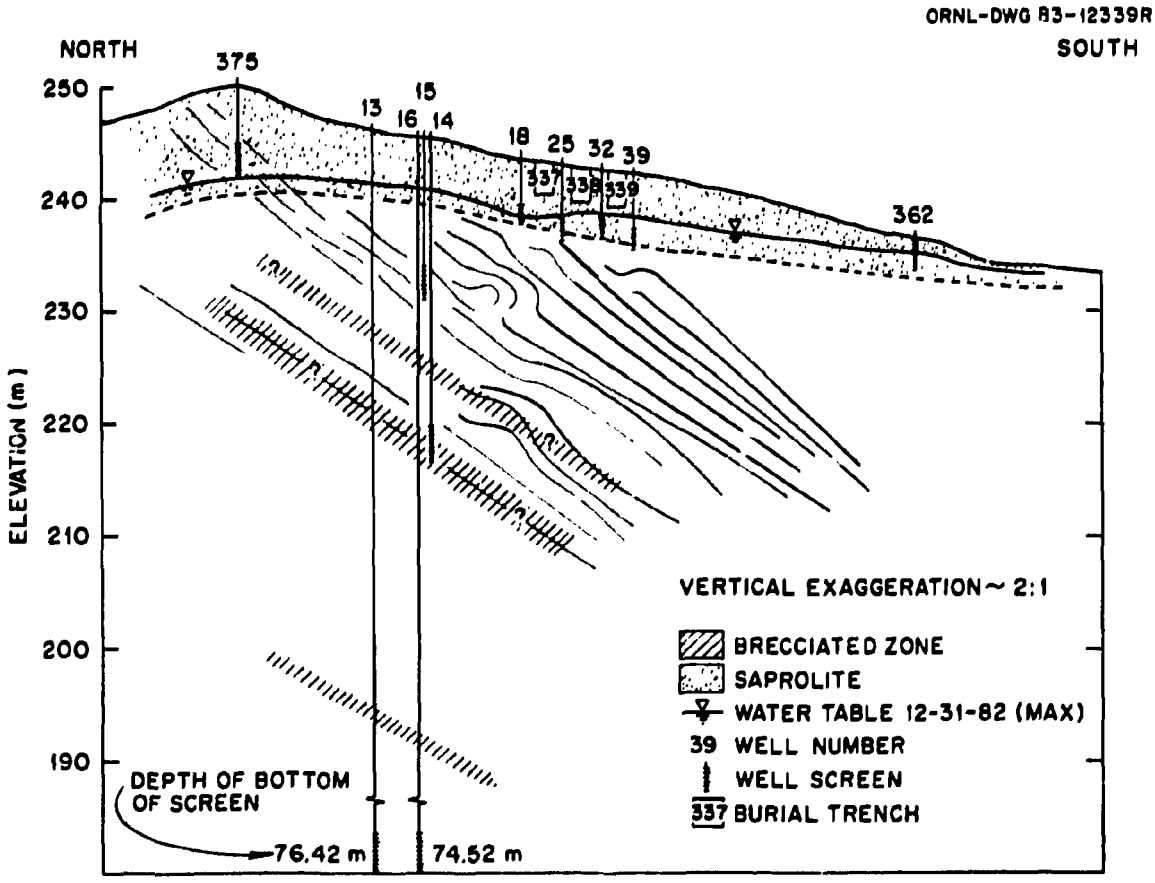

Fig. 43. Cross section 2 of the Engineered Test Facility site. See Fig. 41 for exact location.

ETF-14 and -15 and ETF-14 and -16. The gradient was upward to well ETF-15 and downward to ETF-16. This vertical gradient is about one-tenth the average horizontal gradient in the area.

In summary, groundwater flow is not only controlled locally by the geology at the site but also by the general topography of the area. Local permeability variations may be extemely important during recharge events. Vertical components to groundwater flow are also important at the site, especially during recharge events. The deeper groundwater system may be composed of a series of semi-independently acting "aquifers," one of which is apparent from the monitoring well network at the ETF.

Potentiometric data collected for the period 1980–1983 are being used to construct a hydrologic model for the site. In this stage of model testing, the objective is to have the model reproduce the general equipotential contours during a period when groundwater elevations are relatively stable, such as in late summer. As the model is refined to adequately simulate steady-state conditions at the site, its predictive capabilities will be investigated over a shorter time step by assuming various pertubations (extreme precipitation events or groundwater withdrawal) and comparing the model results to actual field measurements. The water-table monitoring program developed for the ETF site was designed to supply the necessary field data and, aside from the short periods of downtime due to equipment malfunction, has proved to be quite reliable.

4.3.3.4 Water chemistry

In order to measure changes in water quality due to the burial of low-level radioactive waste, or for conducting tracer work, background water quality must be known. To determine background water quality at the ETF site, samples have been routinely collected from wells ETF-1 through -12 and from the two surface drainage streams. Water samples were taken approximately every 2 months from October 1980 through 1981 and then accelerated to twice a month through June 1982. The flumes were sampled less often, but pH and conductivity measurements have been taken on a weekly basis (see Sect. 4.3.2). All samples were analyzed for major cations and anions, as well as trace metals and radioisotopes. As one means of checking the quality and consistency of chemical analyses, a charge balance was made. Results indicated that analyses were consistent; that is, there were only minor differences between anion and cation content. Detailed results of the water chemistry analyses are included in Appendix E.

A trilinear plot of mean water analyses for wells ETF-1 through -12 and Flumes I and II is shown in Fig. 44. All the wells have calcium as the dominant cation (approximately 80% of the

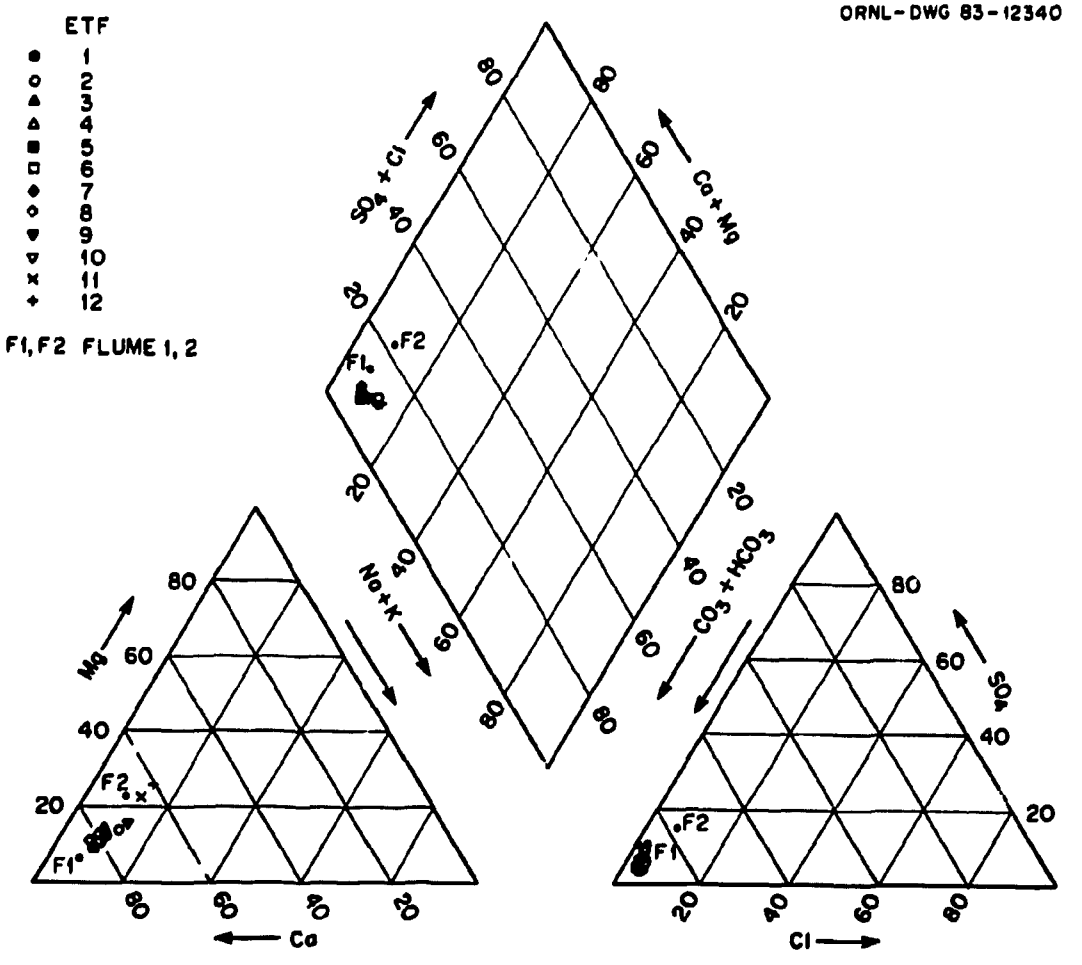

Fig. 44. Trilinear diagram of water analyses for wells ETF-1 through -12 and Flumes I and II.

total) and bicarbonate as the dominant anion (approximately 90% of the total). This water chemistry reflects the lithology at the ETF. The calcium-carbonate water is typical of limestone terrains, while the high silicon dioxide (SiO_2) reflects the high pH and silt content of the Maryville Limestone. Magnesium is the next most abundant cation, indicating that some dolomite or high-magnesium calcite is present in the formation. The only noticeable difference between the analyses, as plotted on the trilinear diagram, is that wells ETF-11 and -12 and Flume II have higher magnesium contents than wells ETF-1 through -10. As discussed earlier, wells ETF-11 and -12 are about 6 m deeper than wells ETF-1 through -10. The two flumes also show slightly higher sulfate contents than the groundwater at the site.

In general, the groundwater at the ETF site is very low in total dissolved solids (TDS), has very low electrical conductivity, and has a neutral to slightly alkaline pH. The surface waters are neutral to slightly acidic but also low in conductivity and TDS. The difference between surface and groundwater analyses may be partially explained by the fact that fertilizer is periodically used on adjacent areas. Nitrate, sulfate, and chloride contents would be especially affected by fertilizer use. The SiO_2 analyses for the flumes are slightly lower than the test wells, and along with pH indicate water derived directly from runoff or very near surface groundwater that has not reacted extensively with the surrounding rock. Correlations between measured parameters have been performed and are summarized in Table 29. The correlations of total alkalinity and magnesium with calcium are obvi-

Table 29. Correlations among several water quality parameters from samples taken at the Engineered Test Facility site

(99.9% level of significance)

Variables	r values	Number of observations
Total alkalinity—Ca	.668	245
Tritium—SO_4	.541	50
Mg—Ca	.668	245
Tritium—Cl	.662	50
TOC[a]—pH	−.704	24

[a]TOC = total organic carbon.

ous ($r \sim 0.7$). The correlations of tritium with SO_4 and chlorine and pH with total organic carbon (TOC) are primarily the result of the surface water analyses, which do indicate contamination from surrounding burial ground operations. Further statistics on all water quality parameters being monitored can be found in Appendix E.

The radionuclide analyses of water samples show essentially no ^{137}Cs, ^{60}Co, or ^{90}Sr. Gross alpha and ^{3}H values are at background levels. Hence, the water contains only background amounts normally found in the environment. Again, values for tritium in the flumes (especially Flume II) do indicate above-background concentrations, evidence of contamination from burial activities to the east of the ETF. The water quality data collected at the ETF are an integral part of the site modeling effort. Background quality has been established, and continued sampling will be used to interpret results of tracer tests designed to map water flow and contaminant transport in the unsaturated

and saturated zones. Because of the low levels of radionuclides in the groundwater at the ETF site, contamination from the nine experimental trenches should be easily detectable in future ground and surface-water samplings.

4.3.3.5 Evaluation

Like the geologic characterization, the hydrologic characterization of the site made use of a variety of measurements and data sources. The focus of work was near surface and in close proximity to the experimental trenches. All methods utilized appear to have value, though limitations were noted.

Hydrologic data reported in this section appear to be adequate to begin fitting a numerical hydrologic model to the site. Areas of uncertainty related to the measurement of downward flow gradients in the saturated zone indicate the potential importance of downward flow in transporting contaminants from disposal sites. Further definition of the vertical dimension at this location, using two or more additional well nests or multilevel monitoring devices, would be a useful adjunct to the study.

Effective porosity is possibly the most difficult measurement to make on the rocks of the Conasauga Group. Tracer tests, fracture measurements, and laboratory measurements should increase the knowledge of porosity magnitude and variability at the ETF. Knowing effective porosity is critical for future predictions of the mass transport in the underlying aquifer.

4.3.4 Unsaturated Zone Hydrology

4.3.4.1 Background

Perhaps the most critical property of the soil formation at a given disposal site is the hydraulic conductivity of the zone in which the waste is to be buried. Ideally, the hydraulic conductivity as a function of water content, over its range of seasonal variation, should be determined. The hydraulic conductivity, at differing moisture contents and suctions, can be mathematically described as a function of the saturated hydraulic conductivity and moisture content (Yeh and Tamura 1982). This can be done either empirically (e.g., Luxmoore 1982, Campbell 1974) or by taking a more general theoretical approach (e.g., Jackson et al. 1965). Thus an accurate estimation of the saturated hydraulic conductivity of the unsaturated zone should be quite adequate for a site characterization. In humid regions, where by definition annual precipitation exceeds evapotranspiration, most of a formation's annual percolation occurs under saturated or near saturated conditions. Thus the saturated hydraulic conductivity exerts the greatest control on the amount of annual percolation through the profile of the unsaturated zone.

This unsaturated zone can exhibit a less-than-simple relationship between hydraulic conductivity and depth within its profile. Such depth variations can be inherited from the stratification of the geologic parent material or arise from spatial variation in the soil's genetic development or its depositional mode. Unless some evidence exists that differing lithologies can be identified within significantly sized or regularly spaced horizons of the unsaturated zone, the most useful approach to measuring hydraulic conductivity would be to obtain an average whole-profile value rather than attempt to measure these hydraulic properties in depth increments. Such a whole-profile value would be heavily weighted by its more conductive horizons or regions. Disposal trenches are generally quite large in relation to any identifiable pattern in the vertical or horizontal spatial variability

of hydraulic properties. At ORNL, at an adjacent site within the Conasauga Group, patterning of horizontal spatial variability could not be detected at the greater than 2-m scale (Luxmoore et al. 1981). If any such patterning does exist, it must be at a scale smaller than 2 m. Trenches are normally constructed at a scale much larger than this (i.e., typically 3 m wide by 3 m deep by 15 m long), so any patterning of hydraulic properties on a smaller scale than this would not be useful to learn. Because an excavated trench would intersect many zones of higher hydraulic conductivity, identification and patterning of small-scale variability would not be expected to be useful in describing waste leaching source terms.

Perhaps the only mathematically tractable method to describe such a random distribution of hydraulic properties would be to obtain enough measurements at more or less random positions within the formation to determine the nature of the population distribution and an estimate of its variance. Extensive previous work with the subsoils of a hillock within the Conasauga Group ORNL (Luxmoore et al. 1981) has shown that the population of hydraulic conductivities is described by a log-normal frequency distribution. Thus the useful statistics for describing such a population distribution would be its log-normalized mean and its coefficient of variation. Such log-normal frequency distributions have been observed by many other workers for regions of quite differing lithologies (Rao et al. 1979, Sisson and Wierenga 1981, and Sharma et al. 1980). Thus such log-normal distributions are to be expected rather than excepted for almost all types of soil and rock formations.

To sample such a population, hydraulic conductivity should be determined at a number of points in the area of interest. At the ETF, this area is defined as the drainage unit of the hillock wherein the trenches are located. Because spatial patterning cannot be expected, there would be no advantage to locating these measuring points on a grid or any other geometric array; actually, a more random selection of locations would have the most statistical validity. In the case of the ETF, locations within or very close to the burial trenches needed to be avoided because backfilled soils will be disturbed and have altered hydraulic properties. At the ETF, there was one apparent difference in soil genesis that was accommodated in the selection of measurement points. Soils on the toeslopes of the hillock receive erosional deposits from the higher elevations; therefore, they are a mixture of material weathered in place and transported material. They may be expected to have differing hydraulic characteristics than the soils on the top and sides of the hillock, which are composed primarily of material weathered in place. Because the hillock comprises most of the area of the ETF site, six measurement points were located within this area and four were located in the toeslope region (Fig. 45).

4.3.4.2 Methods

The method selected for the determination of saturated hydraulic conductivity was that of a well point filter with falling-head water delivery (Hvorslev 1951). Because water is delivered through a standpipe into a sealed section of borehole, a considerable range of hydraulic conductivities can be measured in reasonable time intervals (i.e., 1 d) by an appropriate selection of standpipe and borehole diameters. Soils of low permeability can be measured using large-diameter boreholes (e.g., 20 cm) with small-diameter standpipes (e.g., 2 cm), while more permeable soils can be measured using a narrower ratio of diameters. Very permeable soils can also be measured using a constant-head delivery system with a reservoir of a diameter much greater than the borehole. Thus the technique is adaptable to almost any hydraulic conductivity and can be easily adapted in the field.

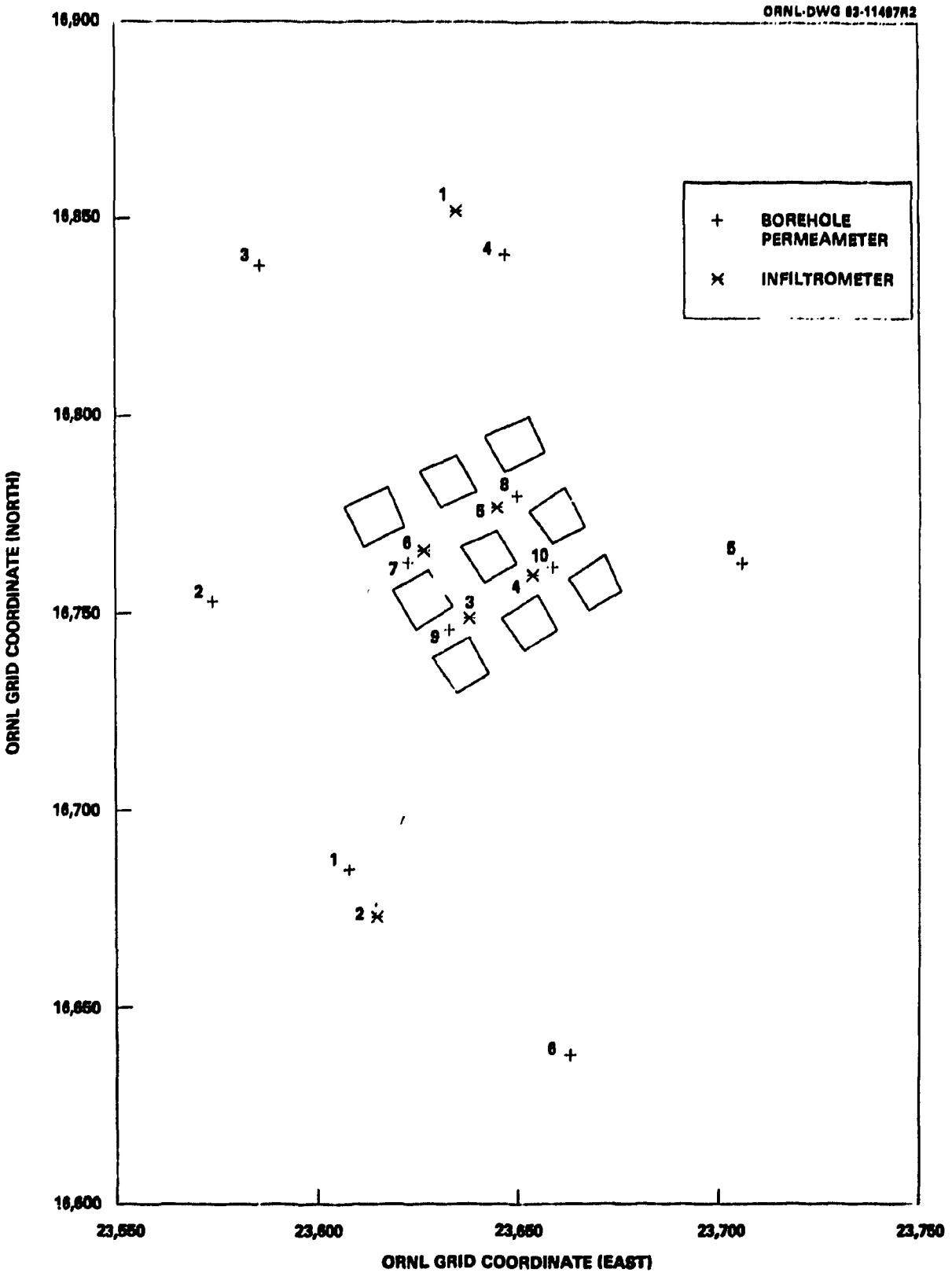

Fig. 45. Location of boreholes and infiltrometers at the Engineered Test Facility site.

In the ETF characterization, boreholes were augered with a gas-powered posthole digger to a depth of approximately 1 m below ground surface. Each 10-cm-diam borehole was then jetted with water for 2 min delivered with a 2.5-cm-diam hose at a rate of 40 L/min to remove sheared soil from the walls and bottom of the borehole. The borehole was then filled to within 30 cm of the ground surface with coarse sand (0.5 mm < diameter < 2 mm). A 2.5-cm-diameter by 91-cm-long glass pipe was inserted into the sand about 5 cm, and a thin (5-cm) concrete collar was poured around it to secure the standpipe in place. The standpipe protruded about 60 cm above the ground surface, facilitating observation of the falling water level. After the concrete had cured for a day, the annulus was filled with sand above the concrete and acrylamide grout (Avanti International 1981) poured in to effect a hydrologic seal for the standpipe. This grout readily permeated the sand and soil formation and set to an impermeable collar material in 20 min. Water was then poured into the standpipe and any trapped air in the sand backfill of the borehole released by agitating with a steel rod. Alternately, a length of rubber tubing could be placed to the bottom of the borehole prior to backfilling with sand to allow entrained air to escape through the annulus of the standpipe when filling the borehole with water; the tubing would have to be stopcocked during permeability measurements.

After pouring at least five standpipe volumes of water, permeability measurements were initiated. Usually two water elevation readings are required for the falling-head measurement: one at time zero and one some time later when the water level in the standpipe has fallen to near the ground surface. These permeability measurements were repeated at least five times to ensure that completely saturated conditions were achieved within the borehole. The two water-level readings within the standpipe were used to calculate the hydraulic conductivity:

$$K = \frac{d^2 \cdot \ln(2mL/D) \cdot \ln(H_1/H_2)}{8L(t_2 - t_1)}, \tag{11}$$

where

K = hydraulic conductivity in meters per second,
d = diameter of standpipe in meters,
D = diameter of borehole in meters,
L = length of open borehole in meters,
m = transformation ratio, assumed = 1,
t = time in seconds,
H = hydraulic head, in meters, at time = t.

For the purpose of calculating the hydraulic head, H, the water table was assumed to be 1.3 m below the bottom of the borehole, and the elevation of water in the standpipe above the bottom of the borehole was added to this assumed water-table depth to compute H. Although this assumption is quite realistic for the ETF site, any error caused by the assumption will exert very little effect on the calculated hydraulic conductivity because only $\ln(H_1/H_2)$ enters the calculation. A slightly different equation would govern the case where a constant-head delivery device were employed (Hvorslev 1951). For formations with extremely low hydraulic conductivities, a pressurized water-delivery-system could be employed, but such a method would not be required for conductivities above about 10^{-9} m/s.

4.3.4.3 Results and discussion

The calculated hydraulic conductivities for the repeated determinations of each borehole are depicted in Fig. 46. The independence of these determinations in repeated measurements is evidence that the zones controlling the hydraulic conductivity of these profiles had been and remained

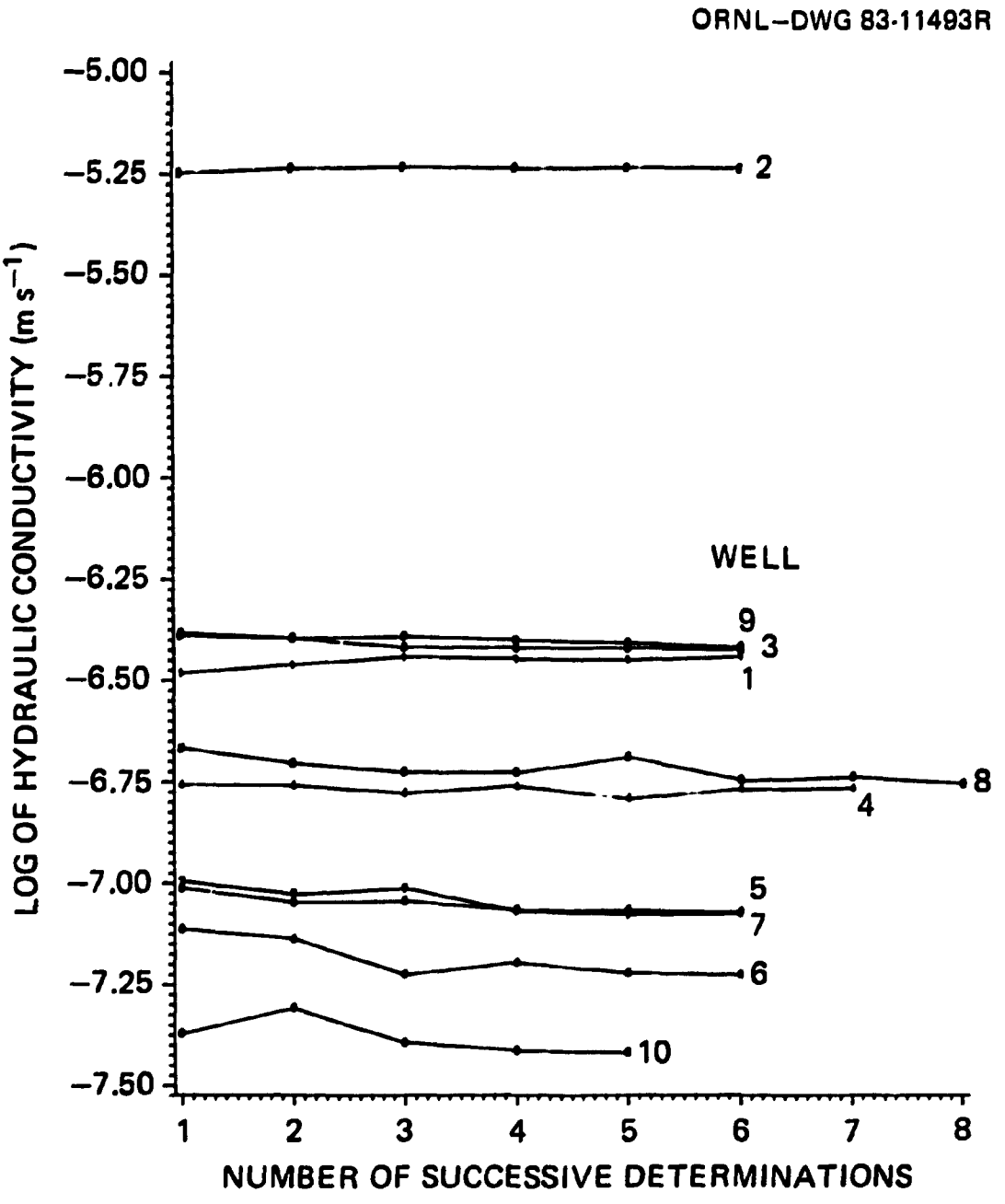

Fig. 46. Calculated hydraulic conductivities for the Engineered Test Facility unsaturated zone based on a number of successive determinations.

saturated. Initial water acceptance rates were much greater during the wetting phase for each borehole and the saturated condition was generally approached within about two borehole void volumes of water. There was no apparent difference between the four toeslope locations (boreholes 1, 2, 4, and 5) and the locations on the hillock. The area can therefore be considered to be a uniform population of hydraulic properties and can be represented by a single frequency distribution. The mean of these ten log-normalized observations was 2.0×10^{-7} m/s, with a coefficient of variation of 122%. Previous investigation in an adjacent hillock area (Luxmoore et al. 1981) found a population of hydraulic conductivities with a log-normalized mean of 2.3×10^{-7} m/s and a coefficient of variation of 129%, employing a sample of 48 locations on a regular grid. Thus the sample set of ten, which was used at the ETF, yielded an adequate description of the frequency distribution of the formation's hydraulic conductivity.

4.3.4.4 Evaluation

The purpose of determining the hydraulic conductivity of the formation's unsaturated zone, in which the waste has been buried, is to model and predict the flux of water leaching the waste. The finite element model for describing the dynamics of water within the formation requires that the hydraulic conductivity of the various finite elements, that is, spatial volumes, be known. Because, as discussed previously, the patterning of spatial variability can be recognized only on a very small scale, the hydraulic conductivity of all finite elements (whose scale will be much larger than the scale of any spatial variability) can probably be represented by the population's log-normalized mean. If many elements for the discretization of the site need to be constructed, then an assignment of their hydraulic conductivities can be made using a Monte Carlo method, with the population frequency distribution as the "dice." The initial discretization of the formation would normally be constructed with a minimum number of finite elements, all with a single hydraulic conductivity value. Any discrepancies between this initial model's predictions and the actual site performance (i.e., water-table elevations) would require increasing the number of finite elements with some incorporation of the population variance of hydraulic conductivity.

If a particular site can be dissected into several hydrologically distinct zones, then each of these zones should be characterized by a separate sample population. Visual, geochemical, or mineralogical differences among zones, however, do not necessarily correlate with hydraulic properties. Therefore, segregation into apparently differing zones should not be attempted until some preliminary determinations indicate that significant differences do exist among the zones.

5. SUMMARY

The ETF is a 0.3-ha study site located in SWSA 6 for purposes of investigating improved SLB methods. As part of the experimental objectives outlined in Chap. 2, a detailed site characterization was initiated in 1981. The purpose of the characterization was not to collect all the information required by NRC and DOE to license a waste disposal site but, rather, to concentrate on information necessary to construct a working hydrologic model. Studies have focused on the major areas of geology, soils, and hydrology (Sects. 4.1, 4.2, and 4.3, respectively), the critical areas where information is needed. The following sections of this report highlight the results of the site characterization study.

5.1 GEOLOGY

1. The ETF is geographically located in Melton Valley, approximately 2 km south of ORNL. It is within the Copper Creek thrust block and is underlain by strata of the Middle to Late Cambrian Conasauga Group. The Conasauga Group is lithologically very heterogeneous, consisting basically of alternating siltstones, silty limestones, limey shales, and mudstones. The ETF site is underlain by such a limestone-rich formation, the Maryville, and is located on one of the hillocks (elevation 243 m MSL) characteristic of SWSA 6.

2. Examination of rock cores taken during drilling of wells indicates that the Maryville is a gray to gray-black massive- to medium-bedded silty interclastic limestone and ribbon-bedded silty limestone interbedded with a thin-bedded mudstone/shale. All of the cores exhibit numerous joints and fractures (mean size = 1–3 mm), some of which are filled with crystalline calcite accompanied by dolomite, pyrite, marcasite, and bladed gypsum.

3. X-ray diffraction studies of selected core samples indicate that chlorite, illite, and mixed layer illite/vermiculite are the major clay mineral constituents.

4. Two major joint/fracture orientations can be found in the Conasauga near the ETF site. The first is a high-angle joint set that is generally found to strike perpendicular to geologic strike. The second type of movement is along bedding planes where slickensides, polishing, and offset can be found, indicating displacement.

5. Measurement of radionuclide Kd's on selected rock samples from a deep core (35 m) showed a decline in ^{85}Sr Kd with depth that parallels the distribution of hardness cations. Two radionuclides, ^{125}I and ^{241}Am, showed little Kd variation with depth, while both ^{134}Cs and ^{58}Co exhibited a gradual decline with depth as less weathered rock was encountered.

6. Chemical properties of the rock samples exhibit a more consistent depth relation with the upper profile, showing a greater total exchangeable cation capacity than deeper samples. Further studies have supported the general conclusion that the Maryville Limestone becomes more inert to cation and radionuclide adsorption with depth.

7. Analysis of seismic refraction data showed two dipping discontinuities at the ETF, which were later identified during trench excavation. Interpretation of soil thickness based on an electrical

resistivity survey compared well with well logs and showed soil thickness to range from 2 to 7 m, being thinnest in the center of the array of experimental trenches (above a major limestone fold).

8. Ground penetrating radar results were confounded by high soil-moisture conditions and were found to be of marginal value in this site characterization.

9. Recommended geologic site characterization activities include: (1) examination of rock cores taken during drilling of monitoring wells; (2) geophysical logging of wells; (3) X-ray diffraction analysis of clay minerals; (4) examination of shallow structure from test excavations; (5) physical, chemical, and radionuclide characterization of rock cores; and (6) employment of various surface geophysical techniques compatible with site conditions.

5.2 SOILS

1. Soil at the ETF site is described as very shallow (A and B horizons), even taking into account the material removed during site clearing. The underlying C horizons are highly leached (strongly acidic) and highly structured due to stratigraphic characteristics inherited from the bedrock. Root penetration is generally not noted below approximately 40 cm.

2. Laboratory batch mode Kd determinations are recommended for determining soil radionuclide Kd's. The ETF soil samples collected during experimental trench excavation exhibited Kd's ranging from a low of 11.7 L/kg (^{125}I) to a high of 64,100 L/kg (^{137}Cs). No observable pattern with depth was noted for any of the soil Kd's. On a larger depth scale extending into comparatively unweathered bedrock, there appeared to be some general decline in most radionuclide Kd's.

3. Soils at the ETF have low pH (4.4) and considerable cation exchange capacities averaging 210 meq/kg. There appeared to be only a minor influence of vegetational nutrient cycling, as evidenced by the modest decline in exchangeable calcium with depth in each soil profile tested.

4. A number of significant correlations were observed among the soil chemical properties measured. Of particular note are the correlations between exchangeable acidity and percent base saturation and pH ($r = 0.80$ and -0.72, respectively). This relationship was expected because the lower the soil pH, the more exchange sites that are occupied by acid cations (Al^{+3} and H^{+}) and, hence, the lower the percentage of these sites that are occupied by basic cations. Calcium dominated these exchangeable bases when the base saturation increased, which accounts for its high correlation ($r = 0.90$) with percent base saturation and its negative correlation with exchangeable acidity ($r = -0.73$).

5. Variation in bulk density and porosity showed no pattern with depth for soil samples tested. Illite and chlorite were identified as the dominant clay minerals.

6. Soils at the ETF site would generally be mapped in the Montevallo series. These are shallow, well-drained upland soils formed from material weathered from acid shale. The soil family is a typic dystrochrept, a strongly leached solum weathering from a rather highly leached parent material.

7. Recommended site characterization activities for soils include: (1) mapping and soil classification, (2) using batch mode methods of determining various radionuclide Kd's, (3) determining soil chemical properties, (4) determining soil physical properties and morphology, and (5) determining clay mineralogy of selected soil samples.

5.3 HYDROLOGY

1. Precipitation measurements at the ETF totaled 1022 mm (1981) and 1295 mm (1982), 19% lower and 2% higher than the average annual rainfall for ORNL 1267 mm. Continuous precipitation monitoring at at least one site in a given study area is recommended.

2. Flow in the two streams draining the ETF ranges from zero (late summer) to highs near 58 L/s (during storm events). Hydrographs of 60 storms were recorded at Flume I, and 120 storms at Flume II. Mean peak discharge for this 30-month period of record was approximately 10 L/s for each stream. Base flow in the two streams at the gauging point is quite low (approximately 0.04 L/s), indicating that the streams are typical headwaters, with most flow occurring during storm events.

3. Chemical analyses of surface water samples indicate runoff from a mixed carbonate and siliceous terrane. Sample pH values are generally in the range of from 7.0 to 7.5, with electrical conductivity values being approximately 150 μS/cm for Stream I and approximately 350 for Stream II. Part of this increased conductivity in Stream II could be due to periodic fertilizer application to an adjacent hillock. Tritium in concentrations as high as 25,000 Bq/L has been observed in Stream II and can be linked to prior disposal operations on an adjacent hill. No tritium or other radionuclides have as yet been detected in Stream I.

4. Surface infiltration measurements under saturated conditions have been carried out on both undisturbed soil (1.56×10^{-5} cm/s) and trench cover material (13.3×10^{-5} cm/s). The higher infiltration value for the trench cover material is to be expected and will likely decrease with time, approaching the value in the undisturbed soil

5. Water-table fluctuations have been measured for a period of 2 years and indicate that the yearly cycle is approximately 1 m, exhibiting a maximum in December–February and a minimum in July–September. Response of water levels to rainfall events is rapid, usually on the order of 5–10 h, and requires several days to return to prestorm conditions.

6. Tracer tests have been interpreted as showing rapid (60–65 d to peak concentration) movement of tracer along strike, between injection well ETF-1 and monitoring well ETF-3. The resulting value of linear velocity is 19.7×10^{-5} cm/s (0.17 m/d).

7. Values of hydraulic conductivity have been measured in each well at the ETF and appear to be spatially related to the fault structure found during trench construction. Mean hydraulic conductivity, based on these individual well slug tests, is 6.31×10^{-5} cm/s. Pump test data have been evaluated using a curve-matching technique based on the Theis equation. From this analysis an aquifer transmissivity of 2.54×10^{-3} m^2/min (3.66 m^2/d) and a storage coefficient of 0.01 were calculated.

8. Analyses of groundwater samples show calcium as the dominant cation (80% of the total) and bicarbonate as the dominant anion (90% of the total). The $CaCO_3$ water is typical of limestone terrains, while the high SiO_2 reflects the high pH and silt content of the Maryville Limestone. Radionuclides in groundwater have been found to be at background levels normally found in the environment.

9. Hydraulic conductivity was determined in the unsaturated zone (area where waste is normally buried) at several locations and found to be 2.0×10^{-5} cm/s. This value compares well with the value of 1.56×10^{-5} cm/s found in the surface infiltration measurements.

10. Recommended hydrologic site characterization activities include: (1) precipitation measurement, (2) runoff measurement in streams draining the site, (3) water-table fluctuations on an annual and storm cycle, (4) surface infiltration, (5) aquifer characteristics, (6) hydraulic conductivity in the saturated and unsaturated zones, and (7) surface and groundwater chemistry.

REFERENCES

Allison, L. E. 1965. "Organic Carbon," in *Methods of Soil Analysis*, Pt. 2. *Agronomy* 9, 1372–1376, American Society Agron., Madison, Wis.

American Public Health Association. 1980. *Standard Methods for the Examination of Water and Wastewater*, American Public Health Association, Washington, D.C.

American Society of Agronomy. 1982. *Methods of Soil Analysis*, Pt. 2, *Chemical and Microbiological Properties*, 2d ed., ed. A. L. Page, American Society Agron., Madison, Wis.

American Society for Testing Materials. 1958. *Procedures for Testing Soils, America Society for Testing Materials*, Philadelphia.

Avanti International. 1981. *Safe Operating Practices for AV-100 Chemical Grout*, Avanti International, Houston.

Baes, C. F., III, and Sharp, R. D. 1983. "A Proposal for Estimation of Soil Leaching and Leaching Constants for Use in Assessment Models," *J. Environ. Qual.* 12, 17–28.

Bertrand, A. R. 1965. "Rate of Water Intake in the Field," in *Methods of Soil Analysis*, Pt. 1, *Agronomy* 9, 197–209, American Society Agron., Madison, Wis.

Boegly, W. J., Jr., and Davis, E. C. 1983. *Design and Construction of a Low-Level Waste Shallow Land Burial Experimental Facility*, Union Carbide Corp. Nuclear Div., ORNL/NFW-83/10, Oak Ridge Natl. Lab.

Bolinger, G. A. 1975. *A Catalog of Southeastern United States Earthquakes, 1754 Through 1974*, Research Division Bull. 101, Department Geol. Science, Va. Polytechnic Institute and State Univ., Blacksburg, Va.

Bouwer, H. 1978. *Groundwater Hydrology*, McGraw-Hill, New York.

Boyle, J. W., et al. 1982. *Environmental Analysis of the Operation of Oak Ridge National Laboratory (X-10 site)*, ORNL-5870, Union Carbide Corp. Nuclear Div., Oak Ridge Natl. Lab.

Campbell, G. S. 1974. "A Simple Method for Determining Unsaturated Conductivity from Moisture Retention Data," *Soil Sci.* 117, 311–314.

Chapman, H. D. 1965. "Total Exchangeable Bases," in *Methods of Soil Analysis*, Pt. 2, *Agronomy* 9, 902–904, American Society Agron., Madison, Wis.

Cooper, W. T. 1981. "Interactions Between Organic Solutes and Mineral Surfaces and the Significance in Hydrogeology," Ph.D. thesis, Indiana University, Bloomington, Ind.

Davis, E. C., Spalding, B. P., and Vaughan, N. D. 1982. *Development of Trench Lining and Grouting Techniques for the Field Demonstration of Improved Shallow Land Burial Practices for*

Low-Level Radioactive Solid Waste, ORNL/NFW-82/31, Union Carbide Corp. Nuclear Div., Oak Ridge Natl. Lab.

Day, P. R. 1965. "Particle Fractionation and Particle Size Analysis," in *Methods of Soil Analysis,* Pt. 1. *Agronomy* 9, 545–567. American Society Agron., Madison, Wis.

Dobrin, M. B. 1960. *Introduction to Geophysical Prospecting,* McGraw-Hill, New York.

Douglas, L. A. 1977. "Vermiculites," pp. 259–292 in *Minerals in Soil Environments,* Soil Science Society America, Madison, Wis.

Ellis, B. G., and Knezek, B. D. 1972. "Adsorption Reactions of Micronutrients in Soils," pp. 59–78 in *Micronutrients in Agriculture,* Soil Science Society America, Madison, Wis.

Fenneman, N. M. 1938. *Physiography of Eastern United States,* McGraw-Hill, New York.

Freeze, R. A. 1975. "A Stochastic-Conceptual Analysis of One-Dimensional Groundwater Flow in a Nonuniform Homogeneous Media," *Water Resour. Res.* 11(5), 725–741.

Freeze, R. A., and Cherry, J. A. 1979. *Groundwater,* Prentice-Hall, Englewood Cliffs, N.J.

Geo-Centers Inc. 1982. *Ground Penetrating Radar Proof of Principle Test, Oak Ridge National Laboratory,* GC-TR-82-229, Geo-Centers Inc., Newton Upper Falls, Mass.

Gilbert/Commonwealth. 1980. *Assessment of Alternatives for Management of ORNL Retrievable Transuranic Waste,* ORNL/Sub-79/13837/5, Union Carbide Corp. Nuclear Div., Oak Ridge Natl. Lab.

Gringarten, A. C., and Witherspoon, P. A. 1972. "A Method of Analyzing Pump Test Data from Fractured Aquifers," pp. T3-B-1 to T3-B-8 in *Proceedings of Symposium, Percolation Through Fissured Rock, September 18–19, 1971, Stuttgart, Germany.* Published for International Society for Rock Mechanics and International Association of Engineering Geology by Deutsche Gesellschaft für Erd- und Grundbau, Essen, Federal Republic of Germany.

Haase, C. S., and Vaughan, N. D. 1981. "Stratigraphy and Lithology of the Conasauga Group in the Vicinity of Oak Ridge, Tenn.," *Abstracts with Programs,* Southeastern Section, The Geological Society of America (30th Annual Meeting, Hattiesburg, Miss.), 13(1), 8.

Haase, C. S. *Subsurface Geologic Data for the Conasauga Group on the USDOE O.R. Reservation,* ORNL/TM-9158, to be published at Oak Ridge National Laboratory.

Hasson, K. O., and Haase, C. S. "Lithology and Paleogeography of the Conasauga Group (Middle and Late Cambrian) in the Valley and Ridge Province of East Tennessee," submitted for publication to American Association of Petroleum Geologists.

Hem, J. D. 1959. *Study and Interpretation of Chemical Characteristics of Natural Water,* U.S. Geol. Surv. Water-Supply Paper 1973.

Hobson, G. 1967. "Seismic Methods in Mining and Groundwater Exploration," pp. 148–176 in *Proceedings of the Canadian Centennial Conference on Mining and Groundwater Geophysics,* Econ. Geol. Report 26, Geol. Surv. Canada, Toronto.

Hvorslev, M. J. 1951. *Time Lag and Soil Permeability in Groundwater Observations,* Bull. No. 36. Waterways Experiment Station, U.S. Army Corps of Engineers, Vicksburg, Miss.

Jackson, M. L. 1974. *Soil Chemical Analysis—Advanced Course,* 2d ed., Univ. Wisconsin, Madison, Wis.

Jackson, R. D., Reginato, R. J., and van Bavel, C. H. M. 1965. "Comparison of Measured and Calculuted Hydraulic Conductivities of Unsaturated Soils," *Water Resour. Res.* **1**, 375–380.

Jacobs, D. G., and Tamura, T. 1960. "The Mechanism of Ion Fixation Using Radioisotope Techniques," *Seventh Int. Cong. of Soil Sci. Trans.* **2**, 206–214.

Klute, A. 1965. "Laboratory Measurement of Hydraulic Conductivity of Saturated Soil," in *Methods of Soil Analysis,* Pt. 1, *Agronomy* **9**, 210–221, American Society Agron., Madison, Wis.

Krumhansl, J. L. 1979. *Conasauga Near-Surface Heater Experiment,* SAND 79-1855, Sandia Lab.

Lennox, D. H., and Carlson, V. 1967. "Integration of Geophysical Methods for Groundwater Exploration in the Prairie Provinces, Canada," pp. 517–533 in *Proceedings of the Canadian Centennial Conference on Mining and Groundwater Geophysics,* Econ. Geol. Report 26, Geol. Surv. Canada, Toronto.

Linsley, R. K., Jr., Kohler, M. A., and Paulhus, J. L. H. 1975. *Hydrology for Engineers,* McGraw-Hill, New York.

Lohman, S. W. 1972. *Groundwater Hydraulics.* U.S. Geol. Surv. Prof. Paper 70B.

Luxmoore, R. J., Spalding, B. P., and Munro, I. L. 1981. "Areal Variation and Chemical Modification of Weathered Shale Infiltration Characteristics," *Soil Sci. Soc. Am. J.* **45**, 687–691.

Luxmoore, R. J. 1982. *Physical Characteristics of Soils of the Southern Region—Fullerton and Sequoia Series,* ORNL-5868, Union Carbide Corp. Nuclear Div., Oak Ridge Natl. Lab.

McDonald, H. R., and Wantland, D. 1961. "Geophysical Procedures in Groundwater Study," *Trans. Am. Soc. Civ. Eng.* **126**, 122–135.

McMaster, W. M. 1963. *Geologic Map of the Oak Ridge Reservation, Tennessee* (geologic), ORNL/TM-713, Union Carbide Corp. Nuclear Div., Oak Ridge Natl. Lab.

Peech, M. 1965. "Exchange Acidity," in *Methods of Soil Analysis,* Pt. 2, *Agronomy* **9**, 910–911. American Society Agron., Madison, Wis.

Philip, J. R. 1957. "The Theory of Infiltration: 4. Sorptivity and Algebraic Infiltration Equations," *Soil Sci.* **84**, 257–264.

Rao, P. V., et al. 1979. "Use of Goodness-of-Fit Tests for Spatial Variability of Soil Properties," *Soil Sci. Soc. Am. J.* **43**, 274–278.

Sease, J. D., et al. 1982. "ORNL Radioactive Waste Operations," pp. 133–143 in *Proceedings of the Symposium on Waste Management at Tucson, Arizona,* vol. 2, ed. R. G. Post, Univ. Ariz., Tucson, Ariz.

Sharma, M. L., Grander, G. A., and Hunt, C. G. 1980. "Spatial Variability of Infiltration in a Watershed," *J. Hydrol.* **45**, 101–122.

Siefken, D., et al. 1982. *Site Suitability, Selection, and Characterization,* NUREG-0902, Branch Technical Position--Low-Level Waste Licensing Branch, U.S. Nuclear Regulatory Commission.

Sisson, J. B., and Wierenga, P. J. 1981. "Spatial Variability of Steady-State Infiltration Rates as a Stochastic Process," *Soil Sci. Soc. Am. J.* 45, 699–704.

Sledz, J. J., and Huff, D. D. 1981. *Computer Model for Determining Fracture Porosity and Permeability in the Conasauga Group, Oak Ridge National Laboratory, Tennessee,* ORNL/TM-7695, Union Carbide Corp. Nuclear Div., Oak Ridge Natl. Lab

Spalding, B. P. 1980. "Adsorption of Radiostrontium by Soil Treated with Alkali Metal Hydroxides," *Soil Sci. Soc. Am. J.* 44, 703–709.

Stockdale, P. 1951. *Geologic Conditions at the Oak Ridge National Laboratory (X-10) Area Relevant to the Disposal of Radioactive Waste,* ORO-58, Oak Ridge Operations, U.S. Department Energy.

Stumm, W., and Morgan, J. J. 1981. *Aquatic Chemistry: An Introduction Emphasizing Chemical Equilibria in Natural Waters.* 2d. ed., John Wiley and Sons, New York.

Swann, M. E., et al. 1942. *Roane County, Tennessee, Soil Survey.* U.S. Department Agriculture, Bureau of Plant Industry, Ser. 1936 No. 15.

U.S. Congress. 1976. *Resource Conservation and Recovery Act of 1976,* PL 94-580.

U.S. Department of Agriculture (USDA), Soil Conservation Service. 1951. *Soil Survey Manual.*

U.S. Department of Agriculture (USDA), Soil Conservation Service. 1961. *Soil Survey of Loudon County, Tennessee,* Ser. 1958 No. 2.

U.S Department of Agriculture (USDA), Soil Conservation Service. 1972. *Soil Survey Laboratory Methods and Procedures for Collecting Soil Samples.* Soil Survey Investigation Report No. 1.

U.S Department of Agriculture (USDA), Soil Conservation Service. 1975. *Soil Taxonomy.* Agriculture Handbook No. 436.

U.S Department of Agriculture (USDA), Soil Conservation Service. 1981. *Soil Survey of Anderson County, Tennessee.*

U.S. Department of Commerce (DOC), National Oceanic and Atmospheric Administration. 1972. *Daily, Monthly, and Annual Climatological Data for Oak Ridge, Tennessee, Townsite and Area Stations January 1951 Through December 1971,* National Climatic Center, Asheville, N.C.

U.S. Department of Commerce (DOC), National Oceanic and Atmospheric Administration. 1981. *Local Climatological Data Annual Summary with Comparative Data, Oak Ridge, Tennessee,* National Climatic Center, Asheville, N.C.

U.S. Department of Energy (DOE). 1983. *Radioactive Waste Management,* draft DOE order 5820.

U.S. Environmental Protection Agency (EPA). 1979. Methods for Chemical Analysis of Water and Wastes, Publ. 600/4-79-020.

U.S. Environmental Protection Agency (EPA). 1982. *Hazardous Waste Management System: Permitting Requirements for Land Disposal Facilities*, 47 FR 32274–32388.

U.S. Nuclear Regulatory Commission (NRC). 1979. *USNRC Rules and Regulations, Pt. 20, Standards for Protection Against Radiation, Revised January 1, 1979.*

U.S. Nuclear Regulatory Commission (NRC). 1981. *Licensing Requirements for Land Disposal of Radioactive Waste*, Draft Environmental Impact Statement on 10CFR Pt. 61, Main Report, NUREG-0782, vol. 2.

U.S. Nuclear Regulatory Commission (NRC). 1982. *Licensing Requirements for Land Disposal of Radioactive Waste*, Final Environmental Impact Statement on 10CFR Pt. 61, NUREG-0934, vol. 1.

Vaughan, N. D., et al. 1982. *Field Demonstration of Improved Shallow Land Burial Practices for Low-Level Radioactive Solid Wastes: Preliminary Site Characterization and Progress Report*, ORNL/TM-8477, Union Carbide Corp. Nuclear Div., Oak Ridge Natl. Lab.

Whittig, L. D. 1965. "X-ray Diffraction Techniques for Mineral Identification and Mineralogical Composition," in *Methods of Soil Analysis*, Pt. 1. *Agronomy* 9, 671–698, American Society Argon., Madison, Wis.

Wilson, D. G. 1977. *Handbook of Solid Waste Management.* Van Nostrand Reinhold, New York.

Yeh, G. T., and Tamura, T. 1982. "Geohydrological Considerations in Land Disposal of Low-Level Wastes," *Nuc. Sci. Eng.* **82**, 206–219.

Appendix A

REPORTS RELATED TO SWSA 6 AND GENERAL DISPOSAL SITE CHARACTERISTICS

1. Arora, H. S., et al. 1981. *An Assessment of the Effect of a Bentonite Seal on Groundwater Storage in Underlying Waste Disposal Trenches at Oak Ridge National Laboratory,* ORNL/TM-7416, Union Carbide Corp. Nuclear Div., Oak Ridge Natl. Lab.

2. Barnett, J. 1954. *Geological Investigations: Waste Disposal Area, Oak Ridge National Laboratory, Oak Ridge, Tennessee.* U.S. Army Corps of Engineers, Ohio River Division Laboratories, Mariemont, Ohio.

3. Cowser, K. E., Lomenick, T. F., and McMaster, W. M. 1961. *Status Report on Evaluation of Solid Waste Disposal at ORNL: I,* ORNL-3035, Union Carbide Corp. Nuclear Div., Oak Ridge Natl. Lab.

4. Dames and Moore. 1978. *Applicability of a Generic Monitoring Program for Radioactive Waste Burial Grounds at Oak Ridge National Laboratory and Idaho National Engineering Laboratory,* ORNL/SUB-7167/1, Union Carbide Corp. Nuclear Div., Oak Ridge Natl. Lab.

5. Duguid, J. O. July 1975. *Status Report on Radioactivity Movement from Burial Grounds in Melton and Bethel Valleys,* ORNL-5017, Union Carbide Corp. Nuclear Div., Oak Ridge Natl. Lab.

6. Duguid, J. O. October 1976. *Annual Progress R port of Burial Ground Studies at Oak Ridge National Laboratory: Period Ending September 30, 1975,* ORNL-5141, Union Carbide Corp. Nuclear Div., Oak Ridge Natl. Lab.

7. Jacobs, D. G., Epler, J. S., and Rose, R. R. 1980. *Identification of Technical Problems Encountered in the Shallow Land Burial of Low-Level Radioactive Wastes,* ORNL/SUB-80/13619/1, Union Carbide Corp. Nuclear Div., Oak Ridge Natl. Lab.

8. Lomenick, T. F., and Cowser, K. E. 1961. *Status Report on Evaluation of Solid Waste Disposal at ORNL: II,* ORNL-3182, Union Carbide Corp. Nuclear Div., Oak Ridge Natl. Lab.

9. Lomenick, T. F., and Wyrick, H. J. December 1965. *Geohydrological Evaluation of Solid Waste Storage Area 6,* ORNL TM-1327, Union Carbide Corp. Nuclear Div., Oak Ridge Natl. Lab.

10. McClain, W. C., and Meyer, O. H. 1970. *Seismic History and Seismicity of the Southeastern Region of the United States,* ORNL-4582, Union Carbide Corp. Nuclear Div., Oak Ridge Natl. Lab.

11. McMaster, W. M. 1963. *Geologic Map of the Oak Ridge Reservation, Tennessee* (geologic), ORNL/TM-713, Union Carbide Corp. Nuclear Div., Oak Ridge Natl. Lab.

12. McMaster, W. M., and Waller, H. D. 1965. *Geology and Soils of White Oak Creek Basin, Tennessee,* ORNL-1108, Union Carbide Corp. Nuclear Div., Oak Ridge Natl. Lab.

13. McMaster, W. M. 1967. *Hydrologic Data for the Oak Ridge Area, Tennessee,* U.S. Geol. Surv. Water-Supply Paper 1839-N.

14. Oakes, T. W., and Shank, K. E. 1979. *Radioactive Waste Disposal Areas and Associated Environmental Surveillance Data at Oak Ridge National Laboratory,* ORNL/TM-6893, Union Carbide Corp. Nuclear Div., Oak Ridge Natl. Lab.

15. Rogers, J. 1953. *Geologic Map with Explanatory Text* (geologic), Bull. 58, Pt. 2, Tenn. Div. Geol., Nashville, Tenn.

16. Sledz, J. J., and Huff, D. D. 1981. *Computer Model for Determining Fracture Porosity and Permeability in the Conasauga Group, Oak Ridge National Laboratory, Tennessee,* ORNL/TM-7695, Union Carbide Corp. Nuclear Div., Oak Ridge Natl. Lab.

17. Stockdale, P. B. 1951. *Geologic Conditions at the Oak Ridge National Laboratory (X-10) Area Relevant to the Disposal of Radioactive Waste,* ORO-58, Oak Ridge Operations, U.S. Department Energy.

18. Struxness, E. G. 1962. *General Description of Oak Ridge Site and Surrounding Areas—Hazards Evaluation,* vol. 2, ORNL/TM-323, Union Carbide Corp. Nuclear Div., Oak Ridge Natl. Lab.

19. Tamura, T., et al. 1980. *Progress Report of Disposal Area Studies at Oak Ridge National Laboratory: Period of October 1, 1975, to September 30, 1977,* ORNL-5514, Union Carbide Corp. Nuclear Div., Oak Ridge Natl. Lab.

20. U.S. Department of Commerce (DOC), National Oceanic and Atmospheric Administration. July 1972. *Daily, Monthly, and Annual Climatological Data for Oak Ridge, Tennessee, Townsite and Area Stations January 1951 Through December 1971.* National Climatic Center, Asheville, N.C.

21. Webster, D. A. 1976. *A Review of Hydrologic and Geologic Conditions Related to the Radioactive Solid-Waste Burial Grounds at Oak Ridge National Laboratory, Tennessee,* U.S. Geol. Surv. Open File Report 76-727.

22. Webster, D. A. 1979. "Land Burial of Solid Radioactive Waste at Oak Ridge National Laboratory, Tennessee," pp. 731–746 in *Management of Low-Level Radioactive Wastes,* vol. 2, ed. M. W. Carter, A. A. Moghissi, and B. Kahn, Pergamon Press, New York.

23. Webster, D. A., et al. 1981. *Water-Level Data for Wells in Burial Ground 6, Oak Ridge National Laboratory, Tennessee, 1975–1979.* U.S. Geol. Surv. Open File Report 81-57.

Appendix B
STRATIGRAPHIC COLUMNS

DESCRIPTION OF STRATIGRAPHIC COLUMNS

The columns in this appendix are based on recovered core material. Also noted are zones of poor or no recovery. (Material from the residuum was not recovered; therefore, no description of it is included.) From left to right the column shows depth, color, bedding structures, and lithology. The lithologic portion indicates the relative abundance of lithology at a given horizon. The "ragged" edge of the column represents a weathering profile. Narrow areas or hollows indicate a soft, easily weathered zone. Wide zones, or ridges, represent hard zones, usually less easily weathered limestone beds. The weathering profile is based on drilling information as well as percent carbonate in the recovered material. Further descriptions of symbols, with nomenclature, and structures can be found in most general geology texts.

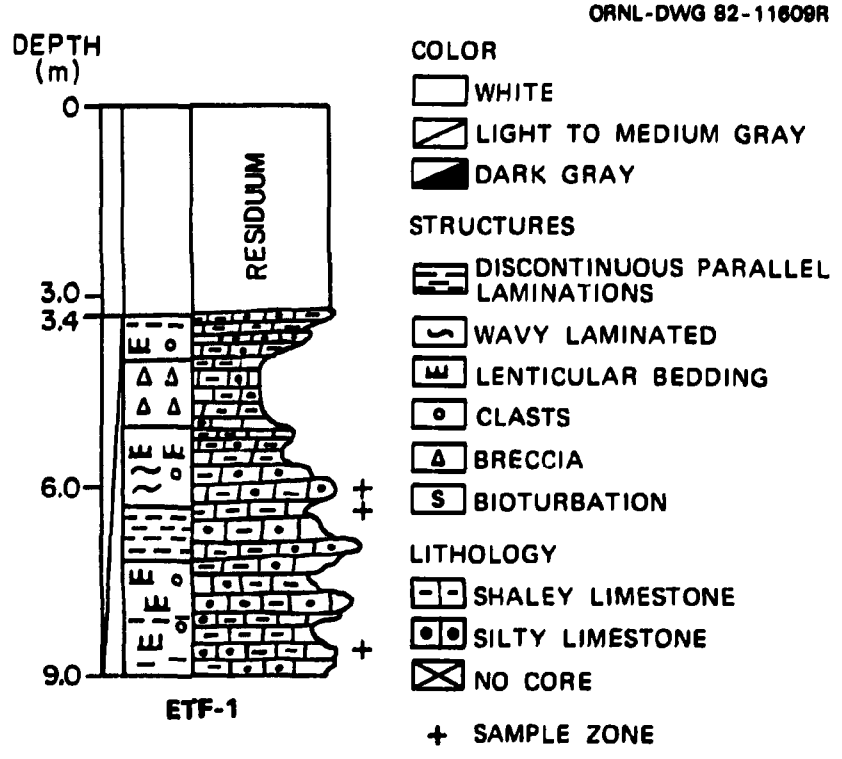

Fig. B.1. Stratigraphic column: ETF-1. Interbedded gray-white interclastic limestone and dark gray to black shale. Fractures numerous, some filled with calcite (white and pink); limestone slightly silty. Occasional solution cavities and brecciated zones. Worm burrows.

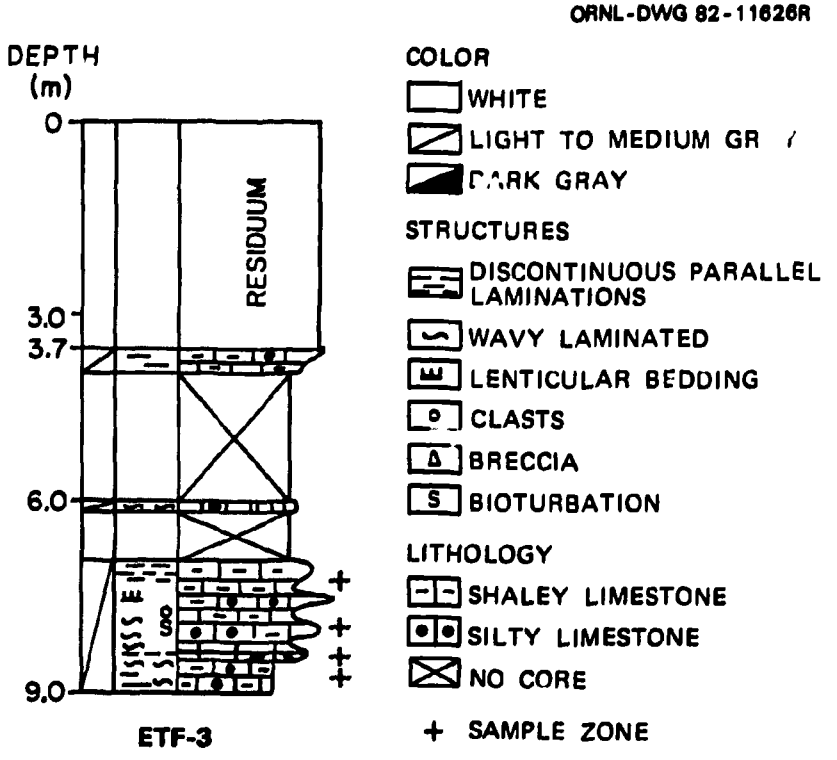

Fig. B.2. Stratigraphic column: ETF-3. Interbedded gray-white silty interclastic limestone and gray, mica-bearing calcareous shale. Clasts surrounded by thin shale layers. Fractures filled with pink and white calcite. Fault (8.5 m) with few millimeters of offset noted. Worm burrows numerous.

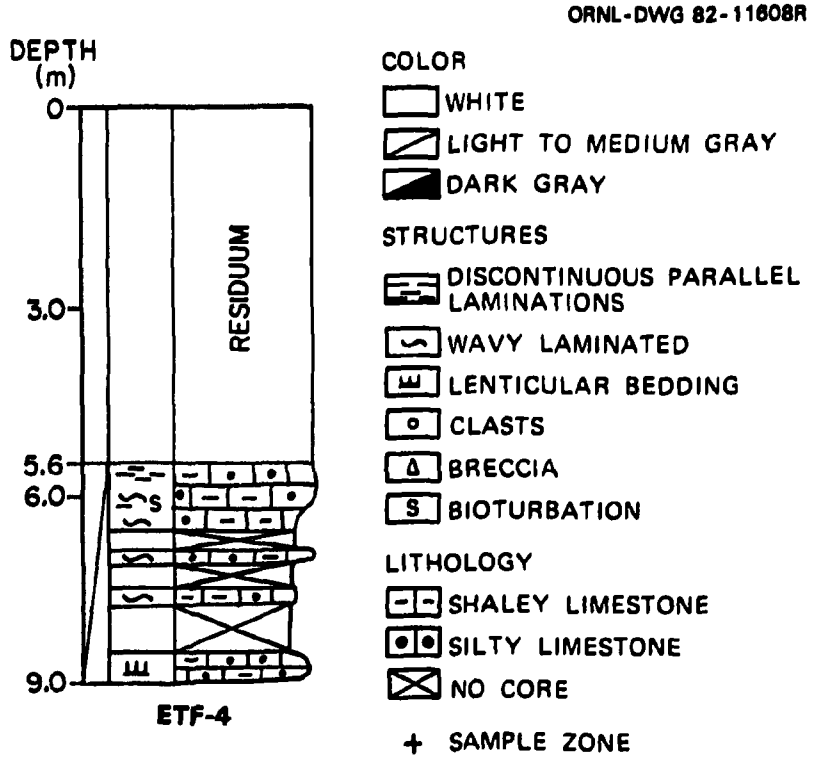

Fig. B.3. Stratigraphic column: ETF-4. Interbedded gray-white interclastic micritic, silty limestone and gray shale. Clasts micritic; shale layers and partings surround clasts. Partings and layers present to give poker-chip-style sections. Fractures, several large, filled with pink and white calcite. Rock pieces in broken zone very weathered.

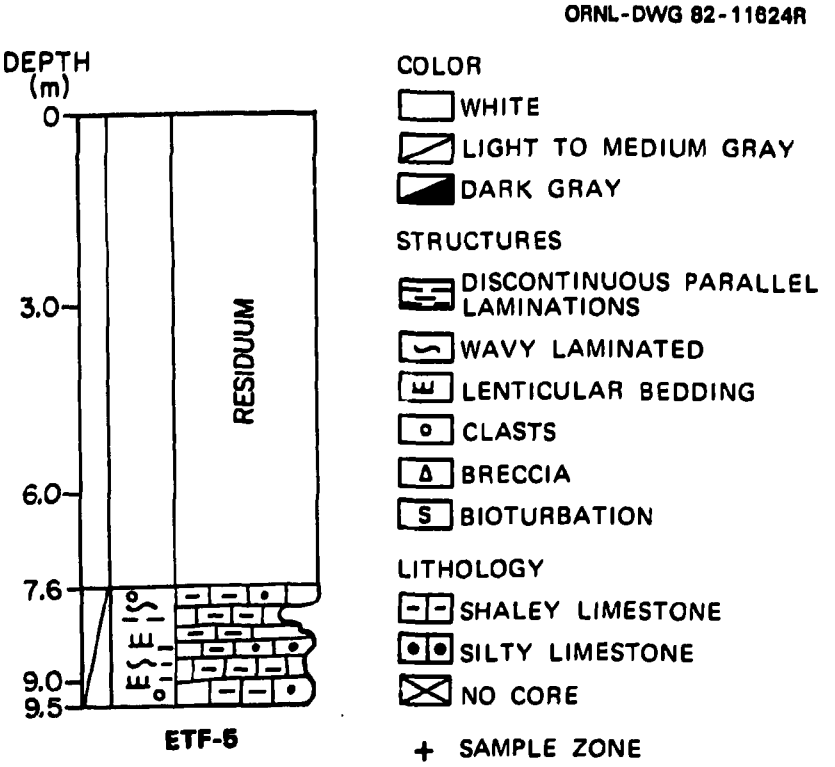

Fig. B.4. Stratigraphic column: ETF-5. Interbedded gray-white interclastic limestone and gray shale. Clasts are micritic; shales, thin-bedded and in irregular lenses. Fractures are calcite filled. Solution cavity filled with shale; worm burrows.

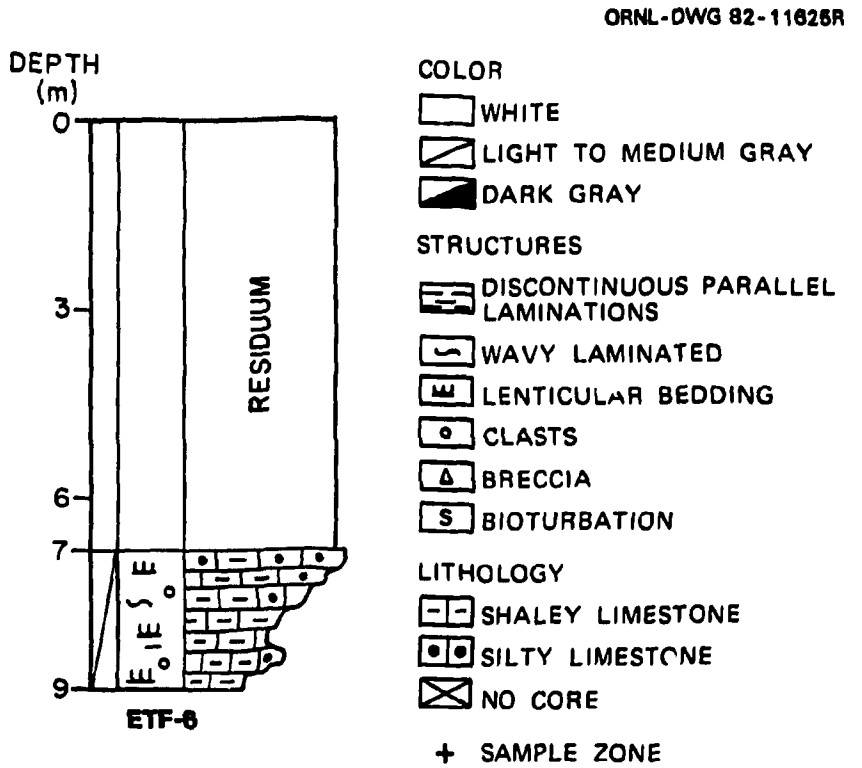

Fig. B.5. Stratigraphic column: ETF-6. Interbedded gray-white micritic limestone and gray shale. Shale lenses are convoluted, with irregular bedding patterns. Fractures calcite filled and cross-cutting beddings. Solution cavities present.

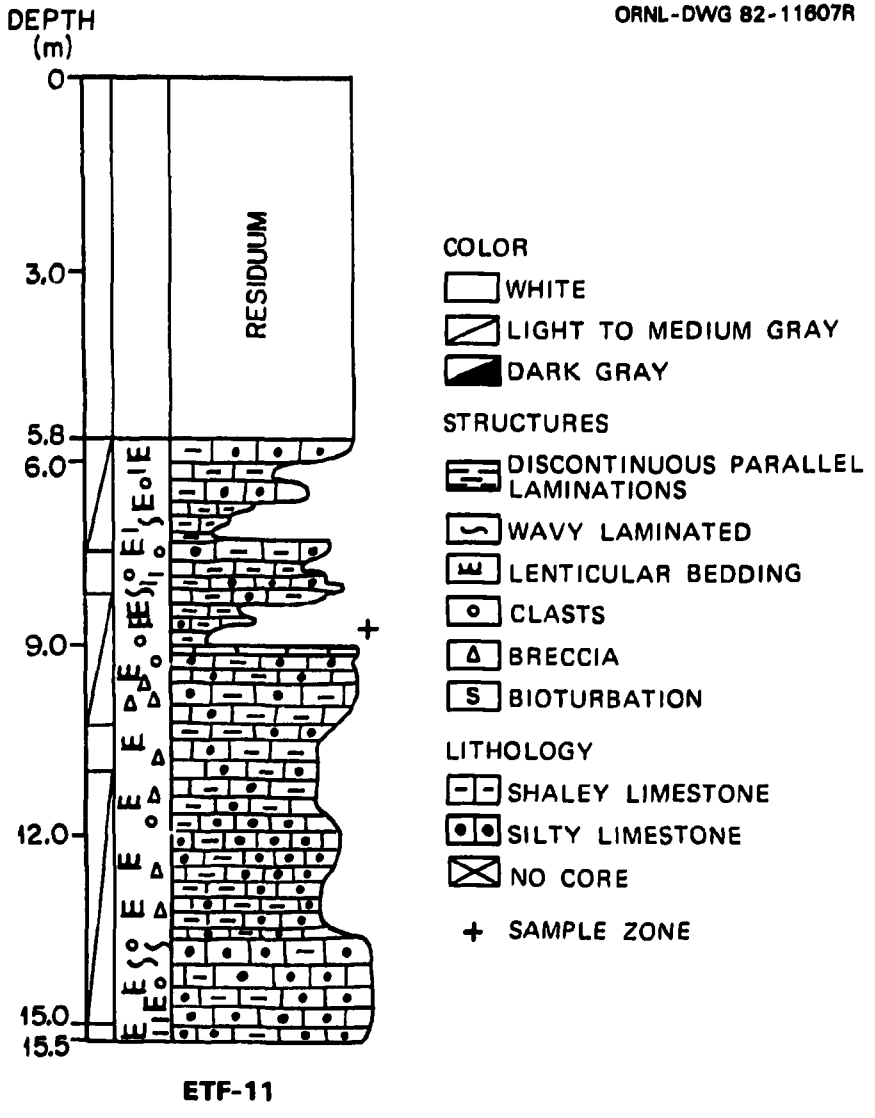

Fig. B.6. Stratigraphic column: ETF-11. Interbedded interclastic gray-white limestone and gray shale. Numerous fractures with calcite veins and fillings present. Pyrite and marcasite (?) present in fractures as well as large, well-developed gypsum-bladed crystals. Numerous solution cavities open and partially filled. Thin shale lenses between clasts.

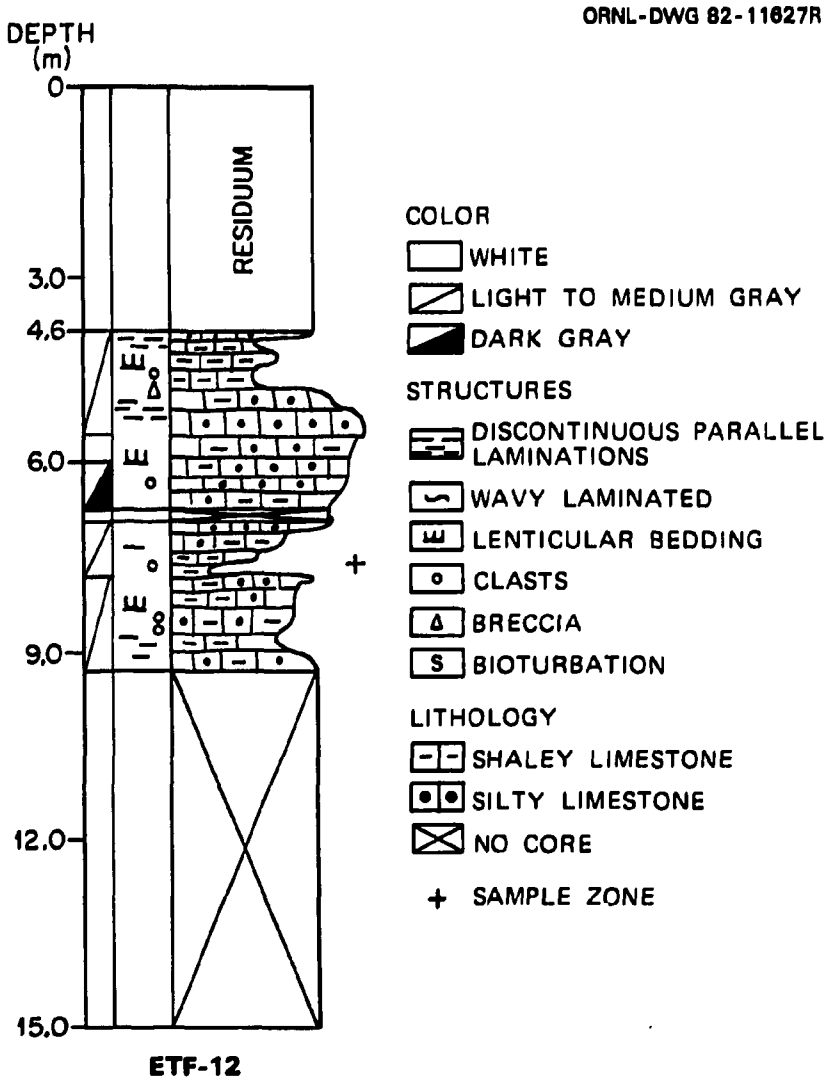

Fig. B.7. Stratigraphic column: ETF-12. Interbedded interclastic gray-white limestone and gray-black shale. Numerous fractures are calcite filled; solution cavities with local iron-oxide coatings. Pyrite, partially oxidized, on some fractures; gypsum crystals. At 6.7 m, 20-cm-thick zone of solution cavities. At 7.6 m, a shear or fracture zone with calcite filling. Pyrite also in shale.

Appendix C
SUMMARY OF DAILY PRECIPITATION

Table C.1. Summary of 1980 daily precipitation

Day	August		September		October		November		December	
	in.	mm	in.	mm	in.	mm	in.	mm	in.	mm
1	*a*	*a*	0.00	0.00	0.00	0.00	0.00	0.00	0.00	0.00
2	*a*	*a*	0.12	3.18	0.03	0.64	0.00	0.00	0.00	0.00
3	*a*	*a*	0.00	0.00	0.00	0.00	0.00	0.00	0.00	0.00
4	*a*	*a*	0.00	0.00	0.00	0.00	0.20	5.08	0.00	0.00
5	*a*	*a*	0.00	0.00	0.00	0.00	0.00	0.00	0.00	0.00
6	*a*	*a*	0.03	0.64	0.00	0.00	0.00	0.00	0.00	0.00
7	*a*	*a*	0.00	0.00	0.00	0.00	0.00	0.00	0.00	0.00
8	*a*	*a*	0.00	0.00	0.00	0.00	0.00	0.00	0.00	0.00
9	*a*	*a*	0.00	0.00	0.00	0.00	0.00	0.00	1.15	29.21
10	*a*	*a*	0.90	22.86	0.00	0.00	0.00	0.00	0.03	0.64
11	0.03	0.64	0.00	0.00	0.00	0.00	0.00	0.00	0.00	0.00
12	0.23	5.72	0.00	0.00	0.00	0.00	0.00	0.00	0.00	0.00
13	0.03	0.64	0.00	0.00	0.00	0.00	0.00	0.00	0.00	0.00
14	0.00	0.00	0.00	0.00	0.00	0.00	0.03	0.64	0.00	0.00
15	0.38	9.53	0.00	0.00	0.00	0.00	0.80	20.32	0.00	0.00
16	0.05	1.27	0.00	0.00	0.00	0.00	0.00	0.00	0.00	0.00
17	0.30	7.62	0.08	1.91	0.00	0.00	0.85[b]	21.59[b]	0.00	0.00
18	0.00	0.00	0.00	0.00	1.00	25.40	0.00[b]	0.00[b]	0.00	0.00
19	0.03	0.64	0.00	0.00	0.00	0.00	0.00	0.00	0.03	0.64
20	0.08	1.91	0.23	5.72	0.00	0.00	0.00	0.00	0.00	0.00
21	0.00	0.00	0.00	0.00	0.00	0.00	0.00	0.00	0.00	0.00
22	0.00	0.00	0.00	0.00	0.00	0.00	0.00	0.00	0.00	0.00
23	0.00	0.00	0.00	0.00	0.00	0.00	0.90	22.86	0.00	0.00
24	0.00	0.00	0.23	5.72	0.20	5.08	0.60	15.24	0.55	13.97
25	0.00	0.00	0.30	7.62	0.20	5.08	0.00	0.00	0.00	0.00
26	0.00	0.00	0.00	0.00	0.00	0.00	0.10	2.54	0.00	0.00
27	0.00	0.00	0.00	0.00	0.33	8.26	0.58	14.60	0.00	0.00
28	0.00	0.00	0.38	9.52	0.03	0.64	0.00	0.00	0.00	0.00
29	0.00	0.00	0.08	1.90	0.00	0.00	0.00	0.00	0.00	0.00
30	0.00	0.00	0.38	9.52	0.00	0.00	0.00	0.00	0.05	1.27
31	0.30	7.62			0.00	0.00			0.00	0.00
Total	1.43	35.59	2.73	68.59	1.79	45.10	4.06	102.87	1.81	45.73

[a]Rainfall gauging station was not in operation until August 10, 1980.

[b]Total precipitation for this day may be inaccurate, because the capacity of the gauge was exceeded.

Table C.2. Summary of 1981 daily precipitation

Day	January		February		March		April		May		June	
	in.	mm	in.	mm	in.	mm	in.	mm	in.	mm	in.	mm
1	0.00	0.00	1.72	43.82	0.00	0.00	0.08	1.90	0.00	0.00	0.05	1.27
2	0.00	0.00	0.00	0.00	0.00	0.00	0.00	0.00	0.00	0.00	0.25	6.35
3	0.00	0.00	0.00	0.00	0.00	0.00	0.00	0.00	0.00	0.00	0.15	3.81
4	0.00	0.00	0.00	0.00	0.52	13.34	0.45	11.43	0.00	0.00	0.52	13.34
5	0.00	0.00	0.00	0.00	0.20	5.08	0.65	16.51	0.00	0.00	0.03	0.64
6	0.15	3.81	0.00	0.00	0.00	0.00	0.00	0.00	0.00	0.00	1.58	40.00
7	0.03	0.64	0.05	1.27	0.00	0.00	0.00	0.00	0.00	0.00	0.00	0.00
8	0.00	0.00	0.08	1.90	0.00	0.00	0.00	0.00	0.00	0.00	0.00	0.00
9	0.00	0.00	0.00	0.00	0.00	0.00	0.55	13.97	0.00	0.00	0.00	0.00
10	0.00	0.00	1.35	34.29	0.00	0.00	0.00	0.00	0.03	0.64	0.68	17.14
11	0.00	0.00	0.20	5.08	0.00	0.00	0.00	0.00	0.00	0.00	0.00	0.00
12	0.00	0.00	0.00	0.00	0.00	0.00	0.00	0.00	0.00	0.00	0.00	0.00
13	0.00	0.00	0.00	0.00	0.00	0.00	0.00	0.00	0.00	0.00	0.00	0.00
14	0.00	0.00	0.00	0.00	0.00	0.00	0.08	1.90	0.22	5.72	0.00	0.00
15	0.00	0.00	0.00	0.00	0.08	1.90	0.00	0.00	0.00	0.00	0.00	0.00
16	0.00	0.00	0.00	0.00	0.05	1.27	0.03	0.64	0.00	0.00	0.00	0.00
17	0.00	0.00	0.65	16.51	0.00	0.00	0.40	10.16	0.00	0.00	0.00	0.00
18	0.00	0.00	0.40	10.16	0.00	0.00	0.10	2.54	0.08	1.90	0.00	0.00
19	0.00	0.00	0.10	2.54	0.00	0.00	0.30	7.62	0.62	15.88	0.00	0.00
20	0.28	6.99	0.00	0.00	0.00	0.00	0.80	20.32	0.00	0.00	0.00	0.00
21	0.03	0.64	0.00	0.00	0.00	0.00	0.00	0.00	0.00	0.00	0.00	0.00
22	0.00	0.00	0.18	4.44	0.62	15.88	0.00	0.00	0.00	0.00	0.58	14.60
23	0.00	0.00	0.05	1.27	0.03	0.64	0.20	5.08	0.00	0.00	0.00	0.00
24	0.00	0.00	0.00	0.00	0.00	0.00	0.00	0.00	0.00	0.00	0.00	0.00
25	0.00	0.00	0.00	0.00	0.00	0.00	0.00	0.00	0.60	15.24	0.80	20.32
26	0.00	0.00	0.00	0.00	0.00	0.00	0.00	0.00	0.30	7.62	0.00	0.00
27	0.18	4.44	0.00	0.00	0.00	0.00	0.00	0.00	0.68	17.14	0.00	0.00
28	0.00	0.00	0.08	1.90	0.00	0.00	0.00	0.00	0.00	0.00	0.00	0.00
29	0.00	0.00			0.10	2.54	0.12	3.18	0.00	0.00	0.00	0.00
30	0.28	6.98			1.15	29.21	0.00	0.00	1.18	29.84	0.00	0.00
31	0.00	0.00			0.00	0.00			0.30	7.62		
Total	0.95	23.50	4.86	123.18	2.75	69.96	3.76	95.25	4.01	101.60	4.64	117.47

Table C.2 (continued)

July		August		September		October		November		December	
in.	mm	in.	mm	in.	mm	in.	mm	in.	mm	in.	mm
0.32	8.26	0.00	0.00	0.40	10.16	0.28	6.98	0.00	0.00	0.55	13.97
0.00	0.00	0.18	4.44	0.00	0.00	0.00	0.00	0.00	0.00	0.00	0.00
0.00	0.00	0.00	0.00	0.15	3.81	0.00	0.00	0.00	0.00	0.00	0.00
0.00	0.00	0.00	0.00	0.45	11.43	0.00	0.00	0.00	0.00	0.03	0.64
1.32	33.66	0.00	0.00	0.00	0.00	0.10	2.54	0.18	4.44	0.00	0.00
0.00	0.00	0.50	12.70	0.00	0.00	0.00	0.00	0.00	0.00	0.00	0.00
0.12	3.18	0.08	1.90	0.00	0.00	0.00	0.00	0.00	0.00	0.00	0.00
0.00	0.00	0.70	17.78	0.00	0.00	0.00	0.00	0.00	0.00	0.00	0.00
0.00	0.00	0.00	0.00	0.00	0.00	0.00	0.00	0.00	0.00	0.00	0.00
0.08	1.90	0.00	0.00	0.00	0.00	0.03	0.64	0.00	0.00	0.00	0.00
0.00	0.00	0.05	1.27	0.00	0.00	0.00	0.00	0.00	0.00	0.00	0.00
0.00	0.00	0.12	3.18	0.00	0.00	0.00	0.00	0.00	0.00	0.00	0.00
0.00	0.00	0.00	0.00	0.00	0.00	0.00	0.00	0.00	0.00	0.00	0.00
0.00	0.00	0.00	0.00	0.20	5.08	0.00	0.00	0.00	0.00	0.73	18.42
0.00	0.00	0.00	0.00	1.60	40.64	0.00	0.00	0.00	0.00	0.12	3.18
0.00	0.00	0.38	9.52	0.00	0.00	0.00	0.00	0.85	21.59	0.00	0.00
0.00	0.00	0.00	0.00	0.00	0.00	0.00	0.00	0.00	0.00	0.20	5.08
0.00	0.00	0.12	3.18	0.00	0.00	0.65	16.51	0.00	0.00	0.00	0.00
0.00	0.00	0.00	0.00	0.00	0.00	0.00	0.00	0.05	1.27	0.00	0.00
0.03	0.64	0.08	1.90	0.00	0.00	0.00	0.00	0.00	0.00	0.00	0.00
0.00	0.00	0.62	15.88	0.00	0.00	0.00	0.00	0.00	0.00	0.60	15.24
0.00	0.00	0.00	0.00	0.00	0.00	0.03	0.64	0.00	0.00	0.60	15.24
0.00	0.00	0.00	0.00	0.00	0.00	0.82	20.96	0.40	10.16	0.15	3.81
0.90	22.86	0.08	1.90	0.00	0.00	0.00	0.00	0.05	1.27	0.00	0.00
0.00	0.00	0.00	0.00	0.00	0.00	0.75	19.05	0.00	0.00	0.25	6.35
0.00	0.00	0.00	0.00	0.00	0.00	0.98	24.76	0.00	0.00	0.00	0.00
0.00	0.00	0.00	0.00	0.00	0.00	0.00	0.00	0.85	21.59	0.03	0.64
0.03	0.64	0.00	0.00	0.00	0.00	0.00	0.00	0.00	0.00	0.00	0.00
0.08	1.90	0.00	0.00	0.00	0.00	0.00	0.00	0.00	0.00	0.00	0.00
0.00	0.00	0.00	0.00	0.00	0.00	0.00	0.00	0.62	15.88	0.00	0.00
0.00	0.00	0.00	0.00			0.00	0.00			0.88	22.22
2.88	73.04	2.91	73.65	2.80	71.12	3.64	92.08	3.00	76.20	4.14	104.79

Table C.3. Summary of 1982 daily precipitation data

Day	January		February		March		April		May		June	
	in.	mm	in.	mm	in.	mm	in.	mm	in.	mm	in.	mm
1	0.00	0.00	0.00	0.00	0.02	0.64	0.00	0.00	0.00	0.00	0.25	6.35
2	0.32	8.26	0.68	17.14	0.00	0.00	0.00	0.00	0.00	0.00	0.00	0.00
3	1.22	31.12	0.25	6.35	0.00	0.00	0.10	2.54	0.00	0.00	0.00	0.00
4[a]	0.75	19.05	0.00	0.00	0.00	0.00	0.00	0.00	0.00	0.00	0.45	11.43
5[a]	0.00	0.00	0.00	0.00	0.20	5.08	0.10	2.54	0.00	0.00	0.00	0.00
6[a]	0.00	0.00	0.12	3.18	0.78	19.68	0.05	1.27	0.00	0.00	0.00	0.00
7	0.20	5.08	0.00	0.00	0.78	19.68	0.00	0.00	0.50	12.70	0.00	0.00
8	0.00	0.00	0.02	0.64	0.00	0.00	0.50	12.70	0.10	2.54	0.00	0.00
9	0.00	0.00	1.18	29.84	0.00	0.00	0.02	0.64	0.00	0.00	0.00	0.00
10	0.00	0.00	0.00	0.00	0.00	0.00	0.00	0.00	0.00	0.00	0.22	5.72
11	0.00	0.00	0.00	0.00	0.00	0.00	0.00	0.00	0.00	0.00	0.00	0.00
12	0.00	0.00	0.22	5.72	0.00	0.00	0.00	0.00	0.00	0.00	0.40	10.16
13	0.00	0.00	0.10	2.54	0.22	5.72	0.00	0.00	0.00	0.00	0.08	1.90
14	0.00	0.00	0.00	0.00	0.05	1.27	0.00	0.00	0.00	0.00	0.00	0.00
15	0.42	10.80	0.20	5.08	1.25	31.75	0.02	0.64	0.00	0.00	0.25	6.35
16	0.05	1.27	1.10	27.94	0.15	3.81	0.00	0.00	0.00	0.00	0.38	9.52
17	0.00	0.00	0.10	2.54	0.28	6.98	0.68	17.14	0.00	0.00	0.00	0.00
18	0.00	0.00	0.10	2.54	0.00	0.00	0.00	0.00	0.00	0.00	0.00	0.00
19	0.42	10.80	0.00	0.00	0.00	0.00	0.00	0.00	0.00	0.00	0.00	0.00
20	.10	2.54	0.00	0.00	0.00	0.00	0.00	0.00	0.00	0.00	0.00	0.00
21	1.10	27.94	0.00	0.00	1.00	25.40	0.00	0.00	0.18	4.44	0.00	0.00
22	0.30	7.62	0.00	0.00	0.00	0.00	0.00	0.00	0.08	1.90	0.28	6.98
23	0.75	19.05	0.00	0.00	0.00	0.00	0.00	0.00	0.05	1.27	0.00	0.00
24	0.00	0.00	0.00	0.00	0.00	0.00	0.00	0.00	0.00	0.00	0.00	0.00
25	0.00	0.00	0.00	0.00	0.28	6.98	0.58	14.60	0.00	0.00	0.00	0.00
26	0.00	0.00	0.25	6.35	0.00	0.00	0.12	3.18	0.00	0.00	0.05	1.27
27	0.00	0.00	0.65	16.51	0.00	0.00	0.18	4.44	0.40	10.16	0.05	1.27
28	0.00	0.00	0.00	0.00	0.00	0.00	0.00	0.00	0.60	15.24	0.00	0.00
29	0.00	0.00			0.00	0.00	0.00	0.00	0.00	0.00	0.18	4.44
30	0.00	0.00			0.00	0.00	0.00	0.00	0.00	0.00	0.10	2.54
31	0.60	15.24			1.28	32.38			0.02	0.64		
Total	6.23	158.77	4.97	126.37	6.29	159.37	2.35	59.69	1.93	48.89	2.69	67.93

Table C.3 (continued)

July		August		September		October		November		December	
in.	mm	in.	mm	in.	mm	in.	mm	in.	mm	in.	mm
0.00	0.00	0.00	0.00	1.00	25.40	0.00	0.00	0.00	0.00	2.45	62.23
0.00	0.00	0.00	0.00	0.80	20.32	0.00	0.00	0.00	0.00	0.00	0.00
0.10	2.54	0.00	0.00	0.00	0.00	0.00	0.00	1.90	48.26	0.00	0.00
0.40	10.16	0.00	0.00	0.00	0.00	0.00	0.00	0.25	6.35	0.00	0.00
0.00	0.00	0.00	0.00	0.00	0.00	0.00	0.00	0.00	0.00	0.88	22.22
0.00	0.00	0.02	0.64	0.00	0.00	0.00	0.00	0.00	0.00	0.00	0.00
0.00	0.00	0.00	0.00	0.00	0.00	0.40	10.16	0.00	0.00	0.00	0.00
0.95	24.13	0.25	6.35	0.00	0.00	0.30	7.62	0.00	0.00	0.00	0.00
0.00	0.00	1.32	33.66	0.00	0.00	0.00	0.00	0.00	0.00	0.00	0.00
0.00	0.00	0.05	1.27	0.00	0.00	0.00	0.00	0.00	0.00	0.15	3.81
1.43	36.20	0.25	6.35	0.00	0.00	0.00	0.00	0.00	0.00	1.00	25.40
0.00	0.00	0.00	0.00	0.02	0.64	1.00	25.40	0.70	17.78	0.15	3.81
0.00	0.00	.00	0.00	0.12	3.1?	0.58	14.60	0.00	0.00	0.00	0.00
0.00	0.00	0.00	0.00	0.00	0.00	0.00	0.00	0.00	0.00	0.00	0.00
0.00	0.00	0.00	0.00	0.00	0.00	0.00	0.00	0.00	0.00	0.85	21.59
0.00	0.00	0.08	1.90	0.00	0.00	0.00	0.00	*b*	*b*	0.00	0.00
0.00	0.00	0.70	17.78	0.00	0.00	0.00	0.00	*b*	*b*	0.00	0.00
0.00	0.00	0.00	0.00	0.00	0.00	0.00	0.00	*b*	*b*	0.00	0.00
0.00	0.00	0.00	0.00	0.00	0.00	0.00	0.00	*b*	*b*	0.20	5.08
0.00	0.00	0.00	0.00	0.08	1.90	0.10	2.54	*b*	*b*	0.00	0.00
0.00	0.00	0.00	0.00	0.00	0.00	0.00	0.00	*b*	*b*	0.00	0.00
0.48	12.06	0.00	0.00	0.00	0.00	0.00	0.00	*b*	*b*	0.00	0.00
0.00	0.00	0.60	15.24	0.00	0.00	0.00	0.00	1.88	47.62	0.20	5.08
0.00	0.00	0.00	0.00	0.00	0.00	0.00	0.00	0.00	0.00	0.02	0.64
0.00	0.00	0.00	0.00	0.38	9.52	0.00	0.00	0.00	0.00	0.02	0.64
0.00	0.00	0.00	0.00	0.05	1.27	0.00	0.00	0.00	0.00	0.38	9.52
0.00	0.00	0.05	1.27	0.00	0.00	0.00	0.00	0.35	8.89	0.00	0.00
0.08	1.90	0.00	0.00	0.00	0.00	0.00	0.00	0.75	19.05	0.60	15.24
0.02	0.64	0.00	0.00	0.00	0.00	0.00	0.00	0.00	0.00	0.00	0.00
0.30	7.62	0.00	0.00	0.00	0.00	0.00	0.00	0.20	5.08	0.00	0.00
1.52	38.74	0.20	5.08			0.00	0.00			0.00	0.00
5.28	133.99	3.52	89.54	2.45	62.23	2.38	60.32	6.03	153.03	6.90	175.26

[a]Total precipitation for this day may be *inaccurate*, because the capacity of the gauge was exceeded.

[b]Instrumentation malfunction. Precipitation occurring on November 16–22, 1982, was summarized and entered on November 23, 1982.

Table C.4. Summary of 1983 daily precipitation

Day	January		February		March	
	in.	mm	in.	mm	in.	mm
1	0.00	0.00	0.90	22.86	0.00	0.00
2	0.35	8.89	0.68[a]	17.14[a]	0.00	0.00
3	0.00	0.00	0.02	0.64	0.00	0.00
4	0.00	0.00	0.00	0.00	0.00	0.00
5	0.00	0.00	0.00	0.00	0.40	10.16
6	0.00	0.00	0.62	15.88	0.12	3.18
7	0.00	0.00	0.05	1.27	0.00	0.00
8	0.00	0.00	0.00	0.00	0.05	1.27
9	0.38	9.52	0.02	0.64	0.00	0.00
10	0.12	3.18	0.95	24.13	0.00	0.00
11	0.10	2.54	0.20	5.08	0.00	0.00
12	0.00	0.00	0.00	0.00	0.00	0.00
13	0.00	0.00	0.00	0.00	0.00	0.00
14	0.00	0.00	0.00	0.00	0.00	0.00
15	0.00	0.00	0.00	0.00	0.00	0.00
16	0.00	0.00	0.00	0.00	0.00	0.00
17	0.00	0.00	0.00	0.00	0.00	0.00
18	0.00	0.00	0.00	0.00	0.08	1.90
19	0.00	0.00	0.00	0.00	0.00	0.00
20	0.00	0.00	0.00	0.00	0.85	21.59
21	0.38	9.52	0.00	0.00	0.00	0.00
22	0.00	0.00	0.48	12.06	0.00	0.00
23	0.00	0.00	0.00	0.00	0.00	0.00
24	0.00	0.00	0.22	5.72	0.00	0.00
25	0.00	0.00	0.00	0.00	0.00	0.00
26	0.00	0.00	0.00	0.00	0.10	2.54
27	0.00	0.00	0.00	0.00	0.50	12.70
28	0.00	0.00	0.00	0.00	0.00	0.00
29	0.08	1.90			0.00	0.00
30	0.10	2.54			0.00	0.00
31	0.00	0.00			0.05	1.27
Total	1.51	38.09	4.14	105.42	2.15	54.61

[a]Total precipitation for this day may be inaccurate, because the capacity of the gauge was exceeded.

Appendix D

SUMMARY OF PEAK DISCHARGES DURING RAINFALL EVENTS

Table D.1. Summary of peak discharges during rainfall events: Flume I

Runoff event	Date	Peak discharge (L/s)	Peak time	Recovery time[a] (h)	Runoff event	Date	Peak discharge (L/s)	Peak time	Recovery time[a] (h)
1	11-27-80	15.1	0400	6.0	31	07-04-82	0.8[b]	0100	0.2
2	04-20-81	6.6	0430	0.5	32	07-08-82	10.5	2200	1.0
3	05-25-81	2.4	1230	0.5	33	07-11-82	33.3	1430	6.0
4	05-27-81	46.4	1940	0.3	34	07-22-82	1.6[b]	1400	0.5
5	05-30-81	6.6	1500	0.2	35	07-31-82	4.1	1030	0.5
6	05-30-81	57.8	1645	0.2	36	07-31-82	19.4	1300	1.0
7	06-04-81	7.4	0700	5.5	37	08-09-82	24.6	1615	9.7
8	06-06-81	44.6	0800	5.0	38	08-17-82	13.4	2145	0.7
9	06-06-81	13.4	1645	0.2	39	08-23-82	4.1	1915	1.2
10	06-22-81	1.6[b]	1915	*c*	40	09-01-82	26.3	1730	2.0
11	07-05-81	28.9	2245	0.2	41	09-02-82	9.1	0930	*d*
12	11-27-81	5.8	0745	0.2	42	09-02-82	9.1	1030	6.0
13	11-27-81	0.8[b]	0900	*c*	43	11-03-82	7.4	0115	0.7
14	11-30-81	0.8[b]	1615	0.2	44	11-03-82	4.9	0330	0.5
15	12-01-81	2.4	0715	0.?	45	11-12-82	4.9	1330	1.5
16	12-14-81	1.6[b]	1330	5.5	46	11-22-82	6.6	0115	0.7
17	01-03-82	2.4	0400	3.0	47	11-28-82	4.9	1645	5.2
18	01-04-82	10.0	0100	4.0	48	11-30-82	22.9	0245	*d*
19	03-06-82	1.6[b]	0200	3.0	49	11-30-82	24.6	0545	6.2
20	03-15-82	8.3	0745	5.2	50	12-05-82	4.9	0545	0.5
21	03-25-82	2.4	1715	0.7	51	12-11-82	4.9	2200	3.0
22	03-31-82	17.7	1530	16.5	52	12-15-82	4.9	1830	*d*
23	04-08-82	1.6[b]	0830	3.5	53	12-15-82	4.9	2130	1.5
24	04-17-82	4.1	0930	2.0	54	12-28-82	10.0	0830	6.5
25	05-07-82	2.4	2300	5.0	55	02-22-83	6.6	1630	2.5
26	05-28-82	4.9	0630	2.5	56	03-20-83	4.9	2030	1.5
27	06-01-82	0.8[b]	0830	0.2	57	04-05-83	9.1	0730	18.0
28	06-04-82	8.3	1430	1.5	58	04-09-83	14.3	0600	*c*
29	06-10-82	0.8[b]	1130	0.2	59	04-09-83	12.6	1000	8.0
30	06-14-82	7.4	1730	0.5	60	04-23-83	3.2	1300	5.0

[a]Time from occurrence of runoff peak to return to base flow.
[b]Measured peak discharge is less than flume minimum design flow; hence the value is an estimate.
[c]A recovery time of less than 10 min.
[d]Stream did not return to base flow before the next rainfall occurred.

Table D.2. Summary of peak discharges during rainfall events: Flume II

Runoff event	Date	Peak discharge (L/s)	Peak time	Recovery time[a] (h)	Runoff event	Date	Peak discharge (L/s)	Peak time	Recovery time[a] (h)
1	11-15-80	4.9	0515	5.7	31	05-30-81	50.8	1645	10.0
2	11-17-80	7.4	1000	7.0	32	05-31-81	6.6	1800	14.5
3	11-23-80	4.1	1300	1.0	33	06-02-81	2.4	0545	*b*
4	11-23-80	4.1	1830	*b*	34	06-02-81	2.4	0830	1.0
5	11-23-80	3.3	2100	1.5	35	06-02-81	2.4	2315	3.2
6	11-24-80	18.5	0400	32.0	36	06-03-81	5.8	1630	1.0
7	11-27-80	5.8	0640	18.3	37	06-04-81	2.4	0430	*b*
8	12-09-80	4.9	0700	2.0	38	06-04-81	10.8	0730	13.5
9	12-09-80	2.4	1000	*b*	39	06-06-81	5.8	1200	*b*
10	12-09-80	5.8	1630	19.5	40	06-06-81	16.0	1730	4.5
11	12-24-80	0.8[c]	0930	0.5	41	06-10-81	8.3	1815	0.7
12	03-22-81	1.6[c]	0830	1.5	42	06-10-81	3.3	2130	1.0
13	03-22-81	2.4	1630	1.5	43	06-22-81	6.6	1915	0.7
14	03-30-81	9.1	0515	8.7	44	06-22-81	1.6[c]	2145	1.0
15	04-05-81	7.4	0100	6.5	45	06-25-81	23.7	1800	14.2
16	04-09-81	4.1	0815	1.7	46	07-01-81	2.4	2300	0.2
17	04-17-81	0.8[c]	0830	1.0	47	07-05-81	10.0	1715	*b*
18	04-19-81	2.4	1730	1.0	48	07-05-81	4.1	1900	1.0
19	04-20-81	10.8	0445	0.7	49	07-05-81	28.1	2245	5.2
20	04-20-81	6.6	0815	10.0	50	08-16-81	5.8	0330	11.5
21	05-14-81	1.6[c]	1930	0.7	51	08-20-81	4.1	2400	10.0
22	05-18-81	2.4	1630	0.2	52	09-01-81	3.3	1100	3.0
23	05-18-81	2.4	2030	0.5	53	09-03-81	0.8[c]	1300	2.0
24	05-18-81	4.1	2315	1.2	54	09-04-81	4.9	2115	4.7
25	05-19-81	5.8	0600	8.0	55	10-01-81	1.6[c]	2200	2.0
26	05-25-81	7.5	1230	7.5	56	10-18-81	3.3	0515	6.2
27	05-26-81	2.4	2230	1.5	57	10-23-81	4.1	0400	11.0
28	05-27-81	40.2	1930	16.5	58	10-25-81	7.5	2145	*b*
29	05-30-81	4.9	1345	*b*	59	10-26-81	4.1	0330	*b*
30	05-30-81	12.6	1445	*b*	60	10-26-81	7.5	2400	32.0

Table D.2 (continued)

Runoff event	Date	Peak discharge (L/s)	Peak time	Recovery time[a] (h)	Runoff event	Date	Peak discharge (L/s)	Peak time	Recovery time[a] (h)
61	11-16-81	4.1	1330	*b*	91	11-03-82	9.1	0115	*b*
62	11-16-81	4.1	1915	13.7	92	11-03-82	8.3	0300	*b*
63	11-23-81	4.1	2330	10.5	93	11-03-82	4.1	1200	*b*
64	11-27-81	10.8	0745	26.7	94	11-03-82	4.1	1330	*b*
65	11-30-81	7.5	1630	*b*	95	11-03-82	5.8	1500	*b*
66	12-01-81	10.0	0800	24.0	96	11-04-82	7.5	0115	10.7
67	12-17-81	1.6[c]	0800	3.0	97	11-21-82	18.5	2430	35.5
68	12-31-81	8.3	1200	21.5	98	11-28-82	10.0	1800	*b*
69	01-02-82	2.4	2200	*b*	99	11-28-82	10.0	2015	1.2
70	01-03-82	17.7	0400	*b*	100	12-01-82	47.2	0300	*b*
71	01-04-82	30.7	0115	12.7	101	12-01-82	49.0	0600	4.0
72	03-06-82	4.1	2145	*b*	102	12-05-82	7.5	0545	0.7
73	03-07-82	6.6	0200	5.0	103	12-11-82	10.0	2100	2.0
74	03-15-82	18.6	0800	4.0	104	12-15-82	11.7	1845	*b*
75	03-21-82	5.8	0730	3.5	105	12-15-82	16.8	2100	1.5
76	03-31-82	21.1	1530	2.5	106	12-28-82	7.5	1100	1.2
77	05-28-82	3.3	0630	0.2	107	02-01-83	49.9	0200	27.0
78	05-28-82	4.9	1430	0.2	108	02-02-83	22.9	0600	3.0
79	07-08-82	15.1	2200	4.0	109	02-10-83	7.5	1600	2.0
80	07-11-82	48.1	1430	18.0	110	02-10-83	10.0	2015	2.2
81	07-31-82	4.9	1030	*b*	111	02-11-83	7.5	0130	1.0
82	07-31-82	36.8	1245	21.7	112	02-22-83	10.8	1615	1.7
83	08-09-82	35.0	1600	*b*	113	03-27-83	4.9	0700	4.0
84	08-09-82	7.5	1745	16.2	114	04-05-83	10.0	0700	*b*
85	08-11-82	2.4	1430	3.5	115	04-05-83	13.4	1300	*b*
86	08-17-82	19.4	2145	14.2	116	04-05-83	16.8	1600	7.0
87	08-23-82	3.3	2015	16.7	117	4-09-83	7.5	0545	*b*
88	09-02-82	18.6	1045	26.2	118	04-09-83	10.0	0930	2.5
89	10-12-82	9.1	2330	*b*	119	04-23-83	1.4[c]	1130	*b*
90	10-13-82	9.1	0300	9.0	120	04-23-83	8.8	1330	10.5
					121	05-03-83	0.8[c]	1145	0.2

[a]Time from occurrence of runoff peak to return to base flow.
[b]Stream did not return to base flow before the next rainfall occurred.
[c]Measured peak discharge is less than flume minimum design flow; hence the value is an estimate.

Appendix E
WATER-TABLE ELEVATION SUMMARY

Table E.1. Water-table elevation summary

Month	Engineered Test Facility well														
	1	2	3	4	5	6	7	8	9	10	11	12	13	14	15
								1981							
Jan	237.90	238.46	237.19					237.51	238.31	238.06	236.82	237.79			
Feb	238.65	238.57	237.86	237.93	238.04	238.04	238.42	238.21	238.60	238.62	237.51	238.58			
Mar	238.74	238.68	237.97	237.84	237.92	237.92	237.85	238.35	238.72	238.43	237.61	238.82			
Apr	238.78	238.71	237.98	237.90	237.96	237.95	237.84	238.36	238.81	239.03	237.67	238.89			
May	238.69	238.62	237.88	237.82	237.88	237.86	237.96	238.25	238.67	238.98	237.55	238.80			
Jun	238.75	238.67	237.93	238.01	237.95	237.93	237.97	238.32	238.74	239.10	237.44	238.88			
Jul	238.64	238.57	237.81	237.72	237.84	237.80	237.83	238.21	238.64	2[illegible].94	237.40	238.79			
Aug	238.65	238.55	237.66	237.66	237.69	237.72	237.72	238.18	238.59	2[illegible].92	237.40	238.74			
Sep	238.63	238.55	237.72	237.74	237.77	237.81	237.79	238.23	238.57	238.93	237.34	238.70			
Oct	238.52	238.43	237.65	237.67	237.76	237.75	237.73	238.18	238.51	238.86	237.22	238.71			
Nov	238.62	238.49	237.78	237.79	237.78	237.85	237.87	238.25	238.56	238.78	237.27	238.76			
Dec	238.70	238.62	238.19	237.95	237.91	237.96	238.14	238.36	238.70	238.81	237.41	238.84			
								1982							
Jan	238.94	238.75	238.21	238.15	238.07	238.14	238.03	238.54	238.90	239.17	237.65	238.93			
Feb	239.17	238.91	238.28	238.40	238.21	238.28	238.15	239.04	238.96	239.19	237.80	239.02			
Mar	238.96	238.93	238.17	238.35	238.27	238.29	238.48	238.72	238.91	239.20	237.78	239.15			
Apr	238.66	238.91	238.19	238.21	238.17	238.15	238.25	238.38	238.91	239.37	237.96	239.20			
May	238.87	238.81	238.04	238.00	238.03	238.00	238.11	238.52	238.83	239.06	237.69	238.99			
Jun	238.59	238.71	237.84	237.78	237.87	238.00	237.89	238.23	238.62	238.85	237.45	239.04			
Jul	238.73	238.72	237.84	237.89	237.91	237.95	237.96	238.35	238.71	239.00	237.55	238.90			
Aug	238.83	238.60	237.90	237.94	238.03	238.00	238.05	238.41	238.80	239.06	237.64	238.93	239.76	341.17	241.14
Sep	238.77	238.65	237.83	237.84	237.94	237.91	237.98	238.23	238.41	239.03	237.53	238.90	239.71	241.14	141.14
Oct	238.73	238.48	237.85	237.94	237.88	237.88	237.93	238.34	238.50	239.01	237.56	238.84	239.60	241.02	241.22
Nov	238.80	238.67	237.96	238.18	238.00	237.98	238.05	238.47	238.89	239.05	237.69	238.91	239.64	241.08	240.97
Dec	238.94	238.75	238.13	238.49	238.22	238.14	238.25	238.60	238.94	239.15	237.82	239.03	239.90	241.37	241.24
								1983							
Jan	238.86	238.81	238.05	238.51	238.11	238.10	238.17	238.50	238.86	239.15	237.75	239.00	239.93	241.42	241.28
Feb	238.97	238.90	238.21	237.86	238.25	238.23	238.33	238.67	239.08	239.20	237.87	239.06	239.92	241.34	241.57

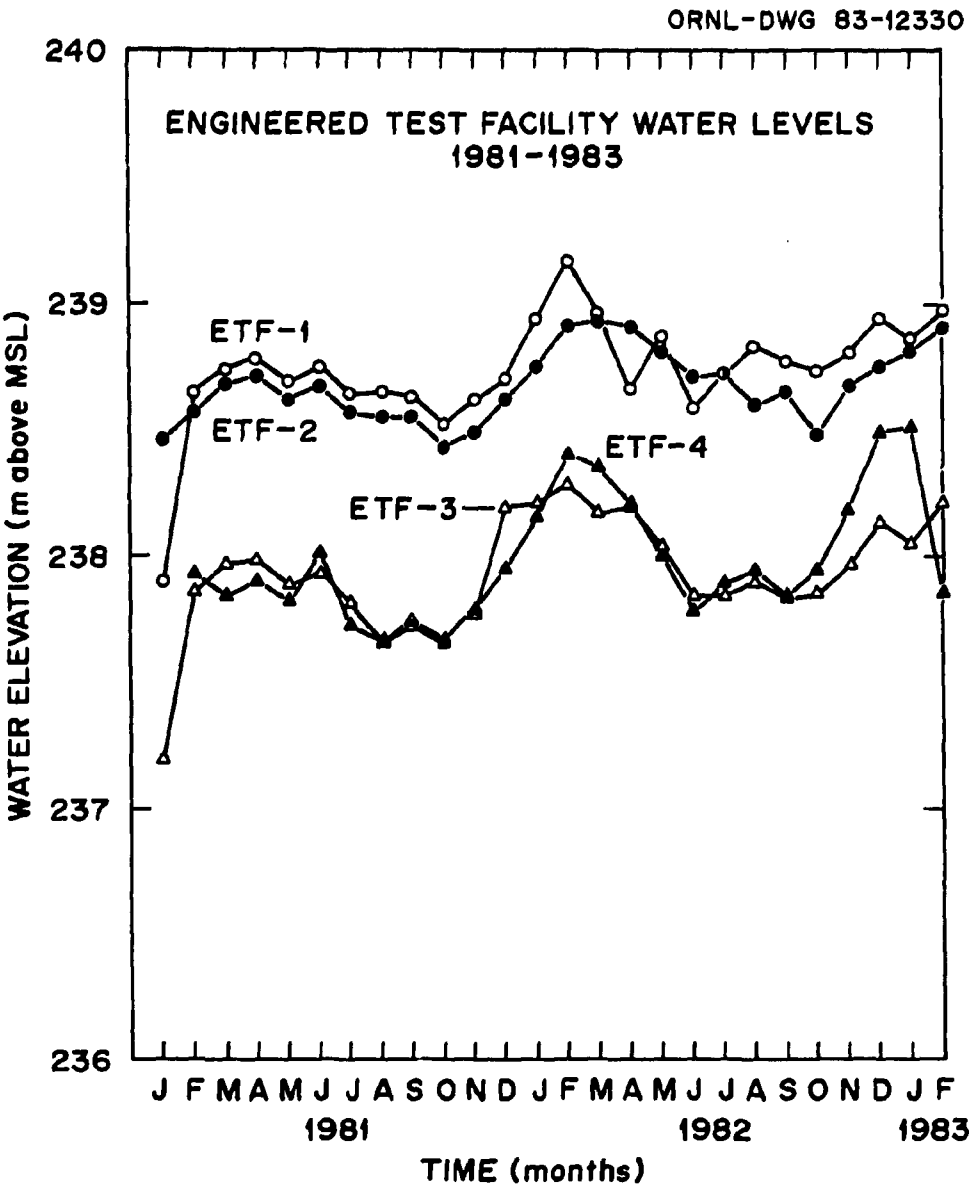

Fig. E.1. Water-table elevation, 1981–1983: ETF-1, -2, -3, and -4.

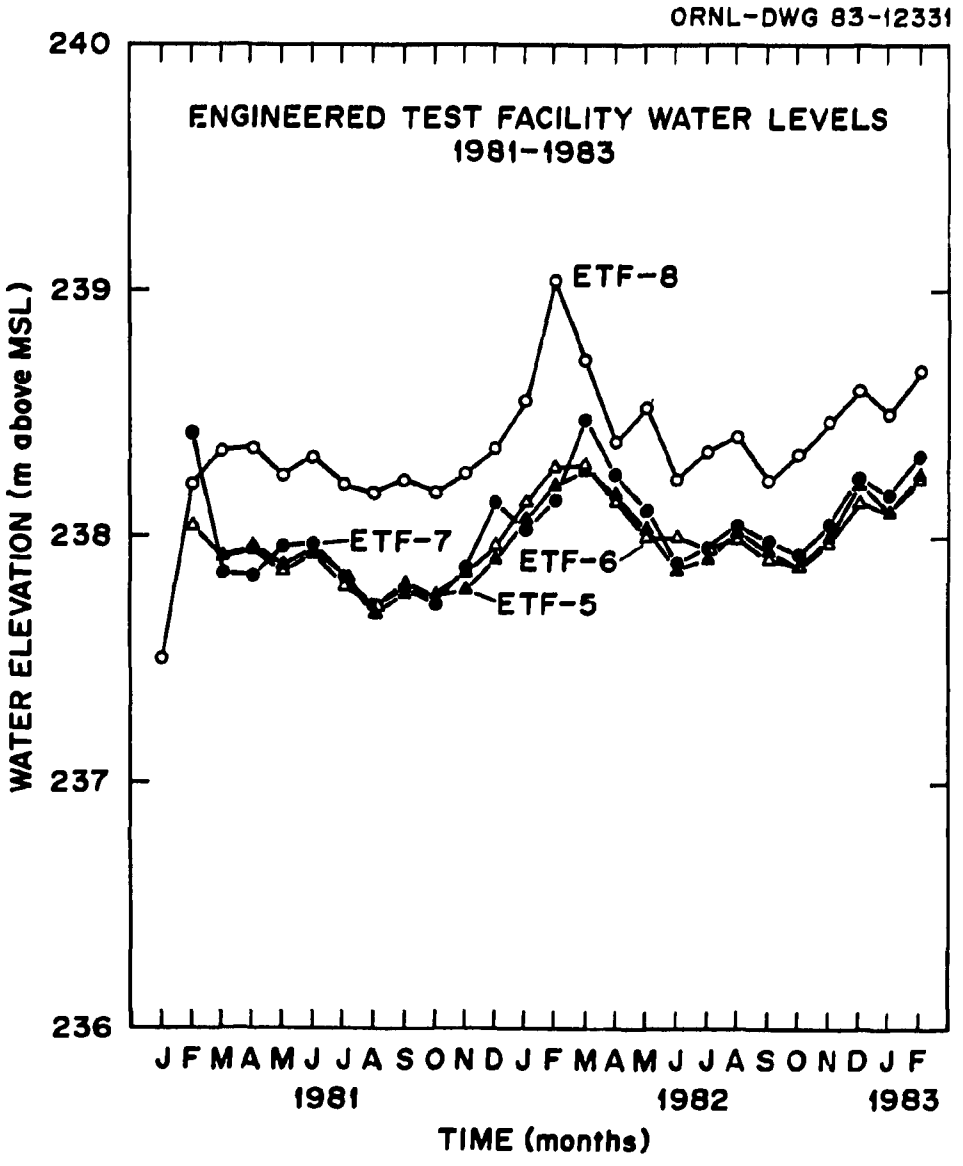

Fig. E.2. Water-table elevation, 1981–1983: ETF-5, -6, -7, and -8.

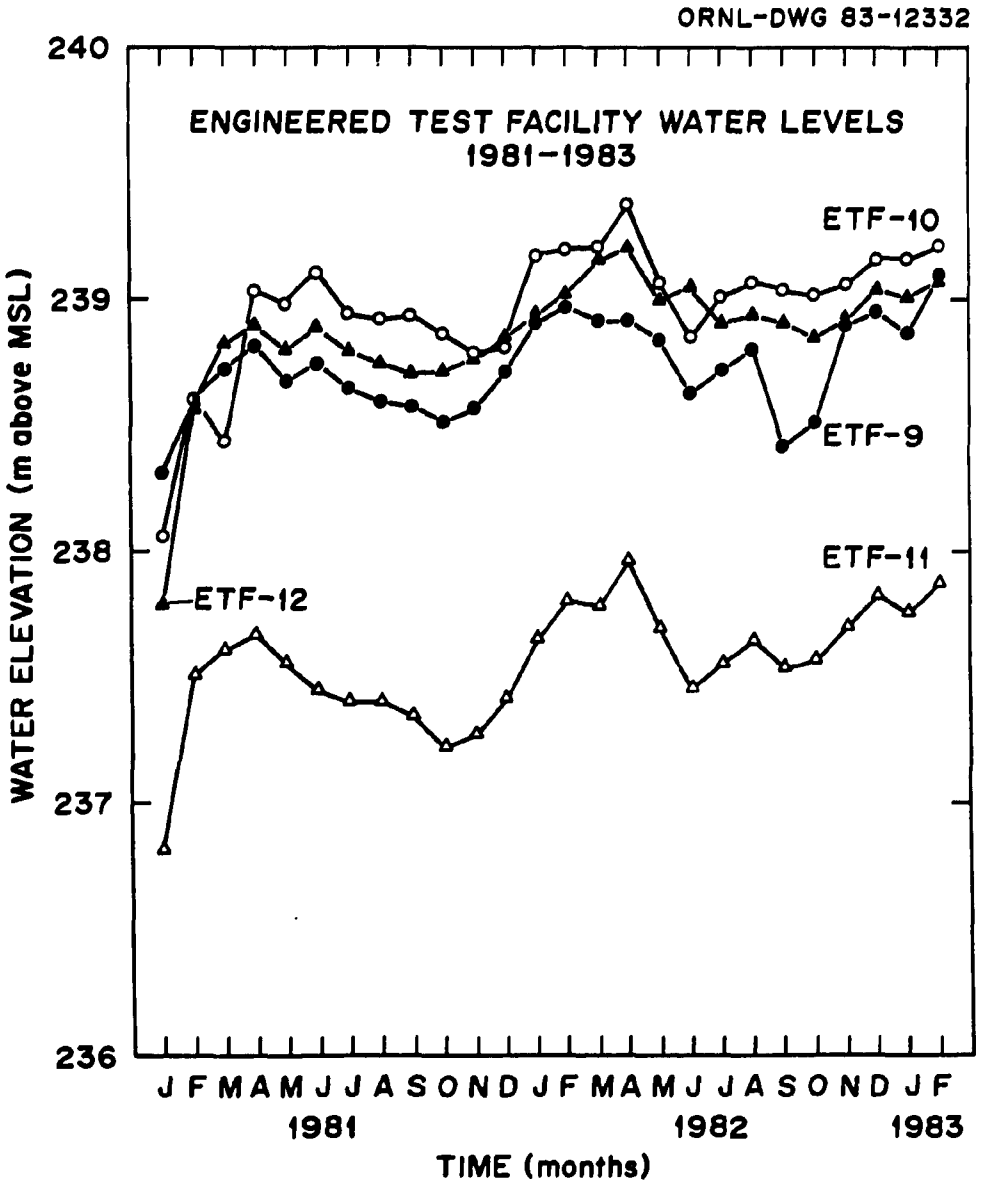

Fig. E.3. Water-table elevation, 1981–1983: ETF-9, -10, -11, and -12.

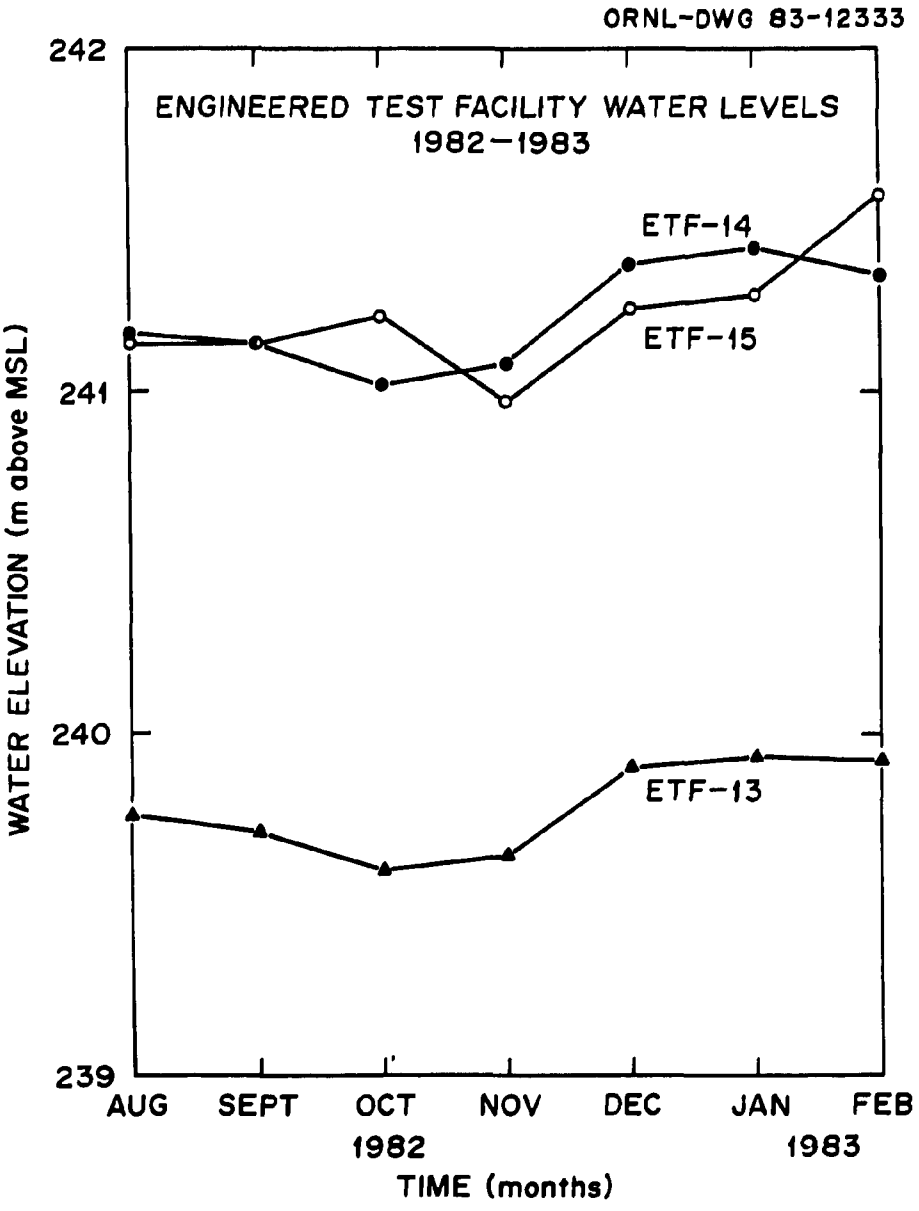

Fig. E.4. Water-table elevation, 1982–1983: ETF-13, -14, and -15.

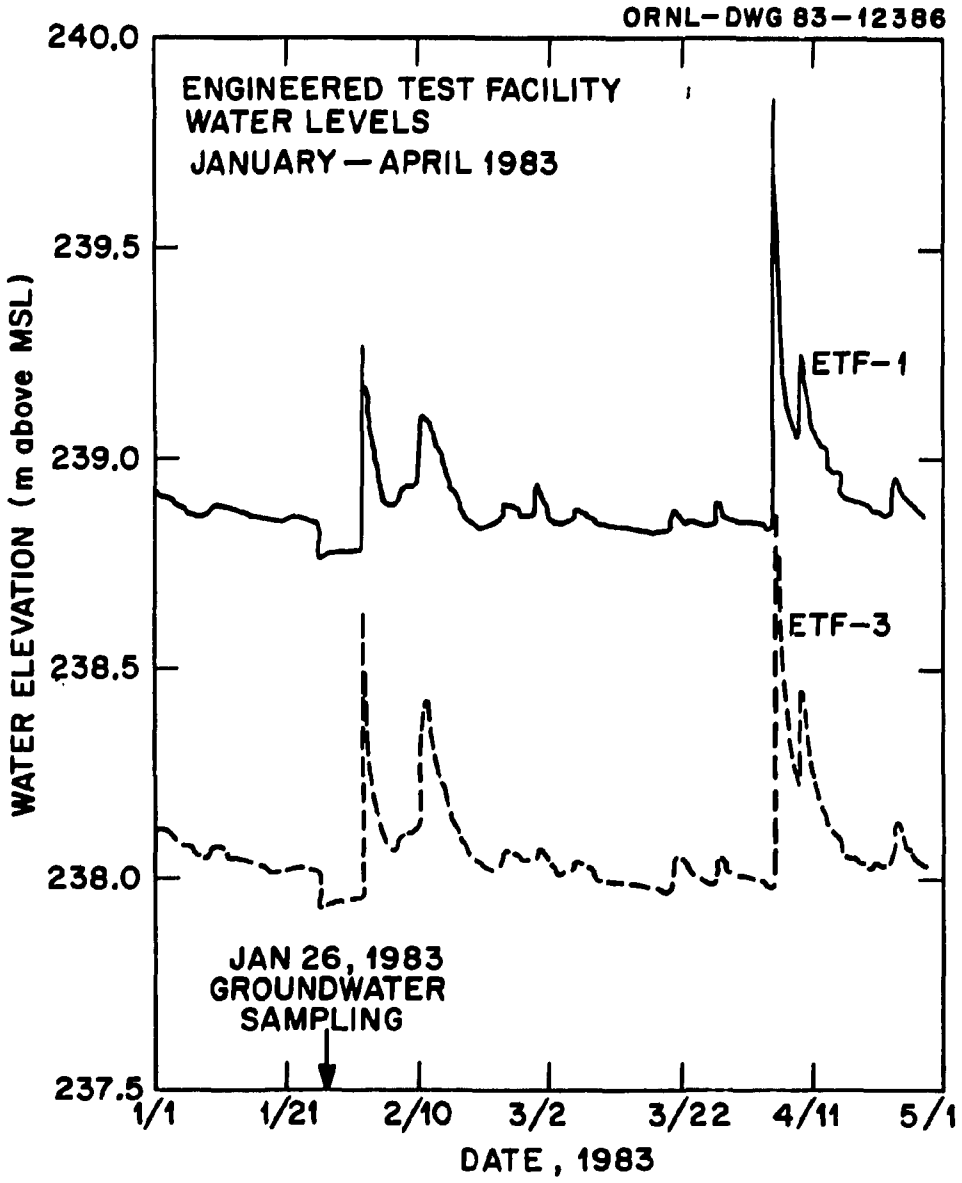

Fig. E.5. Water-table elevation, 1983: ETF-1 and -3.

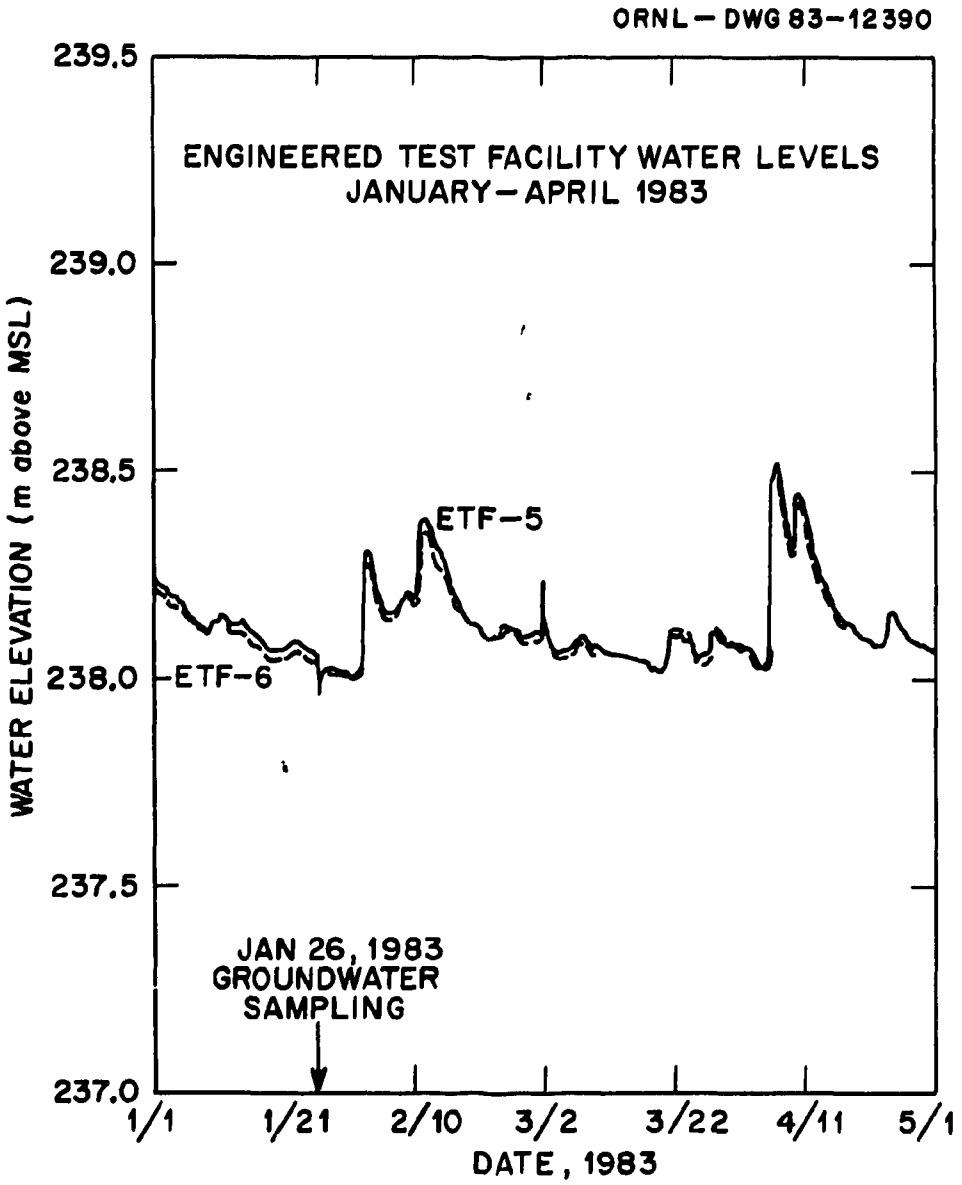

Fig. E.6. Water-table elevation, 1983: ETF-5 and -6.

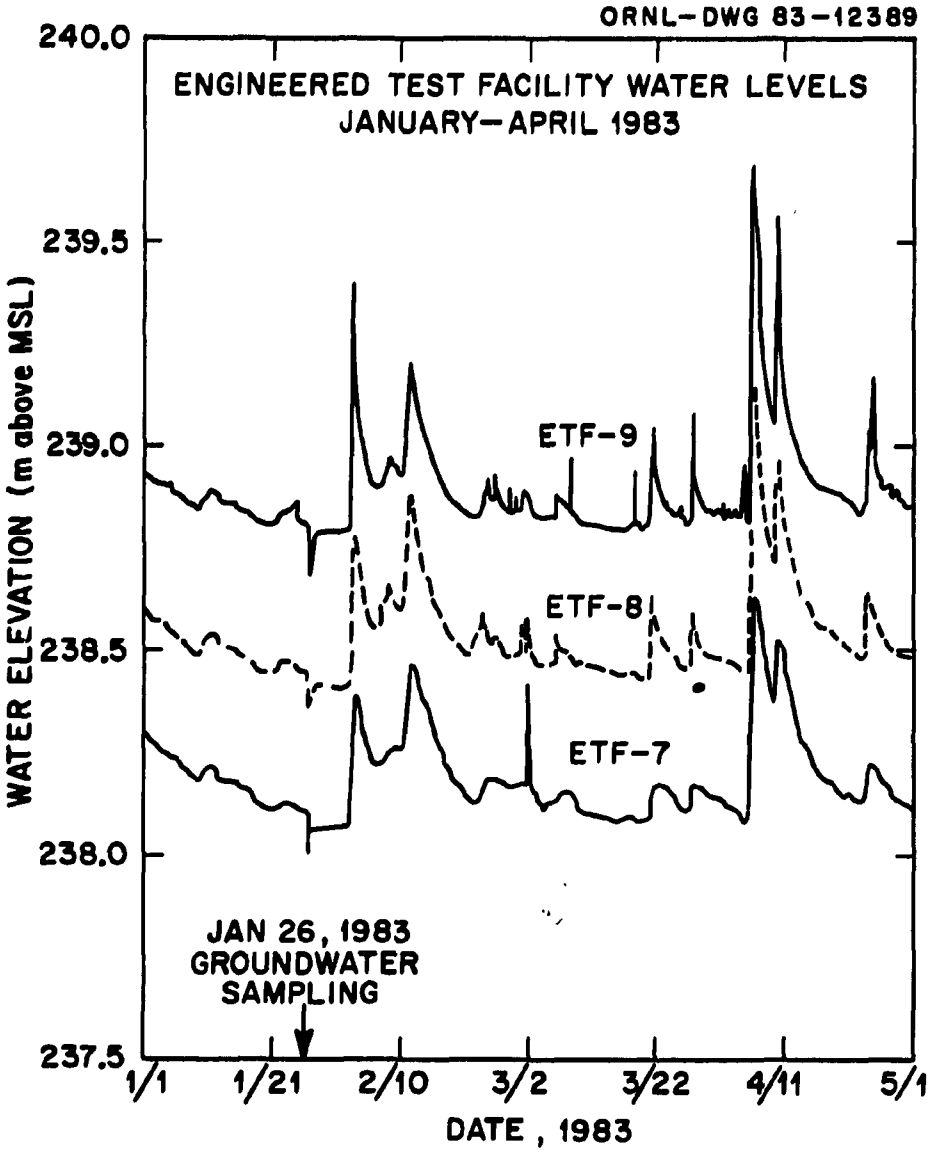

Fig. E.7. Water-table elevation, 1983: ETF-7, -8, and -9.

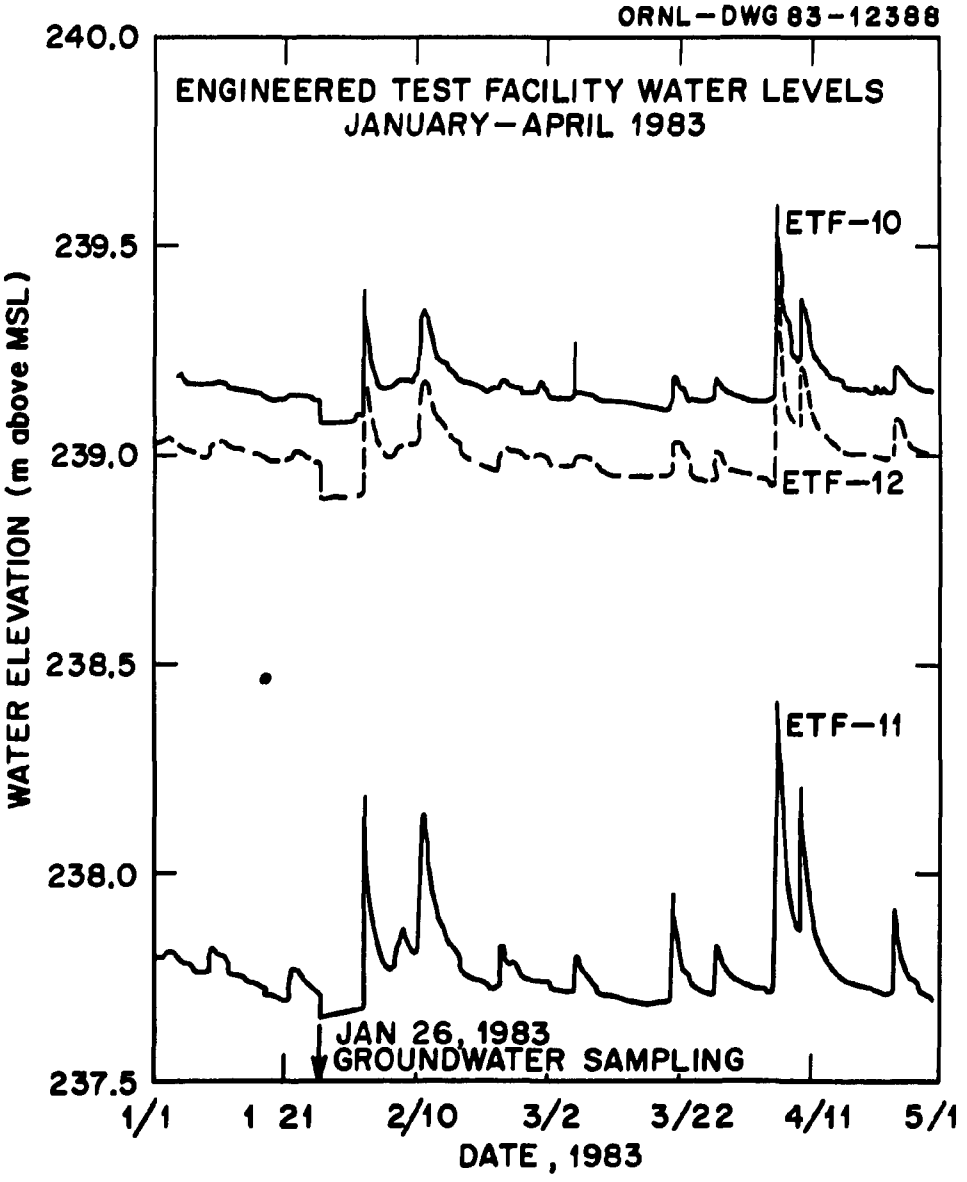

Fig. E.8. Water-table elevation, 1983: ETF-10, -11, and -12.

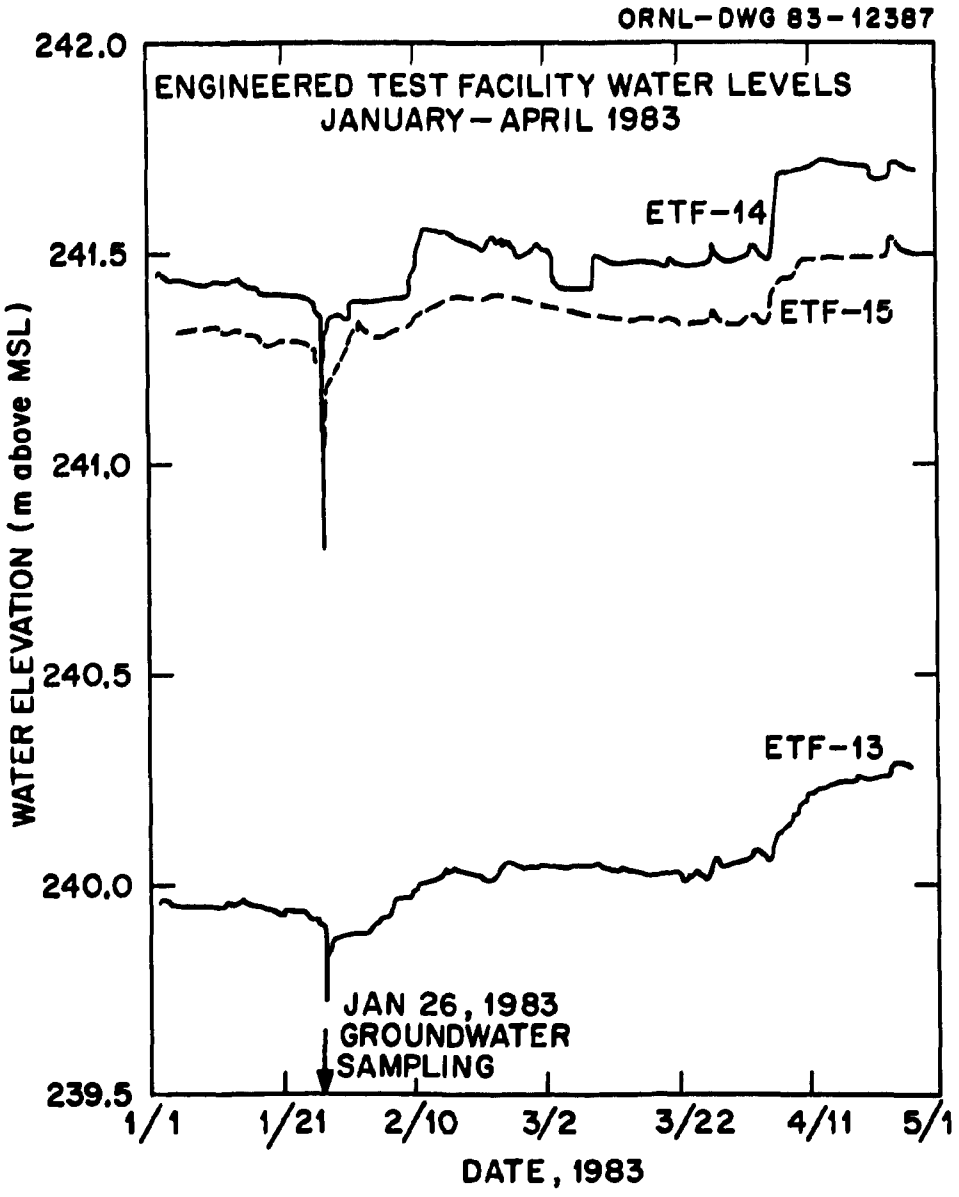

Fig. E.9. Water-table elevation, 1983: ETF-13, -14, and -15.

Appendix F
ETF WATER QUALITY

ETF WATER QUALITY DATA

The chemical analyses in this appendix represent background water quality at the ETF. Given for each well or flume, by analysis, are the number of samples having that analysis performed, the mean of analyses, the standard deviation, and the maximum and minimum. Very often the quantity of a chemical constituent is below the analytical detection limit. If more than 50% of the samples were below detection, no mean or statistics are presented. If less than 50% of samples were below detection, a maximum mean (determined by assigning the detection limit as the value for the analysis) is given. Because detection limits vary through time, they have not been listed.

The radiochemical analyses are also included in this appendix. The only analysis that is statistically significant is the tritium content in Flume II. The uncertainty associated with the radiochemical analyses makes all other statistics insignificant.

Table F.1. Engineered Test Facility water quality: Flume I

Constituent	Unit	Number of samples	Mean	Standard deviation	Minimum value	Maximum value
Al	mg/L	3	0.532	0.840	0.004	1.500
B[a]	mg/L	3	0.026	0.020	0.012	0.050
Br	mg/L	1	[b]			
Ca	mg/L	3	46	31	17	79
Cl	mg/L	3	2.4	2.0	0.9	4.6
F[a]	mg/L	3	0.2	0.2	0.1	0.4
Fe	mg/L	3	[b]			
I	mg/L	1	[b]			
K	mg/L	3	2.68	0.68	2.04	3.40
Mg[a]	mg/L	3	1.89	1.65	0.02	3.14
Mn[a]	mg/L	3	0.039	0.053	0.0003	0.100
Na	mg/L	3	2.29	0.95	1.20	2.88
NO_2-N	mg/L					
NO_3-N	mg/L	3	1.4	2.4	0.001	4.2
P (total)	mg/L	2	0.012	0.010	0.005	0.019
PO_4-P	mg/L					
SiO_2	mg/L	3	8.50	1.25	7.50	9.90
SO_4	mg/L	3	13.4	10.4	2.9	23.6
Sr	mg/L	3	[b]			
Total alkalinity	mg/L as $CaCO_3$	3	120	75	40	188
Conductivity	μS/cm	1	120			
pH	pH units	1	6.6			
TOC	mg/L	1	4.9			
Tritium	Bq/L[a]	3	48	29	24	81
^{90}Sr	Bq/L	3	[b]			
Gross alpha	Bq/L	3	0.74	0.46	0.28	1.20
^{137}Cs	Bq/L	3	[b]			
^{60}Co	Bq/L	3	[b]			

[a]Majority of values above detection limit; therefore, mean = maximum mean.
[b]Majority of values below detection limit; therefore, no mean is reported.

Table F.2 Engineered Test Facility water quality: Flume II

Constituent	Unit	Number of samples	Mean	Standard deviation	Minimum value	Maximum value
Al	mg/L	3	0.158	0.261	0.006	0.459
B[a]	mg/L	3	0.032	0.018	0.014	0.050
Br	mg/L	1	*b*			
Ca	mg/L	3	44	7	36	50
Cl	mg/L	3	8.7	5.2	4.6	14.6
F	mg/L	3	0.1	0.0	0.1	0.1
Fe	mg/L	3	*b*			
I	mg/L	1	*b*			
K	mg/L	3	2.60	0.51	2.01	2.90
Mg	mg/L	3	9.18	3.41	6.20	12.90
Mn[a]	mg/L	3	0.041	0.052	0.0004	0.100
Na	mg/L	3	4.25	0.51	3.70	4.70
NO_2-N	mg/L					
NO_3-N[a]	mg/L	3	2.0	3.4	0.003	5.9
P (total)	mg/L	2	0.022	0.029	0.001	0.042
PO_4-P	mg/L					
SiO_2	mg/L	3	7.50	3.05	5.39	11.00
SO_4	mg/L	3	23.9	12.7	13.0	37.8
Sr	mg/L	3	*b*			
Total alkalinity	mg/L as $CaCO_3$	3	134	16	121	152
Conductivity	μS/cm	1	320			
pH	pH units	1	6.9			
TOC	mg/L	1	3.3			
Tritium	Bq/L[a]	3	13,667	1527	12,000	15,000
^{90}Sr	Bq/L	3	*b*			
Gross alpha	Bq/L	3	0.50	0.11	0.40	0.62
^{137}Cs	Bq/L	3	*b*			
^{60}Co	Bq/L	3	*b*			

[a]Majority of values above detection limit; therefore, mean = maximum mean.
[b]Majority of values below detection limit; therefore, no mean is reported.

Table F.3. Engineered Test Facility water quality: ETF-1

Constituent	Unit	Number of samples	Mean	Standard deviation	Minimum value	Maximum value
Al[a]	mg/L	20	0.049	0.039	0.007	0.170
B[a]	mg/L	19	0.057	0.055	0.001	0.200
Br	mg/L	17	*b*			
Ca	mg/L	20	32.5	5.3	22.9	49.0
Cl	mg/L	20	*b*			
F	mg/L	20	*b*			
Fe	mg/L	20	*b*			
I	mg/L	17	*b*			
K[a]	mg/L	20	2.55	4.24	0.001	19.0
Mg	mg/L	21	137.19	81.29	1.00	264.00
Mn[a]	mg/L	19	0.007	0.004	0.0001	0.018
Na[a]	mg/L	20	3.61	2.39	1.77	11.97
NO_2-N	mg/L	9	*b*			
NO_3[a]-N	mg/L	20	2.6	2.6	0.001	10.0
P (total)[a]	mg/L	17	0.31	0.31	0.04	1.10
PO_4-P	mg/L	10	*b*			
SiO_2	mg/L	19	12.07	2.09	8.09	15.80
SO_4[a]	mg/L	20	6.9	2.4	4.0	10.0
Sr[a]	mg/L	20	0.062	0.017	0.048	0.100
Total alkalinity	mg/L as $CaCO_3$	20	97	10	65	111
Conductivity	μS/cm	19	142	36	70	200
pH	pH units	19	7.3	0.6	6.4	8.3
TOC	mg/L	2	2.6	0.5	2.2	2.9
Tritium	Bq/L[a]	5	35	16	22	61
^{90}Sr[a]	Bq/L	5	1.29	1.20	0.120	3.00
Gross alpha	Bq/L	5	0.35	0.15	0.20	0.54
^{137}Cs	Bq/L	5	*b*			
^{60}Co	Bq/L	5	*b*			

[a]Majority of values above detection limit; therefore, mean = maximum mean.
[b]Majority of values below detection limit; therefore, no mean is reported.

Table F.4. Engineered Test Facility water quality: ETF-2

Constituent	Unit	Number of samples	Mean	Standard deviation	Minimum value	Maximum value
Al[a]	mg/L	20	0.055	0.045	0.01	0.17
B[a]	mg/L	19	0.051	0.039	0.001	0.115
Br	mg/L	17	*b*			
Ca	mg/L	20	25.1	8.7	10.0	38.0
Cl	mg/L	20	*b*			
F	mg/L	20	*b*			
Fe	mg/L	20	*b*			
I	mg/L	17	*b*			
K[a]	mg/L	20	2.94	4.65	0.001	17.00
Mg	mg/L	20	2.66	1.42	1.22	8.00
Mn	mg/L	20	0.038	0.046	0.001	0.201
Na[a]	mg/L	20	2.78	1.29	1.03	5.77
NO_2-N	mg/L	9	*b*			
NO_3-N	mg/L	20	*b*			
P (total)	mg/L	16	*b*			
PO_4-P	mg/L	10	*b*			
SiO_2	mg/L	19	7.52	3.04	2.10	14.20
SO_4[a]	mg/L	20	6.5	2.6	3.6	10.0
Sr[a]	mg/L	20	0.049	0.025	0.013	0.100
Total alkalinity	mg/L as $CaCO_3$	20	72	25	1.2	102
Conductivity	μS/cm	19	123	42	70	220
pH	pH units	19	7.3	0.4	6.6	8.05
TOC	mg/L	2	1.8	0.2	1.7	2.0
Tritium	Bq/L[a]	5	35	19	16	65
^{90}Sr	Bq/L	5	*b*			
Gross alpha	Bq/L	5	0.23	0.13	0.04	0.36
^{137}Cs	Bq/L	5	*b*			
^{60}Co	Bq/L	5	*b*			

[a]Majority of values above detection limit; therefore, mean = maximum mean.
[b]Majority of values below detection limit; therefore, no mean is reported.

Table F.5. Engineered Test Facility water quality: ETF-3

Constituent	Unit	Number of samples	Mean	Standard deviation	Minimum value	Maximum value
Al	mg/L	20	[a]			
B[b]	mg/L	19	0.106	0.221	0.002	1.00
Br	mg/L	17	[a]			
Ca	mg/L	20	33.1	2.9	28.3	38.7
Cl[b]	mg/L	20	1.4	0.5	0.8	2.2
F	mg/L	20	[a]			
Fe	mg/L	20	[a]			
I	mg/L	17	[a]			
K[a]	mg/L	20	3.10	5.29	0.001	22.00
Mg	mg/L	20	3.57	0.48	2.42	4.53
Mn	mg/L	20	0.111	0.061	0.003	0.204
Na[b]	mg/L	20	2.97	1.10	1.98	6.44
NO_2-N	mg/L	9	[a]			
NO_3-N	mg/L	20	[a]			
P (total)	mg/L	16	[a]			
PO_4-P	mg/L	10	[a]			
SiO_2	mg/L	19	9.50	1.35	7.15	11.80
SO_4	mg/L	20	8.3	1.8	4.0	10.0
Sr[b]	mg/L	20	0.066	0.016	0.048	0.100
Total alkalinity	mg/L as $CaCO_3$	20	103	6	94	117
Conductivity	μS/cm	19	162	50	114	300
pH	pH units	19	7.5	0.6	6.6	8.6
TOC	mg/L	2	1.5	1.3	0.6	2.4
Tritium	Bq/L[b]	5	27	18	2	50
^{90}Sr[b]	Bq/L	5	1.31	1.18	0.13	3.00
Gross alpha	Bq/L	5	0.36	0.30	0.07	0.80
^{137}Cs	Bq/L	5	[a]			
^{60}Co	Bq/L	5	[a]			

[a]Majority of values below detection limit; therefore, no mean is reported.
[b]Majority of values above detection limit; therefore, mean = maximum mean.

Table F.6. Engineered Test Facility water quality: ETF-4

Constituent	Unit	Number of samples	Mean	Standard deviation	Minimum value	Maximum value
Al	mg/L	20	[a]			
B[b]	mg/L	19	0.050	0.047	0.002	0.140
Br	mg/L	17	[a]			
Ca	mg/L	20	43.7	7.4	25.0	52.3
Cl	mg/L	20	2.6	0.7	1.0	3.1
F	mg/L	20	[a]			
Fe	mg/L	20	[a]			
I	mg/L	17	[a]			
K[b]	mg/L	20	2.82	4.03	0.001	15.00
Mg	mg/L	20	3.78	0.67	2.20	4.66
Mn	mg/L	20	0.017	0.018	0.0002	0.060
Na[b]	mg/L	20	3.17	1.22	1.59	6.71
NO_2-N	mg/L	9	[a]			
NO_3-N	mg/L	20	[a]			
P (total)	mg/L	16	[a]			
PO_4-P	mg/L	10	[a]			
SiO_2	mg/L	19	11.90	2.55	5.39	15.60
SO_4[b]	mg/L	20	7.8	2.0	4.0	10.0
Sr[b]	mg/L	20	0.079	0.012	0.060	0.100
Total alkalinity	mg/L as $CaCO_3$	20	133	29	66	230
Conductivity	μS/cm	19	177	58	120	290
pH	pH units	19	7.3	0.4	6.5	8.2
TOC	mg/L	2	2.3	1.8	1.0	3.6
Tritium	Bq/L[b]	5	35	9	22	45
^{90}Sr[b]	Bq/L	5	1.25	1.24	0.12	3.00
Gross alpha	Bq/L	5	0.46	0.20	0.27	0.76
^{137}Cs	Bq/L	5	[a]			
^{60}Co	Bq/L	5	[a]			

[a]Majority of values below detection limit; therefore, no mean is reported.
[b]Majority of values above detection limit; therefore, mean = maximum mean.

Table F.7. Engineered Test Facility water quality: ETF-5

Constituent	Unit	Number of samples	Mean	Standard deviation	Minimum value	Maximum value
Al	mg/L	20	*a*			
B[b]	mg/L	19	0.046	0.042	0.001	0.140
Br	mg/L	17	*a*			
Ca	mg/L	20	43.2	5.8	36.0	54.3
Cl[b]	mg/L	20	1.8	0.5	1.0	3.0
F	mg/L	20	*a*			
Fe	mg/L	20	*a*			
I	mg/L	17	*a*			
K[b]	mg/L	20	2.39	3.70	0.001	14.00
Mg	mg/L	20	2.95	0.39	2.46	3.60
Mn[b]	mg/L	20	0.005	0.005	0.0002	0.023
Na[b]	mg/L	20	3.17	1.18	2.50	6.81
NO_2-N	mg/L	9	*a*			
NO_3-N	mg/L	20	*a*			
P (total)	mg/L	16	*a*			
PO_4-P	mg/L	10	*a*			
SiO_2	mg/L	19	13.20	1.72	9.82	16.91
SO_4[b]	mg/L	20	6.6	2.6	3.0	10.0
Sr[b]	mg/L	20	0.095	0.096	0.060	0.500
Total alkalinity	mg/L as $CaCO_3$	20	137	47	99	330
Conductivity	μS/cm	19	168	44	110	255
pH	pH units	19	7.4	0.5	6.5	8.3
TOC	mg/L	2	1.6	0.5	1.3	2.0
Tritium	Bq/L[b]	5	39	19	16	61
^{90}Sr[b]	Bq/L	5	1.24	1.25	0.10	3.00
Gross alpha[b]	Bq/L	5	0.31	0.36	0.02	0.92
^{137}Cs	Bq/L	5	*a*			
^{60}Co	Bq/L	5	*a*			

[a]Majority of values below detection limit; therefore, no mean is reported.
[b]Majority of values above detection limit; therefore, mean = maximum mean.

Table F.8. Engineered Test Facility water quality: ETF-6

Constituent	Unit	Number of samples	Mean	Standard deviation	Minimum value	Maximum value
Al	mg/L	20	*a*			
B[b]	mg/L	19	0.048	0.045	0.002	0.130
Br	mg/L	17	*a*			
Ca	mg/L	20	41.5	5.5	25.8	50.6
Cl[b]	mg/L	20	1.8	0.4	1.0	2.4
F	mg/L	20	*a*			
Fe	mg/L	20	*a*			
I	mg/L	17	*a*			
K[b]	mg/L	20	3.20	5.56	0.001	23.00
Mg	mg/L	20	3.26	0.44	1.90	3.96
Mn	mg/L	20	0.070	0.036	0.002	0.120
Na[b]	mg/L	20	3.34	1.02	1.98	5.54
NO_2-N	mg/L	9	*a*			
NO_3-N	mg/L	20	*a*			
P (total)	mg/L	16	*a*			
PO_4-P	mg/L	10	*a*			
SiO_2	mg/L	19	11.05	1.89	7.30	13.70
SO_4[b]	mg/L	20	6.4	3.1	1.4	10.0
Sr[b]	mg/L	20	0.341	1.238	0.010	5.600
Total alkalinity	mg/L as $CaCO_3$	20	127	15	71	149
Conductivity	μS/cm	19	162	45	118	255
pH	pH units	19	7.3	0.5	6.4	8.3
TOC	mg/L	2	2.4	1.5	1.3	3.4
Tritium	Bq/L[b]	5	26	14	8	42
^{90}Sr[b]	Bq/L	5	1.29	1.20	0.06	3.00
Gross alpha	Bq/L	5	0.44	0.25	0.13	0.76
^{137}Cs	Bq/L	5	*a*			
^{60}Co	Bq/L	5	*a*			

[a]Majority of values below detection limit; therefore, no mean is reported.
[b]Majority of values above detection limit; therefore, mean = maximum mean.

Table F.9. Engineered Test Facility water quality: ETF-7

Constituent	Unit	Number of samples	Mean	Standard deviation	Minimum value	Maximum value
Al	mg/L	20	*a*			
B[b]	mg/L	18	0.054	0.045	0.002	0.120
Br	mg/L	16	*a*			
Ca	mg/L	20	38.8	4.7	28.8	47.4
Cl[b]	mg/L	20	2.0	0.6	1.0	3.0
F	mg/L	20	*a*			
Fe	mg/L	20	*a*			
I	mg/L	16	*a*			
K[b]	mg/L	20	3.21	5.27	0.001	21.00
Mg	mg/L	20	3.54	0.44	2.60	4.42
Mn	mg/L	20	0.030	0.040	0.0001	0.169
Na[b]	mg/L	20	3.28	1.57	2.13	9.03
NO_2-N	mg/L	9	*a*			
NO_3-N	mg/L	20	*a*			
P (total)	mg/L	16	*a*			
PO_4-P	mg/L	10	*a*			
SiO_2	mg/L	19	11.57	1.79	8.09	14.77
SO_4[b]	mg/L	20	6.5	2.6	3.0	10.0
Sr[b]	mg/L	19	0.070	0.018	0.010	0.100
Total alkalinity	mg/L as $CaCO_3$	20	122	14	82	147
Conductivity	μS/cm	19	157	62	3	300
pH	pH units	19	7.3	0.5	6.5	8.2
TOC	mg/L	2	1.4	0.4	1.1	1.6
Tritium	Bq/L[b]	5	30	23	8	65
Gross alpha	Bq/L	5	0.35	0.17	0.10	0.56
^{137}Cs	Bq/L	5	*a*			
^{60}Co	Bq/L	5	*a*			

[a]Majority of values below detection limit; therefore, no mean is reported.
[b]Majority of values above detection limit; therefore, mean = maximum mean.

Table F.10. Engineered Test Facility water quality: ETF-8

Constituent	Unit	Number of samples	Mean	Standard deviation	Minimum value	Maximum value
Al	mg/L	20	[a]			
B[b]	mg/L	19	0.043	0.039	0.003	0.110
Br	mg/L	17	[a]			
Ca	mg/L	20	44.9	7.6	36.2	60.2
Cl[b]	mg/L	20	2.6	1.0	1.0	4.0
F	mg/L	20	[a]			
Fe	mg/L	20	[a]			
I	mg/L	17	[a]			
K[b]	mg/L	20	2.19	2.78	0.001	9.40
Mg	mg/L	20	3.42	0.57	2.50	4.50
Mn	mg/L	20	0.006	0.003	0.002	0.014
Na[b]	mg/L	20	3.10	1.38	2.28	7.31
NO_2-N	mg/L	9	[a]			
NO_3-N[b]	mg/L	20	4.8	6.4	0.001	21.0
P (total)	mg/L	16	[a]			
PO_4-P	mg/L	10	[a]			
SiO_2	mg/L	19	10.66	2.76	0.79	14.12
SO_4[b]	mg/L	20	9.0	1.0	7.0	10.0
Sr[b]	mg/L	20	0.073	0.020	0.010	0.100
Total alkalinity	mg/L as $CaCO_3$	20	126	13	106	149
Conductivity	μS/cm	18	173	48	115	280
pH	pH units	18	7.4	0.4	6.8	8.2
TOC	mg/L	2	1.4	1.1	0.6	2.1
Tritium	Bq/L[b]	5	47	15	30	65
^{90}Sr	Bq/L	5	[a]			
Gross alpha[b]	Bq/L	5	0.17	0.06	0.07	0.24
^{137}Cs	Bq/L	5	[a]			
^{60}Co	Bq/L	5	[a]			

[a]Majority of values below detection limit; therefore, no mean is reported.

[b]Majority of values above detection limit; therefore, mean = maximum mean.

Table F.11. Engineered Test Facility water quality: ETF-9

Constituent	Unit	Number of samples	Mean	Standard deviation	Minimum value	Maximum value
Al	mg/L	20	[a]			
B[b]	mg/L	19	0.047	0.040	0.004	0.115
Br	mg/L	17	[a]			
Ca	mg/L	20	35.0	5.8	19.0	42.9
Cl[b]	mg/L	20	1.6	0.7	1.0	4.0
F	mg/L	20	[a]			
Fe	mg/L	20	[a]			
I	mg/L	17	[a]			
K[b]	mg/L	20	4.02	7.27	0.001	32.0
Mg	mg/L	20	4.83	0.79	3.10	6.30
Mn[b]	mg/L	20	0.028	0.038	0.0002	0.160
Na[b]	mg/L	20	3.52	1.30	2.50	7.14
NO_2-N	mg/L	9	[a]			
NO_3-N	mg/L	20	[a]			
P (total)	mg/L	16	[a]			
PO_4-P	mg/L	10	[a]			
SiO_2[b]	mg/L	19	7.32	2.54	0.20	13.60
SO_4[b]	mg/L	20	10.3	1.8	4.0	13.6
Sr[b]	mg/L	20	0.073	0.016	0.039	0.100
Total alkalinity	mg/L as $CaCO_3$	20	114	10	86	131
Conductivity	μS/cm	19	178	60	118	300
pH	pH units	19	7.4	0.4	6.7	8.2
TOC	mg/L	2	1.9	1.6	0.8	3.0
Tritium	Bq/L[b]	5	35	19	16	65
^{90}Sr[b]	Bq/L	5	1.70	1.02	0.28	3.00
Gross alpha[b]	Bq/L	5	0.35	0.32	0.12	0.90
^{137}Cs	Bq/L	5	[a]			
^{60}Co	Bq/L	5	[a]			

[a]Majority of values below detection limit; therefore, no mean is reported.
[b]Majority of values above detection limit; therefore, mean = maximum mean.

Table F.12. Engineered Test Facility water quality: ETF-10

Constituent	Unit	Number of samples	Mean	Standard deviation	Minimum value	Maximum value
Al[a]	mg/L	20	0.053	0.060	0.001	0.260
B[a]	mg/L	19	0.044	0.045	0.001	0.140
Br	mg/L	17	*b*			
Ca	mg/L	20	30.5	8.5	6.8	42.3
Cl	mg/L	20	*b*			
F	mg/L	20	*b*			
Fe	mg/L	20	*b*			
I	mg/L	17	*b*			
K[a]	mg/L	20	2.14	3.59	0.001	14.00
Mg	mg/L	20	2.40	0.62	0.56	3.38
Mn[a]	mg/L	20	0.053	0.180	0.0001	0.810
Na[a]	mg/L	20	273	1.42	0.41	6.65
NO_2-N	mg/L	9	*b*			
NO_3-N	mg/L	20	*b*			
P (total)	mg/L	16	*b*			
PO_4-P	mg/L	10	*b*			
SiO_2[a]	mg/L	19	10.97	3.89	0.20	15.41
SO_4[a]	mg/L	20	6.1	2.8	3.0	10.0
Sr[a]	mg/L	20	0.056	0.021	0.024	0.100
Total alkalinity	mg/L as $CaCO_3$	20	96	22	12	115
Conductivity	μS/cm	19	150	55	85	300
pH	pH units	19	7.5	0.5	6.9	8.3
TOC	mg/L	2	3.4	2.3	1.7	5.0
Tritium	Bq/L[a]	5	43	25	22	86
^{90}Sr	Bq/L	5	*b*			
Gross alpha	Bq/L	5	0.34	0.37	0.08	1.00
^{137}Cs	Bq/L	5	*b*			
^{60}Co	Bq/L	5	*b*			

[a]Majority of values above detection limit; therefore, mean = maximum mean.
[b]Majority of values below detection limit; therefore, no mean is reported.

Table F.13. Engineered Test Facility water quality: ETF-11

Constituent	Unit	Number of samples	Mean	Standard deviation	Minimum value	Maximum value
Al	mg/L	20	[a]			
B[b]	mg/L	19	0.045	0.039	0.004	0.120
Br	mg/L	17	[a]			
Ca	mg/L	20	30.5	6.4	13.0	49.0
Cl[b]	mg/L	20	1.4	0.5	1.0	2.6
F	mg/L	20	[a]			
Fe	mg/L	20	[a]			
I	mg/L	17	[a]			
K[b]	mg/L	20	3.96	4.89	0.001	14.00
Mg	mg/L	20	6.77	1.02	3.30	8.10
Mn	mg/L	20	0.039	0.019	0.0003	0.066
Na[b]	mg/L	20	3.85	1.41	2.50	7.88
NO_2-N	mg/L	9	[a]			
NO_3-N	mg/L	20	[a]			
P (total)	mg/L	16	[a]			
PO_4-P	mg/L	10	[a]			
SiO_2	mg/L	19	12.54	1.91	9.05	15.70
SO_4	mg/L	20	9.78	2.06	4.00	13.00
Sr[b]	mg/L	20	0.119	0.022	0.054	0.158
Total alkalinity	mg/L as $CaCO_3$	20	114	10	88	149
Conductivity	μS/cm	18	173	68	85	320
pH	pH units	19	7.5	0.4	6.9	8.2
TOC	mg/L	2	1.6	0.4	1.3	1.8
Tritium[b]	Bq/L[b]	5	16	15	2	34
^{90}Sr	Bq/L	5	[a]			
Gross alpha	Bq/L	5	0.15	0.10	0.06	0.09
^{137}Cs	Bq/L	5	[a]			
^{60}Co	Bq/L	5	[a]			

[a]Majority of values below detection limit; therefore, no mean is reported.
[b]Majority of values above detection limit; therefore, mean = maximum mean.

Table F.14. Engineered Test Facility water quality: ETF-12

Constituent	Unit	Number of samples	Mean	Standard deviation	Minimum value	Maximum value
Al	mg/L	20	[a]			
B[b]	mg/L	19	0.055	0.046	0.005	0.136
Br	mg/L	17	[a]			
Ca	mg/L	20	26.6	5.0	8.9	31.8
Cl	mg/L	20	[a]			
F	mg/L	20	[a]			
Fe	mg/L	20	[a]			
I	mg/L	17	[a]			
K[b]	mg/L	20	5.18	7.06	0.001	23.0
Mg	mg/L	20	7.18	1.69	2.90	9.19
Mn	mg/L	20	0.013	0.011	0.002	0.040
Na[b]	mg/L	20	3.67	1.50	2.50	6.79
NO_2-N	mg/L	9	[a]			
NO_3-N	mg/L	20	[a]			
P (total)	mg/L	16	[a]			
PO_4-P	mg/L	10	[a]			
SiO_2	mg/L	19	13.45	2.05	9.80	16.00
SO_4[b]	mg/L	20	10.8	2.4	4.0	14.0
Sr[b]	mg/L	19	0.124	0.025	0.044	0.152
Total alkalinity	mg/L as $CaCO_3$	19	106	8	76	113
Conductivity	μS/cm	19	157	48	118	300
pH	pH units	19	7.7	0.9	7.0	11.0
TOC	mg/L	2	2.2	1.8	0.9	3.5
Tritium[b]	Bq/L[b]	5	19	16	2	37
^{90}Sr[b]	Bq/L	5	1.03	0.96	0.02	2.0
Gross alpha	Bq/L	5	0.39	0.34	0.11	0.90
^{137}Cs	Bq/L	5	[a]			
^{60}Co	Bq/L	5	[a]			

[a] Majority of values below detection limit; therefore, no mean is reported.
[b] Majority of values above detection limit; therefore, mean = maximum mean.

ORNL/TM-9146

INTERNAL DISTRIBUTION

1. T. L. Ashwood
2–3. S. I. Auerbach
4. L. D. Bates
5–9. W. J. Boegly, Jr.
10. J. Bolinsky, Jr.
11. B. Cannon
12. R. B. Clapp
13. J. H. Coobs
14. K. E. Cowser
15. N. H. Cutshall
16–20. E. C. Davis
21. D. L. DeAngelis
22. L. R. Dole
23. L. D. Eyman
24. N. D. Farrow
25. C. W. Francis
26. W. F. Furth
27. J. R. Gissel
28. T. Grizzard
29–33. C. S. Haase
34. S. G. Hildebrand
35. F. J. Homan
36–40. D. D. Huff
41. R. Jordan
42. R. H. Ketelle
43. E. M. King
44. D. W. Lee
45. L. J. Mezga
46. M. S. Moran
47. F. R. Mynatt
48. T. E. Myrick
49. T. W. Oakes
50. C. R. Olsen
51. B. D. Patton
52. F. G. Pin
53. D. E. Reichle
54. C. R. Richmond
55. L. W. Rickert
56. R. D. Roop
57–61. E. R. Rothschild
62. T. H. Row
63. T. G. Scott
64. O. M. Sealand
65. E. D. Smith
66–70. B. P. Spalding
71. R. G. Stansfield
72. W. P. Staub
73. S. H. Stow
74–83. L. E. Stratton
84. J. Switek
85. T. Tamura
86. D. M. Walls
87. D. S. Wilkes
88. R. G. Wymer
89. G. T. Yeh
90. H. E. Zittel
91–92. Central Research Library
93–102. ESD Library
103–104. Laboratory Records Department
105. Laboratory Records, RC
106. ORNL Patent Office
107. ORNL Y-12 Technical Library

EXTERNAL DISTRIBUTION

108. S. W. Ahrends, Oak Ridge Operations, U.S. Department of Energy, P.O. Box E, Oak Ridge, TN 37831
109. J. Albaugh, Program Manager, Solid Waste Processing and Disposal, Rockwell Hanford Operations, P.O. Box 800, Richland, WA 99353

110. E. L. Albenesius, Savannah River Laboratory, P.O. Box A, Aiken, SC 29801
111. M. Barainca, Program Manager, Low-Level Waste Management Program, U.S. Department of Energy, 550 Second Street, Idaho Falls, ID 83401
112. D. R. Brown, Manager, ORO Radioactive Waste Management Program, Oak Ridge Operations, U.S. Department of Energy, P.O. Box E, Oak Ridge, TN 37831
113. P. W. Caspar, Assistant Manager for Safety and Environment, Oak Ridge Operations, U.S. Department of Energy, P.O. Box E, Oak Ridge, TN 37831
114. T. C. Chee, R&D and Byproducts Division, DP-123 (GTN), U.S. Department of Energy, Washington, D.C. 20545
115. Peter Colombo, Group Leader, Nuclear Waste Research, Brookhaven National Laboratory, Building 701, Upton, NY 11973
116. E. F. Conti, Office of Nuclear Regulatory Research, Nuclear Regulatory Commission, MS-1130-SS, Washington, D.C. 20555
117. J. J. Davis, Office of Nuclear Regulatory Research, Nuclear Regulatory Commission, MS-1130-SS, Washington, D.C. 20555
118. J. L. Deichman, Program Director, Waste Management Program Office, Rockwell Hanford Operations, P.O. Box 800, Richland, WA 99353
119. J. E. Dieckhoner, Acting Director, Operations and Traffic Division, DP-122 (GTN), U.S. Department of Energy, Washington, D.C. 20545
120. Carl Gertz, Chief, Radioactive Waste Technology Branch, Idaho Operations Office, U.S. Department of Energy, 550 Second Street, Idaho Falls, ID 83401
121. F. F. Hooper, Ecology, Fisheries and Wildlife Program, School of Natural Resources, The University of Michigan, Ann Arbor, MI 48109
122. E. A. Jennrich, Program Manager, Low-Level Waste Management Program, EG&G Idaho, P.O. Box 1625, Idaho Falls, ID 83401
123. J. J. Jicha, Director, R&D and Byproducts Division, DP-123 (GTN), U.S. Department of Energy, Washington, D.C. 20545
124. E. A. Jordan, Low-Level Waste Program Manager, Division of Storage and Treatment Projects, NE-25 (GTN), U.S. Department of Energy, Washington, D.C. 20545
125. J. H. Kittel, Manager, Office of Waste Management Programs, Argonne National Laboratory, 9700 South Cass Avenue, Building 205, Argonne, IL 60439
126. M. R. Kreiter, Waste Isolation, Pacific Northwest Laboratory, Richland, WA 99352
127. Leonard Lane, Los Alamos National Laboratory, P.O. Box 1663, Los Alamos, NM 87545
128. D. E. Large, National Program Manager, ORO Radioactive Waste Management Program, Oak Ridge Operations, U.S. Department of Energy, P.O. Box E, Oak Ridge, TN 37831
129. D. B. Leclaire, Director, Office of Defense Waste and Byproducts Management, DP-123 (GTN), U.S. Department of Energy, Washington, D.C. 20545
130. J. A. Lenhard, Oak Ridge Operations, U.S. Department of Energy, P.O. Box E, Oak Ridge, TN 37831
131. Helen McCammon, Director, Ecological Research Division, Office of Health and Environmental Research, Office of Energy Research, U.S. Department of Energy, MS-E201, ER-75, Room E-233, Washington, D.C. 20545

132. G. L. Meyer, Environmental Protection Agency, 401 M Street, SW., MS-ANR459, Washington, D.C. 20460
133. H. A. Mooney, Department of Biological Sciences, Stanford University, Stanford, CA 94305
134. J. D. Newbold, Stroud Water Research Center, Route 1, Box 512, Avondale, PA 19311
135. D. T. Oakley, Program Manager for Waste Management, Los Alamos National Laboratory, P.O. Box 1663, Los Alamos, NM 87545
136. W. S. Osburn, Jr., Ecological Research Division, Office of Health and Environmental Research, Office of Energy Research, U.S. Department of Energy, MS-E201, EV-33, Room F-216, Washington, D.C. 20545
137. Irwin Remson, Department of Applied Earth Sciences, Stanford University, Stanford, CA 94305
138. P. G. Risser, Office of the Chief, Illinois Natural History Survey, Natural Resources Building, 607 East Peabody Avenue, Champaign, IL 61820
139. Jackson Robertson, U.S. Geological Survey, 410 National Center, Reston, VA 22092
140. E. M. Romney, University of California, Los Angeles, 900 Veteran Avenue, Los Angeles, CA 90024
141. R. J. Starmer, HLW Technical Development Branch, Office of Nuclear Material Safety and Safeguards, U.S. Nuclear Regulatory Commission, Room 427-SS, Washington, D.C. 20555
142. J. G. Steger, Environmental Sciences Group, Los Alamos National Laboratory, P.O. Box 1663, Los Alamos, NM 87545
143. J. A. Stone, Savannah River Laboratory, E. I. Du Pont de Nemours & Company, Building 773-A, Room E-112, Aiken, SC 29808
144. David Swan, Point Road, Wilson Point, South Norwalk, CT 06854
145. N. D. Vaughan, Shell Landing, Route 2, Box 1738, Beaufort, NC 28516
146. E. C. Walls, Route 1, Box 322, Harriman, TN 37748
147. R. L. Watters, Ecological Research Division, Office of Health and Environmental Research, Office of Energy Research, U.S. Department of Energy, MS-E201, ER-75, Room F-226, Washington, D.C. 20545
148. F. J. Wobber, Division of Ecological Research, Office of Health and Environmental Research, Office of Energy Research, U.S. Department of Energy, MS-E201, Washington, D.C. 20545
149. R. W. Wood, Director, Division of Pollutant Characterization and Safety Research, U.S. Department of Energy, Washington, D.C. 20545

150–176. Technical Information Center, Oak Ridge, TN 37831